



COPYRIGHT AND USE OF THIS THESIS

This thesis must be used in accordance with the provisions of the Copyright Act 1968.

Reproduction of material protected by copyright may be an infringement of copyright and copyright owners may be entitled to take legal action against persons who infringe their copyright.

Section 51 (2) of the Copyright Act permits an authorized officer of a university library or archives to provide a copy (by communication or otherwise) of an unpublished thesis kept in the library or archives, to a person who satisfies the authorized officer that he or she requires the reproduction for the purposes of research or study.

The Copyright Act grants the creator of a work a number of moral rights, specifically the right of attribution, the right against false attribution and the right of integrity.

You may infringe the author's moral rights if you:

- fail to acknowledge the author of this thesis if you quote sections from the work
- attribute this thesis to another author
- subject this thesis to derogatory treatment which may prejudice the author's reputation

For further information contact the University's Director of Copyright Services

sydney.edu.au/copyright

**Role of double-stranded RNA
binding proteins in the Arabidopsis
miRNA pathway**

by

Rodrigo Siqueira Reis

A thesis submitted for the degree of

Doctor of Philosophy

at the University of Sydney



THE UNIVERSITY OF
SYDNEY

August 2014

To

*Sebastiao and Ana, my parents, who always gave the highest
priority to education*

Every day is a new day. It is better to be lucky. But I would rather be exact.

Then when luck comes you are ready.

Ernest Hemingway

Declaration of originality

To the best of my knowledge, this thesis contains no copy or paraphrase of work published by another person, except where duly acknowledged in the text. This thesis contains no material which has been previously presented for a degree at the University of Sydney or any other university.

I declare this thesis to be wholly my own work, unless stated otherwise.

Rodrigo Siqueira Reis _____

Publications

Journal articles published or in preparation and conference abstracts presented during this Ph.D. candidature:

Reis, R.S., Hart-Smith, G., Eamens, A., Wilkins, M. and Waterhouse, P.M., *Gene regulation by translational inhibition is determined by Dicer partnering proteins. Nature Plants*, 1(3). doi:10.1038/nplants.2014.27.

Reis, R.S., Hart-Smith, G., Eamens, A., Wilkins, M. and Waterhouse, P.M., *Regulation of protein accumulation by double-stranded RNA binding proteins DRB1 and DRB2. In preparation.*

Reis, R.S., Eamens, A., Roberts, T.H. and Waterhouse, P.M., *Structural determinants of the in vivo activity of Arabidopsis double-stranded RNA binding proteins. In preparation.*

Reis, R.S., Hart-Smith, G., Eamens, A., Wilkins, M. and Waterhouse, P.M., *Quantitative Proteomic Analysis of Arabidopsis thaliana DOUBLE-STRANDED RNA BINDING2 (DRB2) Knockout Mutant Plants – Role in Translation Inhibition. The Non-Coding Genome (poster), 2013.*

Reis, R.S., Hart-Smith, G., Eamens, A., Wilkins, M. and Waterhouse, P.M., *Quantitative proteomic analysis of Arabidopsis thaliana DOUBLE-STRANDED RNA BINDING2 (DRB2) knockout mutant plants. 24th International Conference on Arabidopsis Research (ICAR) (poster), 2013.*

Reis R.S., Litholdo Junior C.G., Mackay J. and Waterhouse P., *Application of silencing suppressor in single cell co-expression of target proteins. ComBio2012 (poster), 2012.*

Abstract

MicroRNAs (miRNAs) are small regulatory RNAs that are produced by Dicer proteins and regulate gene expression in development and adaptive responses to the environment. The components and mechanism(s) that determine whether a plant miRNA ultimately regulates its targets by guiding transcript cleavage or translation inhibition are unknown. In this thesis I show that the form of regulatory action directed by a plant miRNA is determined by DOUBLE-STRANDED RNA BINDING PROTEIN2 DRB2, a DICER-LIKE1 (DCL1) partnering protein. The dependence of DCL1 on DRB1 for miRNA biogenesis is well characterized, but I show that it is required only for miRNA-guided transcript cleavage. DRB2 determines miRNA-guided translational inhibition and represses *DRB1* expression, thereby allowing the active selection of miRNA regulatory action. Furthermore, the results reveal that the core silencing proteins ARGONAUTE1 (AGO1) and SERRATE (SE) are regulated by miRNA-guided translational inhibition. DRB2 has been remarkably conserved throughout plant evolution, with its functional domains retaining ~80% amino acid sequence identity from mosses to eudicots, while DRB1, although also present in all multicellular plant clades, is much less conserved. This raises the possibility that translational repression is the ancient form of miRNA-directed gene regulation in plants, and that Dicer partnering proteins, such as human TRBP, might play a similar role in other eukaryotic systems. In addition, DRB1 and DRB2 have similar but functionally different domains, such as their dsRBD2 and C-terminus. The results presented here suggest that DRB1 and DRB2 act as bridging proteins that assemble different component proteins, and even different RNAs, into the core of the dicing bodies (D-bodies), thus altering the properties of the D-bodies and the functionality of the miRNA pathway as a whole. DRB1 and DRB2 are also shown to play major, but different, roles in environmental adaptation, suggesting that cleavage and translation inhibition, respectively, are independent mechanisms, an insight that has not been experimentally shown before.

Keywords: DRB2, DRB1, translation inhibition, Arabidopsis, proteomics, miRNA

Acknowledgements

I thank my supervisors Peter Waterhouse, Marc Wilkins, Andrew Eamens and Thomas Roberts for their encouragement, support and wisdom. Peter's enthusiasm for research is very contagious, and he's never put limits to my absurdities. Thank you for your patience and for always supporting my work. Thanks Marc for our discussions that helped me to take the most of the proteomics in my work, also thanks for getting Gene Hart-Smith on board. After one year struggling with my initial project, I couldn't see how to move forward. Andy was crucial in that moment and the reason I'm now part of the DRB group. Thanks for showing support when I needed it the most, and for being a great supervisor throughout this thesis. I'll be always indebted to Tom for having me as his student when Peter moved to Queensland, and for being supportive and encouraging in the critical moment of thesis writing. A very special thankyou to Gene for your engagement with the proteomics project; it was fantastic to work with you.

I had a great time and a lot of fun in Peter's lab. I thank Craig Jackson for being the amazing lab manager he was, which made my life a lot easier than it would've been otherwise. I thank Adriana Fusaro for encouraging me to undertake a PhD thesis, and for helping me in the first steps of my thesis. Thanks Kenlee Nakasugi for being such a great bioinformatician and for patiently helping me. Thanks Julia Bali for your kindness and support during the tough times. Thanks Celso Litholdo for the encouragement, friendship and many goals we scored together playing football! Thanks Kiwook Kim and Marcus McHale for the invaluable discussions and advice; I'll miss our beers at the Royal! Glen McIntyre, thanks for being weird and questioning literally everything. Thanks Amanda Huen for our discussions and your advice on various techniques. Kate Chamberlain, thanks for our discussions and your positive attitude. Thanks Deborah Barton for your beautiful microscopy images.

I also thank my 'new' group at ATP. Thank you all for the inspiration, discussions and support during the tough times of my last semester. A special thanks to Peri Tobias for our insightful discussions, to Juan Pablo Risopatron for your encouragement and friendship, and to Hugh Goold for your interesting viewpoints. Thanks to Brian Jones for helpful discussions and advice. Thanks to Claudia Carrasco, Janet Basani, Lai Poon (Cheryl) and Sebastian Ugbaje for the good time together in our office.

From the moment I met Ana Julia, now my wife, to this very day she has filled my life with courage, balance, kindness and love. Thank you for the support during my thesis, and everything I could only achieve with you.

Preface

This thesis contains a compilation of results obtained with my research from late 2011 to mid of 2014.

The thesis has six parts:

Part I: Introduction

Part II: Experimental procedures

Part III: Results and discussion

Part IV: General discussion and conclusion

Part V: Supplementary data

Part VI: Bibliography

The Results and discussion part is organized into three chapters. The General discussion and conclusion part brings together the main findings and their relevance.

Contents

Declaration of originality	ii
Publications	iii
Abstract	iv
Acknowledgements	v
Preface	vi
List of Figures	x
List of Tables	xi
Abbreviations and acronyms	xii
PART I - INTRODUCTION	1
Chapter 1 – History of eukaryotic RNA silencing	2
1.1 Virus immunity left researchers puzzled.....	3
1.2 Co-suppression and homology-dependent virus resistance in plants.....	3
1.3 Antisense RNAs in animals.....	4
1.4 dsRNA: the trigger of RNA silencing.....	5
1.5 The discovery of small-interfering RNAs (siRNAs).....	5
1.6 RNA-dependent RNA polymerases unites the kingdoms.....	6
1.7 siRNA biogenesis: Dicer proteins.....	7
1.8 sRNA activity: Argonaute proteins.....	8
1.9 miRNAs: more nodes to the network	9
1.10 Hitting hard with plant miRNAs.....	10
Chapter 2 – miRNA biogenesis and activity	12
2.1 miRNA biogenesis	13
2.1.1 miRNA biogenesis and RISC assembly in plants: components required.....	15
2.1.2 microRNA biogenesis in plants: still a sea of possibilities	18
2.1.3 miRNA biogenesis in plants: role of DRB proteins	19
2.2 miRNA activity.....	23
2.2.1 Transcript cleavage directed by plant miRNA.....	23
2.2.2 Translation inhibition directed by plant miRNA.....	24
2.2.3 Function of miRNA-guided translation inhibition: growing evidence	27
Chapter 3 – miRNA activity in the age of systems biology	29
3.1 Plant and systems biology: still catching up	30
3.2 Proteomics, just another “OMICS” to make sense of interactomes?.....	31

3.3	Quantitative proteomics in plants.....	32
Chapter 4 – Project hypothesis.....		34
PART II – EXPERIMENTAL PROCEDURES		36
Chapter 5 – Experimental procedures.....		37
5.1	Plant lines and growth condition.....	37
5.1.1	Plant growth conditions for proteomics analysis.....	37
5.1.2	Salt stress treatment.....	37
5.1.3	Germination under abscisic acid treatment.....	38
5.2	Construction of expression vectors and plant transformation.....	38
5.3	Reporter gene expression analysis.....	39
5.1	RNA analysis.....	41
5.1.1	Small RNA deep sequencing.....	41
5.1.2	Analysis of miRNA synthesis accuracy and strand selection.....	41
5.1.3	Northern blot and real time RT-PCR.....	41
5.1.4	miRNA real time RT-PCR.....	42
5.1.5	Microarray analysis.....	44
5.2	Protein extraction and Western blots.....	44
5.3	Proteomics analysis.....	44
5.3.1	Sample preparation.....	44
5.3.2	Mass spectrometry.....	45
5.3.3	MS/MS inclusion lists.....	46
5.3.4	Sequence database searches and protein quantification.....	46
5.4	Construction of the Shoot Apex Interactome and network analysis.....	47
5.5	Gene ontology enrichment analysis.....	47
PART III – RESULTS AND DISCUSSION		48
Chapter 6 – Gene regulation by translational inhibition is determined by Dicer partnering proteins		49
6.1	Phenotypes displayed by <i>drb1</i> and <i>drb2</i> mutant plants.....	50
6.2	Characterization of <i>DRB1</i> and <i>DRB2</i> expression.....	52
6.3	miRNA production is altered in <i>drb2</i> mutant.....	54
6.4	miRNA target gene expression in the <i>drb2</i> shoot apex.....	56
6.5	miRNA target protein levels are disproportionately elevated in <i>drb2</i>	58
6.6	DRB2 directs miRNA-guided translational inhibition in flowers.....	63
6.7	Protein machinery required for miRNA-directed translational inhibition.....	65

6.8	DRB2 represses <i>DRB1</i> expression.....	66
6.9	DRB1 and DRB2 are evolutionary conserved in plants	68
6.10	Chapter highlights.....	72
Chapter 7 – Regulation of protein accumulation by double-stranded RNA binding proteins DRB1 and DRB2		73
7.1	Arabidopsis Shoot Apex Interactome	74
7.2	Altered protein accumulation in <i>drb1</i> and <i>drb2</i> shoot apex	77
7.3	Network rewiring in <i>drb1</i> and <i>drb2</i> mutants.....	77
7.4	Functions and processes enriched in <i>drb1</i> and <i>drb2</i> mutants.....	82
7.5	Biotic and abiotic responses in <i>drb1</i> and <i>drb2</i> mutants.....	88
7.6	Chapter highlights.....	90
Chapter 8 – Structural determinants of the <i>in vivo</i> activity of Arabidopsis double-stranded RNA binding proteins		91
8.1	Evolutionary conservation of DRB1 non-canonical dsRNA binding domain.....	93
8.2	Expression of chimeric gene series in <i>drb1</i> plants.....	95
8.3	miRNA accumulation and gene regulation in transgenic plants	98
8.4	Abscisic acid treatment of the <i>drb1</i> transformant lines	100
8.5	Chapter highlights.....	101
PART IV – GENERAL DISCUSSION AND CONCLUSION		102
Chapter 9 – General discussion, conclusion and future directions		103
9.1	Role of translation inhibition in plants.....	104
9.2	Auto-regulation of the miRNA pathway.....	106
9.3	DRBs as scaffold proteins	106
9.4	Structural determinants for DRB1 and DRB2 <i>in vivo</i> activity.....	107
9.5	Conclusion.....	107
9.6	Future directions	108
PART V – SUPPLEMENTARY DATA		110
Sequence of synthesized DNA		111
Map of cloning vectors.....		114
Microarray data		115
Gene ontology enrichment and protein accumulation		121
PART VI - BIBLIOGRAPHY		136
Bibliography		137

List of Figures

Figure 2-1. miRNA biogenesis and activity.	14
Figure 2-2. Schematic representation of miRNA biogenesis and RISC assemble.	17
Figure 2-3. Secondary structure of RBD1 and RBD2 of Arabidopsis DRB1.	20
Figure 2-4. Amino acid alignment of DRB1 and DRB2 RBD orthologs.	22
Figure 2-5. The action stage of the Arabidopsis miRNA pathway.	26
Figure 5-1. Construction of expression vectors to transform <i>drb1</i> mutants.	40
Figure 6-1. <i>DRB1</i> and <i>DRB2</i> knockout mutant phenotypes.	51
Figure 6-2. <i>DRB1</i> and <i>DRB2</i> expression profiles.	53
Figure 6-3. Strand selection and miRNA processing inaccuracy in <i>drb2</i> mutant.	55
Figure 6-4. Gene expression in <i>drb2</i> mutant.	57
Figure 6-5. Histogram of protein accumulation ratios in <i>drb1</i> and <i>drb2</i>	58
Figure 6-6. DRB2 is required for miRNA-guided translational inhibition in the shoot apex.	60
Figure 6-7. DRB3 and DRB5 are not required for miRNA-guided translational inhibition in the shoot apex.	61
Figure 6-8. miRNA targets accumulate at protein level in shoot apex of <i>drb2</i>	62
Figure 6-9. DRB2 is required for miRNA-guided translational inhibition in flowers.	64
Figure 6-10. Translation inhibition machinery.	65
Figure 6-11. DRB2 represses <i>DRB1</i> expression in shoot apex.	67
Figure 6-12. Evolutionary conservation of DRB1 and DRB2.	69
Figure 6-13. Alignment of dsRNA binding domains (RBD) of DRB1 and DRB2 orthologs.	71
Figure 7-1. Shoot apex interactome.	76
Figure 7-2. Clusters of proteins with differential accumulation in <i>drb1</i> and <i>drb2</i>	80
Figure 7-3. Gene ontology enrichment of proteins of <i>drb1</i> and <i>drb2</i> shoot apex.	83
Figure 7-4. Gene ontology enrichment of proteins with differential accumulation.	85
Figure 7-5. Distribution of proteins according to GO in <i>drb1</i> and <i>drb2</i>	87
Figure 7-6. Abiotic and biotic response GOs and salt stress treatment in <i>drb1</i> and <i>drb2</i>	89
Figure 8-1. dsRNA-binding domains of Arabidopsis DRB proteins.	94
Figure 8-2. Phenotype of wild-type, <i>drb1</i> and transgenic plants.	97
Figure 8-3. miRNA accumulation and their target levels in wild-type, <i>drb1</i> and transgenic plants.	99
Figure 8-4. Effects of exogenous ABA on wild-type, <i>drb1</i> and transgenic plants.	100
Figure 9-1. Proposed model for the role of DRB1 and DRB2 in the miRNA pathway.	108

List of Tables

Table 2-1. Proteins required for miRNA biogenesis and RISC assembly.	16
Table 5-1. List of DNA oligos and probes.....	43
Table 5-2. Source and working dilution of antibodies used for western blot analysis. ...	44
Table 6-1. miRNA accumulation profile of detected miRNA in shoot apex of 3-week-old Arabidopsis wild-type (Col-0) and <i>drb2</i> mutant plants (n = 1).	54
Table 6-2. DRB1 and DRB2 putative orthologs in plant species.	70
Table 7-1. Accumulation and function of proteins with differential accumulation clustered (sub-networks) in <i>drb1</i> and <i>drb2</i>, relative to wild-type.	81
Table 9-1. Transcript expression level of miRNA targets in shoot apex in <i>drb2</i> and wild-type.	115
Table 9-2. Accumulation of proteins enriched in GO terms (p-value<0.05).	121

Abbreviations and acronyms

3'UTR	3' untranslated region
ABA	Abscisic acid
ABRC	Arabidopsis Biological Resource Centre
ACT2	ACTIN 2 (AT3G18780)
AFB1	AUXIN SIGNALING F BOX PROTEIN 1 (AT4G03190)
AGO	Argonaute
AGRf	Australian Genome Research Facility
AKR4C8	ALDOKETO REDUCTASE FAMILY 4 MEMBER C8 (AT2G37760)
amiRNA	Artificial miRNA
AMP1	ALTERED MERISTEM PROGRAM1 (AT3G54720)
ANNAT1	ANNEXIN1 (AT1G35720)
ANNAT4	ANNEXIN4 (AT2G38750)
ANOVA	Analysis of variance
AP2	APETELA2 (AT4G36920)
APS1	ATP SULFURYLASE 1 (AT3G22890)
ARPN	PLANTACYANIN (AT2G02850)
ATDJ1A	DJ-1 HOMOLOG1-A (AT3G14990)
ATHB-14	A. THALIANA HOMEBOX PROTEIN14 (AT2G34710)
BioGRID	Biological General Repository for Interaction Datasets
BMP	Bone morphogenetic protein
BXL7	Probable beta-D-xylosidase 7 (AT1G78060)
CAF	CARPEL FACTORY, renamed DCL1 (AT1G01040)
CDC5	CELL DIVISION CYCLE5 (AT1G09770)
CPL1	C-TERMINAL DOMAIN PHOSPHATASE-LIKE1 (AT4G21670)
CPN60B	CHAPERONIN 60 BETA (AT1G55490)
cRNAs	Complementary RNAs
CSD1	COPPER/ZINC SUPEROXIDE DISMUTASE 1 (AT1G08830)
CSD2	COPPER/ZINC SUPEROXIDE DISMUTASE2 (AT2G28190)
CUC2	CUP SHAPED COTLEDONS2 (AT2G28190)
CYP71B6	CYTOCHROME P450 71B6 (AT2G24180)
DAS	Days after stratification
DAVID	Database for Annotation, Visualization and Integrated Discovery
D-body	Dicing body
DCL1	DICER-LIKE1 (AT1G01040)
DDL	DAWDLE (AT3G20550)
DELTA-TIP	DELTA TONOPLAST INTEGRAL PROTEIN (AT3G16240)
DIGE	Differential in Gel Electrophoresis
DRB	dsRNA-binding
dsRNA	Double-stranded RNA
ER	Endoplasmic reticulum

FAMT	FARNESOIC ACID CARBOXYL-O-METHYLTRANSFERASE (AT3G44860)
FHA	Phosphothreonine binding forkhead-associated domain
FKBP15	FK506-BINDING PROTEIN 15 KD-1 (AT3G25220)
FLC	FLOWERING LOCUS C (AT5G10140)
FVE	MULTICOPY SUPPRESSOR OF IRA1 4 (AT2G19520)
GO	Gene ontology
GPX2	GLUTATHIONE PEROXIDASE2 (AT2G31570)
GUS	β-glucuronidase
HAP2-1	"NUCLEAR FACTOR Y, SUBUNIT A1" (AT5G12840)
HDA16	HISTONE DEACTYLATION16 (AT3G18520)
HEN1	HUA ENHANCER 1 (AT4G20910)
HOS1	HIGH EXPRESSION OF OSMOTICALLY RESPONSIVE GENES1 (AT2G39810)
hpRNA	Hairpin RNA
KTN1	KATANIN1 (AT1G80350)
LAC2	LACCASE 2 (AT2G29130)
LAC3	LACCASE 3 (AT2G30210)
LACS7	LONG-CHAIN ACYL-COA SYNTHETASE7 (AT5G27600)
m ⁷ G	5'-7-methylguanosine
MBP1	MYROSINASE-BINDING PROTEIN 1 (AT1G52040)
MBP2	MYROSINASE-BINDING PROTEIN 2 (AT1G52030)
miRISC	miRNA-loaded RISC
miRNA	MicroRNA
miRNA*	Passenger strand
MOS2	MODIFIER OF SNC1, 2 (AT1G33520)
MS (medium)	Murashige and Skoog
MS (proteomics)	Mass spectrometry
NAC089	NAC DOMAIN CONTAINING PROTEIN89 (AT5G22290).
NB-LRR	Nucleotide-binding site leucine-rich repeat
NGS	Next-generation sequencing
NOT2b	NEGATIVE ON TATA LESS2b (AT5G59710)
NTL9	NAC TRANSCRIPTION FACTOR-LIKE9 (AT4G35580)
OEP16	OUTER ENVELOPE PROTEIN 16 (AT2G28900).
PAGE	polyacrylamide gel electrophoresis
PEX11C	PEROXIN 11C (AT1G01820)
PEX11D	PEROXIN11D (AT2G45740)
PIP1B	PLASMA MEMBRANE INTRINSIC PROTEIN 1B (AT2G45960)
PIP2A	PLASMA MEMBRANE INTRINSIC PROTEIN 2 (AT3G53420)
PIP2E	PLASMA MEMBRANE INTRINSIC PROTEIN 2E (AT2G39010)
PIP3	PLASMA MEMBRANE INTRINSIC PROTEIN 3A (AT4G35100)
Pol II	RNA polymerase II

PPI	Protein-protein interaction
pri-miRNA	Primary miRNA transcript
PTGS	Post-transcriptional gene silencing
QDE	Quelling-defective
RAB8	GTPASE HOMOLOG 8 (AT3G53610)
RACK1	RECEPTOR FOR ACTIVATED C KINASE1 (AT1G18080)
RBD	dsRNA-binding domain
RCA	RUBISCO ACTIVASE (AT2G39730)
RDR	RNA-dependent RNA polymerase
REV	REVOLUTA (AT5G60690)
R-gene	Resistance gene
RISC	RNA-induced silencing complex
RNAi	RNA interference
RT-PCR	Reverse-transcription PCR
SAI	Shoot Apex Interactome
SAM	Shoot apical meristem
SAT3	SERINE ACETYLTRANSFERASE 3 (AT3G13110)
SE	SERRATE (AT2G27100)
SEC61b	SUPPRESSORS OF SECRETION-DEFECTIVE 61 BETA (AT2G45070)
SIC	SICKLE (AT4G24500)
SIN1	SHORT INTEGUMENTS1, renamed DCL1 (AT1G01040)
siRNAs	Small-interfering RNAs
SOX	SULFITE OXIDASE (AT3G01910)
SPL4	SQUAMOSA PROMOTER BINDING PROTEIN-LIKE 4 (AT1G53160)
sRNA	Small RNA
ssRNA	Single-stranded RNA
STA1	STABILIZED1 (AT4G03430)
stRNA	Small temporal RNA
SUMO1	SMALL UBIQUITIN-LIKE MODIFIER 1 (AT4G26840)
SUMO3	SMALL UBIQUITIN-LIKE MODIFIER 3 (AT5G55170)
SUO	'SHUTTLE' IN CHINESE (AT3G48050)
SUS1	SUSPENSOR1, renamed DCL1 (AT1G01040)
TAC	Transcriptome Analysis Console
T-DNA	Transfer-DNA
TGH	TOUGH (AT5G23080)
TRV	<i>Tobacco ring spot virus</i>
VCS	VARICOSE (AT3G13300)
WHY3	WHIRLY 3 (AT2G02740)

PART I - INTRODUCTION

Chapter 1 – History of eukaryotic RNA silencing

In eukaryotes, RNA silencing is triggered by double-stranded RNA (dsRNA) that is processed into small RNAs (sRNAs) by a member of the Dicer protein family (Bernstein et al., 2001). These sRNAs are in turn loaded into a member of the Argonaute (AGO) protein family to form the catalytic core of the RNA-induced silencing complex (RISC) (Hammond et al., 2001). Endogenous or exogenous transcripts carrying complementary sequences to the AGO-loaded sRNA are targeted by RISC, which, depending on the AGO family member at its catalytic core, mediates expression inhibition at either the transcriptional or posttranscriptional level (Zamore et al., 2000). Plant sRNAs also require the activity of the sRNA-specific methyltransferase, HUA ENHANCER1 (HEN1), to stabilise the sRNA post Dicer processing and prior to AGO loading, via 2'-O-methylation of the 3' terminal nucleotide (Yu et al., 2005).

In this chapter, the main discoveries that have led to our current understanding of RNA silencing are discussed, with a specific focus on plant miRNA biogenesis and action.

1.1 Virus immunity left researchers puzzled

RNA silencing was probably first reported in 1928 (reviewed by Baulcombe, 2004), when tobacco plants infected with *Tobacco ring spot virus (TRV)* became progressively less symptomatic over time. Intriguingly, new leaves that emerged post *TRV* infection appeared to have 'recovered' from the initial infection and were shown to be resistant to secondary infection with either the same, or to closely related, viruses (Wingard, 1928). Half a century later, plant virologists started to uncover the molecular mechanisms behind virus-induced resistance.

1.2 Co-suppression and homology-dependent virus resistance in plants

In plants, two related theories led to the first advance towards our current understanding of RNA silencing: co-suppression and homology-dependent virus resistance. Silencing of a selectable marker gene, introduced to the plant via *Agrobacterium tumefaciens* (*Agrobacterium*)-mediated transformation, was observed upon the introduction of a second plant expression vector carrying a different selectable marker gene, when the expression of both selectable marker genes was driven by the same strong viral promoter (Matzke et al.,

1989). In addition, the constitutive expression of reintroduced copies of endogenous genes via the use of viral promoters was shown to result in silencing of both the endogenous and transgene-introduced copy (van der Krol, 1990; Napoli et al., 1990). Further variations of these initial co-suppression experiments were repeatedly confirmed in subsequent studies (de Carvalho et al., 1992; Smith et al., 1990; Vaucheret et al., 1995). Similarly, homology-dependent virus resistance was observed with transformed plants harbouring viral-derived transgenes, which, upon plant genome integration, mediated resistance to viruses with homologous sequences to those present in the integrated transgene (Lindbo et al., 1993; Mueller et al., 1995). It did not take long for researchers to realise that a similar mechanism was underpinning the phenomena observed in silencing endogenous genes as well as with plant-acquired resistance to viruses (Ratcliff, 1997). Both phenomena shared high target specificity, leading to the hypothesis that they may be guided by a nucleic acid molecule. Several independent groups concluded that 'silenced' plants failed to accumulate gene products encoded by homologous genes, even though the corresponding loci remained transcriptionally active. This suggested that the observed silencing was occurring at the posttranscriptional level, and was thus termed posttranscriptional gene silencing, or PTGS (Angell and Baulcombe, 1997; Baulcombe, 1996; Carr and Zaitlin, 1991; Metzclaff et al., 1997; Ratcliff, 1997; Ruiz, 1998). At this time, however, it remained a matter of debate as to whether it was a DNA- or RNA-based molecule that was directing the observed posttranscriptional regulation (reviewed by Baulcombe and English, 1996).

1.3 Antisense RNAs in animals

By the mid-1990s, the use of antisense RNA as a tool to repress complementary gene expression was commonplace in animal research, but an understanding of the molecular mechanism(s) that led to this repression remained unknown (Nellen and Lichtenstein, 1993). It was well-established that natural antisense RNAs – endogenous transcripts with sequences complementary to sense transcripts – were widely distributed amongst prokaryote genomes, and that they controlled numerous biological functions, including transposition, plasmid replication and regulation of gene expression (reviewed by Wagner and Simons, 1994). Moreover, in eukaryotes, additional evidence of natural antisense RNAs strongly suggested that antisense RNA was part of a general, evolutionary-conserved mechanism for the control of gene expression, as opposed to solely acting as a defence mechanism against invading exogenous nucleic acids (Vanhée-Brossollet and Vaquero, 1998).

1.4 dsRNA: the trigger of RNA silencing

The breakthrough that has enabled our current understanding of RNA silencing as a widespread eukaryote gene expression regulatory mechanism came in the year 1998. Fire et al. (1998) demonstrated that dsRNA was the sole trigger required to initiate RNA silencing. The authors reported highly robust and specific RNA silencing of complementary genes that was readily and reproducibly achievable following the injection of dsRNA into the nematode *Caenorhabditis elegans* (*C. elegans*). The gene silencing by dsRNA-triggered RNA silencing was, hence, termed RNA interference (RNAi). Interestingly, this discovery was inspired by the puzzling observation that sense and antisense RNA are equally effective in RNA silencing (Guo and Kemphues, 1995). The paradox was resolved by showing that the preparations of sense and antisense RNA contained small amounts of dsRNA, enough to trigger RNA silencing (Fire et al., 1998). Therefore, the authors concluded that the observed RNA silencing was likely a consequence of dsRNA formation in the cell.

By the mid 1990s, an understanding of the molecular mechanisms of RNA silencing in plants had already started to form. The identification and characterisation of a tomato RNA-DEPENDENT RNA POLYMERASE (RDR) (Schiebel et al., 1993) led to the hypothesis that the role of RDRs was to transcribe complementary RNAs (cRNAs) from transgene-encoded transcripts (Baulcombe, 1996). The RDR-transcribed cRNA could hybridise with a corresponding target RNA to form a hybrid substrate for dsRNA-specific RNases, leading to the arrest of translation (Baulcombe, 1996; Waterhouse et al., 1998). In this context, the breakthrough demonstration in plants was provided by Waterhouse et al. (1998), showing that PTGS is also induced by a dsRNA trigger. In the same year that the Fire and Waterhouse studies were published, molecules of dsRNA were shown to also be effective triggers of RNA silencing in other organisms, such as flies (Kennerdell and Carthew, 1998) and protozoa (Ngô et al., 1998).

1.5 The discovery of small-interfering RNAs (siRNAs)

Although dsRNA was rapidly established as the trigger for eukaryote RNA silencing, the molecular mechanisms that led to the repression of gene expression remained to be determined. The first definitive piece of this puzzle came from plants: the identification of small-interfering RNAs (siRNAs). Hamilton and Baulcombe (1999) showed that transgene-

or virus-induced PTGS resulted in the accumulation of small RNA (sRNA) molecules of an approximately uniform length of 25 nucleotides (nt). Furthermore, the authors went on to show that the level of 25 nt sRNA accumulation tightly correlated with the degree of RNA silencing. However, it remained uncertain whether these 25 nt sRNAs were responsible for directing the observed silencing itself, or whether they were just byproducts resulting from the RNA silencing process. Long molecules of dsRNA were later shown to be processed into a population of 21–23 nt sRNAs *in vitro*, and targeted mRNA was only cleaved in regions complementary to the triggering dsRNA (Zamore et al., 2000). Moreover, the mRNA was cleaved at approximate 21–23 nt intervals, the same size as the detected sRNAs. These findings suggested that sRNAs, or siRNAs, derived from processing of the triggering dsRNA, were able to direct cleavage of complementary mRNAs. Several subsequent studies revealed siRNA-directed repression of gene expression across eukaryotes (Elbashir et al., 2001a; Parrish et al., 2000; Wianny and Zernicka-Goetz, 2000).

1.6 RNA-dependent RNA polymerases unites the kingdoms

The first cellular component required for siRNA-directed RNA silencing was identified in a screen for mutants defective in transgene-induced RNA silencing in the filamentous fungus *Neurospora crassa*, with the identified mutants termed *quelling-defective* (*qde*) (Cogoni and Macino, 1997, 1999). The gene product encoded by *QDE1* (the mutated locus in the *qde1* mutant background) was found to be similar to the previously characterised RDR in tomato (Cogoni and Macino, 1999). Furthermore, the silencing-impaired *C. elegans* and *Arabidopsis thaliana* (Arabidopsis) mutants *ego-1* and *sgs2/sde1*, respectively, were also determined to harbour mutations in genes encoding orthologs of the tomato RDR (Dalmay et al., 2000; Mourrain et al., 2000; Smardon et al., 2000). The identification of RDR orthologs as conserved components in the RNA silencing pathways provided experimental evidence for the previously proposed model based on RDR-catalysed cRNA production (Baulcombe, 1996; Waterhouse et al., 1998). More importantly, RDR gene identification across eukaryotes established that PTGS and RNAi phenomena were mechanistically related (Cogoni and Macino, 2000). The RDR-based model did, however, raise three major questions: (i) Are RDRs necessary to produce large molecules of dsRNA from aberrant single-stranded RNA (ssRNA) templates? (ii) How are long dsRNA molecules processed into siRNAs (siRNA biogenesis)? and (iii) How are siRNAs effective in repressing gene expression (siRNA activity).

In plants, the demonstration that the RDR, SDE1/SGS2, produces dsRNA using the targeted RNA as a template, also revealed spreading of the siRNA silencing signal from the original target site of the triggering dsRNA into adjacent 5' and 3' regions (Vaistij et al., 2002). This research also further identified RDRs as central components of siRNA-directed RNA silencing mechanisms across diverse species.

1.7 siRNA biogenesis: Dicer proteins

Bernstein et al. (2001) showed in an elegant experiment that siRNA production, and siRNA action, are separate processes and that a RNase III-like endonuclease is required for siRNA production from the dsRNA trigger. The authors applied differential centrifugation to show that the activity of the previously identified RISC (Hammond et al., 2000) and the siRNA generating enzyme of the same RNA silencing pathway did not co-fractionate. Therefore, a nuclease specific for processing of the triggering dsRNA, such as an RNase III endonuclease, was suggested to be a central requirement for dsRNA processing and siRNA production. The *Drosophila melanogaster* (Drosophila) RNase III CG4792 was demonstrated to produce siRNA guide sequences of approximately 22 nt in length from much longer, almost perfectly dsRNA triggers. Due to the ability of CG4792 to 'dice up' the dsRNA trigger into siRNAs, CG4792 was renamed Dicer (Bernstein et al., 2001). Dicer was subsequently shown to be evolutionarily conserved across several eukaryote species, including Arabidopsis (*SIN1/SUS1/CAF*), *C. elegans* (K12H4.8) and mammals (Helicase-MOI) (Bernstein et al., 2001). In the tale of the blind men and an elephant, a group of blind men touch an elephant to learn what it is like, but each one feels a different and unique part in such a way that they come to different conclusions as to the nature of an elephant. This tale vividly describes the identification of a Dicer homolog in Arabidopsis (Schauer et al., 2002). The *SHORT INTEGUMENTS1* (*SIN1*), *SUSPENSORI* (*SUS1*) and *CARPEL FACTORY* (*CAF*) alleles had been previously extensively studied in embryo, ovule and flower development, respectively, as individual loci thought to encode different proteins (Errampalli et al., 1991; Jacobsen et al., 1999; Robinson-Beers et al., 1992). However, it was later determined that *SIN1/SUS1/CAF* were all mutant alleles of a single locus encoding a RNase III-like endonuclease similar to the *Drosophila* Dicer protein, and that this locus was therefore renamed *DICER-LIKE1* (*DCL1*) (Finnegan et al., 2003; Golden et al., 2002).

Dicer proteins often belong to multimember families, with each family member characterized by RNase III, PAZ, RNA helicase and dsRNA binding domains. For example, the Arabidopsis genome encodes four Dicer proteins, DCL1 to DCL4, which differ in the size of the protein and the presence and organization of each functional domain (Schauer et al., 2002). The diversity in sRNA biogenesis proteins in Arabidopsis suggested that the dsRNAs processed, as well as the resulting sRNA species produced, act through multiple parallel RNA silencing pathways. The first experimental evidence that Dicer proteins have distinct roles in RNA silencing was obtained in an study on Arabidopsis where DCL1 was shown to not be an essential protein component for PTGS or siRNA production (Finnegan et al., 2003).

1.8 sRNA activity: Argonaute proteins

The core protein component of the siRNA effector complex RISC was revealed via a biochemical approach. A *Drosophila* ribonucleoprotein complex (~500 kDa) with RISC activity was purified and micro-sequenced to reveal the presence of an AGO protein (Hammond et al., 2001). However, the first AGO to be isolated was Arabidopsis AGO1. As outlined for Arabidopsis DCL1, the Arabidopsis AGO1 gene was initially identified via a mutagenesis screening, and was named after the appearance that resembles the molluscs known as argonaut (a group of pelagic octopuses) (Bohmert et al., 1998). Although, members of the AGO protein family had been shown to affect the dsRNA response in *Neurospora* (QDE-1), *C. elegans* (RDE-1) and Arabidopsis (AGO1) (Fagard et al., 2000; Macino et al., 2000; Tabara et al., 1999), the 'slicer' activity of an AGO protein was not realised until after the crystal structure of the *Pyrococcus furiosus* AGO protein was resolved (Song et al., 2004) and an extensive mutational analysis of human *Ago2* had been performed (Liu et al., 2004).

AGO family members are characterised by the presence of three conserved functional domains, namely the PAZ (similar to Dicer), MID and PIWI domains. Arabidopsis and human genomes are known to encode ten and four AGO proteins, respectively, indicating large functional diversification of the action stage of the parallel RNA silencing pathways in eukaryotes (Song et al., 2004). Indeed, by the time AGO's slicer activity had been experimentally validated, Dicer and AGO mutant characterisation had already revealed that sRNA-directed RNA silencing was central to a diverse array of biological processes (reviewed by Carmell et al., 2002).

1.9 miRNAs: more nodes to the network

The *C. elegans lin-4* RNA is recognised as the founding member of an extensive and highly specific class of small regulatory RNAs, termed microRNAs (miRNAs) (Bartel, 2004). Curiously, the approximately 22 nt *lin-4* (Lee et al., 1993) and *let-7* (Reinhart et al., 2000; Slack et al., 2000) sRNAs had been studied as the only two examples of small temporal RNA (stRNA) products for almost a decade until the identification of over one hundred stem loop-structured RNAs that, upon Dicer cleavage, generate 21 to 24 nt non-coding small regulatory RNAs similar to stRNAs, which were later collectively called miRNAs (Lagos-Quintana et al., 2001; Lau et al., 2001; Lee and Ambros, 2001). miRNAs have been shown to be evolutionary conserved, similar to the *lin-4* and *let-7* stRNAs, and are typically (i) derived from independent transcriptional units; (ii) processed from stem loop precursor RNAs by Dicers, and (iii) able to regulate the expression of a large set of genes via RISC-mediated mechanisms (reviewed by Bartel, 2004).

In contrast to siRNAs, miRNAs do not trigger the amplification and spreading of secondary silencing signals via the activity of an RDR (Lagos-Quintana et al., 2001; Lau et al., 2001; Lee and Ambros, 2001). Furthermore, miRNA-directed RNA silencing was initially shown to lead exclusively to translation repression of the targeted transcript in animals, and to solely mediate RNA silencing via a mRNA cleavage-based mechanism in plants (Llave et al., 2002; Tang et al., 2003). In animals and flies, siRNA- and miRNA-loaded RISC, termed siRISC and miRISC, have different complementarity requirements for target transcript recognition. siRISC recognises and regulates the expression of target transcripts that harbour target sequences with high complementarity to the loaded siRNA. miRISC target regulation, on the other hand, has been shown to be based on low miRNA:mRNA complementarity requirements (Elbashir et al., 2001a, 2001b). Furthermore, it has since been demonstrated that mammalian miRNAs bearing high complementarity to their targeted transcript(s) also guide mRNA cleavage and, conversely, that exogenously supplied siRNAs can inhibit the expression of lowly complementary mRNAs without inducing any detectable transcript cleavage (Doench et al., 2003; Zeng et al., 2003). It is now known that the AGO protein, assembled with either a miRNA or siRNA, determines which mechanism of RNA silencing the loaded sRNA will direct in animals and insects (Filipowicz et al., 2005).

Plant miRNAs were initially thought to act through a mechanism similar to siRNAs, because of the extensive miRNA:mRNA base pairing requirement (Tang et al., 2003). However, the authors concluded that plant miRNAs, since they lacked RdRP-dependent amplification and

spreading steps, act through a similar mechanism to that in animals and insects. Nevertheless, it was widely accepted by the plant sRNA research community at this time that AGO1, at the catalytic core of plant miRISCs, was mechanistically similar to cleavage-competent human Ago2, as opposed to directing translation inhibition (Filipowicz et al., 2005; Tang et al., 2003). This paradigm that plant miRNAs direct only transcript cleavage was initially challenged by Xuemei Chen's work on the Arabidopsis miR172-*AP2* silencing module. miR172 was shown to regulate the expression of its targeted gene, *APETELA2* (*AP2*), predominantly via translation repression (Chen, 2004a). Later, other workers demonstrated that translation repression is a widespread silencing mechanism directed by either miRNAs or siRNAs (Brodersen et al., 2008). It is currently well established that plant miRNAs can act through either transcript cleavage or translation repression. It is interesting to note that, although RDRs were the first cellular component to exhibit the evolutionary conservation of RNA silencing, the demonstration that miRNAs act independently of RDR activity in plants was also responsible for setting apart the plant miRNA pathway from those of other organisms. It is therefore not surprising that plant miRNA-guided translation repression had been discounted for many years.

1.10 Hitting hard with plant miRNAs

In plants, RNA silencing has been artificially achieved since the early 1990s via the introduction of exogenous sequences into their genome through the use of modified *Agrobacterium* transfer-DNA (T-DNA) expression vectors. Initially, PTGS was achieved via the use of T-DNA constructs encoding either antisense (Hamilton et al., 1990) or co-suppression RNAs (Jorgensen, 1995). However, such an approach typically resulted in a low efficiency of silenced individuals within generated transformant populations. The identification of dsRNA-triggered PTGS led to the subsequent development of much more powerful tools that offered almost 100% PTGS efficiency via the introduction of T-DNA constructs encoding hairpin RNAs (hpRNAs) (Chuang and Meyerowitz, 2000; Wesley et al., 2001). More recently, the expression of modified miRNA stem loop precursor transcripts, which incorporate artificial miRNA (amiRNA) sequences targeting genes of interest, has enabled the silencing of highly specific target genes (Schwab et al., 2006).

To date, the over-expression of endogenous miRNA precursor transcripts has been widely documented to be a useful tool for the characterisation of native miRNA target genes and to

study the effects of miRNA mis-expression (Llave et al., 2002). Conversely, studying the consequences of miRNA target gene mis-expression has been largely achieved via expression of endogenous miRNA target genes harbouring silent mutations within the miRNA binding site (Baker et al., 2005; Mallory et al., 2005). More recently, via an indirect approach, the over-expression of non-cleavable miRNA target mimic sequences, to either sequester (Franco-Zorrilla et al., 2007) or completely degrade (Yan et al., 2012a) the regulating endogenous miRNA, has been used to study miRNA/mRNA target interactions *in vivo*. In contrast to animal miRNAs, the requirement of plant miRNAs for extensive base pairing to their target mRNA(s) has enabled such a specific transgene-based approach for the determination of their biological function. Together, these approaches have revealed that plant miRNAs play an important role throughout plant development (Rubio-Somoza and Weigel, 2011), as well as to mediate tolerance or adaptation responses to biotic and abiotic stress (Ding et al., 2013; Khraiwesh and Zhu, 2012; Sunkar et al., 2012). Therefore, plant miRNAs are obvious targets for molecular modification of plants to increase current crop yield and improve food security (Li et al., 2013a). Indeed, several successful examples of biotechnological applications of amiRNAs have been reported (reviewed by Khraiwesh et al., 2012).

Chapter 2 – miRNA biogenesis and activity

2.1 miRNA biogenesis

Eukaryotes have evolved a diverse and complex set of miRNA-guided gene expression inhibition pathways (Ameres and Zamore, 2013; Chang et al., 2012; Rogers and Chen, 2013). In the canonical miRNA pathway (Figure 2-1), primary miRNA transcripts (pri-miRNA) are transcribed by RNA polymerase II (Pol II) to produce non-coding RNAs with mRNA-like features, including a 5'-7-methylguanosine (m⁷G) cap and 3'-poly(A) tail. Due to partial self-complementarity, pri-miRNAs fold to form stem-loop structures that are cleaved in the nucleus to produce smaller sized precursor miRNA (pre-miRNA) intermediate molecules. This cleavage is performed by a Dicer protein, assisted by a dsRNA-BINDING (DRB) protein. Such protein partnerships include Drosha/DGCR8 in mammals, Drosha/Pasha in flies, and DICER-LIKE1 (DCL1)/DRB1 in plants (Gregory et al., 2004; Kurihara and Watanabe, 2004; Landthaler et al., 2004). In mammals and flies, the pre-miRNA is exported to the cytoplasm and further processed into a miRNA/miRNA* duplex by a second Dicer/DRB partnership, the Dicer/TRBP and Dicer-1/Loqs interaction, respectively (Bernstein et al., 2001; Hutvagner et al., 2001; Lee et al., 2004). In plants, both the pri-miRNA and pre-miRNA precursor processing steps occur in the nucleus, in specialised nuclear bodies termed 'dicing bodies' or D-bodies, and only require the single DCL1/DRB1 protein partnership (Kurihara and Watanabe, 2004). The resulting miRNA/miRNA* duplex is then loaded by an AGO protein that, in mammals and flies, removes the miRNA* passenger strand (via AGO-catalysed endonucleolytic cleavage), resulting in an active miRISC (Czech and Hannon, 2010). In plants, however, the exact mechanism by which the miRNA is selected for miRISC incorporation over the corresponding miRNA* strand remains unknown, although the preferential selection and AGO loading of the miRNA guide strand has been shown to be directed by DRB1 (also called HYL1) (Eamens et al., 2009). Figure 2-1 outlines the core protein machinery components of the canonical miRNA pathways of animals, flies and plants.

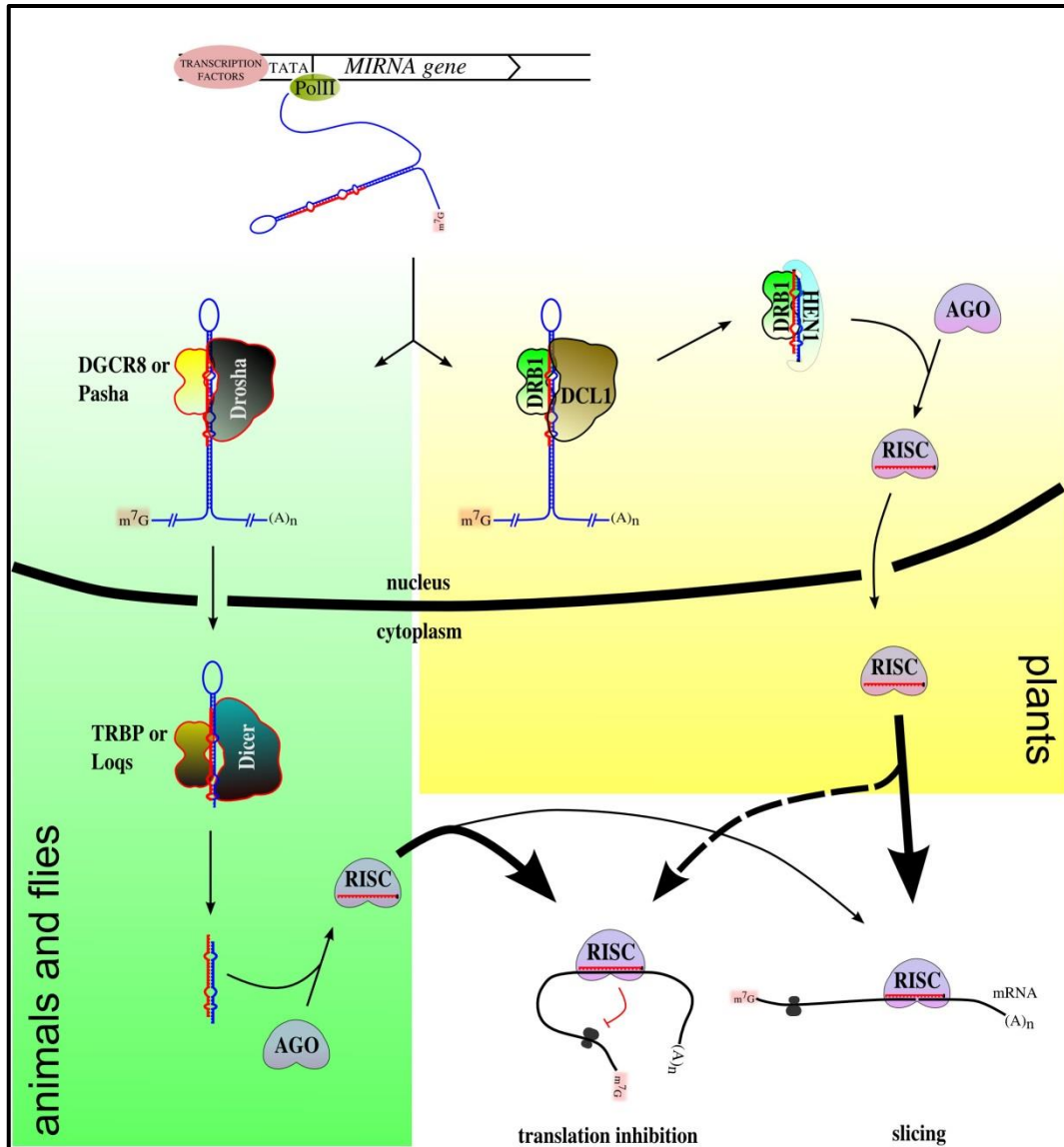


Figure 2-1. miRNA biogenesis and activity.

Primary miRNA transcripts (pri-miRNA) are transcribed from MIR genes by Pol II. In animals and insects (left, green), the pri-miRNA is processed into the pre-miRNA by Droscha/Pasha and exported to the cytoplasm where it is further processed into the miRNA/miRNA* duplex by Dicer/Loqs. The mature miRNA is loaded by AGO forming miRISC, and miRISC uses the loaded sRNA to direct a translation inhibition mechanism of RNA silencing. In plants (right, yellow), DCL1/DRB1 mediate the processing steps of pri-miRNA to pre-miRNA, and pre-miRNA to miRNA/miRNA* duplex. Following DRB1-directed miRNA guide strand loading into miRISC, miRISC can regulate miRNA target gene expression via either an mRNA cleavage or translational repression mode of RNA silencing.

2.1.1 miRNA biogenesis and RISC assembly in plants: components required

Our knowledge of miRNA biogenesis in plants has advanced greatly in recent years. Table 2-1 summarises the role(s) of the core protein machinery components (DCL1, DRB1 and SE) as well as the more recently identified components experimentally demonstrated to play a role in the Arabidopsis miRNA pathway. Supporting Table 2-1, Figure 2-2 provides a schematic of the stage(s), miRNA biogenesis or RISC assembly, at which each of the identified proteins is potentially acting. It is important to note that, although we still do not have a complete understanding of the functional intricacies of the Arabidopsis miRNA pathway, the proposed model presented in Figure 2-2 is based on experimental protein-protein interaction studies, and is as accurate as current knowledge permits.

Table 2-1. Proteins required for miRNA biogenesis and RISC assembly.

Protein	Protein function	Interaction ¹	Reference ²
miRNA biogenesis			
DCL1	RNaseIII activity; processing of pri- and pre-miRNA; required for miRNA accumulation	DRB1, SE, TGH, NOT2, DDL, CBP20, CDC5	(Finnegan et al., 2003; Kurihara et al., 2006)
DRB1/HYL1	Binds dsRNA; promotes accuracy of pri- and pre-miRNA processing; required for miRNA accumulation; required for selective loading of mature miRNA into AGO1	DCL1, SE, TGH	(Dong et al., 2008; Han et al., 2004)
SE	Binds pri-miRNA; promotes accuracy of pri- and pre-miRNA processing; required for miRNA accumulation; required for mRNA splicing	DCL1, DRB1, CPL1, TGH, NOT2, CBP20, RACK1, CDC5	(Christie and Carroll, 2011; Dong et al., 2008; Lobbes et al., 2006)
PollI	Required for MIRNA transcription	Mediator, NOT2, CDC5	(Kawashima et al., 2009)
Mediator	Required for MIRNA transcription	PollI	(Kim et al., 2011)
DDL	Required for pri-miRNA and miRNA accumulation	DCL1	
CBP20	Required for pri-miRNA processing and miRNA accumulation; form the cap-binding complex (CBC) required for splicing of first intron	CBP80, DCL1, SE, NOT2	(Laubinger et al., 2008; Raczynska et al., 2010)
CBP80/ABH1	Required for pri-miRNA processing and miRNA accumulation; form the cap-binding complex (CBC) required for splicing of first intron	CBP20, NOT2	(Laubinger et al., 2008; Raczynska et al., 2010)
TGH	Binds ssRNA; enhances pri-miRNA processing by DCL1; required for miRNA and siRNA accumulation; required for proper DRB1-pri-miRNA interaction; strong genetic interaction with AMP1	DCL1, DRB1, SE	(Calderon-villalobos et al., 2005; Ren et al., 2012)
CPL1	Dephosphorylation of DRB1; required for accurate processing, miRNA accumulation and strand selection (indirect)	SE	(Manavella et al., 2012)
DRB2	Binds dsRNA; required for miRNA accumulation	DCL1, DRB1	(Eamens et al., 2012)
MOS2	Binds pri-miRNA and required for miRNA accumulation; required for proper DRB1-pri-miRNA interaction and DRB1 localization in D-bodies	NA	(Wu et al., 2013)
NOT2	Required for DCL1 localization in the D-bodies; interacts with PollI and is required for efficient transcription of both MIR and protein coding genes	PollI, DCL1, CBP20/80, SE	(Wang et al., 2013)
RACK1	Required for pri-miRNA processing and miRNA accumulation; might be required for miRNA-guided transcript translational inhibition	SE, AGO1	(Speth et al., 2013)
SIC	Required for pri-miRNA processing and miRNA accumulation; co-localizes with DRB1 in D-bodies; required for splicing of mRNA	NA	(Zhan et al., 2012)
STA1	Required for pri-miRNA processing and miRNA accumulation; required for splicing of mRNA	NA	(Ben Chaabane et al., 2013)
CDC5	Required for MIRNA transcription; pri-miRNA processing	PollI, DCL1, SE	(Zhang et al., 2013)
RISC assemble			
HSP70	Required for RISC assemble	AGO1	(Iki et al., 2012)
HSP90	Required for RISC assemble	AGO1, CYP40/SQN	(Iki et al., 2010, 2012)
CYP40/SQN	Required for RISC assemble	AGO1, HSP90	
SDA2/EMA1	Negative regulator of RISC assemble	NA	(Wang et al., 2011)
PP5/TPR	Negative regulator of RISC assemble	AGO1, HSP90	(Iki et al., 2012)

¹ Reference is provided accordingly to non-core proteins, except for the core proteins (DCL1, DRB1 and SE). Not available (NA).

² Refers to protein function and protein interaction (see above).

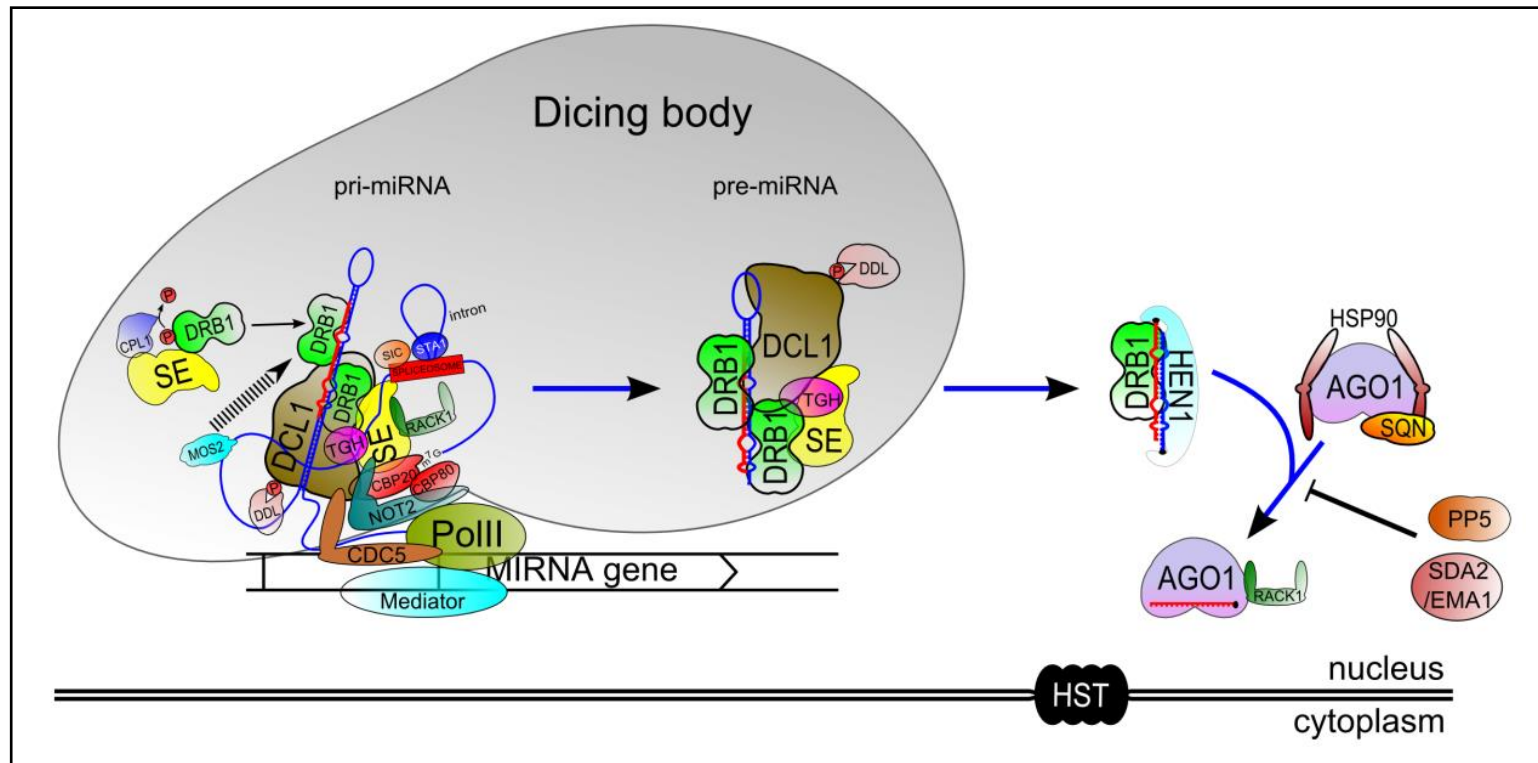


Figure 2-2. Schematic representation of miRNA biogenesis and RISC assemble.

It has been extensively documented that Pol II is responsible for transcription of the pri-miRNA precursor transcripts from MIR loci. In dicing bodies (D-bodies), pri-miRNA is processed into a pre-miRNA intermediate molecule, and subsequently into the miRNA/miRNA* duplex by DCL1/DRB1. DRB1 is then required for the preferential selection of the miRNA guide strand over the miRNA* passenger strand for miRNA loading into AGO1 to form the catalytic core of Arabidopsis miRISC. The placement of the other proteins represented in this schematic is based on experimentally validated protein-protein interaction studies, and this information has been used for the basis of construction of the above proposed miRNA pathway model.

2.1.2 microRNA biogenesis in plants: still a sea of possibilities

Although our knowledge of the biogenesis and mode of action of plant miRNAs has improved dramatically in recent years, several of the latest findings indicate that some important mechanisms remain poorly characterised. The biogenesis of miRNA/miRNA* from miRNA-containing intermediates occurs in D-bodies, and a growing number of proteins, in addition to well characterized core components, have been demonstrated to be also required at this stage of the miRNA pathway (reviewed by Rogers and Chen, 2013). Only in the past few years have approximately half of the known proteins required for D-body assembly and/or function been identified, including TOUGH (TGH), C-TERMINAL DOMAIN PHOSPHATASE-LIKE1 (CPL1), DRB2, DAWDLE (DDL), MODIFIER OF SNC1, 2 (MOS2), NEGATIVE ON TATA LESS2b (NOT2b), RECEPTOR FOR ACTIVATED C KINASE 1 (RACK1), SICKLE (SIC), STABILIZED1 (STA1) and CELL DIVISION CYCLE5 (CDC5) (Table 2-1). In fact, our knowledge of miRNA biogenesis is still largely restricted to the function of the core proteins DCL1, DRB and SE (Lobbes et al., 2006; Vazquez et al., 2004). Moreover, forward genetics (Manavella et al., 2012), and to a lesser extent, yeast two-hybrid protein-protein interaction screens (Speth et al., 2013), are the only approaches currently used to discover novel genes relevant to miRNA biogenesis.

The recent identification of new proteins required for miRNA biogenesis suggests that this process is more complex and dynamic than previously thought. For example, NOT2b-Pol II interaction is required for efficient transcription of both protein-coding and non-coding gene transcripts, as well as to mediate the connection of *MIR* gene transcripts to core miRNA biogenesis protein machinery, including DCL1 and SE (Wang et al., 2013). The *not2a not2b* (*not2a2b*) double mutant has reduced pri-miRNA expression and mature miRNA accumulation. Furthermore, in *not2a2b* plants, DCL1 localisation, but not the localisation of DRB1, is affected in D-bodies, suggesting that D-body assembly is independent of DCL1. Interestingly, in the *mos2* mutant, DRB1 fails to localise to D-bodies, but MOS2 does not interact with the core proteins DRB1, DCL1 or SE (Wu et al., 2013). However, the pri-miRNA binding affinity of DRB1, and hence pri-miRNA processing, were greatly reduced in the *mos2* mutant background. These findings led the authors to propose that the function of MOS2 is to facilitate pri-miRNA recruitment to the D-body, and that MOS2-recruited pri-miRNAs might act as scaffolding proteins for D-body formation.

CPL1 and DDL have also recently been shown to play a role in miRNA biogenesis, and their functions add another level of complexity to this silencing pathway. The identification of CPL1 revealed that DRB1 is inactive when phosphorylated, requiring CPL1 activity for its dephosphorylation and subsequent activation (Manavella et al., 2012). However, the kinase responsible for DRB1 phosphorylation remains unknown and, more importantly, the biological significance of having a pool of inactive, phosphorylated, DRB1 is still unclear. Hyperphosphorylated DRB1 was readily detectable in cellular lysates, leading the authors to speculate that there is a substantial reservoir of inactive DRB1 that can be dephosphorylated and activated when required, for instance to mediate developmentally-important processes, such as seed germination (Manavella et al., 2012). DDL is required in miRNA biogenesis to bind pri-miRNAs and to interact with phosphorylated DCL1 (Engelsberger and Schulze, 2012; Machida and Yuan, 2013; Yu et al., 2008a). Interestingly, *DDL* encodes a phosphothreonine binding forkhead-associated (FHA) domain, a domain often encoded by proteins that function in signal transduction pathways (Machida and Yuan, 2013). The SMAD signal transducer, which is structurally similar to DDL (Machida and Yuan, 2013), has been demonstrated to integrate the miRNA biogenesis and signal transduction pathways in humans (Davis et al., 2008). SMAD is recruited to pri-miRNA processing complexes and controls the vascular smooth muscle cell phenotype mediated by the bone morphogenetic protein (BMP) family of human growth factors. Due to their structural similarities, it is possible that DDL, like human SMAD, plays a role in integrating the miRNA biogenesis and signal transduction pathways (Machida and Yuan, 2013). However, to date, no experimental evidence exists to support this proposed role for DDL in plants.

2.1.3 miRNA biogenesis in plants: role of DRB proteins

In animals, miRNAs are processed from their precursor transcripts, pri-miRNA and pre-miRNA, via a sequential two-step process in different cellular compartments. On the other hand, the vast majority of plant miRNAs require DRB1-assisted DCL1 activity for their nuclear production (Eamens et al., 2009; Eamens et al., 2012; Vazquez et al., 2004). DRB1 is a highly characterised DCL1 partner protein, and is required by DCL1 for accurate and efficient miRNA/miRNA* processing from larger sized precursor transcripts (Dong et al., 2008; Kurihara et al., 2006). Furthermore, DRB1 has been demonstrated to mediate an additional step in the Arabidopsis miRNA pathway, the preferential selection of miRNA

guide strands over its anti-sense paired sequence, the miRNA* strand, for loading into AGO1-catalysed miRISC (Eamens et al., 2009). More recently, DRB4, together with DCL4, has been shown to be required for the production of a small number of newly evolved miRNAs that are processed from precursor transcripts that, upon folding, form highly complementary stem loop structures (Pélissier et al., 2011; Rajagopalan et al., 2006). In addition, Eamens et al. (2012a) have shown that in the shoot apex and floral tissues, DRB2 is both synergistic and antagonistic to DRB1 in the biogenesis of different miRNAs. However, the exact role that DRB2 mediates in the miRNA pathway remains to be experimentally determined.

The dsRNA-binding domains (RBDs) are typically ~70 amino acids in length, have an $\alpha\beta\beta\alpha$ fold, and are found in most proteins that recognize dsRNA. However, RBD function is not limited to the recognition and binding of dsRNA, but also involves mediation of DRB protein-protein interactions (reviewed by Daniels and Gatignol, 2012). All plant DRB proteins characterised to date encode two amino-terminal RBDs, and the structure of both RBDs of Arabidopsis DRB1 has been determined (Yang et al., 2010). Surprisingly, DRB1 encodes both a canonical RBD (RBD1) and a non-canonical RBD (RBD2) (Figure 2-3).

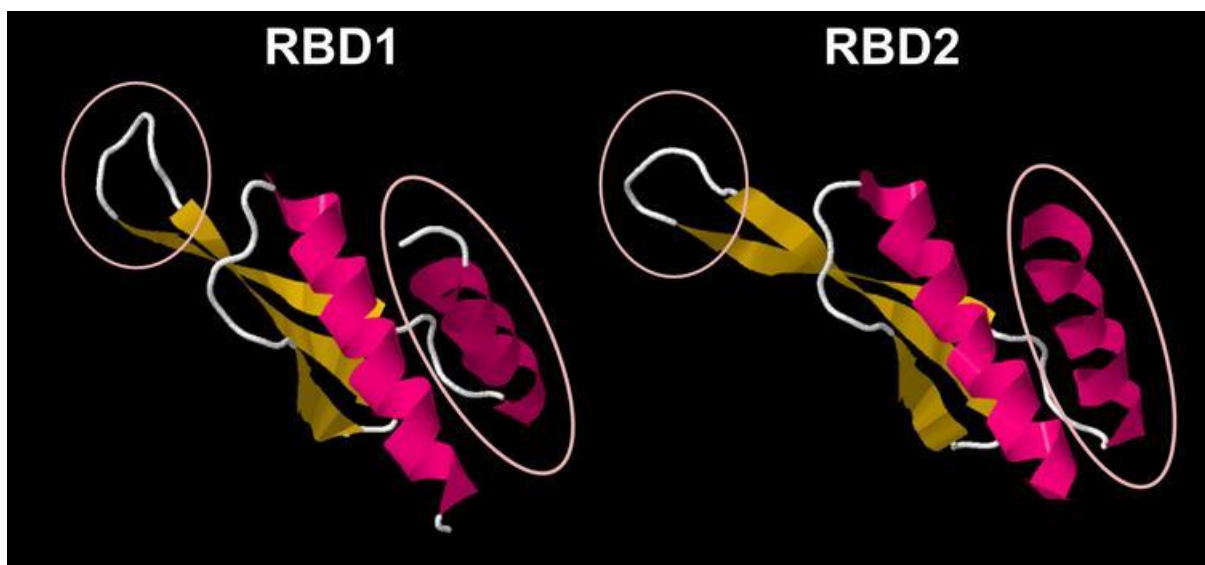


Figure 2-3. Secondary structure of RBD1 and RBD2 of Arabidopsis DRB1.

Structural differences between the canonical RBD1 (3ADJ) and non-canonical RBD2 (3ADG) domains of DRB1 are highlighted (circles).

RBD2 differs from the canonical structure in (i) the loop that recognizes dsRNA minor groove and (ii) the α -helices that recognize both major and minor groove. Both deviations are caused by different electrostatic potential and surface shape, resulting in drastic reduction in binding affinity for pre-miRNA and dsRNA. DRB1 has also been shown to recognise and bind 21 nt dsRNA as homodimer, and Yang et al. (2010) suggested that this may be mediated by the non-canonical structure of DRB1 RBD2. Amino acid sequence alignment of DRB1 and DRB2 RBDs (Figure 2-4) shows that the deviation in loop structure in DRB1 RBD2 appears to be highly conserved in DRB1 orthologs found in other plant species. Interestingly, although DRB2 is required in the miRNA biogenesis pathway (Eamens et al., 2012a), the lack of invariant histidine that defines the non-canonical DRB1 RBD2 is not observed (Figure 2-4).

2.2 miRNA activity

Animal and plant miRNAs have distinct mechanisms of target transcript recognition and expression regulation (Ameres and Zamore, 2013). In animals, the primary determinant for the binding of miRISC to the targeted mRNA(s) is a 6-8 nt domain at the 5' end of the RISC-loaded miRNA, termed the seed region. Furthermore, the vast majority of seed-matched target sequences are located in the 3' untranslated region (3'UTR) of the targeted mRNA(s) (Grimson et al., 2007). In animals, as a consequence of the low target homology requirements of miRNAs, a large number of unrelated genes are regulated by each miRNA (Friedman et al., 2009). The exact mechanism of miRNA-directed target gene expression regulation remains a topic of debate, but it appears to involve translation inhibition and mRNA decay, and to a lesser extent, endonuclease-catalysed mRNA cleavage (Baek et al., 2008; Guo et al., 2010). In contrast, plant miRNAs are highly complementary to their target mRNAs, and their respective target sites are usually located within the coding region of the targeted gene (German et al., 2008; Karginov et al., 2010). The high target complementarity requirements of plant miRNAs result in a small number of closely related target genes, usually a subset of genes belonging to a much larger gene family. Curiously, plant miRNAs can direct either a RISC-mediated endonucleolytic cleavage or translation inhibition to repress the expression of their target genes. Both of these mechanisms are independent of the degree of miRNA:mRNA base pairing or the position of the target site within the coding region of the targeted mRNA (Brodersen et al., 2008; Grant-Downton et al., 2013; Li et al., 2013b).

2.2.1 Transcript cleavage directed by plant miRNA

Argonautes, the RISC effector proteins, contain several functional domains, including PAZ, MID and PIWI (Mallory and Vaucheret, 2010). The MID and PAZ domains bind the 5'-monophosphorylated and 3'-nucleotide of the guide RNA, respectively, and the PIWI domain functions as the ribonucleolytic domain (Song et al., 2004). AGO slicer activity appears to be a three-step process (Wang et al., 2009). In the nucleation step, the 5' end of the miRNA binds to the 3' end of the miRNA target site of the mRNA. Nucleation is followed by the propagation step, characterised by rearrangement of AGO protein and extension of the miRNA:mRNA dsRNA hybrid. During propagation, PAZ domain rotation favours the correct positioning of the mRNA target site with respect to the catalytic PIWI domain. Once the mRNA target site is correctly positioned in AGO, the mRNA is cleaved at the phosphodiester

bond linking mRNA nucleotides opposite to miRNA positions 10 and 11 (Wang et al., 2009). The slicer role of Arabidopsis AGO1 in miRNA pathway is well documented; however several of the other nine Arabidopsis AGO proteins also encode a functional PAZ domain, and exhibit slicer activity, indicating that other AGOs may also perform a similar role to AGO1 in the miRNA pathway (Baumberger and Baulcombe, 2005; Carbonell et al., 2012). Interestingly, Carbonell et al. (2012) recently demonstrated that a mutated, slicer-defective AGO1 forms miRISC more efficiently with its targeted mRNA(s) than wild-type AGO1, indicating that a functional PAZ domain is not a requirement for miRISC target recognition in plants.

2.2.2 Translation inhibition directed by plant miRNA

In plants, miRNA activity has been almost exclusively assessed at the transcript level, while translation inhibition was assumed to be a less important mechanism of silencing operating via an alternative pathway (Rogers and Chen, 2013). However, rapidly growing evidence suggests that in specific plant tissues, such as floral tissues, translation inhibition, and not target mRNA slicing, is the predominant miRNA-directed silencing mechanism (Chen, 2004a; Grant-Downton et al., 2013). Furthermore, Li et al. recently showed that expression of amiRNAs in plants predominantly mediated highly specific translation repression and limited mRNA decay or cleavage (Li et al., 2013a). This finding has a direct impact on the design and evaluation of amiRNA efficacy in a biotechnological context, but it also reveals that translation inhibition has been largely underappreciated in plants.

Forward genetics has recently allowed identification of a number of novel genes required for miRNA-guided translation inhibition, including *KATANINI* (*KTNI*) (Brodersen et al., 2008), *VARICOSE* (*VCS*) (Brodersen et al., 2008), *ALTERED MERISTEM PROGRAM1* (*AMP1*) (Li et al., 2013b) and '*SHUTTLE*' IN CHINESE (*SUO*) (Yang et al., 2012). The encoded proteins appear to be required for either trafficking or localisation of miRISC, and/or for mRNA stability. *KTNI* encodes a microtubule severing enzyme required for the correct organisation of cortical microtubules (Burk et al., 2007), suggesting that the trafficking or assembly of the cellular components required for translation inhibition may require the microtubule network. The involvement of AMP1, an integral endoplasmic reticulum (ER) enzyme (Li et al., 2013b), in translation inhibition further shows that, post assembly, RISC is transported from the nucleus to specific cytoplasmic sites. Interestingly, AGO1 is essential for the slicing

activity of miRISC, and AGO1 activity has also been demonstrated to be required for miRNA-directed translation inhibition (Brodersen et al., 2008; Lanet et al., 2009). Taken together, these recent findings suggest that miRNA trafficking and miRNA complex assembly steps are crucial in the rewiring of AGO1 activity from slicer to repressor. The proteome landscape may determine the identity of additional proteins with which AGO1-catalysed miRISC interacts; these interactions in turn may mediate the ability of the complex to direct either mRNA cleavage or translation inhibition.

RACK1 orthologs are evolutionarily conserved and contain seven WD40- β -propeller domains. These domains have been shown to be involved in mediating simultaneous interactions with multiple proteins and hence allow RACK1 proteins to act as scaffolding proteins in large and dynamic protein complexes (Adams et al., 2011). Arabidopsis RACK1 was identified in a yeast two-hybrid screen that used SE as the bait. Subsequent analyses revealed that the *rack1* mutant accumulates less mature miRNA than in wild type plants (Speth et al., 2013), unlike the increased mature miRNA accumulation previously demonstrated in animal mutants of RACK1 orthologs (Jannot et al., 2011). The Arabidopsis RACK1 alters miRNA accumulation and activity via distinct mechanisms: (i) it is required for efficient and precise pri-miRNA processing, possibly via its interaction with SE, in miRNA biogenesis, and (ii) RACK1 is also part of the AGO1-catalysed miRISC, suggesting that RACK1 also has a role in miRNA activity (Speth et al., 2013). Although the exact role of RACK1 in the AGO1-catalysed miRISC remains unclear, RACK1 does not alter the slicer activity of AGO1. Also, in *rack1* mutants, miR398 targets CSD1, CSD2 and CCS showed increased protein accumulation without a corresponding transcript elevation, suggesting that RACK1 is involved in miR398-guided translational inhibition. However, miR398 accumulation is reduced in *rack1* mutants, which may directly explain the observed elevation in accumulation of miR398 target proteins (Speth et al., 2013). The role of RACK1 in both the biogenesis and action stages of the Arabidopsis miRNA pathway makes it experimentally challenging to assess its function only in relation to miRNA activity. Nonetheless, RACK1 is involved in protein translation in mammals and yeast (Ceci et al., 2003), and a recent report supports a similar role for Arabidopsis RACK1 (Guo et al., 2011). Hence, the observation that RACK1 scaffold protein is involved in both miRNA biogenesis and activity raises the possibility that RACK1 is required for miRISC trafficking from nucleus to the ER.

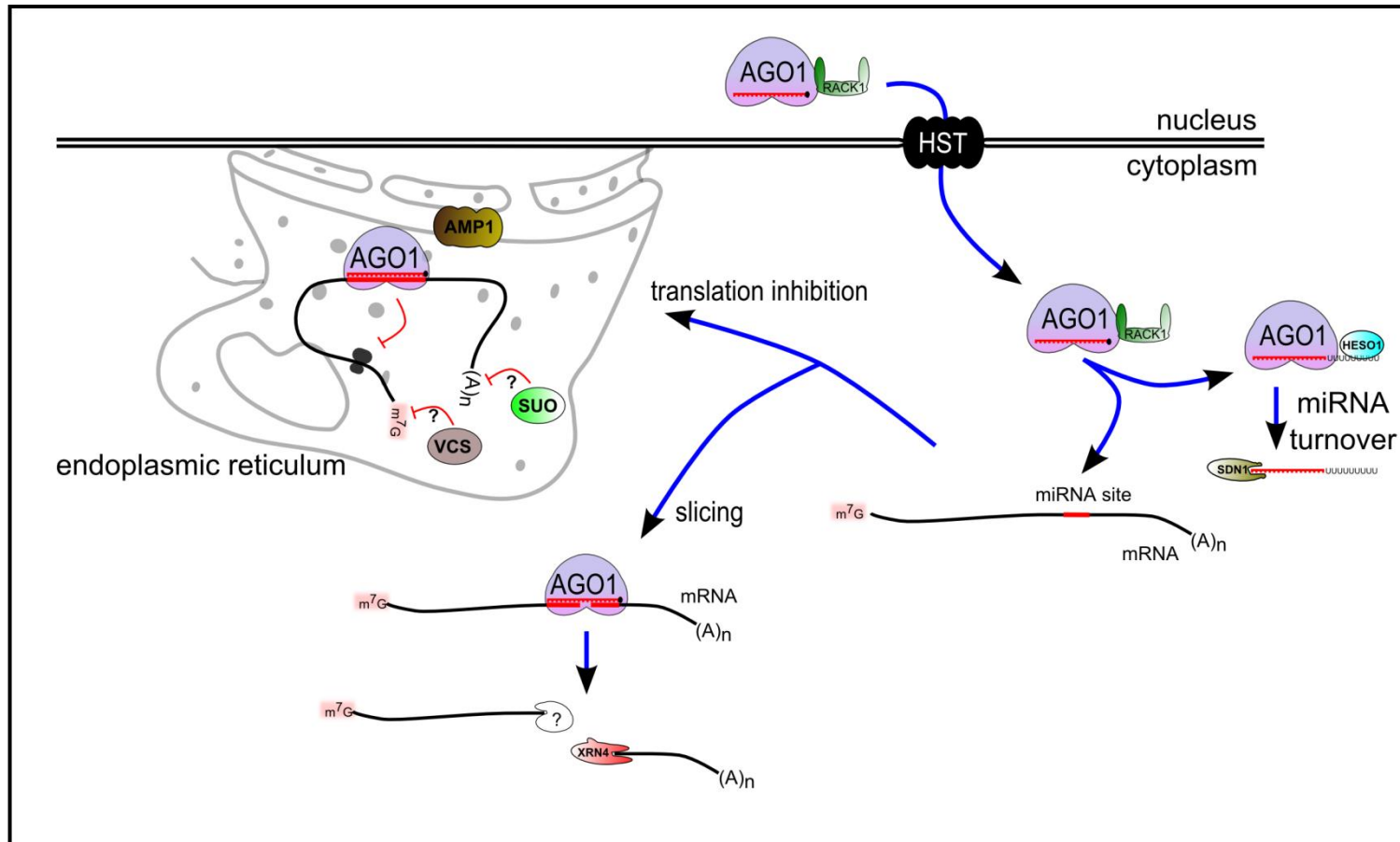


Figure 2-5. The action stage of the Arabidopsis miRNA pathway.

Following precursor transcript processing and miRISC assembly in the nucleus, the miRISC guides either an mRNA cleavage or translation inhibition mechanism of silencing to regulate the expression of miRNA target genes. All experimentally validated protein-protein interactions have been included.

2.2.3 Function of miRNA-guided translation inhibition: growing evidence

Although widely documented in animals, insects and (more recently) plants, the biological relevance of miRNA-guided translational inhibition, over that of transcript cleavage, remains largely unknown. A plant miRNA can guide either of these modes of action to control expression of a gene, thus providing an ideal model to study the biological relevance of translation inhibition and transcript cleavage.

In leguminous plants, the formation of nitrogen-fixing nodules (nodulation) upon bacterial infection is an important evolutionary adaptation to low nitrogen conditions (reviewed by Smith and Smith, 2011). More recently, this process in legumes has been shown to involve miRNA activity, including miR166 and miR169 (Boualem et al., 2008; Combier et al., 2006). Furthermore, Reynoso et al. (2013) demonstrated that the interaction of *Medicago truncatula* (a model legume) with *Sinorhizobium meliloti* results in the differential accumulation of miRNAs in polysomal complexes, and that this in turn leads to differential levels of miRNA target proteins. Enrichment of miRNAs, notably miRNAs miR169 and miR172, in the polysomes revealed their association with translation machinery. Interestingly, upon infection, accumulation of miR169 is reduced in polysomal complexes and, as a consequence, the level of the miR169 target protein, HAP2-1 is elevated. The authors proposed that reduced miR169 polysome accumulation may contribute to translation de-repression of HAP2-1 mRNA immediately following inoculation with *S. meliloti*. miR169-guided HAP2-1 cleavage precedes its translational de-repression, and may act to restrict the expression of HAP2-1 to nodule meristems for cell identity preservation (Reynoso et al., 2013).

The differential accumulation of miRNAs in polysomal complexes suggests that plants may actively control miRNA activity in order to either preserve or remove target mRNAs. Olivier Voinnet proposed that (i) miRNAs and siRNAs could operate primarily through transcript cleavage to produce irreversible gene expression changes required to establish permanent cell fates (e.g., during cell differentiation), or (ii) they could guide translational repression of sRNA target transcripts in a reversible manner, thus allowing the cell to still be able to respond rapidly to environmental challenges (Voinnet, 2009). Although the reversibility of translation repression can be intuitively understood, it has not been experimentally validated in plants. In animals, miRNAs induce gene silencing, with translational inhibition occurring first, which impairs the function of the eIF4F initiation complex, and being required for

subsequent mRNA destabilization (Meijer et al., 2013). However, animal and plant miRNAs are distinct in that plant miRNAs do not show very clear preference towards one mode of action, while the animal counterparts appear to act preferentially through translational repression. Thus, it is reasonable to argue that plant miRNAs guide two functionally different mechanisms to regulate the expression of their target genes.

Plants need to trigger a rapid response against non-beneficial infection. If reversibility is a predominant feature of miRNA action, miRNA- and/or siRNA-guided target transcript translation inhibition may have evolved in plants to confer adaptive advantages against pathogen infection. Reversible sRNA-directed silencing response would allow for the storage of sRNA target transcripts during periods of biotic or abiotic stress. The beneficial plant-bacterial interaction in nodule development in legumes (outlined above) supports such a proposed model. Furthermore, nucleotide-binding site leucine-rich repeat (NB-LRR) genes, a major plant resistance gene (R-gene) class, are required for the recognition of specific pathogens and are encoded by very large gene families in plant genomes (reviewed by Tobias and Guest, 2014). Recent reports have revealed that miRNAs, and a number of classes of siRNAs, are crucial regulators of NB-LRR gene expression in plants (Fei et al., 2013; Zhai et al., 2011). The biological relevance of a RNA silencing-based mechanism to regulate NB-LRR expression remains debated, but it has been shown to be a conserved regulatory mechanism in plants. Moreover, Lucas et al. (2014) have demonstrated that siRNA-directed NB-LRR gene expression regulation is not limited to target transcript cleavage. The authors showed that upon infection of *Brachypodium distachyon* with the fungus *Fusarium culmorum*, 31 miRNAs that were predicted to target NB-LRR genes had altered accumulation. However, the authors did not observe any change to the targets at the mRNA level, suggesting that translation inhibition may play a role in the regulation of R-genes NB-LRR.

**Chapter 3 – miRNA activity in the age
of systems biology**

Ideker et al. (2001) defined systems biology as “the study of biological systems by systematically perturbing them (biologically, genetically, or chemically); monitoring the gene, protein, and informational pathway responses; integrating these data; and ultimately, formulating mathematical models that describe the structure of the system and its response to individual perturbations”.

In this Chapter, the concepts of systems biology studies through protein-protein interaction network and network rewiring are presented. These concepts are further reviewed in the context of plant biology, and the incorporation of miRNAs and their biological effect are also discussed.

3.1 Plant and systems biology: still catching up

An important aspect of systems biology studies is the large-scale analysis of protein-protein interaction (PPI) networks, and their rewiring as consequence of a perturbation. An interaction network “simplifies” complex systems, summarizing them as components (nodes) and interactions (edges) between them (Vidal et al., 2011). This simplified approach applied to PPI has enabled discoveries that were not previously possible, such as large-scale identification of new candidate disease genes or modifier genes of known disease genes (Kemmeren et al., 2014; Lage et al., 2007; Sharma et al., 2013). Such discoveries were only possible because individual proteins and their interactions are analysed in the context of the entire system. The premise underlying this analysis is that phenotypic variations of an organism (e.g., a diseases) arise from perturbations of interactome networks (Vidal et al., 2011). In protein-protein interaction networks, nodes represent proteins and edges represent a physical interaction between two proteins. Currently, various methodologies are used to map PPIs, but two are in wide use for large-scale mapping: primarily yeast two-hybrid (Y2H) systems (Arabidopsis Interactome Mapping Consortium, 2011; Yu et al., 2008b), and isolation and identification of constituents of protein complexes using mass spectrometry (Guruharsha et al., 2011). Furthermore, genes and proteins act in concert in molecular interaction networks, such that gene expression, together with posttranscriptional modifications, defines the proteome landscape, which in turn controls the gene expression. Therefore, gene mutation or gain of function can alter the proteome landscape, rewiring the interaction network, as observed during evolution caused by gene duplication (Reece-Hoyes

et al., 2013). PPI network rewiring caused by gene mutation has proven informative particularly in cases where the gene is a regulator, such as a transcription factor (Kemmeren et al., 2014; Reece-Hoyes et al., 2013).

The knowledge of plant PPI network has greatly improved after the recent work of the Arabidopsis Interactome Mapping Consortium (Arabidopsis Interactome Mapping Consortium, 2011). Currently, BioGRID, the main repository for plant PPI datasets (Chatr-Aryamontri et al., 2013), combines the PPI data generated from 1,407 publications, and lists 17,162 non-redundant binary PPIs for 7,116 unique Arabidopsis proteins. For comparison, the human and yeast interactomes, which are the most extensively characterised, have ~157,000 and ~111,000 binary interactions reported, respectively (Wodak et al., 2013). Although it is still a relatively small database, the Arabidopsis interactome has been applied successfully to studies focusing on floral transition (He et al., 2010), the identification of protein interaction motifs (Leal Valentim et al., 2012), and the determination of mechanisms of transcription factor co-repression (Causier et al., 2012). Predicted interactomes have also been attempted in order to increase the coverage of the current plant PPI landscape (Cui et al., 2008; Geisler-Lee et al., 2007; Gu et al., 2011; Lee et al., 2010; Lin et al., 2011). Furthermore, the importance of biotic and abiotic stress to plants led to specialized interactomes, such as PPIs for Arabidopsis-pathogen (Mukhtar et al., 2011) and rice-abiotic/biotic stresses (Seo et al., 2011). Systems biology extends our knowledge beyond the long list of genes and proteins obtained with modern sequencing and proteomics methods to the functional whole plant. Hence, plant systems biology has the potential to provide additional, and a more detailed understanding of the regulatory networks controlling plant developmental, physiological and pathological processes.

miRNAs and other sRNAs play important roles in regulatory network wiring, and their action can alter target transcript or protein levels, but not necessarily both under a given condition (i.e. miRNA-guided transcript cleavage or translational inhibition). Therefore, a major challenge of plant systems biology is to combine genomics, proteomics and sRNA data to explain plant phenotypes.

3.2 Proteomics, just another “OMICS” to make sense of interactomes?

Interactomes are primarily built on screenings of binary PPIs and, therefore, do not reflect the complex and dynamic nature of cells and whole organisms. Thus, to integrate interactome

data to systems biology studies, the analysis of large-scale gene and protein accumulation is essential as they provide the biological context for an interactome. Next-generation sequencing (NGS) is likely to become a routine analysis in the near future, allowing the comparison of whole genomes and transcriptomes (Faino and Thomma, 2014). In parallel, recent advances in proteomics also provide an unprecedented ability to survey protein abundances (Mallick and Kuster, 2010). It has long been known that regulatory mechanisms translationally and posttranscriptionally regulate protein synthesis and control protein degradation. NGS and proteomics demonstrate a substantial role for these processes in controlling steady-state protein abundances, and intriguing results with non-steady-state (perturbed) systems revealed that our understanding of those regulatory mechanism is still incomplete (reviewed by Vogel and Marcotte, 2012).

NGS has a great dynamic range and can sequence and quantify virtually all nucleic acid species present within a sample. Recent advances in proteomics has allowed for a similar depth of analysis (Picotti et al., 2009). However, high-throughput proteome studies are still limited by relatively low dynamic range (Arsova et al., 2012a). A proteome map for Arabidopsis, generated for different organs, developmental stages, and undifferentiated cultured cells, provided evidence for ~13,000 proteins; while the total number of predicted genes was ~27,000 (Baerenfaller et al., 2008). Furthermore, contrary to genes and transcripts, proteins can undergo a much larger set of modifications that (i) might alter their function and (ii) can be analyzed by large-scale analysis. Proteomics, therefore, provides important pieces to the systems biology puzzle.

3.3 Quantitative proteomics in plants

Quantitative proteomics can be mass spectrometry (MS)-based or non-MS-based. Non-MS-based protein quantification often relies on comparative analysis of 2D-polyacrylamide gel electrophoresis (PAGE) gels (e.g., Differential in Gel Electrophoresis; DIGE), and it is limited by the resolution of the gel (Lei et al., 2005). Conversely, MS-based quantification is primarily limited by the accuracy of the mass spectrometer and can be performed using label-free or metabolic labeled samples (Arsova et al., 2012a). The label-free approach is suitable for tissues that are difficult or expensive to metabolically label (e.g., flowers and fruits) (Arsova et al., 2012a); however, comparison between different samples is challenging (Griffin et al., 2010). Recently, metabolic labelling with a stable nitrogen isotope has been

widely applied to plants (reviewed by Arsova et al., 2012b). In this approach, plants are cultivated on either light (^{14}N) or heavy (^{15}N) nitrogen, combined during harvesting and extracted proteins are identified and quantified using mass spectrometry. Since the proteins undergo similar experimental conditions after extraction, error is reduced compared to a label-free approach. The proteins are relatively easily identified and quantified because heavy and light peaks appear together and their intensity is proportional to protein expression.

Heavy nitrogen metabolic labeling has been successfully applied to study *Arabidopsis* under different treatments (e.g., light and oxidative stress) (Bindschedler et al., 2008; Skirycz et al., 2011). Importantly, the proteome of wild-type plants was not altered by the metabolic labeling treatment itself, under the tested conditions (Bindschedler et al., 2008; Lanquar et al., 2007). Thus, it is possible that metabolic labeling is a suitable tool to study plants in the context of systems biology. Furthermore, together with NGS, it might aid the complete integration of the effect of miRNA on targeted transcript and protein accumulation, revealing the effects of transcript cleavage and translation inhibition activities.

Chapter 4 – Project hypothesis

Our group recently demonstrated that DRB2 is required for miRNA biogenesis (Eamens et al., 2012a), leading to the following question: Is there biological significance for the action of at least two DRB proteins, DRB1 and DRB2, mediating similar functional roles in the Arabidopsis miRNA pathway?

Plant miRNAs can guide both a target mRNA cleavage or translation inhibition to regulate the expression of their targeted genes. Also, mounting evidence indicates that plant miRNAs direct their mode of RNA silencing independently of the degree of complementarity to, or the position of, their target site sequence in their targeted transcripts (Brodersen et al., 2008; Grant-Downton et al., 2013; Li et al., 2013b). To date, the machinery proteins identified to be involved in translation inhibition appear to be involved in the trafficking and cellular localisation of RISC, and/or the stabilisation of the targeted mRNA. Thus, the function of these recently identified translation inhibition machinery proteins does not provide a mechanistic explanation for how a miRNA is directed, from its biogenesis, into either the transcript cleavage or translation inhibition pathway.

I hypothesise that DRB1 and DRB2 mediate different functional roles in the miRNA biogenesis. More specifically, I hypothesise that DRB1 and DRB2 mediate the determination of the 'silencing fate' of a miRNA. To test this hypothesis I studied alterations in miRNA target gene expression at both the mRNA and protein level in the Arabidopsis *drb1* and *drb2* mutant lines.

PART II – EXPERIMENTAL PROCEDURES

Chapter 5 – Experimental procedures

5.1 Plant lines and growth condition

The *drb* T-DNA knockout insertion, *DRB* promoter:GUS reporter gene fusion and *DRB2* overexpression plant lines have been described previously (Curtin et al., 2008; Eamens et al., 2012a). The *lue1* and *suo-2* T-DNA knockout insertion lines were obtained from the Arabidopsis Biological Resource Centre (ABRC) collection and have been described previously (Bouquin et al., 2003; Yang et al., 2012). All Arabidopsis lines used in this study were cultivated under standard growth conditions of 16 hours (h) light/8 h dark at a constant temperature of 24°C. Prior to soil transfer, all Arabidopsis lines were germinated on Murashige and Skoog (MS) agar media containing 1% sucrose for PCR-based genotyping to confirm genetic backgrounds. All DNA oligonucleotides used as primers for PCR-based genotyping are listed in Table 5-1.

5.1.1 Plant growth conditions for proteomics analysis

For proteomics experiments, plants were grown on a modified MS medium containing half nitrogen concentration (0.825 g/L NH_4NO_3 and 0.95 g/L KNO_3) supplemented with 0.4512 g/L KCl to compensate for potassium reduction (Martin et al., 2002). Metabolic ^{15}N labeling was achieved by replacing the nitrogen source with $^{15}\text{NH}_4^{15}\text{NO}_3$ and K^{15}NO_3 (Cambridge Isotope Laboratories Inc.; >98% enriched in ^{15}N). The average ^{15}N -labeling efficiency of the proteins was determined to be 97.6(\pm 0.2) atom%, as calculated using monoisotopic (M) and M-1 peak ratios (Schaff et al., 2008).

5.1.2 Salt stress treatment

Salt stress treatment was performed in seedlings previously cultivated on MS medium for 6 d after stratification (DAS) under standard conditions. Six-day-old seedlings were then transferred to MS medium supplemented with 0, 100 or 150 mM NaCl. Plants were analysed after 10 d of cultivation on salt-supplemented media.

5.1.3 Germination under abscisic acid treatment

Arabidopsis wild-type, mutant and transformant seeds were placed on filter paper saturated with either water (control) or 0.5 μ M abscisic acid (ABA), incubated at 4⁰C for 48 h, and then transferred to growth cabinets for germination under standard growth conditions.

5.2 Construction of expression vectors and plant transformation

The construction of the expression vectors used to transform *drb1* mutants (see Figure 5-1) was performed using standard cloning techniques, Gateway® cloning (Invitrogen) and synthesized DNA sequences. The binary vector used to transform the plants was a Gateway vector, pKCTAP, obtained from Plant Systems Biology (VIB, Belgium; <http://gateway.psb.ugent.be/>), and it has been previously described (Van Leene et al., 2007). The selectable marker cassette from pORE-O1 (Coutu et al., 2007), containing a *Pat* gene driven by *P_{HPL}* (*A. thaliana* hydroperoxide lyase promoter), was amplified using oligos that contained overhanging restriction sites for *RsrII* at both 5' and 3' ends. pKCTAP was digested with *RsrII* and the *Pat* gene cassette was inserted into the vector via the ligation of complementary single- stranded regions of the restriction sites.

To prepare the gene constructs to be inserted into the modified pKCTAP, a series of ~500 nt DNA sequences, termed gBlocks®, were designed in-house and synthesized by Integrated DNA Technologies (IDT). Each gBlock contained sequences coding the dsRNA binding domain of DRB1 and/or DRB2 (gBlocks are listed and described in Supplementary Data). The gBlocks were designed to contain 5' *HindIII* and *MfeI* and a 3' *NheI* restriction site, which were subjected to restriction enzymatic digestion, followed by ligation, to aid their insertion into a vector containing either the *DRB1* (*MfeI* and *NheI*) or *DRB2* (*HindIII* and *NheI*) sequence, as outlined in Figure 5-1A. The obtained constructs, as well as the dsRNA binding domains of *DRB1*, *DRB1* full-length, and *DRB2* full-length sequences, were collectively called genes of interest (GOIs) (Figure 5-1A). GOIs were amplified using a pair of primers designed to introduce a 5' CACC overhanging sequence to allow their directional cloning into pENTR/D-TOPO® (Invitrogen), generating the pENTR/D-TOPO::*GOI* (Figure 5-1A).

The *DRB1* promoter region, containing the 5'UTR of *DRB1* and 538 nt genomic sequence, previously described (Curtin et al., 2008), was modified to also include the first exon and intron of the *DRB1* gene. The longer *DRB1* promoter region was amplified from genomic

DNA using oligos that added 5' *SphI* and a 3' *SalI* overhanging restriction sites (Figure 5-1B). The PCR-amplified sequence was digested and ligated into a modified pEN::L4-2-R1 (also obtained from Plant Systems Biology, VIB). The pEN::L4-2-R1 vector originally encodes the *Cauliflower mosaic virus (CMV)* 35S promoter; thus, to remove the 35S promoter, pEN::L4-2-R1 was amplified using oligos specific to its L4 and R1 *att* site pairs oriented to amplify the entire vector but the 35S promoter.

The modified linear vector was digested with *SpeI* (restriction site included via PCR) and re-circularized, resulting in an L4/R1-containing vector that contained a multiple cloning site (MCS), which was also included via PCR. This vector was then digested with *SphI* and *SalI* and ligated with the longer *DRB1* promoter sequence, generating the pEN::L4-*DRB1pro*-R1. Finally, gateway cloning was performed using the entry vectors pENTR/D-TOPO::*GOI*, pEN::L4-*DRB1pro*-R1, pEN::R2-GStag-L3 and the modified destination vector, pKCTAP (Figure 5-1C). The resulting expression vector was used to transform *drb1* mutant plants via *Agrobacterium*-mediated transformation using the floral dip method (Clough and Bent, 1998). Plants were selected for resistance to the herbicide glufosinate. The sequences of oligos used are listed in Table 5-1, and a map of cloning vectors is shown in Supplementary Data.

5.3 Reporter gene expression analysis

To visualize GUS activity in *pDRB1::GUS* and *pDRB2::GUS* transformant lines (Curtin et al., 2008; Eamens et al., 2012a), seedlings and other selected tissue samples were treated as previously described (Jefferson et al., 1987).

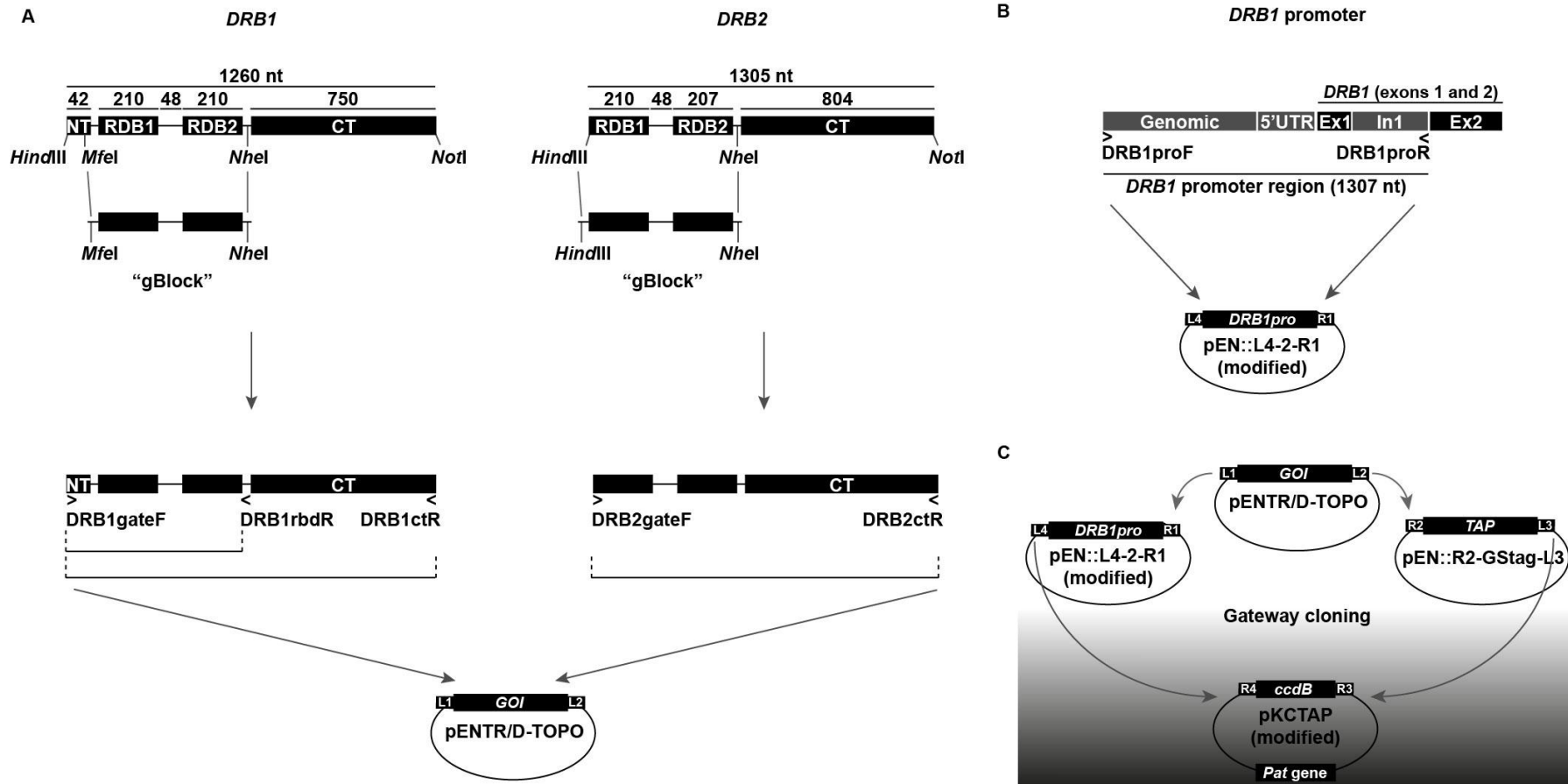


Figure 5-1. Construction of expression vectors to transform *drb1* mutants.

Construction of vectors containing *DRB* genes and chimeric genes (A), isolation of promoter region of *DRB1* (B) and gateway cloning (C).

5.1 RNA analysis

For all RNA analysis, total RNA was isolated using TRIzol Reagent according to the manufacturer's instruction (Invitrogen).

5.1.1 Small RNA deep sequencing

Ten micrograms of total RNA, from shoot apex of wild-type and *drb2* mutant plants, were sent for deep sequencing analysis using the Illumina Hi Seq 2000 system provided by Australian Genome Research Facility (AGRF). The publically available UEA small RNA Workbench was used to determine the normalised expression levels of sRNAs (18-25 nt) that matched any of the annotated Arabidopsis miRNA sequences in the miRNA database, miRBase 20 (<http://www.mirbase.org>; October 2013) (Stocks et al., 2012). Each miRNA with a normalised read count of greater than two reads, and that was detected in both the wild-type Col-0 and *drb2* mutant sample, was selected for further bioinformatic analysis to assess miRNA accumulation in the *drb2* mutant for comparison to wild-type Arabidopsis.

5.1.2 Analysis of miRNA synthesis accuracy and strand selection

Small RNA (sRNA) sequences, obtained by deep sequencing and homologous to miRNAs in wild-type and *drb2*, were considered accurately processed if the 5' and 3' termini of each detected sRNA were identical to a currently known Arabidopsis miRNA, and inaccurately processed if non-identical. The read number of inaccurately processed miRNA was normalized to the total read number obtained for each miRNA family.

Strand selection was indirectly calculated by measuring the normalised accumulation of miRNA passenger strands (miRNA*). miRNA* accumulation was normalised to the total number of reads (miRNA and miRNA*) for each miRNA family.

5.1.3 Northern blot and real time RT-PCR

Northern blot analysis was performed as previously described (Eamens et al., 2012a). DNA probes are listed in Table 5-1.

Synthesis of cDNA for real-time reverse-transcription PCR (RT-PCR) was performed using SuperScript® III Reverse Transcriptase following manufacturer's instructions (Life Technologies). RT-PCR was performed using Brilliant III SYBR® MM according to the Agilent Technologies protocol. The sequences of oligos are listed in **Table 5-1**.

5.1.4 miRNA real time RT-PCR

RT-PCR for the quantification of miRNA accumulation was performed according to a previous report (Chen et al., 2005). SuperScript® III Reverse Transcriptase (Life Technologies) and Brilliant III SYBR® MM (Agilent Technologies) were used to perform the cDNA synthesis and RT-PCR, respectively, following the manufacturer's instructions. Arabidopsis *SnoR101* was used to normalize the miRNA accumulation. The sequences of primers are listed in **Table 5-1**.

Table 5-1. List of DNA oligos and probes.

Oligo name	Specificity*	Sequence (5' to 3')	Oligo name	Specificity*	Sequence (5' to 3')
Real Time RT-PCR					
ACT2_qPCR_FW	AT3G18780	GCAGATGTGGATCTCCAAGGCCGA	miR162_probe	miR162	TTTGATTGAAGGGAGCTCTA
ACT2_qPCR_RV		TTTCTGTGAACGATTCTGGACCTGCC	miR168_probe	miR168	TTCCCGACCTGCACCAAGCGA
AFB1_qPCR_FW	AT4G03190	ACTGTTACGCGGTCAAGTCTGTCT	miR172_probe	miR172	ATGCAGCATCATCAAGATTCT
AFB1_qPCR_RV		ATCCACGGCCAAGCATAACCACCC	miR398_probe	miR398	CAGGGGTGACCTGAGAACACA
AGO1_qPCR-FW	AT1G48410	TGGACCTTCTTGGACCAACCGCA	miR408_probe	miR408	GCCAGGGAAGAGGCAGTGCAT
AGO1_qPCR-RV		GGTGAGGTAGCTTATGACAGCTCGG	miR863-3p_probe	miR863-3p	ATTGAGATCAACAAGACATAA
AKR4C8_qPCR-FW	AT2G37760	CGCCAAAGTGGCTCTCCGTTG	U6_probe	U6	AGGGCCATGCTAATCTTCTCTG
AKR4C8_qPCR-RV		GGCAAACCTAGTAGCTCGGCAAA			
AP2_qPCR_FW	AT4G36920	AGCGGAGGCGGATTCTCACTGTT	miRNA RT-PCR (Stem Loop)		
AP2_qPCR_RV		TCGTCGAGGCCGACCATCAA	SL_RT-snoR101	SnoR101	GTCGTATCCAGTGCAGGGTCCGAGGTATTCGCA
APS1_qPCR_FW	AT3G22890	GGATTAATCGCTCCCGACGGTGGT			CTGGATACGACAGCATC
APS1_qPCR_RV		TCTCGCCGCTTTGGCTCTTCCA	SL_RT-miR164abc	miR164abc	GTCGTATCCAGTGCAGGGTCCGAGGTATTCGCA
APS3_qPCR_FW	AT4G14680	GGAAACCGAGACGGCGAGAGAAGAA			CTGGATACGACAGCGACG
APS3_qPCR_RV		CGCCGTCAATCTCACTCTCGGCAA	SL_RT-miR165/166	miR165/166	GTCGTATCCAGTGCAGGGTCCGAGGTATTCGCA
ARPN_qPCR-FW	AT2G02850	ATGGCCAAAGGGAAGAGGGCAGT			CTGGATACGACGGGGA
ARPN_qPCR-RV		ACGTGCGCGGCTCTAAAGTGTGTTG	SL_RT-miR398a-c	miR398a-c	GTCGTATCCAGTGCAGGGTCCGAGGTATTCGCA
AT1G15125_qPCR_FW	AT1G15125	TTGCTTTGCTCCCTCCCAACGCC			CTGGATACGACMAGGGG
AT1G15125_qPCR_RV		ATGGCAAGTCGGAGAGCCAGCAGA	SL_RT-miR408	miR408	GTCGTATCCAGTGCAGGGTCCGAGGTATTCGCA
ATHB14_qPCR-FW	AT2G34710	AGAAGCTTCCACCCGCTGTGCT			CTGGATACGACGCCAGG
ATHB14_qPCR-RV		CAGCAGCATAAGCATCCACGCCA	URP	SL adaptor	CCAGTGCAGGGTCCGAGGT
BXL7_qPCR-FW	AT1G78060	TGGAAACTACGCTGGTCCGCTT	SL_qPCR-snoR101	SnoR101	CACAGGTAAGTTCGTTGTTG
BXL7_qPCR-RV		TCGCAAGCTTAGAGCAAGCCAC	SL_qPCR-miR164ab	miR164ab	TGGAGAAGCAGGGCAGCTGC
CSD1_qPCR-FW	AT1G08830	TCAGCTGGCTACTGGAACCGCA	SL_qPCR-miR165ab	miR165ab/166a-g	TCGGACCAGGCTTCATYCCC
CSD1_qPCR-RV		CCTGGAGACCAATGATGCCGCAAG			
CSD2_qPCR-FW	AT2G28190	CAATGCCGATGGCGTGGCAAA	SL_qPCR-miR398bc	miR398bc	GGTGTGTTCTCAGGTCACCCCTG
CSD2_qPCR-RV		GCCACCCTTCCGAGGTCATCCTT	SL_qPCR-miR408	miR408	ATGCACTGGCTTCCCTGGC
DCL1_qPCR-FW	AT1G01040	TGGCAATGAGCTGGATGCAGAGGT			
DCL1_qPCR-RV		ATCCCATGGTGTCTGGAGGGT	Genotyping		
DRB1_qPCR-FW	AT1G09700	TCCACTGATGTTTCTCTGG	drb1_gen-FW	SALK_064863	CTTCTGGAAATTGGATTGCAGTG
DRB1_qPCR-RV		GATCTCATAAACAGGCGTTGG	drb1_gen-RV		GCCCCCTAACGTATTCTCACAGC
DRB2_qPCR-FW	AT2G28380	CCAGTCTTGCCATGATGCTTG	drb2_gen-FW	GK348A09016243	GCTAAACCCCTCAACGATTTTCC
DRB2_qPCR-RV		CGGTCTCTCTTCGATGAAT	drb2_gen-RV		GAGATCTCAGCACCGACCTAATAAG
FAMT_qPCR-FW	AT3G44860	CGTCCGCGTTTAAAGGTCACTGTTGG	drb3_gen-FW	SALK_003331	CCAACATCTCTTGTACTGTGGAGC
FAMT_qPCR-RV		ATTGCATTCAGGTTTGGCTTTGGCT	drb3_gen-RV		GTTTCTAATCTAATTTGGTAATGAC
GRF2_qPCR-FW	AT4G37740	GGACTTCAGCTGTTGCGATGCGGTG	drb5_gen-FW	SALK_031307	CCAATGGAGAAGAAGAACAAGTCAAC
GRF2_qPCR-RV		TGTTCCAACAGCAGCGGCAAGG	drb5_gen-RV		CTATCATGGGTTGATCCAAAATCTCG
HTA8_qPCR-FW	AT2G38810	TCTAGCTGCGAAGACGACGGCA	suo-2_gen-FW	CS67883	TCATTCTATCGACCTAATGTG
HTA8_qPCR-RV		GCAGCAGTGGCACCACCTTCCCA	suo-2_gen-RV		GCTCATCACGACAACAAGTG
LAC2_qPCR-FW	AT2G29130	TTAACCCGGCCCGTGACCCAAA			
LAC2_qPCR-RV		GCTCGAGCCCTACAACAGCGCAA	Cloning		
LAC3_qPCR-FW	AT2G30210	ACCACGGCCACGCTTGTGGGA	PATcassetteF	35S promoter	atctaaCGGTCCGaacgtggatactggcagtg
LAC3_qPCR-RV		AGTAAGGGTACAACCTCACCGCCT	PATcassetteR	NOS terminator	caggatGATATCCGGACCGgatctagtagatgacaccgc
MBP1_qPCR-FW	AT1G52040	GCTTTCCATGGAATCCGGCAAGT	DRB1gateF	DRB1/AT1G09700	CACCATGACCTCCACTGATGTTTCC
MBP1_qPCR-RV		CGGGACTAATCGCGGGCAGCTAAA	DRB1dbd2R	DRB1/AT1G09700	GCTAGCTGACTGGATCGCTAAAAGAG
MBP2_qPCR-FW	AT1G52030	TGTCGTAGCTTCCACCAACGGCT	DRB1ctR	DRB1/AT1G09700	TGCGTGGCTTGCTCTGTCTC
MBP2_qPCR-RV		GGGATCCTCAGGAGTGGGCTTTGT	DRB2gateF	DRB2/AT2G28380	CACCATGTATAAAGAACAGCTAC
MYB33_qPCR-FW	AT5G06100	TGGAGGATTTCCGGGCTCGTATG	DRB2ctR	DRB2/AT2G28380	GATCTTTAGGTTCTCCAGTC
MYB33_qPCR-RV		GTGGTTCAGCAACGTCAGCAGCAA	DRB1proFW	upstream DRB1	aagttgGCATGCaGAACGAAAAGGAAAGTGG
PHV_qPCR-FW	AT1G30490	GCCTTGCAAAGGAACTCCGCCAA	DRB1proRV	DRB1/AT1G09700	ttatagTGCACaCAATTGGAACACCTGAGCAGG
PHV_qPCR-RV		TCGATCGGACGCTGAAGTCGATG	pENL42R1-F	pEN::L4-2-R1	ggcgccgactagtagatgac
SAT3_qPCR-FW	AT3G13110	TCGCCAACGCAGCTTCCAACGAAC	pENL42R1-R	pEN::L4-2-R1	tagtagACTAGTtatagTGCAGctggtaaCCGCGGtgacgtCTC
SAT3_qPCR-RV		TGGTTCGGGTTGGTAAAGGGCA			GAGtagatGCATGctatagtgacctaaatc
SE_3'UTR_qPCR-FW	AT2G27100	CGCTTTAGTGAGTGAATTTGGAGGAAC			
SE_3'UTR_qPCR-RV		GGTAGCATCAATCGTGGTGGCTCGT			
SPL4_qPCR-FW	AT1G53160	GCTAAGCGCCTCCTGCAACTTCTC			
SPL4_qPCR-RV	AT2G42200	GTGGTGGTGGATCCGGGCTTCTT			
SPL9_qPCR-FW		TGGCACCTTGGTATCTGACCCGAC			
SPL9_qPCR-RV	AT5G12250	GCTCGCAGTGAACCTCATTCTTCC			
TUB6_qPCR-FW		AGTGCACGGTACTGCTGAGACCCAC			
TUB6_qPCR-RV	AT2G02740	TCCAGATGGTCTGGCCGCTT			
WHY3_qPCR-FW		TGCGGCAAGACGAAGTTGAAAGCA			
WHY3_qPCR-RV					

* Refers to locus amplified or DNA probe for northern blot. ABRC stock number is provided for genotyping oligos.

5.1.5 Microarray analysis

One microgram of total RNA, extracted from the shoot apex of wild-type and *drb2* Arabidopsis mutant lines, was shipped to the Ramaciotti Centre for Gene Function Analysis for the gene expression service on an Affymetrix Arabidopsis gene 1.0ST array. The statistical analysis was performed using Transcriptome Analysis Console (TAC) software and Expression Console software (ANOVA; p -value<0.05). Functional annotation clustering of differentially expressed genes was determined using the Database for Annotation, Visualization and Integrated Discovery (DAVID) analysis (Da Wei Huang et al., 2008).

5.2 Protein extraction and Western blots

Proteins were extracted as previously described (Skirycz et al., 2011). Powdered tissue was resuspended in solubilization buffer (40 mM Tris, pH 8.0, 5 mM MgCl₂, 40 mM dithiothreitol (DTT), 4% (w/v) SDS, and one tablet of proteinase inhibitor Complete ULTRA tablets, Roche, per 10 mL of buffer) and the resulting supernatant collected after centrifugation at 16,000xg for 15 min at 4°C. Protein concentration was determined using a bicinchoninic acid (BCA) protein assay kit according to the manufacturer's instructions (Pierce). Western blots were performed using the antibodies listed in Table 5-2.

Table 5-2. Source and working dilution of antibodies used for western blot analysis.

Antibody	Antibody dilution	Source
anti-ACT	1 : 2,500	Agrisera (AS132640)
anti-AP2	1 : 6,000	Agrisera (AS122609)
anti-AGO1	1 : 7,000	Agrisera (AS09527)
anti-ARPN	1 : 2,000	Gift from Prof. Elizabeth M. Lord (University of California, Riverside) (Dong et al., 2005)
anti-DRB1 (HYL1)	1 : 1,000	Agrisera (AS06136)
anti-CSD1	1 : 5,000	Gift from Dr. Kuo-Chen Yeh (Agricultural Biotechnology Research Center of Academia Sinica) (Chen et al., 2011)
anti-CSD2	1 : 1,000	Agrisera (AS06170)
anti-DCL1	1 : 1,000	Agrisera (AS122102)
anti-SE	1 : 1,000	Agrisera (AS09532)

5.3 Proteomics analysis

5.3.1 Sample preparation

Shoot apical meristem (SAM) and surrounding tissue (shoot apex, for simplicity) was sampled from 4-week-old wild-type Arabidopsis and *drb* mutant plants, and mixed at an

approximate 1:5 (w/w) ratio, as previously described (Arsova et al., 2012a). Two samples were prepared for each *drb* mutant: (i) a mixture of unlabeled wild-type with ¹⁵N-labeled mutant, and (ii) a mixture of ¹⁵N-labeled wild-type with unlabeled mutant. Extracted proteins were separated in 1D SDS-PAGE, stained with colloidal coomassie G-250 and gel lanes were cut into 29 pieces from low to high protein mass. Each polyacrylamide gel slice was destained, reduced and alkylated following the procedure described by Shevchenko et al. (1996). For protein digestion, 40 ng of trypsin (Stratagene, #204310) in 120 µL of 0.1 M NH₄HCO₃ was used for each gel slice and incubation was for 16 h at 37°C. The digest solutions were removed to new microfuge tubes and the gel slices treated with the following solutions sequentially for 30 min each: 80 µL 0.1% (v/v) formic acid/67% (v/v) acetonitrile; and 80 µL 100% acetonitrile. The pooled digest and peptide extraction solutions were then dried (Savant SPD1010, ThermoFisher Scientific) before resuspending in 20 µL of 0.1% (v/v) formic acid.

5.3.2 Mass spectrometry

Proteolytic peptide samples were separated by nano-LC using an UltiMate 3000 HPLC and autosampler system (Dionex, Amsterdam, Netherlands), and ionized using positive ion mode electrospray following experimental procedures described previously (Hart-Smith and Raftery, 2012). MS and MS/MS were performed using an LTQ Orbitrap Velos Pro (Thermo Electron, Bremen, Germany) hybrid linear ion trap and Orbitrap mass spectrometer. Survey scans *m/z* 350–2000 were acquired in the Orbitrap (resolution = 30,000 at *m/z* 400, with an initial accumulation target value of 1,000,000 ions in the linear ion trap; lock mass applied to polycyclodimethylsiloxane background ions of exact *m/z* 445.1200 and 429.0887). Precursor ions were selected for MS/MS using a mixed targeted and untargeted approach. Up to the five most abundant ions from an inclusion list (see below), followed by up to the 10 most abundant ions (>5,000 counts) with charge states of >+2 were sequentially isolated and fragmented via collision-induced dissociation (CID) with an activation *q* = 0.25, an activation time of 30 ms, normalized collision energy of 30% and at a target value of 10,000 ions; fragment ions were mass analyzed in the linear ion trap.

Samples containing *drb2* mutant-derived proteins were subjected to two mixed targeted and untargeted LC-MS/MS experiments, each associated with distinct inclusion lists; samples

containing *drb1* or *drb235* mutant-derived proteins were subjected to one mixed targeted and untargeted LC-MS/MS experiment (see below).

5.3.3 MS/MS inclusion lists

To ensure that peptides associated with the selected proteins of interest were targeted for fragmentation during LC-MS/MS, MS/MS inclusion lists were generated with the aid of Skyline (version 0.7.0.2494, University of Washington). Amino acid sequences for the proteins listed in Table S2 were imported into Skyline, and m/z values for doubly charged theoretical proteotypic peptide ions (unlabeled light and fully ¹⁵N-labeled heavy) associated with these proteins were generated using the following parameters: Enzyme: Trypsin (zero missed cleavages); Structural modifications: Carbamidomethyl cysteine; Isotope modifications: ¹⁵N for all amino acids. Exported m/z values were incorporated into inclusion lists and used for the mixed targeted and untargeted LC-MS/MS experiments described above.

5.3.4 Sequence database searches and protein quantification

Peak lists derived from LC-MS/MS were submitted to the database search program Mascot (version 2.3, Matrix Science) via Proteome Discoverer (version 1.3, Thermo Scientific). Separate searches were conducted for unlabeled and fully ¹⁵N-labeled peptides. For unlabeled peptides, the following search parameters were employed: instrument type was default; precursor ion and peptide fragment mass tolerances were ± 5 ppm and ± 0.4 Da respectively; variable modifications included were acrylamide (C), carbamidomethyl (C) and oxidation (M); enzyme specificity was trypsin with up to two missed cleavages; and all taxonomies in the Swiss-Prot database (July 2013 release, 540,732 sequence entries) were searched. For ¹⁵N-labeled peptides, search parameters were identical to the above, with the following fixed modifications included: ¹⁵N(1) (A,C,D,E,F,G,I,L,M,P,S,T,V,Y), ¹⁵N(2) (K,N,Q,W), ¹⁵N(3) (H) and ¹⁵N(4) (R).

Proteome Discoverer was used to quantify peak intensities for unlabeled and ¹⁵N-labeled peptide pairs; this was performed separately for the search outputs obtained from unlabeled and fully ¹⁵N-labeled peptide sequence database searches. These data were then combined within Proteome Discover to produce consensus quantitative datasets. Only peptides deemed

to be statistically significant ($p < 0.05$) according to the Mascot expect metric were used for quantification.

Average heavy to light peptide ratios for each identified protein were imported into R (version 3.1.0), and analyzed using custom code. Specifically, the following established procedures (Ting et al., 2009), were performed using the limma library (version 3.20.1) in Bioconductor (version 2.14): heavy-to-light protein ratios for each wild-type with the *drb* mutant mixture were lowess normalized; a linear model was fitted for proteins quantified in both ^{14}N : ^{15}N label reversals for each *drb* mutant; and p values associated with average protein fold-changes were calculated using empirical Bayes moderated *t* statistics.

5.4 Construction of the Shoot Apex Interactome and network analysis

The Shoot Apex Interactome (SAI) was constructed based on binary protein-protein interactions obtained from the Biological General Repository for Interaction Datasets (BioGRID, v3.2.109 released in February 1, 2014) (Stark et al., 2006). The proteins used to produce the SAI were derived from a combined dataset of proteins that were identified and quantified in *drb1* and/or *drb2* mutants, relative to wild-type. The SAI was visualized and analyzed using Cytoscape (v3.0.2) (Saito et al., 2012).

5.5 Gene ontology enrichment analysis

Gene ontology enrichment was performed using the Database for Annotation, Visualization and Integrated Discovery (DAVID, v6.7) (Huang et al., 2009). The Functional Annotation Tool was used to create a list of enriched GOTERM_BP clusters (p -value < 0.05) using the Arabidopsis genome as background.

PART III – RESULTS AND DISCUSSION

**Chapter 6 – Gene regulation by
translational inhibition is
determined by Dicer
partnering proteins**

MicroRNAs (miRNAs) are small regulatory RNAs produced by Dicer proteins that regulate gene expression in development and adaptive responses to the environment (Ameres and Zamore, 2013; Bologna and Voinnet, 2014; Sunkar et al., 2012). In animals, the degree of base pairing between a miRNA and its target messenger RNA has appeared to determine whether the regulation occurs through cleavage or translation inhibition (Ameres and Zamore, 2013). In contrast, the selection of regulatory mechanism is independent of the degree of mismatch between a plant miRNA and its target transcript (Brodersen et al., 2008). However, the components and mechanism(s) that determine whether a plant miRNA ultimately regulates its targets by guiding cleavage or translation inhibition are unknown (Mallory and Vaucheret, 2010).

In this Chapter I show that the form of regulatory action directed by a plant miRNA is determined by DRB2, a DICER-LIKE1 (DCL1) partnering protein. The dependence of DCL1 on DRB1 for miRNA biogenesis is well characterized (Eamens et al., 2009; Han et al., 2004b; Kurihara et al., 2006), but I show that it is required only for miRNA-guided transcript cleavage. I found that DRB2 determines miRNA-guided translational inhibition and represses *DRB1* expression, thereby allowing the active selection of miRNA regulatory action. Furthermore, the results reveal that the core silencing proteins ARGONAUTE1 (AGO1) and SERRATE (SE) are highly regulated by miRNA-guided translational inhibition. DRB2 has been remarkably conserved throughout plant evolution, with its functional domains retaining ~80% amino acid sequence identity from primitive mosses to modern eudicots, while DRB1, although also present in all multicellular plant clades, is much less conserved. This raises the possibility that translational repression is the ancient form of miRNA-directed gene regulation in plants, and that Dicer partnering proteins, such as human TRBP, might play a similar role in other eukaryotic systems.

6.1 Phenotypes displayed by *drb1* and *drb2* mutant plants

DOUBLE-STRANDED RNA-BINDING1 (DRB1), also known as HYPONASTIC LEAVES1 (HYL1), is regarded as the principal co-factor that aids DCL1 to accurately and effectively excise miRNAs from their primary transcripts and transfer them to AGO1 effector protein complexes (Eamens et al., 2009; Han et al., 2004b; Kurihara et al., 2006). Eamens et al. (2012a) recently showed that DRB2 is required for miRNA biogenesis in *Arabidopsis*.

However, the biological significance of having at least two DRB proteins, DRB1 and DRB2, in this silencing pathway remains unknown. As illustrated in Figure 6-1, *drb1* plants exhibit pleiotropic developmental defects, including smaller-sized hyponastic leaves, and shorter and twisted siliques (Lu and Fedoroff, 2000). The *drb2* mutant displays a mild developmental phenotype characterized by ovoid and flatter rosette leaves with serrated margins, increased anthocyanin production and late flowering (Curtin et al., 2008; Eamens et al., 2012a).

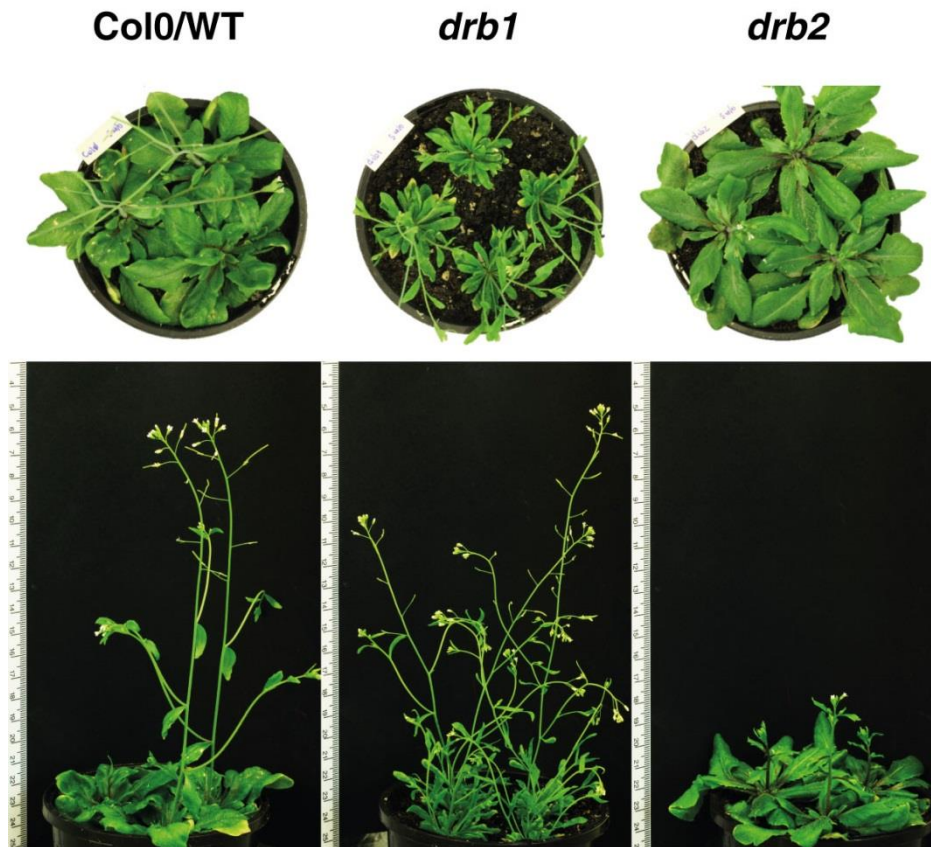


Figure 6-1. *DRB1* and *DRB2* knockout mutant phenotypes.

Five week-old wild-type (Col-0), *drb1* and *drb2* plants. Each pot of plants is shown in both top and side views.

6.2 Characterization of *DRB1* and *DRB2* expression

Eamens et al. (2012a) have previously demonstrated the role of *DRB2*-produced miRNAs in gene expression regulation during the transition to flowering in the shoot apex of *Arabidopsis*. Here, I analyzed younger shoot apex (3 weeks old) to further assess the role of *DRB2* during plant development prior to flowering. *DRB1* and *DRB2* expression was detectable in all assessed tissues, including three-week-old seedlings, roots, shoot apical meristem (SAM) and surrounding tissue (shoot apex, for simplicity) and rosette leaves, as well as in five- to six-week-old floral tissue. The highest levels of *DRB1* and *DRB2* expression were in the shoot apex and floral tissues (Figure 6-2A), as previously reported using the promoter- β -glucuronidase (GUS) approach (Curtin et al., 2008; Eamens et al., 2012a; Lian et al., 2013).

To gain a more detailed picture of *DRB1* and *DRB2* expression in the shoot apex, I sectioned GUS-stained samples of this region of three week old *DRB1pro::GUS* and *DRB2pro::GUS* plants. Upon staining, *DRB1pro::GUS* plants showed high GUS expression in the SAM, rosette leaf primordia, base of emerging leaves, procambium and base of hypocotyl. GUS accumulation was restricted to epicotyl in *DRB2pro::GUS* plants, revealing an apparent boundary between the base of young rosette leaves and the hypocotyl. Intense GUS signals were also observed in the boundary of leaf primordial and SAM region. These results show that *DRB1* is highly expressed throughout the shoot apex, whereas *DRB2* is more intensely expressed in boundary regions of the epicotyl and in leaf primordial (Figure 6-2B).

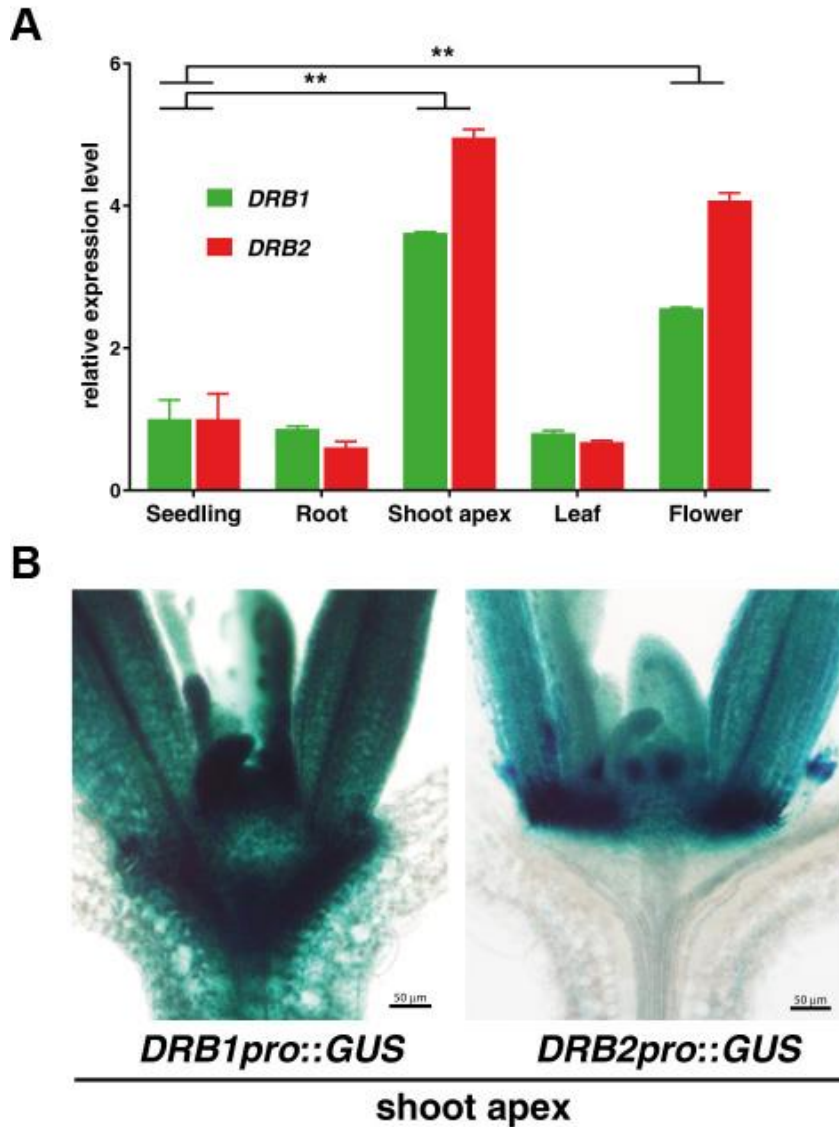


Figure 6-2. *DRB1* and *DRB2* expression profiles.

(A) RT-PCR analysis of *DRB1* and *DRB2* expression of 3-week-old seedling, root, shoot apex and leaf and 5- to 6-week-old floral tissue samples. Values were normalized to *ACT2* (AT3G18780). Gene expression ratios are relative to seedling levels ($n = 3$, $**p < 0.01$, one-way ANOVA, \pm SD).

(B) GUS expression in the shoot apex of 3-week-old transgenic plant carrying the promoter-GUS expression vectors. Reporter gene expression was driven by the *DRB1* (*DRB1pro::GUS*) and *DRB2* (*DRB2pro::GUS*) promoter sequences.

6.3 miRNA production is altered in *drb2* mutant

Figure 6-2 showed that *DRB1* and *DRB2* are highly expressed in the shoot apex. I therefore selected this tissue to further assess the role of *DRB1* and *DRB2* in the miRNA pathway. Initially, small RNA sequencing was performed to identify the miRNA families expressed in wild-type and *drb2* plants. Small RNA sequencing identified 52 miRNA families, of which 19 had reduced accumulation (-5.5 to -2.0 fold change) in the *drb2* compared to wild-type (Table 6-1). *DRB1* has previously been shown to direct the preferential accumulation of the miRNA guide strand over the opposite duplex strand, the miRNA* passenger strand, for loading into AGO1 (Eamens et al., 2009). Although ~37% of detected *MIR* gene families accumulated to lower than wild-type levels in the *drb2* shoot apex, the preferential accumulation of the miRNA guide strand was retained in this mutant background (Figure 6-3A). This result suggests that, unlike *DRB1*, *DRB2* might not be required to direct preferential miRNA guide strand selection in Arabidopsis. However, *DRB2* was required for accurate DCL1-mediated processing of the precursor transcripts of a subset of miRNAs (Figure 6-3B).

Table 6-1. miRNA accumulation profile of detected miRNA in shoot apex of 3-week-old Arabidopsis wild-type (Col-0) and *drb2* mutant plants (n = 1).

miRNA	Col0	<i>drb2</i>	Fold Change (<i>drb2</i> /WT)	miRNA	Col0	<i>drb2</i>	Fold Change (<i>drb2</i> /WT)
miR166	48944.7	12669.13	0.3	miR472	21.06	8.87	0.4
miR165	21487.94	5586.46	0.3	miR395	17.59	14.42	0.8
miR158	10812.07	4839.81	0.4	miR779	16.29	9.43	0.6
miR159	9853.38	5298.67	0.5	miR447	14.55	9.42	0.6
miR319	3859.9	2370.54	0.6	miR1886	13.24	7.2	0.5
miR398	1848.29	1674.63	0.9	miR173	12.59	5.55	0.4
miR396	1282	705.34	0.6	miR781	12.38	8.04	0.6
miR403	858.14	418.38	0.5	miR5642	12.37	4.16	0.3
miR161	685.95	422.26	0.6	miR169	11.28	2.49	0.2
miR157	531.55	313.85	0.6	miR775	10.86	6.93	0.6
miR168	490.74	256.75	0.5	miR164	10.2	9.14	0.9
miR408	266.2	213.76	0.8	miR2111	9.99	5.55	0.6
miR162	209.33	161.09	0.8	miR393	9.77	9.71	1.0
miR397	206.72	194.63	0.9	miR5651	9.12	4.44	0.5
miR156	191.52	82.62	2.3	miR841	9.12	1.66	0.2
miR399	154.39	93.15	0.6	miR400	8.47	3.88	0.5
miR390	150.91	84.01	0.6	miR163	7.61	5.55	0.7
miR394	87.5	32.71	0.4	miR822	5.86	3.32	0.6
miR160	74.69	45.74	0.6	miR823	5.65	1.66	0.3
miR846	64.71	31.33	0.5	miR172	4.99	2.77	0.6
miR858	56.24	39.92	0.7	miR857	4.34	8.59	2.0
miR829	49.51	27.73	0.6	miR840	2.6	0.55	0.2
miR827	48.86	54.62	1.1	miR854	2.53	7.92	3.1
miR167	45.38	11.37	0.3	miR861	2.39	1.11	0.5
miR171	28.01	9.43	0.3	miR869	2.39	0	-
miR824	23.24	21.34	0.9	miR170	2.17	1.11	0.5

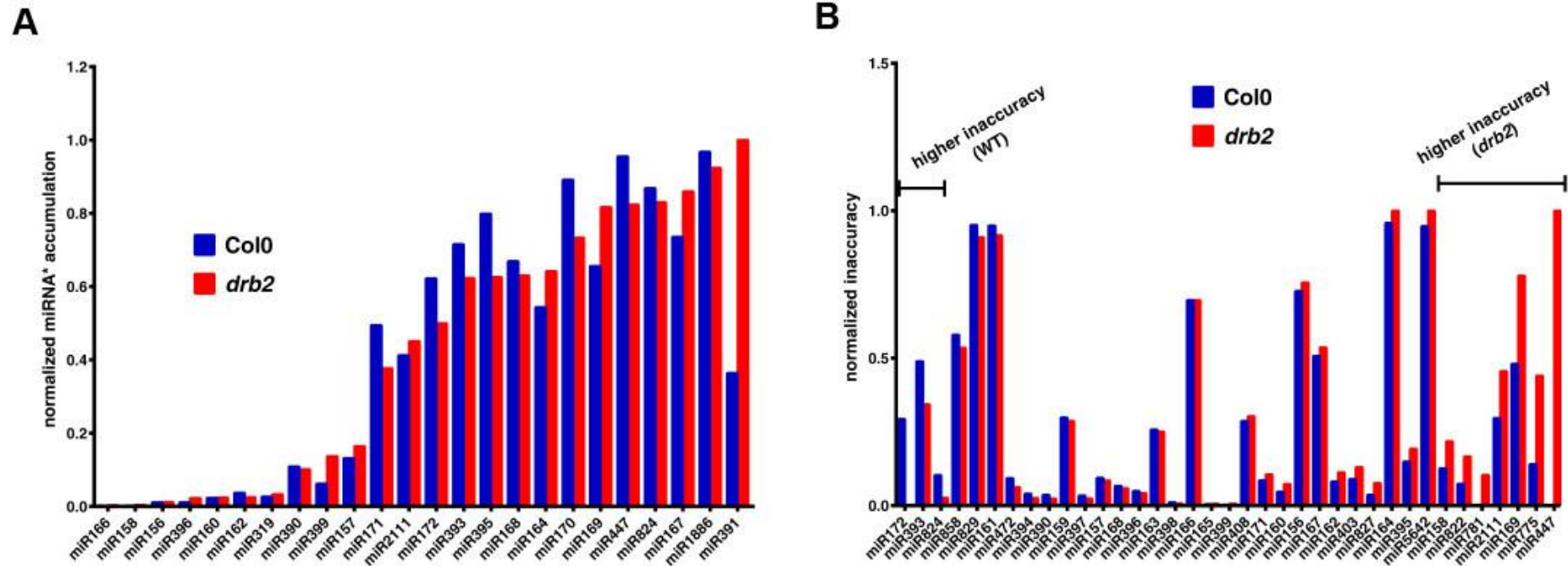


Figure 6-3. Strand selection and miRNA processing inaccuracy in *drb2* mutant.

(A) miRNA* accumulation in the shoot apex of *drb2* plants for each miRNA for which a miRNA* sequence was detectable by sRNA sequencing. Read numbers were normalised to the total miRNA* read number ($n = 1$).

(B) miRNA precursor transcript processing inaccuracy in *drb2* plants compared to wild-type Arabidopsis (*Col-0*). A miRNA was considered accurately processed if its 5' and 3' ends were identical to its canonical miRNA sequence (miRBase 20), and inaccurately processed if non-identical ($n = 1$). The read number of inaccurately processed miRNA was normalized to the total read number obtained for each miRNA family.

6.4 miRNA target gene expression in the *drb2* shoot apex

Following analysis of miRNA targets in the shoot apex, I compiled a list of previously validated and predicted targets of the 52 miRNA families identified via small RNA sequencing (Supplementary Data) and compared their expression profile in *drb2* to wild-type plants via microarray analysis. The transcriptomic analysis revealed that almost all miRNA targets (144 out of 149 assessed) showed wild-type levels in *drb2* (Figure 6-4A and Supplementary Data). Only five miRNA target genes were identified to have altered expression in *drb2*: *AT1G15125* (miR163), *FAMT* (miR163), *SPL4* (miR156), *LAC2* (miR397) and *LAC3* (miR408) (Figure 6-4A). Real time reverse-transcriptase PCR (RT-PCR) analysis confirmed the microarray expression profile for 13 miRNA target transcripts, including the five miRNA target genes with altered expression in *drb2* plants (Figure 6-4B). RT-PCR analysis also showed that most miRNA target transcripts (12 out of 13) had increased accumulation in *drb1*. The analysis also revealed a large set of gene transcripts, non-target of the detected miRNAs, with altered expression in *drb2* plants compared to wild-type; 297 genes were up-regulated and 316 genes were down-regulated ($p < 0.05$; Figure 6-4C). Taken together, the results show that DRB2 plays a role in the regulation of gene expression in the shoot apex, but that the expression of miRNA target transcript is largely unaffected in *drb2* mutants.

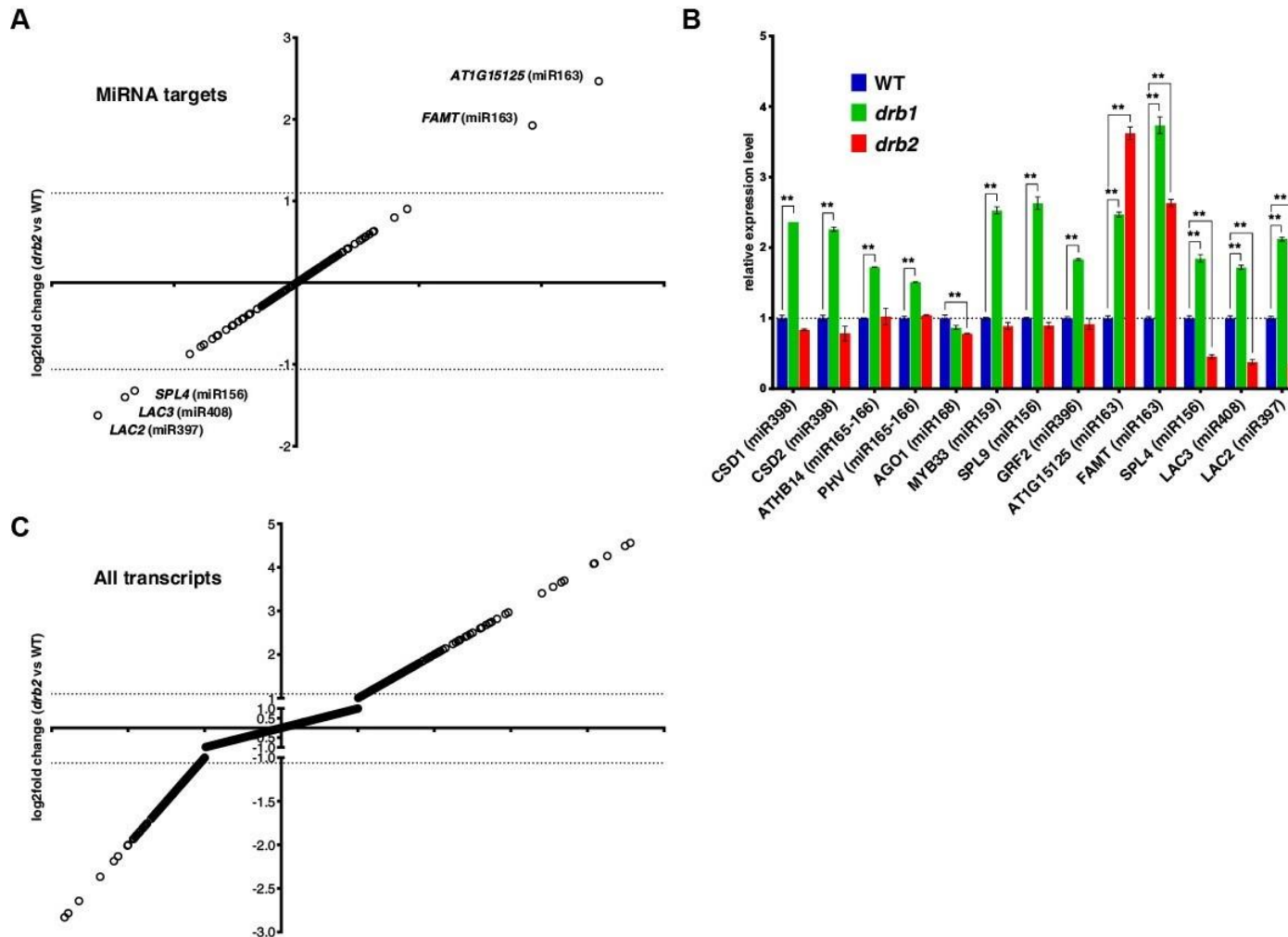


Figure 6-4. Gene expression in *drb2* mutant.

(A) Relative miRNA target transcript expression in *drb2* compared to wild-type. Target genes of the 52 miRNA families detected by small RNA sequencing were included. Of the 149 miRNA target genes assessed, five, namely *AT1G15125* (miR163), *FAMT* (miR163), *SPL4* (miR156), *LAC2* (miR397) and *LAC3* (miR408), were differentially expressed in *drb2*. Dashed lines represent significance threshold ($n = 3$; $p > 0.05$).

(B) RT-PCR analysis of miRNA target gene expression in wild-type (Col-0), *drb1* and *drb2* plants. Expression normalized to *ACT2* (AT3G18780). Gene expression ratios are relative to wild-type levels (dashed line) ($n = 3$, $**p < 0.01$, one-way ANOVA, \pm SD).

(C) Relative transcript expression in *drb2* compared to wild-type. Dashed lines represent significance threshold ($p > 0.05$).

6.5 miRNA target protein levels are disproportionately elevated in *drb2*

In plants, the study of the regulation of miRNA target at the protein level has been restricted by the availability of protein-specific antibodies, and to the expression of epitope-tagged proteins (Brodersen et al., 2008; Grant-Downton et al., 2013; Li et al., 2013b). Thus, a protocol optimized for identification and quantification of miRNA target proteins in *Arabidopsis*, using a ^{15}N metabolic labeling approach coupled with standard mass spectrometry-based proteomics was developed (see Experimental Procedures for details). This protocol was applied as a discovery approach to quantitatively compare the proteomes of the shoot apex of *drb1*, *drb2* and *drb235* to wild-type plants. The *drb235* triple mutant was included in this analysis to test previous hypothesis of either redundancy, or the potential co-involvement of DRB2, DRB3 and DRB5 in an alternate miRNA pathway (Curtin et al., 2008; Eamens et al., 2012a, 2012b). In order to improve the detection and quantification of miRNA target proteins, a tandem mass spectrometry inclusion list was introduced to ensure that peptides derived from these proteins were preferentially targeted for identification (refer to Material & Methods for details). In total, 4,482 unique proteins were identified and 1,845 quantified across the proteomics analyses. The distributions of protein accumulation in *drb1* and *drb2*, relative to wild-type plants, were similar (Figure 6-5). Compared to wild-type, 338 and 243 proteins had altered accumulation (p -value < 0.05) in *drb1* and *drb2* plants, respectively.

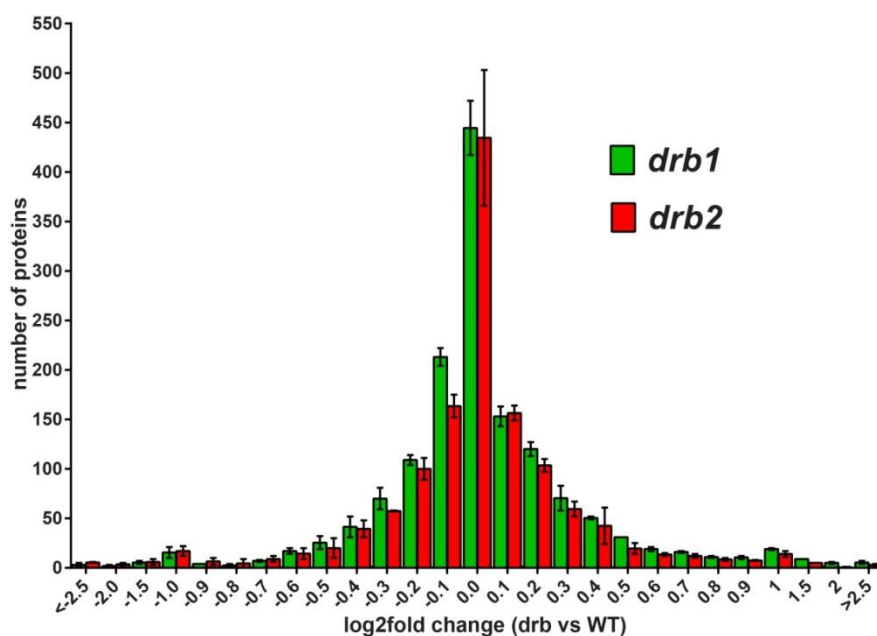


Figure 6-5. Histogram of protein accumulation ratios in *drb1* and *drb2*.

Protein accumulation ratio (log₂fold change) is relative to wild-type (Col-0). Error bars represent +/- SD (n = 2).

The approach above using an inclusion list identified and quantified 10 miRNA target proteins (Figure 6-6A). In *drb1* plants, two previously validated miRNA targets showed altered protein accumulation, AGO1 and WHY3, which are targets of miR168 and miR840 respectively (Figure 6-6A). WHY3 protein and transcript levels were both slightly reduced in *drb1* (Figure 6-6A-B). AGO1 protein accumulation was reduced, but its mRNA remained at wild-type levels (Figure 6-6A-B). The accumulation of two other validated miRNA target proteins, AFB1 (miR393) and APS1 (miR395), were at approximately wild-type levels in *drb1* plants (Figure 6-6A). Five predicted miRNA target proteins were also quantified in *drb1*: MBP1 (miR846), MBP2 (miR846), SAT3 (miR854), BXL7 (miR854) and AKR4C8 (miR781). Four of these five predicted miRNA targets had increased protein levels in *drb1* (Figure 6-6A) and RT-PCR revealed that the target transcripts were elevated accordingly (Figure 6-6B).

In *drb2* plants, the validated miRNA target AGO1 and the predicted miRNA targets MBP1, MBP2, BXL7 and AKR4C8 all over-accumulated relative to wild-type (Figure 6-6A). However, the transcript levels of these miRNA targets remained at approximately wild-type levels in *drb2* (Figure 6-6B). In addition, the proteomics analysis showed that APS1 and APS3 protein levels were reduced and unchanged, respectively, in *drb2* relative to wild-type plants; mRNA levels for these miRNA targets were at approximately wild-type levels in *drb2* (Figure 6-6A-B). For the *drb235* triple mutant, quantitative proteomics data were obtained for the validated miRNA targets AGO1 and APS1, and the predicted miRNA targets MBP2 and BXL7; the accumulation of each of these miRNA target proteins was observed to be comparable to *drb2* plants (Figure 6-7A). Similar to *drb2*, their transcript levels were either unchanged or slightly reduced in *drb235* (Figure 6-7B). Taken together, the proteomics analysis shows that DRB2 is required for miRNA-guided translational inhibition.

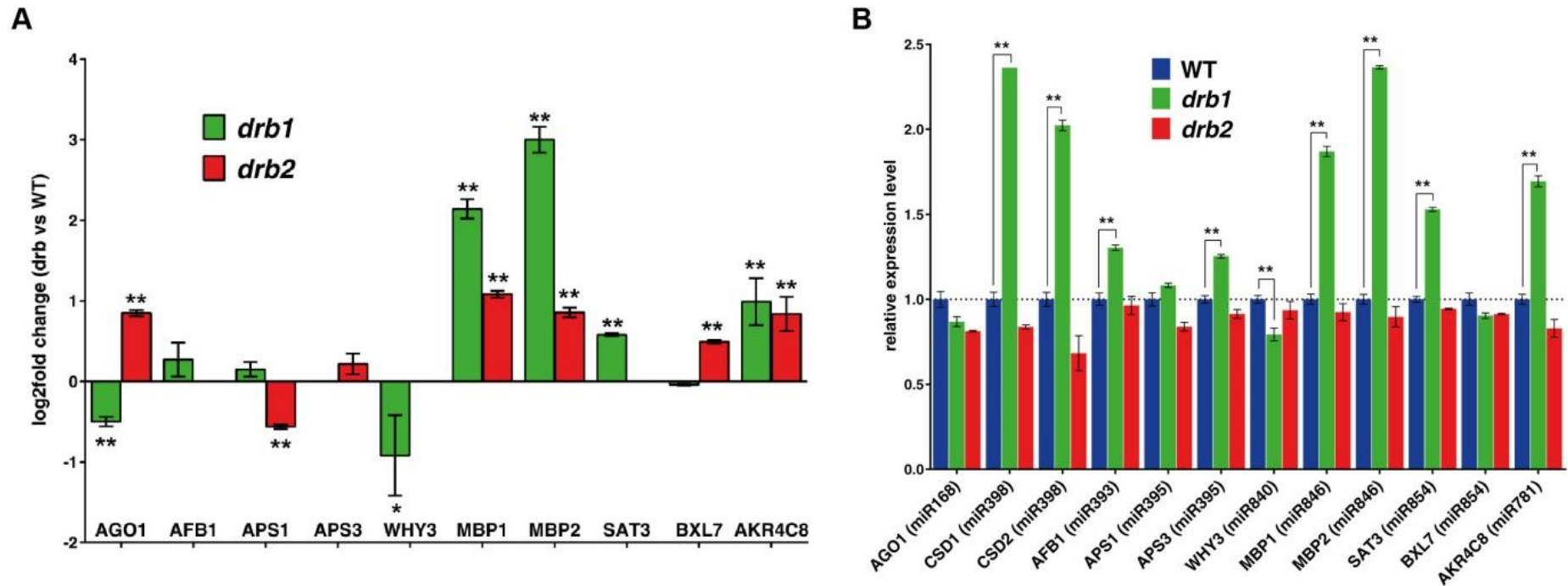


Figure 6-6. DRB2 is required for miRNA-guided translational inhibition in the shoot apex.

(A) Accumulation ratios of miRNA target proteins in *drb1* and *drb2* ($n = 2$; $p < 0.05^*$ or $< 0.01^{**}$; \pm SD). See also Table S6.

(B) RT-PCR analysis of miRNA target gene expression in wild-type (Col-0), *drb1* and *drb2* plants. All values were normalized to *ACT2* (AT3G18780). Gene expression ratios are relative to wild-type levels (dashed line) ($n = 3$, $**p < 0.01$, one-way ANOVA, \pm SD).

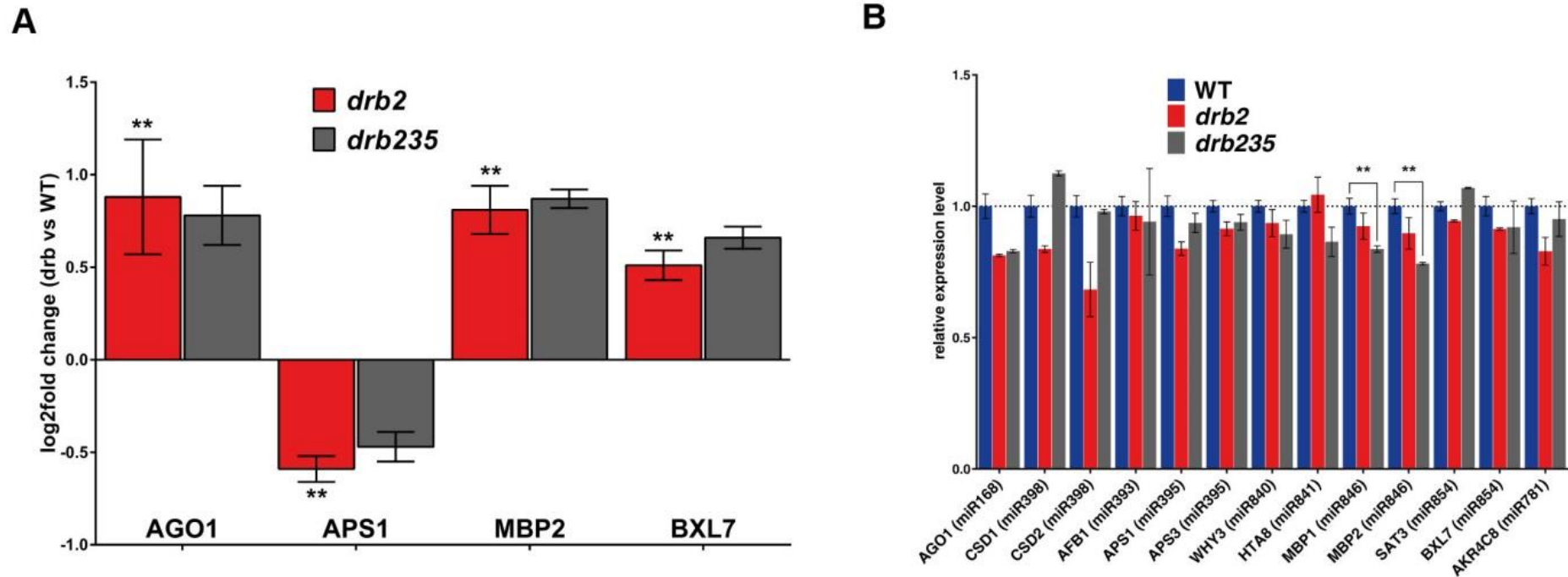


Figure 6-7. DRB3 and DRB5 are not required for miRNA-guided translational inhibition in the shoot apex.

(A) Protein accumulation ratios of miRNA targets identified in *drb2* and *drb235* mutants. Protein accumulation ratios are relative to wild-type (Col-0). Error bars represent +/- SD (n = 2).

(B) RT-PCR analysis of miRNA target gene expression in wild-type (Col-0), *drb2* and *drb235* plants. All values were normalized to *ACT2* (AT3G18780). Gene expression ratios are relative to wild-type levels (dashed line) (n = 3, **p < 0.01, one-way ANOVA, ±SD).

To validate the role of DRB2 in miRNA-guided translational inhibition, I used standard small RNA northern and western blotting approaches. *AGO1*, *CSD1* and *CSD2* have previously been demonstrated to be regulated via miRNA-guided translational inhibition (Brodersen et al., 2008; Dugas and Bartel, 2008; Lanet et al., 2009). In *drb1*, miR168 and AGO1 protein and mRNA levels were all comparable to wild-type (Figure 6-6B and Figure 6-8A-B). MiR398 was reduced in *drb1* (Figure 6-8A), and, as expected, CSD1 and CSD2 proteins and mRNAs over-accumulated (Figure 6-6B and Figure 6-8B). In *drb2* and *drb235*, AGO1, CSD1 and CSD2 proteins had elevated accumulation and, moreover, the elevation was similar between both mutants (Figure 6-8B). In contrast to *drb1*, the observed elevations in protein accumulation were disproportionate to the unchanged miRNA and target transcript levels in *drb2* and *drb235* mutants (Figure 6-7B and Figure 6-8A). Taken together, the results demonstrate that DRB2 is required for miRNA-guided translational inhibition, and suggest that DRB2 is the only DRB protein family member required for that pathway in the shoot apex of Arabidopsis.

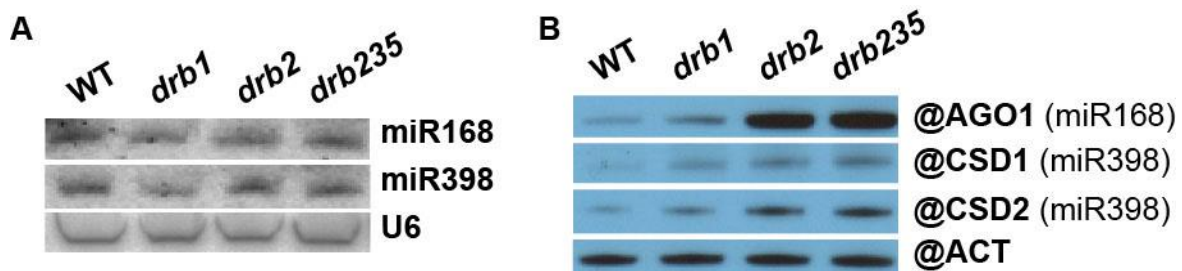


Figure 6-8. miRNA targets accumulate at protein level in shoot apex of *drb2*.

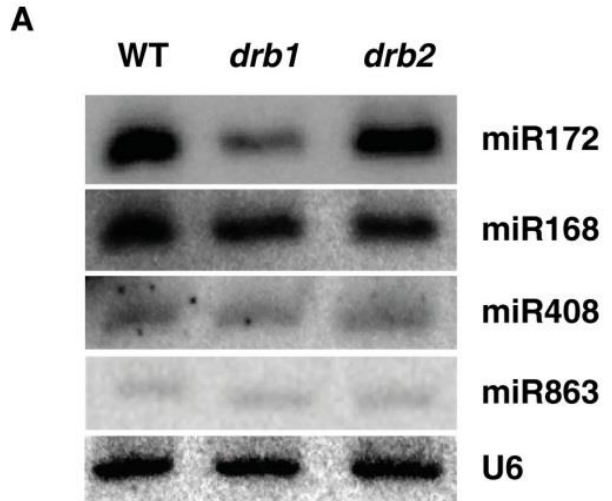
(A) Small RNA northern blot analysis of miR168 and miR398 accumulation in Col-0, *drb1*, *drb2* and *drb235* plants (n = 3). U6 was used as the loading control.

(B) Western blot analysis of AGO1 (miR168), CSD1 (miR398) and CSD2 (miR398) in Col-0, *drb1*, *drb2* and *drb235* plants (n = 3). ACTIN2 (ACT; AT3G18780) was used as the loading control.

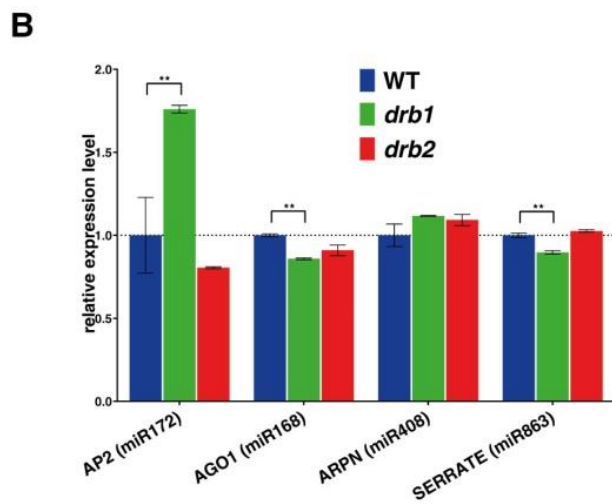
6.6 DRB2 directs miRNA-guided translational inhibition in flowers

Having established that DRB2 determines the translational inhibition mode of action for miRNAs in shoot apices, I examined whether it operates similarly in floral tissue, a known site for miRNA-guided translational inhibition in *Arabidopsis* (Chen, 2004a; Grant-Downton et al., 2013). I analyzed the respective target genes of miR168, miR172, miR408 and miR863, *ARGONAUTE1* (*AGO1*), *APETALA2* (*AP2*), *PLANTACYANIN* (*ARPN*) and *SERRATE* (*SE*). The molecular analyses showed that *AP2* mRNA and protein overaccumulate in *drb1* plants (Figure 6-9B-C) as a consequence of reduced miR172 accumulation (Figure 6-9A). These analyses also revealed that miR172 and *AP2* levels remain unchanged in *drb2* plants (Figure 6-9A-B), but *AP2* is disproportionately elevated (Figure 6-9C). Unlike the miR172/*AP2*/*AP2* relationship observed in *drb1* floral tissues, miR168, miR408 and miR863 accumulation remained unchanged, as did the mRNA and protein levels for their respective target genes (Figure 6-9A-C). miRNA accumulation and target gene expression remained at wild-type levels in *drb2* for miR172, miR168, miR408 and miR863 and their respective target genes (Figure 6-9A-B). However, western blotting showed that *AP2*, *AGO1*, *ARPN* and *SE* levels were disproportionately elevated in *drb2* (Figure 6-9C). Altogether, the results show that DRB2 is required for miRNA translational inhibition activity wherever it is expressed.

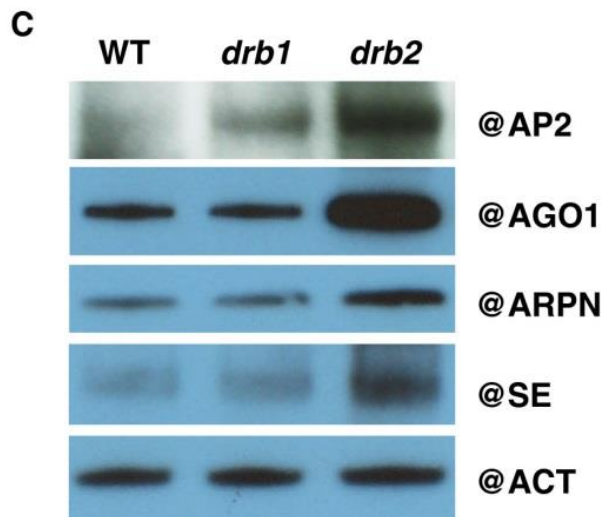
Figure 6-9. DRB2 is required for miRNA-guided translational inhibition in flowers.



(A) Northern blot analysis of miR172, miR168, miR408 and miR863 accumulation in wild-type (Col-0), *drb1* and *drb2* (n = 3). U6 accumulation serves as a loading control.



(B) RT-PCR analysis of miR172, miR168, miR408 and miR863 targets *AP2*, *AGO1*, *ARPN* and *SE*, respectively, in wild-type (Col-0), *drb1* and *drb2*. Values were normalized to *ACT2* (AT3G18780). Gene expression ratios are relative to wild-type levels (dashed line) (n = 3, **p < 0.01, one-way ANOVA, ±SD).



(C) Western blotting analysis of *AP2*, *AGO1*, *ARPN* and *SE* protein accumulation in wild-type, *drb1* and *drb2* (n = 3). *ACT* accumulation serves as loading control.

6.7 Protein machinery required for miRNA-directed translational inhibition

KTNI and *SUO* have been shown to be required for miRNA-guided translational inhibition (Brodersen et al., 2008; Yang et al., 2012). To study the role of *DRB2* in the context of currently known proteins required for that pathway, I compared the miRNA activity in *drb2* to that in *lue-1* (*KTNI*) and *suo2*. MiR168 and miR398 accumulated to approximate wild-type levels in *drb2* and *lue1* plants, but were reduced in *suo-2* (Figure 6-10A). RT-PCR revealed that *AGO1* and *CSD2* mRNA expression remained unchanged in all three mutant backgrounds (Figure 6-10B). Surprisingly, AGO1 protein did not over-accumulate in *lue1* or *suo-2* (Figure 6-10C), but substantially over-accumulated in *drb2*. *CSD2* accumulated to higher than wild-type levels in all three mutant backgrounds, again to a higher level in *drb2* (Figure 6-10C). These results show that miRNA-guided translational inhibition is complex and possibly utilizes a variety of combinatorial components downstream of miRNA biogenesis.

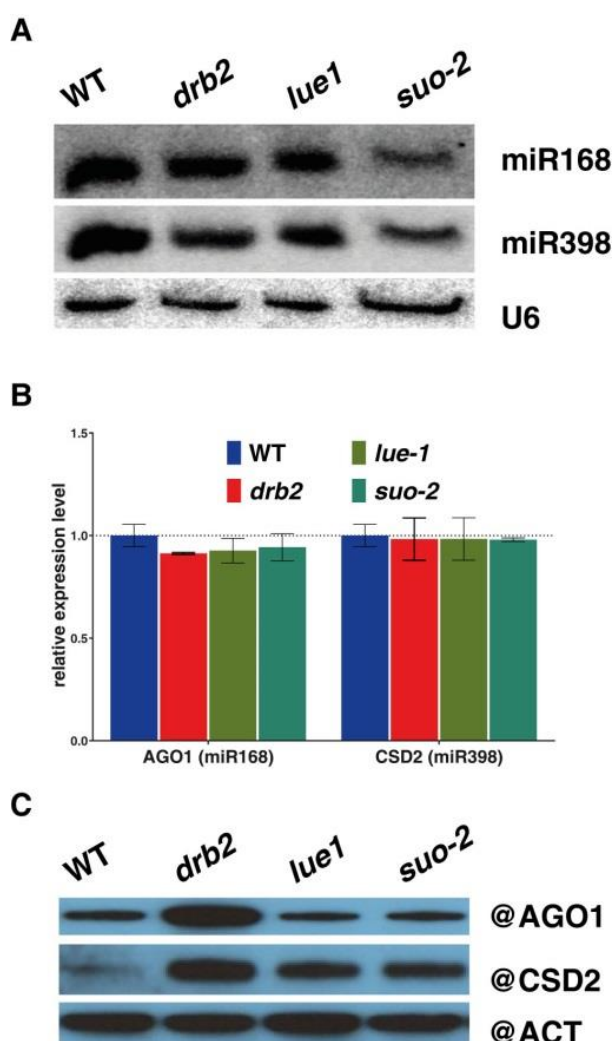


Figure 6-10. Translation inhibition machinery.

(A) Northern blots analysis of miR168 and miR398 accumulation in wild-type (Col-0), *drb2*, *lue1* and *suo-2* (n = 3). U6 accumulation serves as a loading control.

(B) RT-PCR analysis *AGO1* (miR168) and *CSD2* (miR398) in wild-type (Col-0), *drb2*, *lue1* and *suo-2*. Values were normalized to *ACT2* (AT3G18780). Gene expression ratios are relative to wild-type levels (dashed line) (n = 3, **p < 0.01, one-way ANOVA, \pm SD).

(C) Western blotting analysis of AGO1 and CSD2 protein accumulation in wild-type, *drb2*, *lue1* and *suo-2*. ACT accumulation serves as loading control.

6.8 DRB2 represses *DRB1* expression

I also looked at the inter-relationship of DRB1, DRB2 and DCL1. *DCL1* is a target of miR162, which provides an important negative feedback to the miRNA pathway (Xie et al., 2003). In *drb1*, *DCL1* accumulated to higher levels than in the wild-type (Figure 6-11B,C), presumably through decreased cleavage from reduced levels of miR162 (Figure 6-11A). In contrast, the levels of miR162 and *DCL1*, in *drb2*, were similar to those of wild-type plants (Figure 6-11A-C). This suggests that *DCL1* over-accumulates in *drb1*, which may partially compensate for the reduced precision in miRNA production. Surprisingly, DRB1 protein and mRNA levels were elevated in *drb2* plants (Figure 6-11B-C), indicating that *DRB1* expression is repressed at the transcriptional level by DRB2, probably indirectly by miRNA-mediated regulation of transcription factors. The inter-regulation that occurs between DRB1 and DRB2 provides an explanation for the mild developmental phenotype of *drb2* (Figure 6-11D). In these plants, elevated DRB1 levels might be compensating for the lack of DRB2, through DCL1/DRB1 miRNA production and target cleavage, and as a consequence mask the importance of DRB2 under standard growth conditions. To test this, *drb12*, *drb13*, *drb14*, *drb15* and *drb135* double and triple mutants (Curtin et al., 2008; Eamens et al., 2012a, 2012b) were examined. Of the *drb* mutants, *drb12* plants were highly deformed and virtually unable to grow, whereas the others had milder largely *drb1*-like phenotypes (Figure 6-11D). This shows the key role played by DRB2 in plant growth and development.

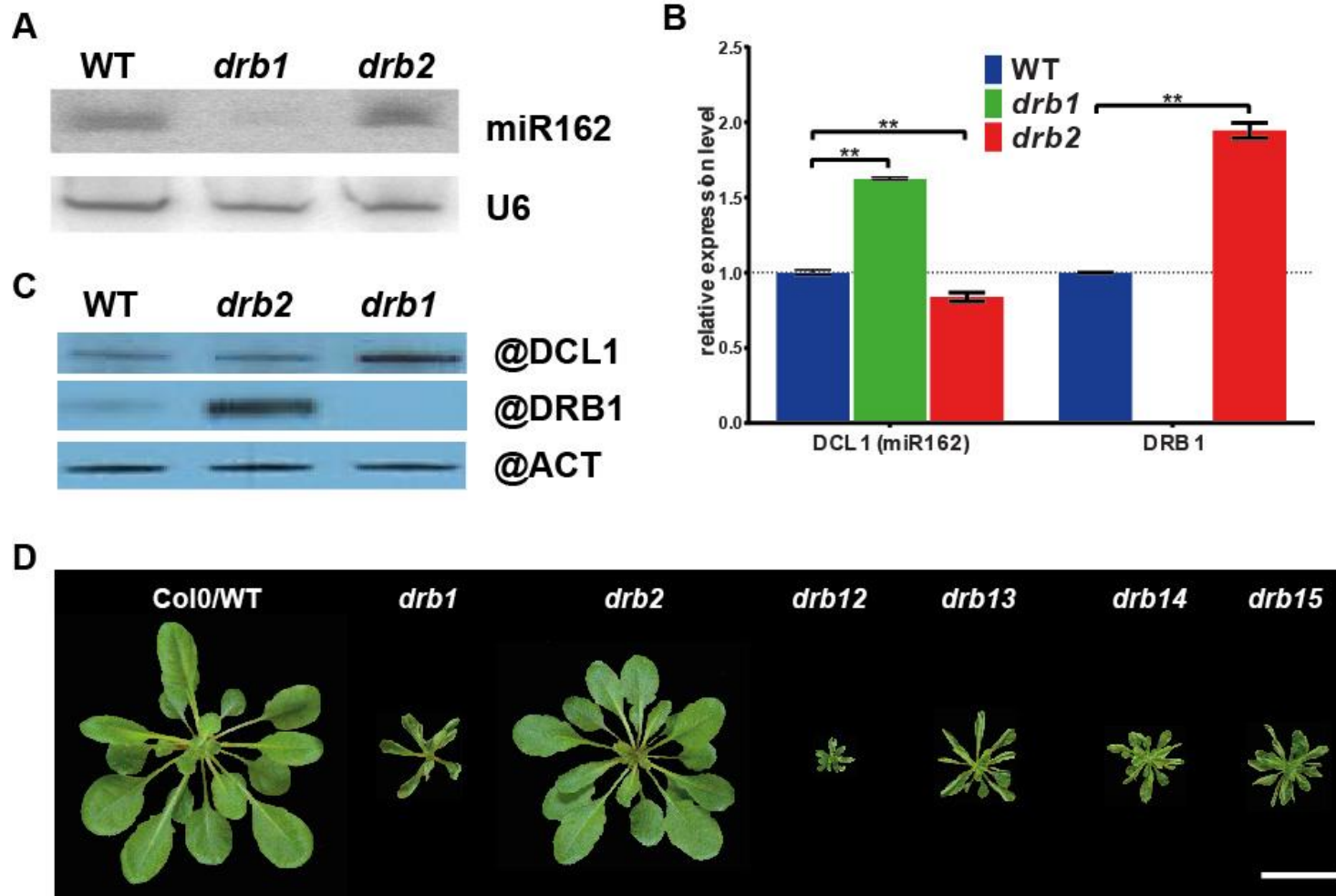
Figure 6-11. DRB2 represses DRB1 expression in shoot apex.

(A) Northern blot analysis of miR162 accumulation in wild-type, *drb1* and *drb2* (n = 3). U6 was loading control.

(B) Transcript levels of *DCL1* (miR162) and *DRB1* in wild-type, *drb1* and *drb2*. Normalized to *ACT2* (AT3G18780) expression; ratios relative to wild-type levels (dashed line) (n = 3, **p < 0.01, one-way ANOVA, ±SD).

(C) Western blot analysis of DCL1 and DRB1 protein accumulation in wild-type, *drb1* and *drb2* (n = 3). ACTIN2 was loading control.

(D) Phenotype of 4-week-old wild-type and *drb* mutant plants under short-day cycle (8 h light/16 h dark). Scale bar, 25 mm.



day cycle (8 h light/16 h dark). Scale bar, 25 mm.

6.9 DRB1 and DRB2 are evolutionary conserved in plants

The importance of DRB2 for growth and development in *Arabidopsis* raised the possibility that it might also be present in other species. Investigating this identified orthologs of *Arabidopsis* DRB1 and DRB2 in the genomes of all 30 multicellular plant species examined. These species ranged from non-vascular moss, through primitive non-flowering and ancient flowering vascular plants, to monocots and eudicots (Figure 6-12A and Table 6-2). Interestingly, the DRB2 orthologs were much more conserved than those of DRB1 (Figure 6-12A). The amino acid sequences of the dsRNA-binding amino-terminal domains (dsRBDs) of *Arabidopsis* DRB2 are approximately 80% identical to *Amborella* (ancient eudicot), *Selaginella* (non-flowering plant) and *Physcomitrella* (moss) orthologs (Figure 6-12B), while the DRB1 domains have 67% identity to *Amborella* and about 40% to *Selaginella* and *Physcomitrella* orthologs (Figure 6-13). This suggests that DRB2 has been a constant and important player during 600 million years of plant evolution and that miRNAs operate not only through cleavage (Floyd and Bowman, 2004) but also by translational repression in primitive plants. Indeed, it is possible that translational repression may have been the primary form of miRNA directed gene regulation in ancient plants.

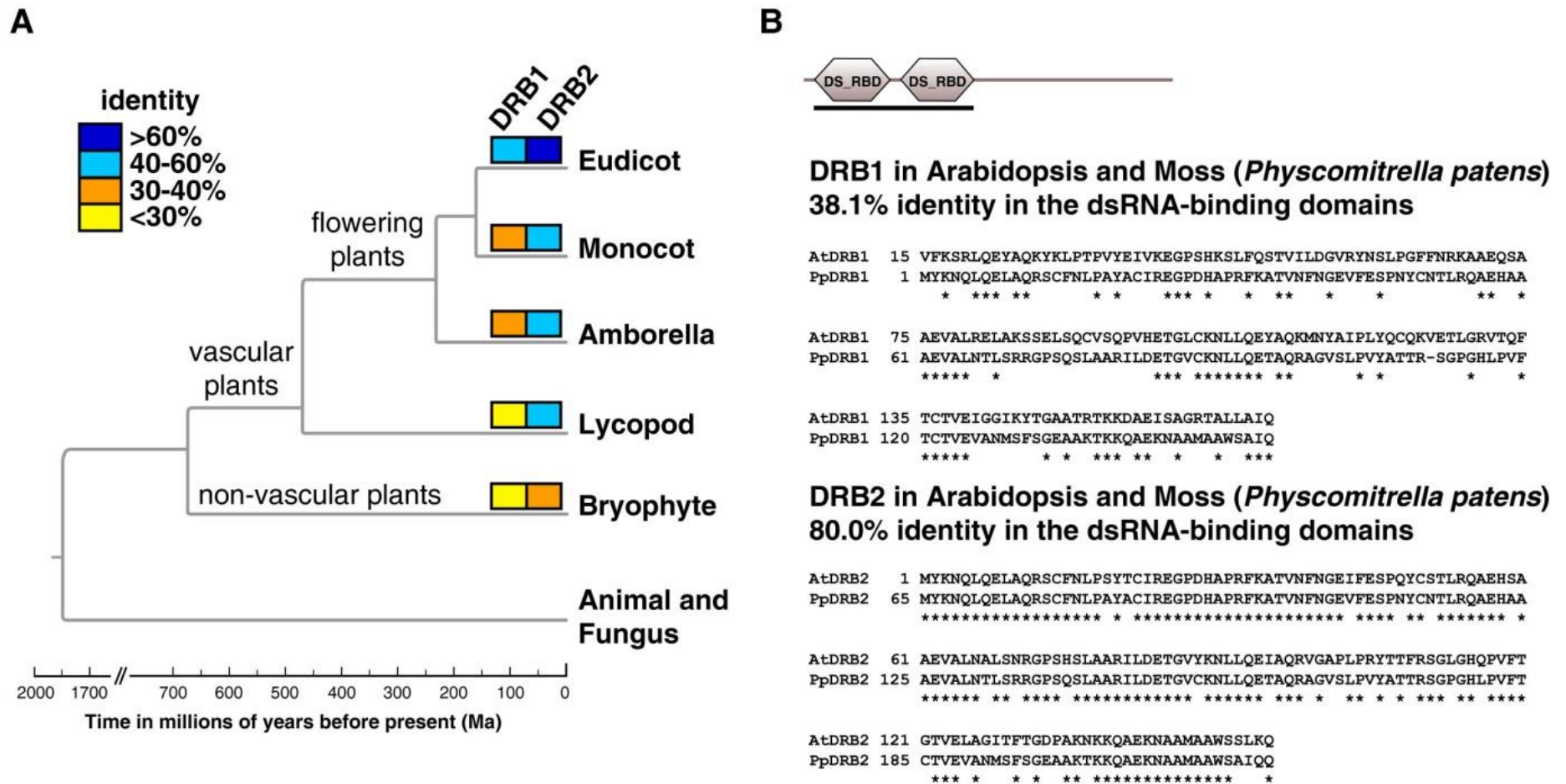


Figure 6-12. Evolutionary conservation of DRB1 and DRB2.

(A) Evolutionary conservation of putative Arabidopsis DRB1 and DRB2 ortholog proteins (full length sequence) across plant species.

(B) Protein sequence alignment of the dsRNA-binding domains (dsRBDs) of Arabidopsis DRB1 and DRB2 with moss (*Physcomitrella patens*) orthologs.

Table 6-2. DRB1 and DRB2 putative orthologs in plant species.

Plant specie	Clade	DRB1 ortholog*	DRB2 ortholog*
<i>Amborella trichopoda</i>	Amborella	AMTR_s00033p00230080	AMTR_s00148p00030810
<i>Physcomitrella patens</i>	Bryophyte	Pp1s173_93V6	PHYPADRAFT_88725
<i>Arabidopsis lyrata</i>	Eudicot	ARALYDRAFT_471071	ARALYDRAFT_481667
<i>Arabidopsis thaliana</i>	Eudicot	AT1G09700	AT2G28380
<i>Aquilegia coerulea</i>	Eudicot	Aquca_007_00512	Aquca_009_00003
<i>Brassica rapa</i>	Eudicot	Bra019999	Bra035704
<i>Capsella rubella</i>	Eudicot	Carubv10009604m.g	Carubv10023224m.g
<i>Carica papaya</i>	Eudicot	evm.TU.contig_34457.2	evm.TU.supercontig_216.1
<i>Citrus sinensis</i>	Eudicot	orange1.1g014809m.g	orange1.1g012154m.g
<i>Cucumis sativus</i>	Eudicot	Cucsa.160550	Cucsa.200460
<i>Eucalyptus grandis</i>	Eudicot	Eucgr.B01706	Eucgr.J00927
<i>Fragaria vesca</i>	Eudicot	gene12149-v1.0-hybrid	gene21565-v1.0-hybrid
<i>Glycine max</i>	Eudicot	Glyma04g10230	Glyma12g08070
<i>Gossypium raimondii</i>	Eudicot	Gorai.010G034400	Gorai.003G142000
<i>Linum usitatissimum</i>	Eudicot	Lus10008862.g	Lus10021471.g
<i>Malus domestica</i>	Eudicot	MDP0000219451	MDP0000188414
<i>Medicago truncatula</i>	Eudicot	Medtr3g100120	Medtr2g094490
<i>Mimulus guttatus</i>	Eudicot	mgv1a009077m.g	mgv1a008321m.g
<i>Phaseolus vulgaris</i>	Eudicot	Phvul.009G036100	Phvul.011G079700
<i>Prunus persica</i>	Eudicot	ppa004305m.g	ppa024708m.g
<i>Ricinus communis</i>	Eudicot	29908.t000326	27538.t000020
<i>Solanum tuberosum</i>	Eudicot	PGSC0003DMG400009356	PGSC0003DMG400008053
<i>Theobroma cacao</i>	Eudicot	Thecc1EG034521	Thecc1EG042059
<i>Vitis vinifera</i>	Eudicot	GSVIVG01009189001	GSVIVG01025192001
<i>Populus trichocarpa</i>	Eudicot	Potri.002G111400	Potri.017G063700
<i>Selaginella moellendorffii</i>	Lycopsid	SELMODRAFT_106185	SELMODRAFT_431451
<i>Brachypodium distachyon</i>	Monocot	Bradi2g35730	Bradi3g28977
<i>Oryza sativa</i>	Monocot	LOC_Os11g01869	LOC_Os10g33970
<i>Setaria italica</i>	Monocot	Si010100m.g	Si034815m.g
<i>Sorghum bicolor</i>	Monocot	Sb08g000900	Sb01g019110
<i>Zea mays</i>	Monocot	GRMZM2G179031	GRMZM2G027462

* Locus identity.

A. thaliana DRB1 vs A. trichopoda putative ortholog

67.3% identity in 156 residues overlap; Score: 528.0; Gap frequency: 1.3%

```

DRB1_D1D2      1 VFKSRLQEYAKYKLPVYIEIVKEGSPSHKSLFQSTVILDGVRVNSLPGFFNRKAAEQSA
Amborella      1 VFKSRLQEYAKGAGIPTVYETVKEGSPSHEPIFRSSVTINDVKYDSLPGFANRKAEEQSA
*****
DRB1_D1D2     61 AEVALRELAKSSELSQCVSQPVHETGLCKNLLQEYAKMNYAIPLYQCQKQVETLGRVTQF
Amborella     61 AEVALMELLKSGTMD-CIPHPVHETGLCKNLLQEYAKMSYSVPSYTCR-DSNSNISF
*****
DRB1_D1D2    121 TCTVEIGGIKYTGAAATRTKKDAEISAGRTALLAIQ
Amborella    119 VCTVEIGGIQYIGGAAKTKKEAEIKAAARTALLAIQ
*****

```

A. thaliana DRB1 vs P. patens putative ortholog

38.1% identity in 155 residues overlap; Score: 263.0; Gap frequency: 0.6%

```

DRB1_D1D2      1 VFKSRLQEYAKYKLPVYIEIVKEGSPSHKSLFQSTVILDGVRVNSLPGFFNRKAAEQSA
Physcomitr     1 MYKNQLQELAQSCFNLPAYACIREGPDHAPRFKATVNFNGEVFESPNYCNTLRQAEHAA
*****
DRB1_D1D2     61 AEVALRELAKSSELSQCVSQPVHETGLCKNLLQEYAKMNYAIPLYQCQKQVETLGRVTQF
Physcomitr     61 AEVALNTLSRRGPSQSLAARILDETVGCKNLLQETAQRAGVSLPVYATTR-SGPGHLPVF
*****
DRB1_D1D2    121 TCTVEIGGIKYTGAAATRTKKDAEISAGRTALLAIQ
Physcomitr    120 TCTVEVANMSFSGEAAKTKKQAEKNAAMAASAIQ
*****

```

A. thaliana DRB1 vs S. moellendorffii putative ortholog

43.9% identity in 155 residues overlap; Score: 317.0; Gap frequency: 0.6%

```

DRB1_D1D2      1 VFKSRLQEYAKYKLPVYIEIVKEGSPSHKSLFQSTVILDGVRVNSLPGFFNRKAAEQSA
Selaginell     1 MYKSQLEFAQKSGWTPQYDSIKQGLPHLPRFQASVEVNGVKYSEDFPNLKAEEHSA
*****
DRB1_D1D2     61 AEVALRELAKSSELSQCVSQPVHETGLCKNLLQEYAKMNYAIPLYQCQKQVETLGRVTQF
Selaginell     61 AKKALDSLTTGGANGASTDASGSSMTGLCKNVLQEYQRNGFSLPIYQIE-ITGSPSHNSVF
*****
DRB1_D1D2    121 TCTVEIGGIKYTGAAATRTKKDAEISAGRTALLAIQ
Selaginell    120 AATVEIGGVLYKGGTAKSKKEAEVKAARTAILAIK
*****

```

A. thaliana DRB2 vs A. trichopoda putative ortholog

87.1% identity in 155 residues overlap; Score: 704.0; Gap frequency: 0.0%

```

DRB2_D1D2      1 MYKNQLQELAQSCFNLPYSYTCIREGPDHAPRFKATVNFNGEIFESPQYCSLTLRQAEHSA
Amborella      1 MYKNQLQELAQSCFNLPYSYTCIREGPDHAPRFKAAVNFNGEVFESPGFCTTLRQAEHAA
*****
DRB2_D1D2     61 AEVALNALSNRGPSHSLAARILDETVGYKNLLQEIAQRVGAAPLPRYTTFRSGLGHQPVFT
Amborella     61 AEVALNTLSNRGPSQSLAARILDETVGYKNLLQEIAQRAGAALPVYTTVRSGLGHLPVFT
*****
DRB2_D1D2    121 GTVELAGITFTGDPARNKKQAEKNAAMAASLQ
Amborella    121 CTVELAGISFSGEPAKSKKQAEKNAAMAASLQ
*****

```

A. thaliana DRB2 vs P. patens putative ortholog

80.0% identity in 155 residues overlap; Score: 648.0; Gap frequency: 0.0%

```

DRB2_D1D2      1 MYKNQLQELAQSCFNLPYSYTCIREGPDHAPRFKATVNFNGEIFESPQYCSLTLRQAEHSA
Physcomitr     1 MYKNQLQELAQSCFNLPAYACIREGPDHAPRFKATVNFNGEVFESPNYCNTLRQAEHAA
*****
DRB2_D1D2     61 AEVALNALSNRGPSHSLAARILDETVGYKNLLQEIAQRVGAAPLPRYTTFRSGLGHQPVFT
Physcomitr     61 AEVALNTLSRRGPSQSLAARILDETVGCKNLLQETAQRAGVSLPVYATTRSGPGHLPVF
*****
DRB2_D1D2    121 GTVELAGITFTGDPARNKKQAEKNAAMAASLQ
Physcomitr    121 CTVEVANMSFSGEAAKTKKQAEKNAAMAASAIQ
*****

```

A. thaliana DRB2 vs S. moellendorffii putative ortholog

81.3% identity in 155 residues overlap; Score: 665.0; Gap frequency: 0.0%

```

DRB2_D1D2      1 MYKNQLQELAQSCFNLPYSYTCIREGPDHAPRFKATVNFNGEIFESPQYCSLTLRQAEHSA
Selaginell     1 MYKNQLQELAQSCFNLPAYSICIREGPDHAPRFKAAVNFNGEVFESPNYCSTLRQAEHAA
*****
DRB2_D1D2     61 AEVALNALSNRGPSHSLAARILDETVGYKNLLQEIAQRVGAAPLPRYTTFRSGLGHQPVFT
Selaginell     61 AELALNVLSRRGPSQSLAARILDETVGFKNLLQETAQRANVPLPTTYTTFRSGPGHLPVF
*****
DRB2_D1D2    121 GTVELAGITFTGDPARNKKQAEKNAAMAASLQ
Selaginell    121 CVVEVAGMNFSGDAGTKKQAEKNAAMAASLQ
*****

```

Figure 6-13. Alignment of dsRNA binding domains (RBD) of DRB1 and DRB2 orthologs.*Amborella trichopoda* (ancient eudicot), *Selaginella moellendorffii* (non-flowering plant) and *Physcomitrella patens* (moss) orthologs.

6.10 Chapter highlights

- ✦ sRNA sequencing revealed ~38% of miRNAs are reduced in shoot apex of *drb2*.
- ✦ miRNA strand selection was unaffected in *drb2*, but some miRNAs were inaccurately processed.
- ✦ miRNA target transcript expression remains unchanged (144/149 transcripts) in *drb2*.
- ✦ miRNA accumulation and target gene expression do not correlate in *drb2* shoot apex, in contrast with a clear correlation in *drb1* plants.
- ✦ Transcriptomic analysis (microarray) revealed changes in gene expression of a large number of transcripts in *drb2* shoot apex.
- ✦ Metabolic labelling allowed detection and quantification of thousands of proteins in the shoot apex of wild-type and *drb1*, *drb2* and *drb235* mutants.
- ✦ Ten proteins, product of miRNA targets, were reliably detected and quantified.
- ✦ Proteomics, western blotting, northern blotting and RT-PCR revealed that DRB2 is required for miRNA-directed translational inhibition in the shoot apex.
- ✦ No evidence for requirement of DRB3 and DRB5 in translation inhibition.
- ✦ DRB2 is required for translational inhibition in floral tissue, suggesting its general requirement in this pathway.
- ✦ DRB2, but not SUO and KTN1, appears to be a determining factor for miRNA-guided translational inhibition.
- ✦ Study of *drb1* and *drb2* mutants revealed previously unknown miRNA-guided translational inhibition of SERRATE (SE) and PLANTACYANIN (ARPN) in flowers.
- ✦ Study of *drb1* and *drb2* also revealed that translational inhibition plays a major role in the autoregulation of miRNA pathway through the regulation of SE and AGO1.
- ✦ DRB2 represses *DRB1* expression, possibly via a transcription factor regulated by miRNA translational inhibition activity.
- ✦ Regulation of DRB1 by DRB2 suggests that miRNA-guided cleavage and translation inhibition are mutually exclusive modes of action in a given cell or tissue.
- ✦ Regulation of DRB1 by DRB2 also suggests that, in the *drb2* mutant, *DRB1* over-expression functions as a compensatory mechanism explaining its mild developmental phenotype.
- ✦ DRB2 is strikingly conserved in evolution, suggesting that translational repression may have been the primary form of miRNA directed gene regulation in ancient plants.

**Chapter 7 - Regulation of protein
accumulation by double-
stranded RNA binding
proteins DRB1 and DRB2**

Dicers interact with a double-stranded RNA (dsRNA)-binding (DRB) protein to produce miRNAs, small RNAs with regulatory functions (Fukunaga et al., 2012; Han et al., 2004a, 2004b). A miRNA can regulate its target genes by translation inhibition or by transcript cleavage, and these two forms of control have different characteristics and consequences (Ameres and Zamore, 2013; Gandikota et al., 2007; Meijer et al., 2013). In the previous chapter, I showed that Arabidopsis DRB2 determines miRNA-guided translation inhibition and represses DRB1, the driver for transcript cleavage. However, the biological significance of having these two mechanistically distinct miRNA-directed RNA silencing pathways remains unknown. In this chapter, I examined the differential accumulation of proteins in shoot apex, a developmentally important tissue, of *drb1* and *drb2* mutants.

In the previous chapter, a large set of proteins with altered accumulation in *drb1* and *drb2* were identified in the proteomics analysis. I then took a systems biology approach to study their biological significance. First, experimentally determined binary protein-protein interactions (PPIs) were used to build a shoot apex interactome. Next, proteins differentially accumulated in *drb1* and *drb2* were assigned functions according to their protein interactions and gene ontology. Binary PPIs were assigned to about one third of all differentially expressed proteins and, together with gene ontology (GO) analysis, several regulatory hubs were identified within these proteins. DRB1 and DRB2 were determined to have different impacts on specific physiological and metabolic processes, including photosynthesis, glycoside metabolism and stress response. Interestingly, individual proteins within PPI clusters often showed co-regulation by DRB1 and/or DRB2, providing evidence for tight regulation of certain processes. Furthermore, several processes known to be regulated by miRNAs showed pronounced protein over-accumulation of non-miRNA targets, suggesting that miRNAs are triggers for rewiring of entire processes. Moreover, both PPI network and GO analysis indicated a response to salt stress, and further experiments revealed an opposite effect of *DRB1* and *DRB2* null mutation – hypersensitivity and resistance, respectively. Taken together, the results reveal regulatory clusters involving different miRNA modes of action, show that they are more specific than previously thought, and points to processes that might be specific to either miRNA-guided transcript cleavage or translational inhibition.

7.1 Arabidopsis Shoot Apex Interactome

Interactomes are often built on binary protein-protein interactions, and their biological relevance relies on the differential expression of each individual protein (Arabidopsis Interactome Mapping Consortium, 2011; Braun et al., 2013; Mallick and Kuster, 2010). To

understand the patterns of protein expression in Arabidopsis, Baerenfaller et al. (2008) assembled a comprehensive proteome map for different Arabidopsis tissues, including roots, leaves and flowers. Although it provides plant researchers with invaluable experimental data, developmentally important tissues, such as shoot apex, were not included in the proteome map. Pre-flowering shoot apex (as previously defined here) is in the interface between roots and leaves, and contains the shoot apical meristem (SAM), a stem cell niche.

To study the proteome and interactome of the shoot apex, wild-type and *drb1* and *drb2* mutants were metabolically labeled. Proteins were extracted from shoot apex and identified and quantified by standard mass spectrometry-based proteomics (see Experimental Procedures and previous Chapter for details). This approach identified and quantified 1664 unique proteins among *drb1* and *drb2*, relative to wild-type, in pre-flowering shoot apex (three week old plants) (Figure 7-1A). Next, a shoot apex interactome was assembled based on experimentally validated PPI (obtained from BioGRID v3.2.109, released in February 1, 2014). To build an interaction network, identified and quantified proteins and their interactors, either identified or not, were considered. Binary PPIs were assigned to 460 of the 1664 (28%) total identified and quantified proteins (Figure 7-1A), and the resulting network had 1917 proteins (nodes) with 2802 interactions (edges) (Figure 7-1B). Compared to BioGRID, a main repository for Arabidopsis PPIs (Chatr-Aryamontri et al., 2013), which currently hosts 17,162 non-redundant binary PPIs for 7,116 unique Arabidopsis proteins, the shoot apex interactome showed a large subset of known interactions.

A

Proteins	<i>drb1</i>	<i>drb2</i>	Combined	Shared
Total	1397	1238	1664	961 (58%)
Differential	319	226	464	81 (18%)
Decrease	121	110	202	29 (15%)
Increase	198	116	261	53 (20%)

Network	
PPI assigned	460 (28%)
Differential	153 (28%)
Nodes (total)	1917
Nodes (differentials)	366
Edges	2802

B

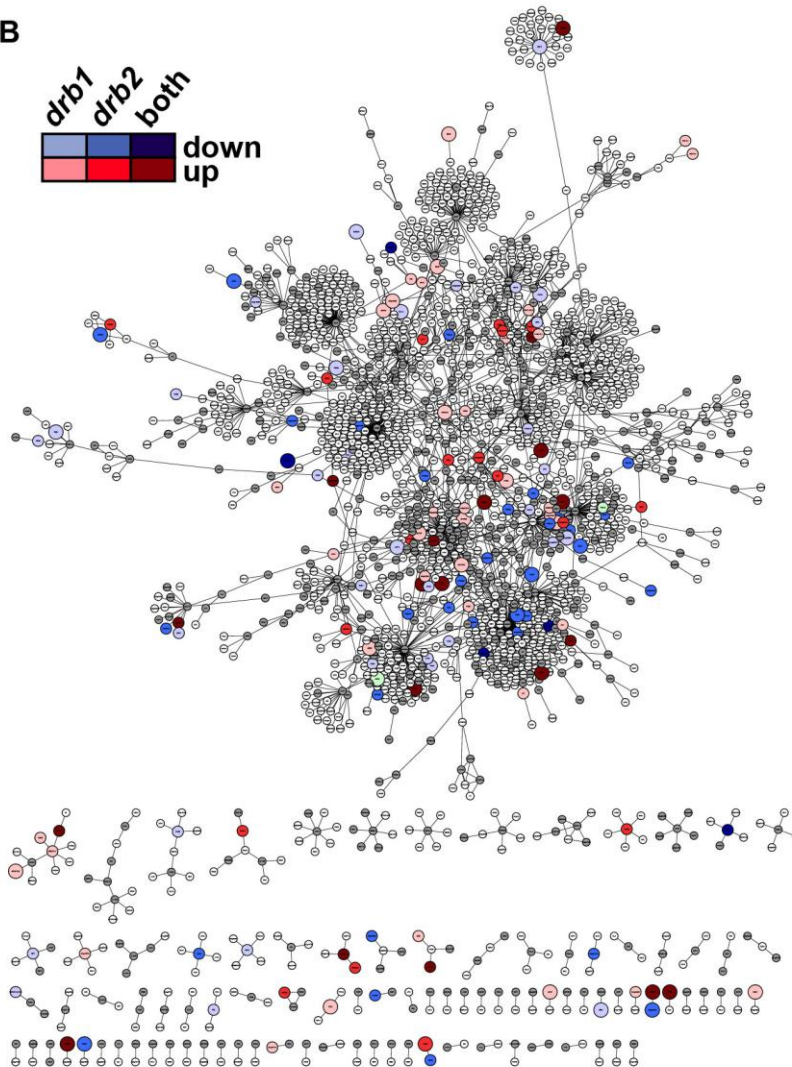


Figure 7-1. Shoot apex interactome.

(A) Distribution of identified proteins and interaction network. Number of non-redundant proteins among *drb1* and *drb2* (“combined” dataset) and protein sharing similar profiles (“shared” dataset) are shown (top). The network was built on PPI assigned to identified proteins (node). Each interaction (edge) has been experimentally determined elsewhere (refer to Experimental Procedures for details).

(B) Interaction network of proteins in shoot apex. Colours refer to differential expression in *drb1*, *drb2* or both, relative to wild-type. White, not detected; grey, detected to wild-type levels. Circle sizes refer to statistical *p*-value (see Experimental Procedures for details): large ($p < 0.01$), medium ($p < 0.5$) and small ($p \geq 0.5$, or not detected).

7.2 Altered protein accumulation in *drb1* and *drb2* shoot apex

The results presented in the previous chapter show that DRB2 determines miRNA-guided translational inhibition and represses *DRB1*, the driver for transcript cleavage. To understand the biological consequences of this functional dichotomy in miRNA modes of action, I generated and analyzed the shoot apex interactome of *drb1* and *drb2* plants, and compared the protein expression to that of wild-type Arabidopsis. These mutants shared a total of 81 proteins with differential accumulation (~20% of all differentials). In *drb1* more proteins were observed with increased accumulation (198) than reduced (121), whereas increased and reduced proteins were in similar proportion in *drb2* (Figure 7-1A). It was possible to include a total of 153 proteins with differential accumulation to the shoot apex interactome, which corresponds to ~30% of all non-redundant differentials identified in *drb1* and *drb2* (Figure 7-1B).

7.3 Network rewiring in *drb1* and *drb2* mutants

Protein-protein interaction rewiring occurs as a consequence of altered accumulation of protein(s) that lead to new interactions (Goel and Wilkins, 2012), and this may have major impacts on development and adaptive responses to the environment (Arabidopsis Interactome Mapping Consortium, 2011). Network rewiring caused by null mutation of *DRB1* and *DRB2* in the shoot apex showed subnetworks, or clusters (Table 7-1) containing different combinations of altered protein accumulation, such as reduced accumulation in both *drb1* and *drb2* (e.g., cluster 2), antagonistic effect (e.g., cluster 6) and increased accumulation in both mutants (e.g., cluster 22) (Figure 7-2). Table 7-1 provides identification and quantification parameters, as well as biological function, for each clustered protein.

Clusters of proteins may represent functional complexes, hence, clusters that have more than one differential protein might indicate coordinated regulation of an entire process (Fung et al., 2012). Cluster 2 showed reduced accumulation of FVE and HOS1 in *drb1* and *drb2*, respectively, suggesting that flowering time and response to cold are regulated synergistically by DRB1 and DRB2 (Figure 7-2 and Table 7-1). RCA (light activation of Rubisco) and CPN60B (Caperonin) were, however, only reduced in *drb2* (Cluster 3). CPN60B has been shown to play a role in photosynthesis acclimatization to heat stress, possibly by protecting RCA from thermal denaturation (Salvucci, 2008); hence, Cluster 3 suggests a role for DRB2 in this process. The dark green coloration and enhanced anthocyanin levels displayed by *drb2*

aerial tissues, rosette leaves and rosette leaf petioles (Curtin et al., 2008; Eamens et al., 2012a), supports that photosynthesis pathway is altered in *drb2* plants.

Several putative SUMOylated proteins were also identified (Cluster 6). The covalent attachment of SUMO (small ubiquitin-like modifier) to other proteins posttranscriptionally affects a broad range of processes, including maintenance of genome integrity, transcriptional regulation, nuclear transport and signal transduction, as well as protecting proteins from ubiquitin addition (Praefcke et al., 2012). The role SUMOylation plays in *drb1* and *drb2* is difficult to predict, as SUMO1 and SUMO3 accumulation was either unchanged or undetected (Table 7-1). However, Cluster 6 is enriched in plant defense, flowering time and cold stress-related proteins, suggesting a coordinated regulation of these processes. Protein modifiers ubiquitin and SUMO are structurally and functionally related (Praefcke et al., 2012). Ubiquitin UBI1 interactors PCNA2 and MBP1, which are involved in DNA repair and plant defense, respectively, were also altered in *drb1* and *drb2* mutants, but UBI1 was also not detected (Cluster 7).

Cluster 10 is a combination of two protein smaller clusters in contact through the transcription factors PIP3 and NTL9 and NAC089. The water transport smaller cluster (PIP proteins) has four members with reduced accumulation in *drb1*, but unchanged level in *drb2*, relative to wild-type, suggesting that DRB1 and DRB2 play different roles in response to osmotic stress. The other smaller cluster is functionally heterogeneous and has seven proteins that over-accumulated in either or both *drb* mutants (Cluster 10). These proteins are involved in various processes, such as signal transduction (RAB8), metabolism (CYP71B6), protein transport (SEC61 BETA), protein folding (FKBP15-1), water and ammonium transport (DELTA-TIP), and cold and light stress (OEP16-1). This result raises the possibility that these seemingly unrelated proteins might be co-regulated and involved in similar process(es), such as Golgi-dependent protein modification and transport.

Interestingly, PPI clusters related to oxidative stress had increased protein accumulation in either or both *drb* mutants (Cluster 17, 19, 20 and 21) (Figure 7-2 and Table 7-1). Peroxisome-related proteins, PEX11D and PEX11C (Cluster 17), and SOX (Cluster 21), had increased accumulation in *drb1*; annexin ANNAT4 (Cluster 19) and glutathione peroxidase GPX2 (cluster 20) were elevated in *drb2*; ANNAT1 (Cluster 19), AT3G14990 (Cluster 20) and peroxisomal LACS7 (Cluster 21) were elevated in both *drb* mutants. The increased accumulation of several proteins involved in oxidative stress responses suggests that both *drb*

mutants were under oxidative stress, possibly caused by loss of cellular and metabolic homeostasis.

Four proteins involved in sulfur metabolism (e.g., sulfur assimilation and cysteine biosynthesis), Cluster 22, over-accumulated in either *drb1* or both *drb* mutants. Plants play an important role in the sulfur cycle through its assimilation from the environment and conversion into methionine and cysteine and, furthermore, the sulfur assimilation pathway is highly regulated by miRNAs, such as miR395 (Kawashima et al., 2009). Cluster 22 shows proteins that are not known miRNA targets but that are regulated via action of DRB1 and DRB2, suggesting that miRNA regulation of related genes is coordinated beyond the presence of the miRNA target site.

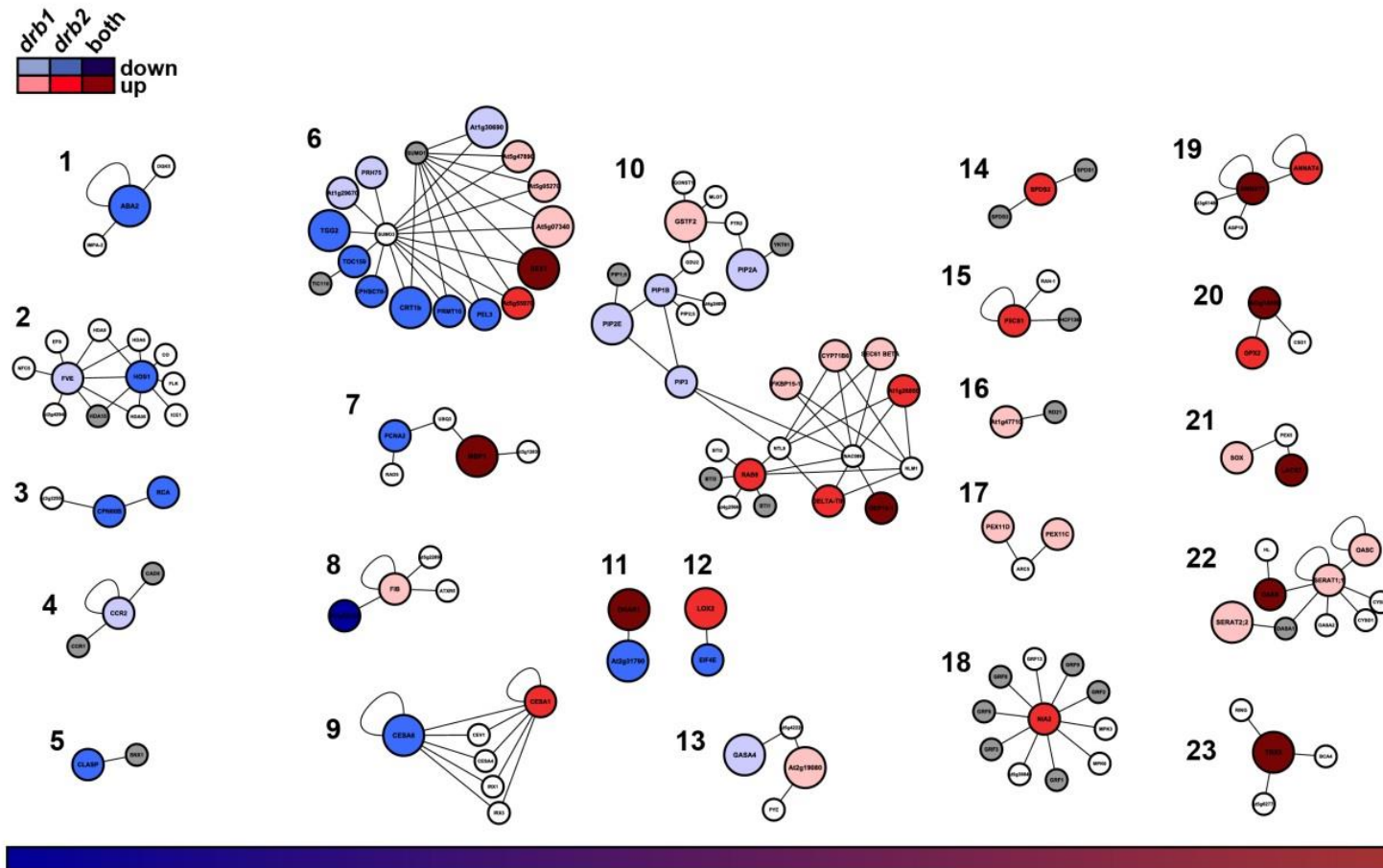


Figure 7-2. Clusters of proteins with differential accumulation in *drb1* and *drb2*.

Sub-networks of proteins with differential accumulation in *drb1* and *drb2*, relative to wild-type. Circle colour refers to differential expression in *drb1*, *drb2* or both. White, not detected; grey, detected to wild-type levels. Circle size refer to statistical *p*-value (see Experimental Procedures for details): large ($p < 0.01$), medium ($p < 0.5$) and small ($p \geq 0.5$, or not detected). Clusters are arranged according to the predominance of reduced or increased protein accumulation (gradient bar, bottom).

Table 7-1. Accumulation and function of proteins with differential accumulation clustered (sub-networks) in *drb1* and *drb2*, relative to wild-type.

Cluster	Protein	Gene Locus	<i>drb1</i>			<i>drb2</i>			Function ²
			log2FC (±SD)	Peptides ¹	p-value	log2FC (±SD)	Peptides ¹	p-value	
1	ABA2	AT1G52340	-0.06±0.13	2	0.75	-1.35±0.29	1.5	0.01	ABA biosynthesis; salt stress
2	FVE	AT2G19520	-0.20±0.79	1.5	0.09	-0.31±0.05	11.5	0.03	Flowering time
	HOS1	AT2G39810	ND	ND	ND	-0.28±0.02	3	0.04	Cold stress; flowering time
	HDA15	AT3G18520	0.61±0.48	1	0.27	ND	ND	ND	Histone deacetylase
3	RCA	AT2G39730	-0.40±0.16	29	0.06	-0.28±0.06	62	0.03	Light activation of rubisco
	CPN60B	AT1G55490	-0.34±0.10	13.5	0.05	-0.43±0.04	12.5	0.01	Caperonin
4	CAD5	AT4G34230	ND	ND	ND	0.67±0.55	2	0.37	Cinnamyl alcohol dehydrogenase
	CCR2	AT2G21660	0.36±0.04	29	0.01	0.45±0.07	18.5	0.01	Circadian rhythm; cold and salt stress
	CCR1	AT4G39260	0.17±0.17	19.5	0.62	0.20±0.12	17.5	0.25	Circadian rhythm; cold and salt stress
5	CLASP	AT2G20190	-0.46±0.07	2	0.01	0.22±0.05	6.5	0.09	Microtubule stability
	SNX1	AT5G06140	-0.10±0.32	2	0.11	ND	ND	ND	Endocytic protein sorting
6	SUMO3	AT5G55170	ND	ND	ND	ND	ND	ND	Post-translational modification
	TOC159	AT4G02510	-0.40±0.25	9	0.18	-0.37±0.05	27	0.02	Chloroplast biogenesis
	SUMO1	AT4G26840	-0.07±0.1	2.5	0.98	ND	ND	ND	Post-translational modification
	AT5G07340	AT5G07340	1.52±0.48	1.5	0.01	0.23±0.27	10	0.81	Unknown
	CRT1b	AT1G09210	-0.11±0.04	1.5	0.39	-0.47±0.01	4.5	0.01	Plant defense (calreticulin)
	PRH75	AT5G62190	-0.53±0.35	3	0.01	ND	ND	ND	DEAD/DEAH box RNA helicase
	AT5G05270/CHIL	AT5G05270	0.29±0.29	3.5	0.03	ND	ND	ND	Chalcone isomerase
	AT1G30690	AT1G30690	-0.76±0.10	4	0	-0.01±0.10	17.5	0.36	Unknown
	TGG2	AT5G25980	0.24±0.16	30.5	0.29	-1.34±0.14	12.5	0	Insect defense (myrosinase)
	AT1G29670	AT1G29670	-0.35±0.01	7	0.02	0.23±0.19	8.5	0.05	Unknown
	PEL3	AT5G23940	-0.34±0.18	6.5	0.14	-0.61±0.27	5	0.02	Cuticle and trichomes formation
	AT5G47890	AT5G47890	0.33±0.02	1.5	0.03	ND	ND	ND	Unknown
	AT5G55070	AT5G55070	0.24±0.12	4.5	0.17	0.33±0.07	10	0.04	Unknown
	PRMT10	AT1G04870	ND	D	ND	-0.20±0.09	7	0.05	Flowering time
	SEX1	AT1G10760	0.62±0.01	8.5	0	0.24±0.13	6	0.04	Starch degradation and freezing tolerance
	CPHSC70-1	AT4G24280	-0.21±0.07	5	0.15	-0.31±0.13	95.5	0.03	Import to chloroplast
7	UBQ3	AT5G03240	ND	ND	ND	ND	ND	ND	Ubiquitin (modulated by light)
	MBP1	AT1G52040	2.23±0.12	3	0	1.11±0.04	8	0	Plant defense (myrosinase-binding protein)
	PCNA2	AT2G29570	ND	ND	ND	-0.29±0.02	2	0.03	DNA repair (light)
8	FIB	AT4G04020	0.65±0.27	2.5	0.04	ND	ND	ND	Fibrillin precursor; photoprotection
	AT5G55220	AT5G55220	-0.33±0.01	4	0.02	-0.34±0.15	6.5	0.02	Unknown
9	CESA1	AT4G32410	ND	ND	ND	0.28±0.16	6.5	0.04	Cellulose biosynthesis
	CESA6	AT5G64740	-2.16±0.08	1.5	0	ND	ND	ND	Cellulose biosynthesis
10	AT1G26850	AT1G26850	-0.06±0.01	7.5	0.53	0.35±0.05	14	0.03	Unknown
	NLM1	AT4G19030	ND	ND	ND	ND	ND	ND	Aquaporin; drought and salt stress
	NL9	AT4G35580	ND	ND	ND	ND	ND	ND	Osmotic stress; transcriptional repressor
	NAC089	AT5G22290	ND	ND	ND	ND	ND	ND	Flowering time
	RAB8	AT3G53610	0.19±0.08	5	0.23	0.34±0.07	3	0.03	Signal transduction (GTPase)
	CYP71B6	AT2G24180	0.60±0.14	2	0.01	ND	ND	ND	Oxidation-reduction process
	SEC61 BETA	AT2G45070	0.39±0.13	5.5	0.05	0.07±0.51	3.5	0.33	Protein transport
	PIP2A	AT3G53420	-0.68±0.02	16	0	-0.06±0.26	19	0.42	Aquaporin; drought stress
	GSTF2	AT4G02520	1.53±0.22	26.5	0	-0.19±0.04	17.5	0.06	Stress response
	PIP3	AT4G35100	-0.36±0.06	13	0.03	-0.04±0.02	31	0.47	Aquaporin; drought and salt stress
	PIP1B	AT2G45960	-0.60±0.19	5.5	0.02	0.14±0.03	8.5	0.1	Aquaporin; drought stress
	FKBP15-1	AT3G25220	0.24±0.09	1.5	0.03	ND	ND	ND	Peptidyl-prolyl isomerases
	DELTA-TIP	AT3G16240	ND	ND	ND	0.24±0.09	9.5	0.04	Water and ammonium (NH ₃) transport
	PIP2E	AT2G39010	-1.78±0.25	2.5	0	-0.59±0.23	0	0.05	Aquaporin; drought stress
	OEP16-1	AT2G28900	0.39±0.04	19	0.01	0.45±0.07	16	0.01	Cold and light stress
11	DHAR1	AT1G19570	1.68±0.16	81	0	0.77±0.01	26.5	0	Mutualistic symbiosis (fungus)
	AT2G31790	AT2G31790	0.17±0.19	7.5	0.75	-0.48±0.02	28	0.01	Unknown
12	EIF4E	AT4G18040	ND	ND	ND	-0.23±0.05	2.5	0.04	Plant defense (elongation factor)
	LOX2	AT3G45140	-0.40±3.01	15.5	0.24	3.07±0.32	11	0	Plant defense (jasmonate)
13	AT5G42220	AT5G42220	ND	ND	ND	ND	ND	ND	Unknown (Ubiquitin-like superfamily)
	AT2G19080	AT2G19080	-0.59±0.22	2	0.03	ND	ND	ND	Unknown
	CASA4	AT5G15230	-1.22±0.38	2	0.01	ND	ND	ND	Unknown
14	SPDS2	AT1G70310	0.29±0.10	4.5	0.09	0.27±0.02	3.5	0.04	Gibberellin response; redox homeostasis
15	P5CS1	AT2G39800	-0.23±0.07	9.5	0.12	0.97±0.39	1.5	0.04	Plant defense (nematode; spermidine)
16	AT1G47710	AT1G47710	0.22±0.09	3.5	0.04	0.31±0.30	9	0.6	Drought and salt stress
17	PEX11D	AT2G45740	0.40±0.07	4	0.02	0.04±0.09	2.5	0.8	Programmed cell death (SERPIN1)
	PEX11C	AT1G01820	0.34±0.16	1.5	0.02	ND	ND	ND	Peroxisome proliferation
18	GRF1,2,3,6,8,9	-	NS	NS	NS	NS	NS	NS	Peroxisome proliferation
	NIA2	AT1G37130	0.12±0.20	1.5	0.88	0.33±0.09	7	0.05	General regulatory factor (14-3-3 protein)
19	ANNAT1	AT1G35720	0.43±0.09	75	0.02	0.44±0.08	2.5	0.02	Nitrate assimilation
	ANNAT4	AT2G38750	ND	ND	ND	0.26±0.21	2	0.05	Oxidative stress (annexin)
20	GPX2	AT2G31570	ND	ND	ND	0.24±0.14	1.5	0.04	Oxidative stress (annexin)
	AT3G14990	AT3G14990	0.80±0.35	14	0.04	1.29±0.00	24.5	0	Oxidative stress (glutathione peroxidase)
21	PEX5	AT5G56290	ND	ND	ND	ND	ND	ND	Oxidative stress (chloroplast formation)
	LACS7	AT5G27600	0.93±0.32	1.5	0.02	0.38±0.01	4	0.01	Protein transport (peroxisomal)
	SOX	AT3G01910	0.44±0.02	8	0.01	0.11±0.06	18	0.12	Fatty acid metabolism (peroxisomal)
22	SERAT1;1	AT5G56760	0.64±0.45	3	0.04	ND	ND	ND	Oxidative stress; sulfur metabolism
	OASB	AT2G43750	0.49±0.15	8.5	0.03	0.51±0.03	19	0.01	Sulfur metabolism (sulfur assimilation)
	SERAT2;2	AT3G13110	0.59±0.02	4	0	ND	ND	ND	Sulfur metabolism (sulfur assimilation)
	OASC	AT3G59760	0.39±0.03	14	0.02	0.20±0.07	17.5	0.14	Sulfur metabolism (cysteine biosynthesis)
23	TRX5	AT1G45145	1.89±0.06	2	0	0.62±0.20	3.5	0.03	Plant defense and oxidative stress

¹ Averaged number of identified and quantified peptide per protein in each replicate.

² According to annotated gene function obtained from The Arabidopsis Information Resource (TAIR).

7.4 Functions and processes enriched in *drb1* and *drb2* mutants

It is predicted that the Arabidopsis interactome has a total number of binary interactions of 299,000 \pm 79,000 (Arabidopsis Interactome Mapping Consortium, 2011), which is approximately 17 times larger than the current known interactome (~17,000 binary interactions). Consequently, although the currently Arabidopsis interactome is insightful, analysis of protein accumulation requires other approaches to complement network analysis. Applying gene ontology (GO) analysis to the 1664 proteins identified and quantified in the shoot apices of *drb1* and *drb2* mutants showed a wide range of enriched metabolic and cellular processes (Figure 7-3). Enriched GO clusters were pooled together according the functional relatedness (Supplementary Data). Interestingly, the most abundant GO cluster pools were related to response to abiotic stimulus (~16%), such as response to metal ion. Although this result may be partially explained by the elevated number of publications in this area of plant biology, which inevitably results in GO annotation of a large number of proteins (Cabello et al., 2014), it indicates that the shoot apex is an important region for adaptation to environmental stimulus.

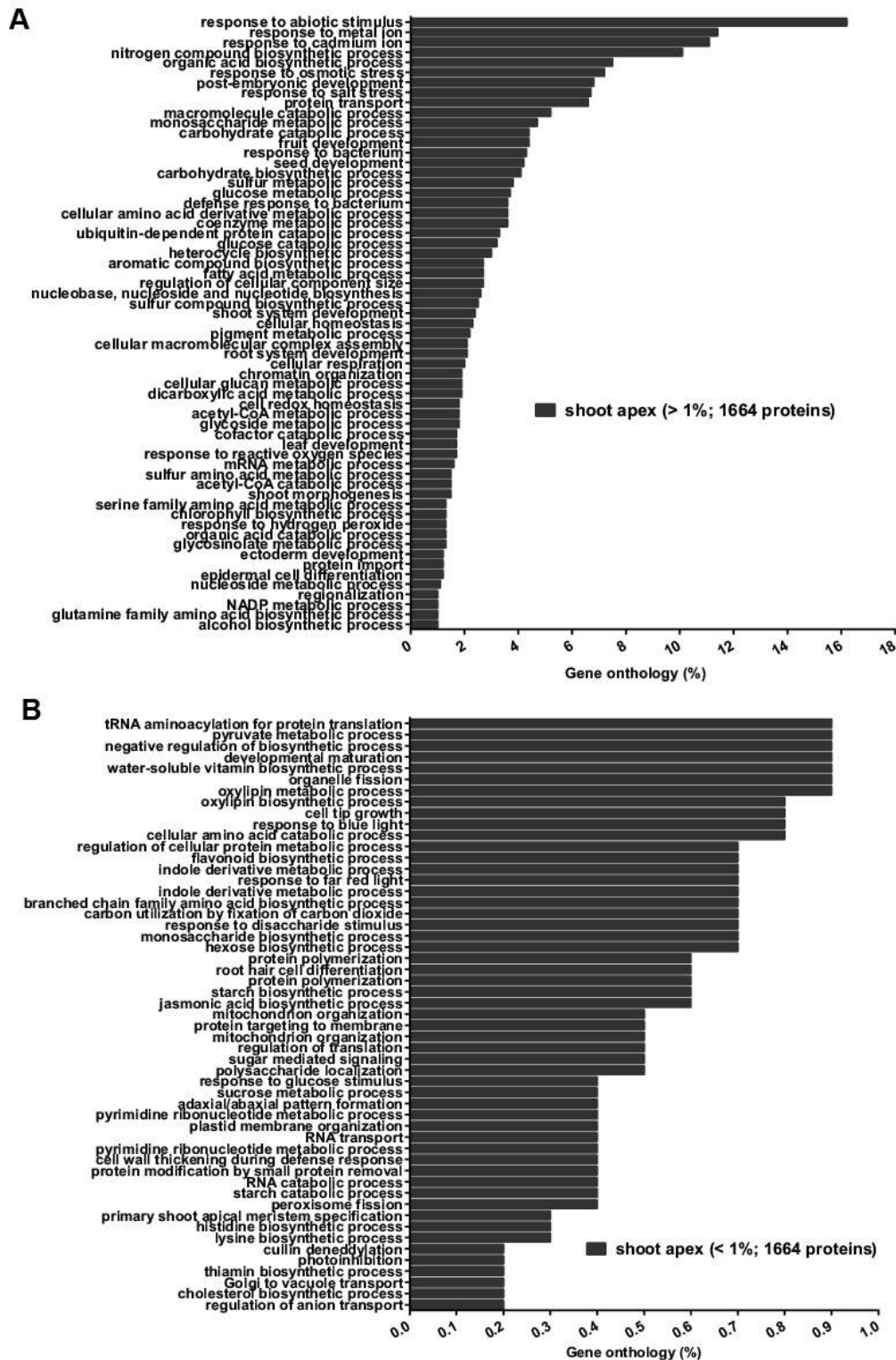


Figure 7-3. Gene ontology enrichment of proteins of *drb1* and *drb2* shoot apex.

(A) More abundant GO enrichment (>1%; p<0.05) of proteins in shoot apex of *drb1* and *drb2* (combined dataset; 1664 proteins).

(B) Less abundant GO enrichment (<1%; p<0.05) of proteins in shoot apex of *drb1* and *drb2* (combined dataset; 1664 proteins).

In the shoot apex of *drb1* plants, GO enrichment revealed that proteins involved in the cellular processes of organic acid biosynthesis, and regulation of cellular size components, were among the most highly reduced (Figure 7-4). It also showed that the accumulation of proteins involved in response to abiotic stimuli (i.e., response to cadmium ion and osmotic stress and salt stress) and defense response were both increased and decreased in *drb1* shoot apex. In *drb2* shoot apex, however, proteins involved in mediating abiotic stress responses were reduced, including response to temperature stimuli and response to metal ion (Figure 7-4). Of the proteins with increased and decreased accumulation in *drb2*, most are involved in mediating response to abiotic stimulus, such as osmotic and salt stress. Similar to *drb1*, a large number of defense response-related proteins were increased *drb2* shoot apex. These results show that DRB1 and DRB2 have both similar and different impacts on metabolism and environmental adaptation of Arabidopsis.

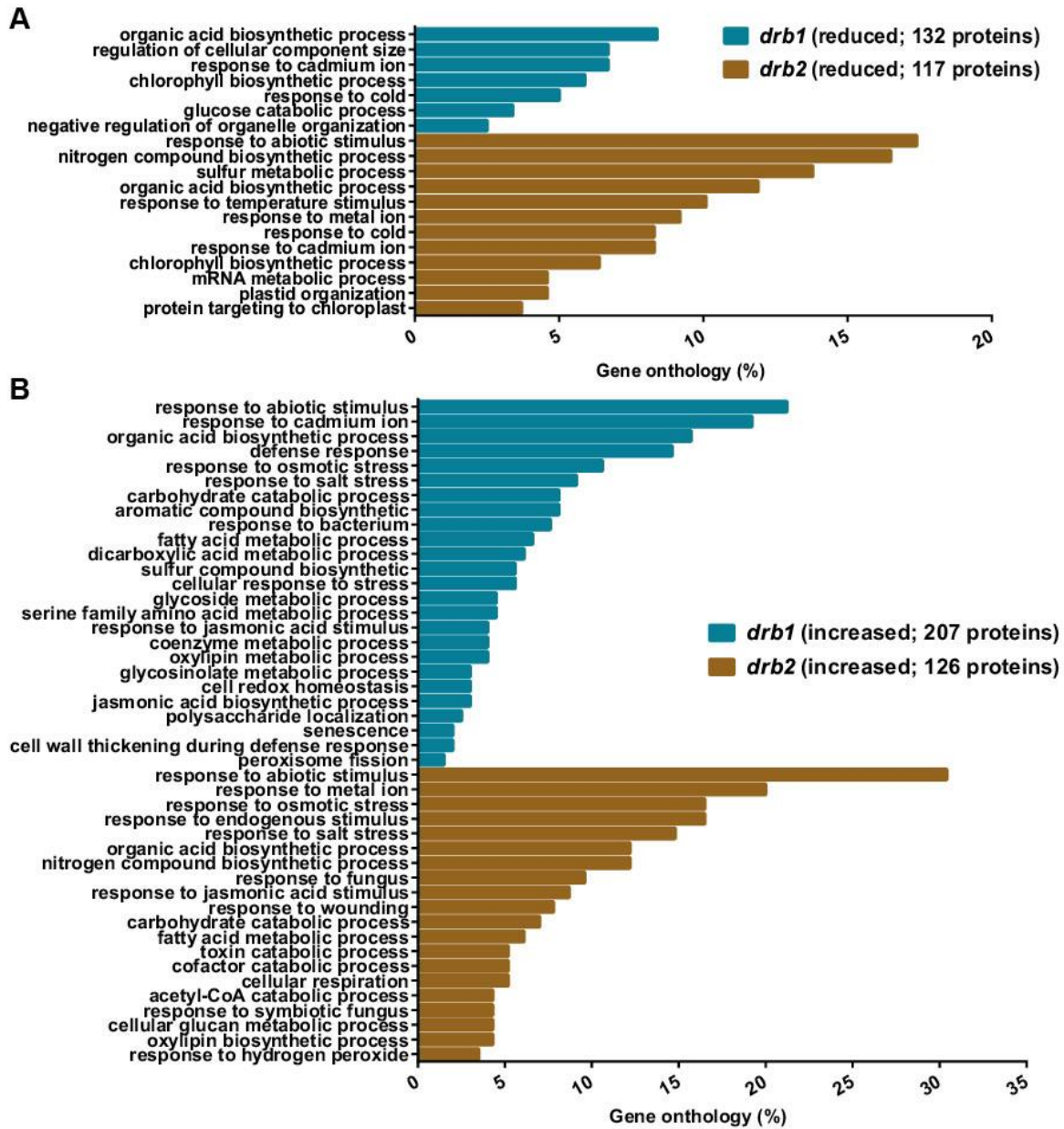


Figure 7-4. Gene ontology enrichment of proteins with differential accumulation.

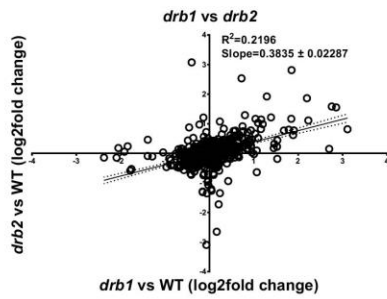
(A) GO enrichment ($p < 0.05$) of proteins with reduced accumulation in shoot apex of *drb1* and *drb2*, relative to wild-type.

(B) GO enrichment ($p < 0.05$) of proteins with increased accumulation in shoot apex of *drb1* and *drb2*, relative to wild-type.

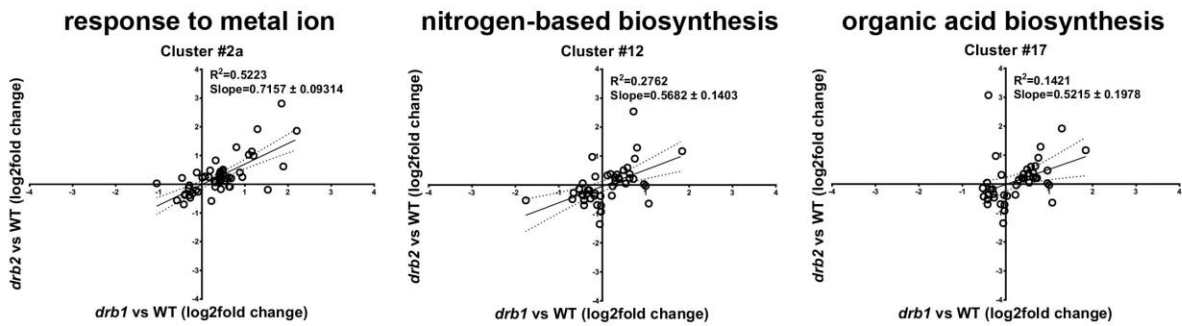
PART III – RESULTS AND DISCUSSION

To study the alteration in functions and processes in *drb1* and *drb2*, I studied the distribution of protein accumulation and GO enrichment (p-value<0.05) in shoot apex of these mutants. Figure 7-5 shows the distribution of all proteins identified and quantified in *drb1* and *drb2*, and their accumulation relative to wild-type. This distribution revealed an apparent correlation between protein accumulation in these mutants ($R^2=0.22$), and slightly biased accumulation towards that in *drb1* (slope=0.38). GO distributions were identified that were either similarly or differently altered in *drb1* and *drb2* mutants (Figure 7-5 and Supplementary Data). Response to metal ion and nitrogen-based and organic acid biosynthesis appear to be altered to a similar extent in both mutants. Interestingly, most proteins related to response to metal ion over-accumulated in *drb1* and *drb2*, suggesting a synergistic effect of loss of DRB1 and DRB2 activity in response to metal ions. More pronounced effects in *drb1* were observed for organelle organization, chlorophyll and chloroplast processes, and mRNA metabolism. Conversely, defense response and sulfur and glycoside metabolism were more altered in *drb2* compared to *drb1*. These results show that DRB1 and DRB2 are both required for regulation of metabolic and cellular processes and environmental adaptation.

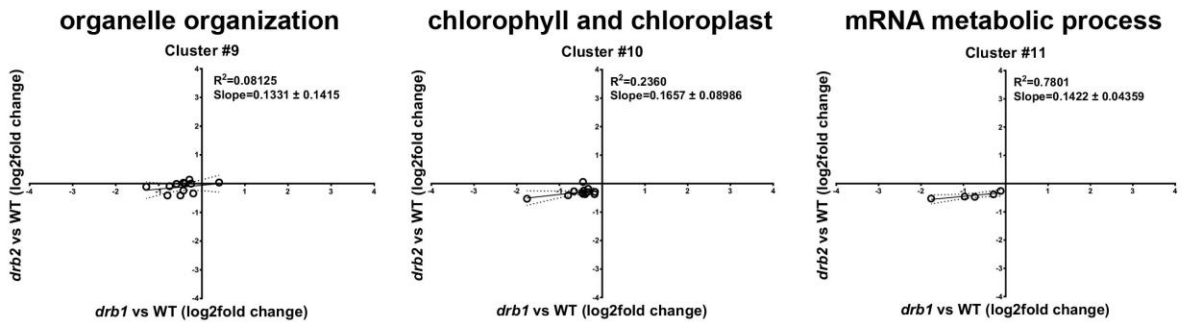
protein accumulation in *drb1* vs *drb2*



similar effect in *drb1* and *drb2*



stronger effect in *drb1*



stronger effect in *drb2*

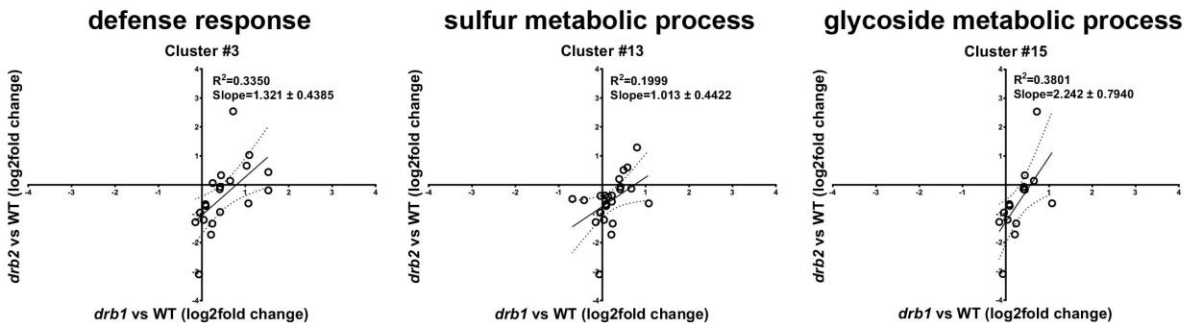


Figure 7-5. Distribution of proteins according to GO in *drb1* and *drb2*.

Correlation of protein accumulation in *drb1* (x-axis) and *drb2* (y-axis), relative to wild-type (top), and distribution of protein accumulation according to different GO annotations. R-squared, Pearson correlation ($p < 0.05$).

7.5 Biotic and abiotic responses in *drb1* and *drb2* mutants

Conserved miRNAs are known to target transcription factors to aid adaptation to stress conditions (Sunkar et al., 2012). However, how plants are altered at the molecular level under stress is still not well understood (Yan et al., 2012b). The study of response to biotic and abiotic stimuli in *drb1* and *drb2*, grown under standard conditions, revealed that several proteins involved in response to salt, temperature and pathogen have altered accumulation in these mutants (Figure 7-6A). Interestingly, GO enriched in response to salt showed proteins that are mostly increased in *drb1* and *drb2*. However, temperature response-related proteins were mostly reduced or unchanged in both mutants. Furthermore, proteins involved in response to pathogen and jasmonic acid biosynthesis highly over accumulated in both *drb* mutants. These results revealed a large set of proteins required for adaptive responses to the environment with altered accumulation in *drb1* and *drb2* mutants.

Both protein interaction network and GO analysis indicated that DRB1 and DRB2 play a role in osmotic response. Interactome Cluster 10 contains four aquaporin water transport proteins that had reduced protein accumulation in *drb1* (Figure 7-2), and GO analysis showed that osmotic stress response proteins were slightly more elevated in *drb1* compared to *drb2* (Figure 7-6A). Thus, the proteomics study indicated a role for these DRB genes in regulating certain stress responsive proteins. To test this, I studied the effect of salt treatment on wild-type and *drb1* and *drb2* mutant plants. Six-day-old wild-type and *drb* mutant plants, cultivated in standard MS media, were transferred to media containing various salt concentrations and were analyzed after 10 days of treatment (Figure 7-6B). Compared to wild-type, *drb1* plants developed mildly bleached, yellowish, rosette leaves on 100 mM NaCl, and completely photobleached (white) rosette leaves on the 150 mM NaCl supplemented media. In contrast to *drb1*, *drb2* seedlings cultivated on the two assessed salt concentrations showed considerably less developmental stress. Furthermore, when compared to wild-type, *drb2* seedlings were more resistant to 100 and 150 mM NaCl, developing large rosette leaves and a more highly developed root system (Figure 7-6B). These results show that DRB1 and DRB2 play important yet functionally distinct roles in response to salt stress, and suggest that their regulation is important for stress responses.

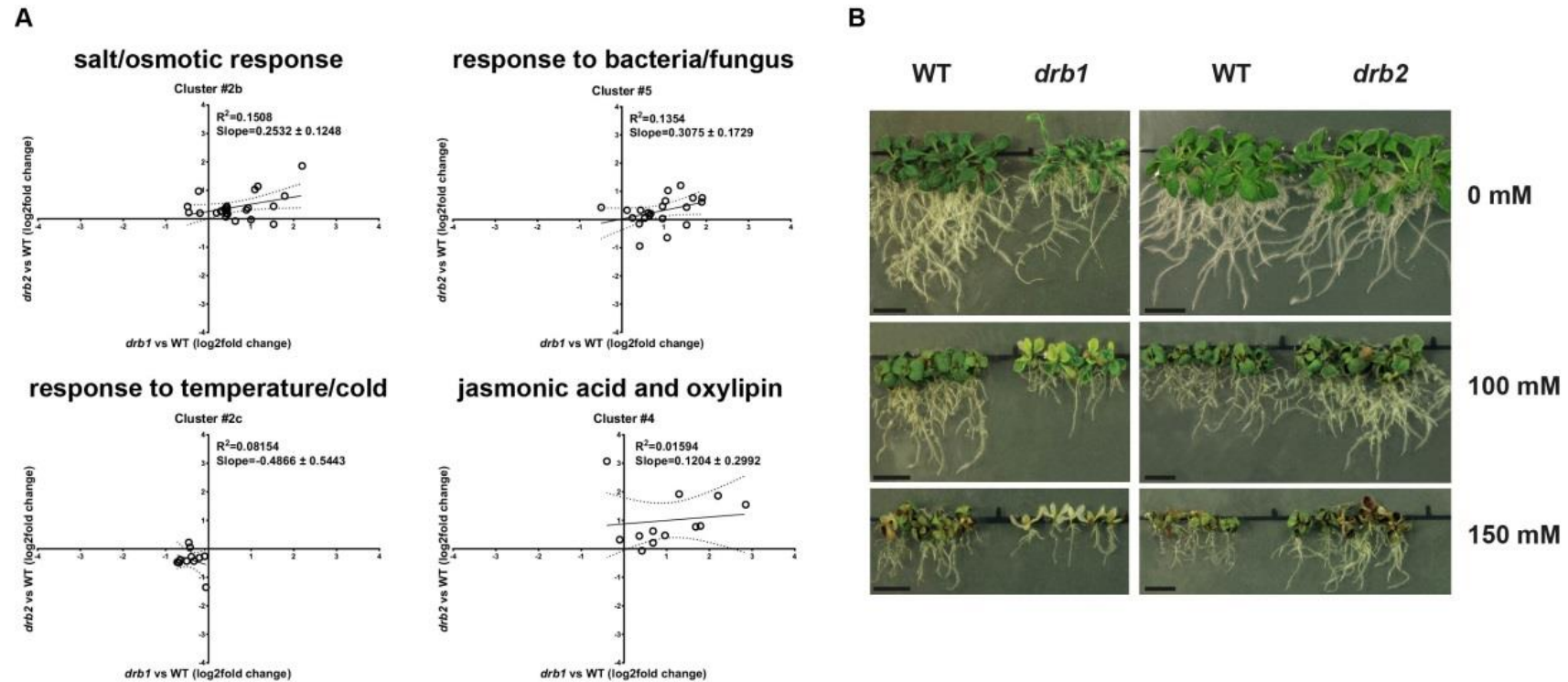

















Figure 7-6. Abiotic and biotic response GOs and salt stress treatment in *drb1* and *drb2*.

(A) Distribution of protein accumulation according to abiotic (left) and biotic (right) GO in *drb1* (x-axis) and *drb2* (y-axis), relative to wild-type. R-squared, Pearson correlation ($p < 0.05$).

(B) Salt stress treatment of *drb1* and *drb2* plants. Six day old seedlings, cultivated on standard MS media for 6 d, were transferred to salt-supplemented media and cultivated for further 10 d ($n = 6$).

7.6 Chapter highlights

-  A Shoot Apex Interactome (SAI) was built on experimentally validated protein-protein interactions.
-  SAI 460 identified and quantified proteins, 1917 nodes and 2802 edges.
-  *drb1* and *drb2* shoot apex share a total of 81 differentially expressed proteins, corresponding to ~20% of all differentially accumulated proteins.
-  SAI comprises 153 proteins with differential accumulation, representing ~30% of all non-redundant differentials identified in *drb1* and *drb2*.
-  Network rewiring, caused by null mutation of *DRB1* and *DRB2*, resulted in alterations in the SAI landscape.
-  SAI clusters of proteins with differential accumulation suggested co-regulation and new functions to these proteins.
-  Reduced accumulation of FVE and HOS1 in *drb1* and *drb2*, respectively, suggests that flowering time and response to cold are regulated synergistically by DRB1 and DRB2.
-  RCA (light activation of Rubisco) and CPN60B (Caperonin) were reduced only in *drb2*, suggesting a role for DRB2 in photosynthesis acclimatization to heat stress.
-  Aquaporin proteins had reduced accumulation only in *drb1*, suggesting that DRB1 and DRB2 play different roles in response to osmotic stress.
-  Several proteins involved in oxidative stress had increased accumulation in both *drb* mutants, suggesting that they lost cellular and metabolic homeostasis.
-  Several proteins involved in sulfur metabolism (non-miRNA targets) over-accumulated in *drb* mutants, suggesting that miRNAs regulate this process beyond the presence of the miRNA target site.
-  Gene ontology enrichment of the 1664 proteins identified in the shoot apices indicates that this tissue is an important region for adaptation to environmental stimulus.
-  GO enrichment showed that DRB1 and DRB2 have both similar and different impacts on metabolism and environmental adaptation of Arabidopsis.
-  A large set of proteins required for adaptive responses to the environment had altered accumulation in *drb1* and *drb2* mutants.
-  DRB1 and DRB2 play important yet functionally distinct roles in response to salt stress.

**Chapter 8 – Structural determinants of
the *in vivo* activity of
Arabidopsis double-
stranded RNA binding
proteins**

The canonical double-stranded RNA (dsRNA)-binding domain (RBD) is characterized by a $\alpha 1\beta 1\beta 2\beta 3\alpha 2$ secondary structure that recognizes dsRNA (Chang and Ramos, 2005). The Arabidopsis genome encodes five DOUBLE-STRANDED RNA (dsRNA)-BINDING (DRB) proteins involved in small RNA pathways, and each has two N-terminal RBDs (Curtin et al., 2008). DRB1 and DRB2 are required for the miRNA pathway, and I showed in this thesis that they define the miRNA mode of action. Interestingly, structural studies have revealed that DRB1 has both a canonical and a non-canonical RBD (Yang et al., 2010). Its second RBD (101-170) has significant structural differences to its first canonical RBD (15-84), such as an arginine residue (R130), as opposed to the “invariant” histidine. The lack of H130 re-orientates a loop that is important for dsRNA minor groove recognition, and this appears to explain the low affinity of DRB1 RBD2 for dsRNA (Yang et al., 2010).

Although DRB1 has an unusual RBD composition that may shed light on its function, *in vivo* studies to assess the biological relevance of its structural components are still missing. Hence, to better understand the structural determinants for DRB1 and DRB2 function in the miRNA pathway, I developed and analyzed *drb1* mutants genetically engineered to express a series of chimeric genes. These transgenic plants expressed different functional parts of DRB1 and DRB2 proteins under control of the *DRB1* native promoter. Initially, amino acid sequence alignment revealed that DRB1 RBDs differ significantly to those of DRB2 and, interestingly, the invariant histidine is only missing in DRB1 RBD2. Protein structure predictions further suggested that DRB1 RBD2 is the sole non-canonical RBD among members of the Arabidopsis DRB family (DRB1-5). This *in silico* analysis showed sequence and structural differences between DRB1 and DRB2. The analysis of the expression of chimeric genes in *drb1* mutants showed that, in accordance with the *in silico* analysis, DRB1 RBD2 is essential to DRB1 activity. It also showed that DRB2 RBD1 can replace its DRB1 counterpart to complement *drb1* severe developmental defects, suggesting that DRB2 RBD1 also folds into a canonical RBD. However, although DRB2 RBD2 was predicted to be canonical, it failed to functionally replace DRB1 canonical RBD1, suggesting that the second RBD of DRB2 plays role(s) other than binding to dsRNA, possibly aiding protein-protein interactions specific to DRB2. Altogether, the results identify the second domain of both DRB1 and DRB2 as key structural features for their *in vivo* activity.

8.1 Evolutionary conservation of DRB1 non-canonical dsRNA binding domain

The structure of DRB1 revealed a non-canonical dsRNA-binding domain that appears to aid protein-protein interaction instead of mediating dsRNA binding (Yang et al., 2010). In this Chapter I studied whether that is a specific feature of DRB1, its biological relevance, and its evolutionary conservation. The structure for RBDs of Arabidopsis DRB2, DRB3, DRB4 and DRB5, were predicted and superimposed with those previously reported for DRB1 (Yang et al., 2010) (Figure 8-1A). All RBDs were predicted to fold as canonical dsRNA-binding domains, contrasting the non-canonical DRB1 RBD2. Strikingly, the loop linking $\beta 1$ and $\beta 2$ (region 2), required for dsRNA minor groove recognition, was only re-oriented in DRB1 RBD2. DRB1 is evolutionary conserved in multicellular plants (presented earlier in this thesis), therefore, DRB1 RBD2 region 2 was aligned with the corresponding region of DRB1 orthologs of other plant species for comparison (Figure 8-1B). The dsRNA binding activity of region 2 is largely determined by a patch of a positive electrostatic potential surface that contains a histidine residue (Yang et al., 2010). This “invariant” histidine residue is found in some monocots (*Zea mays* and *Brachypodium distachyon*), lycopsid (*Selaginella moellendorffii*) and moss (*Physcomitrella patens*), while it was absent in dicots and some other monocot (*Oryza sativa* and *Sorghum bicolor*) species. In these plants, histidine was replaced by an arginine (R) or, less often, by leucine (L) or lysine (K) residue (Figure 8-1B). These results suggest that arginine residue has been selected in evolution, over histidine, in region 2 of DRB1 RBD2.

DRB1 and DRB2 are both required for the miRNA pathway, and I have shown that they determine the miRNA modes of action (presented earlier in this thesis). Hence, to investigate the sequence determinates for their differential activity, I aligned and compared the amino acid sequence of DRB1 and DRB2 RBDs (Figure 8-1C). Region 1 (recognizes dsRNA major groove) and 3 (recognizes dsRNA minor groove) are conserved in both RBDs of DRB1 and DRB2, while region 2 (recognizes dsRNA minor groove) is more variable. This suggests that region 2 is an important structural determinant for DRB1 in the miRNA pathway. However, previous work has shown that point mutations to the invariant histidine residue (H43, region 2) of DRB1 RBD1 only slightly decreased the dsRNA-binding affinity of this domain (Yang et al., 2010), suggesting that the structural determinants of DRB1 function, and possibly DRB2, are complex and also involve elements other than this specific amino acid sequence.

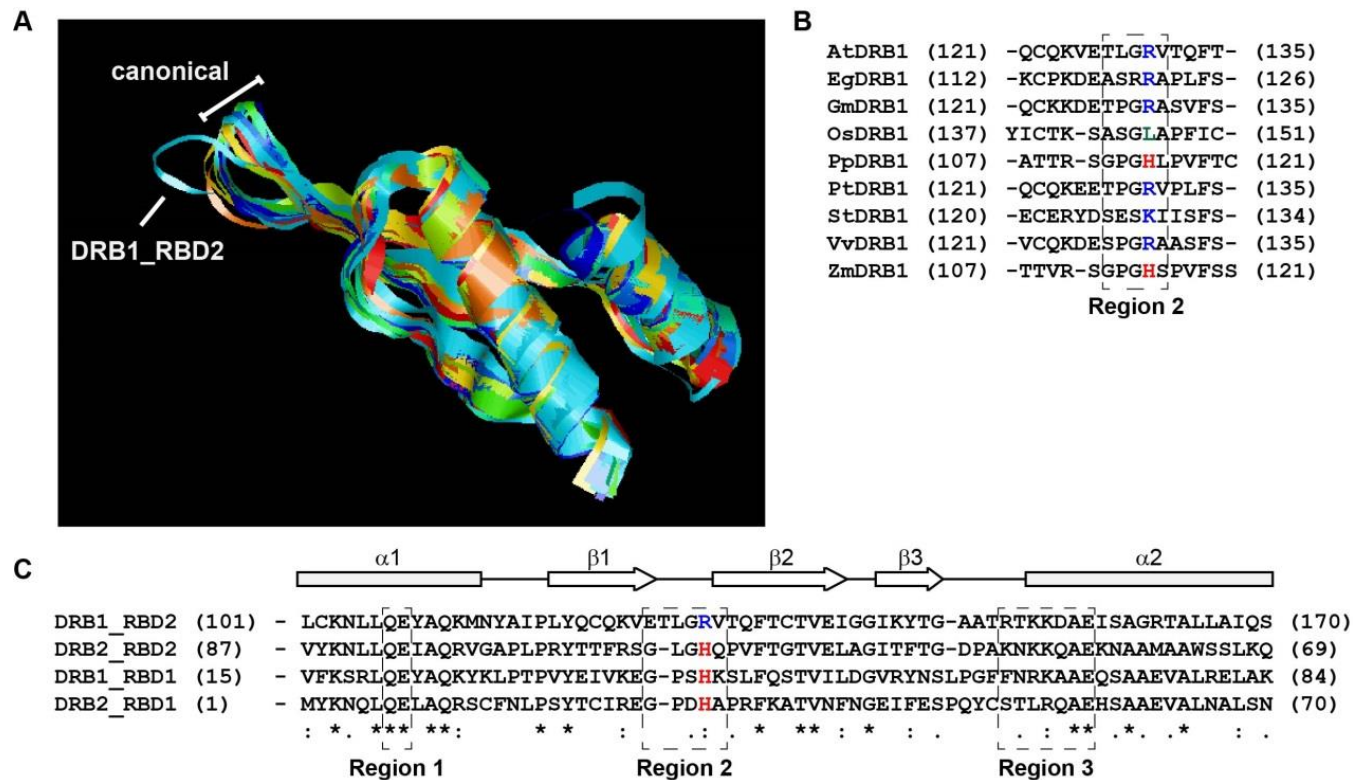


Figure 8-1. dsRNA-binding domains of Arabidopsis DRB proteins.

(A) Alignment of RBD structures of DRB1 (3ADG and 3ADJ) and predicted structure of DRB2, DRB3, DRB4 and DRB5 RBDs. Region 2 of non-canonical DRB1 RBD2 is shown (blue coloured ribbon).

(B) Amino acid sequence alignment of region 2 (loop)-containing sequences of *Arabidopsis thaliana* DRB1 (AtDRB1) RBD2 and orthologs in *Eucalyptus grandis* (EgDRB1), *Glycine max* (GmDRB1), *Oryza sativa* (OsDRB1), *Prunus persica* (PpDRB1), *Populus trichocarpa* (PtDRB1), *Solanum tuberosum* (StDRB1), *Vitis vinifera* (VvDRB1) and *Zea mays* (ZmDRB1). Colours highlight the different amino acids: positively charged arginine (R) and lysine (K) are blue, hydrophobic leucine (L) is green, and “invariant” histidine is red.

(C) Amino acid sequence alignment of Arabidopsis DRB1 and DRB2 RBDs. Secondary folding structures are shown (top). RBD regions (Region 1-3) that interact with major and minor dsRNA grooves are highlighted. Colours highlight the different amino acids as above.

8.2 Expression of chimeric gene series in *drb1* plants

Arabidopsis plants defective in DRB1 activity, *drb1* mutants, exhibit pleiotropic developmental defects, including smaller-sized hyponastic leaves, and shorter and twisted siliques (Figure 8-2) (Lu and Fedoroff, 2000; Wu et al., 2007). To investigate the structural components that determine DRB1 and DRB2 activity in the miRNA pathway, I transformed a *drb1* mutant with a series of vectors to express chimeric genes, each containing functional domains of either DRB (Figure 8-2). Homozygous F2 plants of transgenic lines expressing either a chimeric gene (DRB-C3 to DRB-C9), DRB1 full-length (DRB-C1) or DRB1 RBD1-2 (DRB-C2), all driven by the endogenous promoter sequence of Arabidopsis *DRB1* (Curtin et al., 2008; Eamens et al., 2012a), were compared to Col-0 wild-type and *drb1* mutants (Figure 8-2).

Previous work has shown that expression of the N-terminal dsRNA binding domains of DRB1, driven by a constitutive promoter, are sufficient for complementation of the severe developmental phenotype expressed by *drb1* plants (Wu et al., 2007). Here, I observed that the expression of DRB1 full-length (DRB-C1) or DRB1 N-terminal RBDs (DRB-C2), driven by *DRB1*'s endogenous promoter, in a *drb1* mutant background (*drb1*/DRB-C1 and *drb1*/DRB-C2 plants) also allowed for phenotypic complementation of this mutant (Figure 8-2). This further confirms that the N-terminal RBDs fulfill the function of the whole DRB1. However, transformation of *drb1* mutant with chimeric genes lacking the non-canonical DRB1 RBD2 (DRB-C5, C6 and C8) failed to complement its phenotype. Transgenic lines *drb1*/DRB-C5, *drb1*/DRB-C6 and *drb1*/DRB-C8 expressed *drb1*-like phenotype, showing that the non-canonical domain of DRB1 is essential for its *in vivo* activity. In addition, DRB-C7 chimeric gene also failed to complement the *drb1* phenotype. In DRB-C7 chimeric gene, the canonical first dsRNA-binding domain of DRB1 was replaced with the second domain of DRB2, which was predicted to fold into a canonical RBD (Figure 8-1). *drb1*/DRB-C7 plants showed *drb1*-like phenotype, suggesting that (1) DRB2 RBD2 is a non-canonical dsRNA binder or (2) that it mediates specific protein-protein interactions that impair DRB1 activity. DRB1 interaction with its partnering proteins has been shown to require its second dsRNA binding domain (Yang et al., 2010); hence, it is likely that the second dsRNA binding domain of DRB2 plays a similar role in mediating protein-protein interactions.

Although the C-terminal region of DRB1 appears to be dispensable for its function (Figure 8-2; Wu et al., 2007), the transformation of *drb1* with chimeric genes harboring DRB2 C-

terminal region (DRB-C3 and DRB-C9) resulted in different phenotypes. DRB-C3 has the DRB1 dsRNA binding domains fused to the C-terminal of DRB2, and *drb1*/DRB-C3 displayed *drb1*-like phenotype (Figure 8-2). DRB-C9 chimeric gene, however, is similar to DRB-C3 with the difference that it has the first RDB of DRB1 replaced by DRB2 RDB1. Interestingly, *drb1*/DRB-C9 phenotype was closely related to wild-type, but also had some hyponastic leaves, a characteristic of *drb1* mutants. These results show that the C-terminus of DRB2 can impair DRB1 function in the absence of DRB2 RBD1, which suggests that these domains interact with each other. In addition, DRB-C4 chimeric gene has the first RDB of DRB1 replaced by DRB2 RDB1, and *drb1*/DRB-C4 is wild-type in appearance. Altogether, these results suggest that the first dsRNA binding domain of DRB1 and DRB2 are functionally similar.

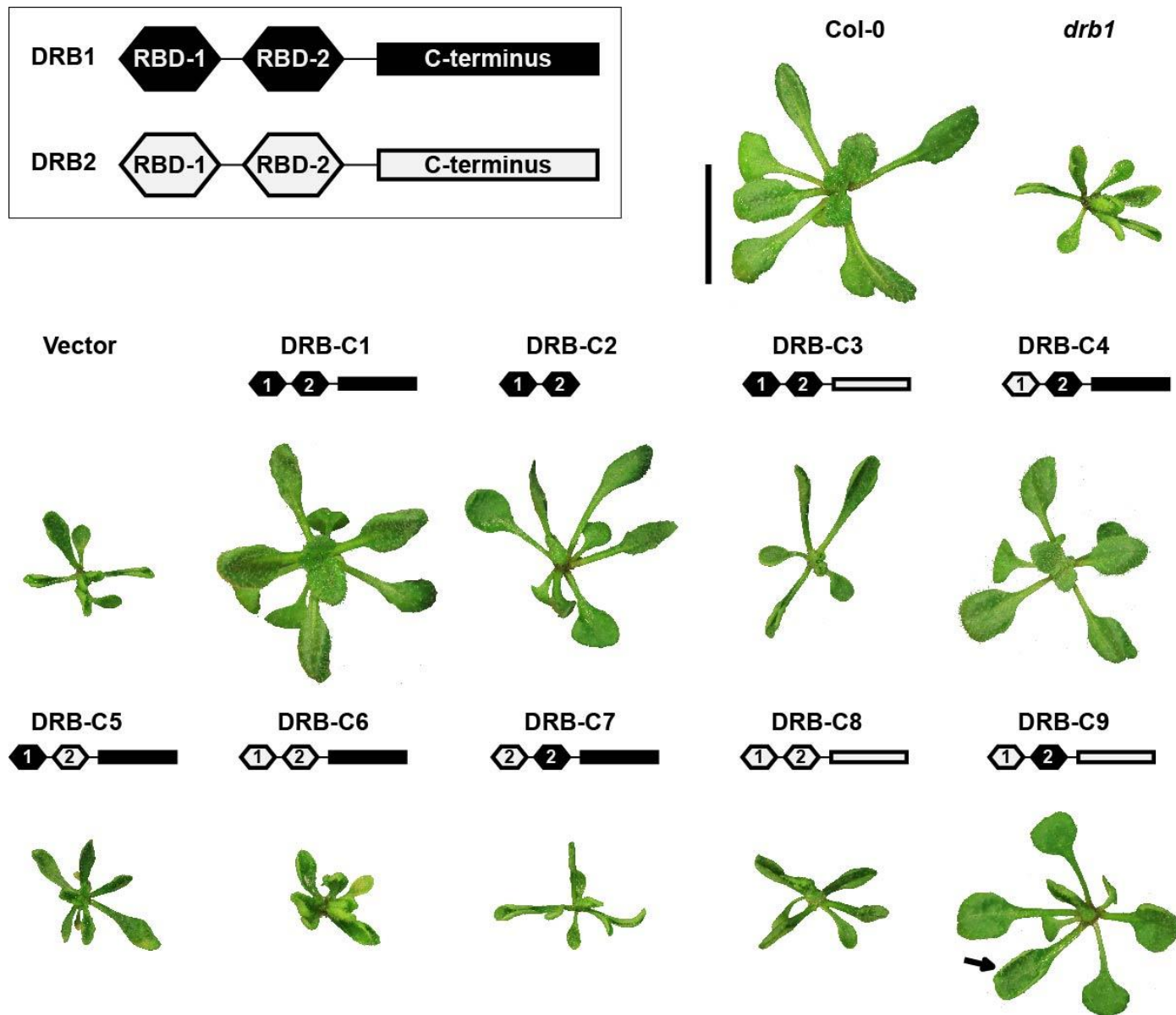


Figure 8-2. Phenotype of wild-type, *drb1* and transgenic plants.

Col-0 wild-type, *drb1* and *drb1* transformed with either DRB1 (DRB-C1), dsRNA binding domains of DRB1 (DRB-C2), or a chimeric gene (DRB-C3 to DRB-C9), driven by the endogenous promoter sequence of Arabidopsis *DRB1*. Protein domains of DRB1 and DRB2, used to construct the vectors for transformation, are depicted in the boxed schematic (top), and domain identities of each vector is shown above each transgenic plant. Arrow (DRB-C9) points to a *drb1*-like hyponastic leaf. Transgenic plants were cultivated on MS medium under long day conditions for 16 d (n > 5). Scale bar, 50 mm.

8.3 miRNA accumulation and gene regulation in transgenic plants

drb1 mutants are characterized by reduced miRNA accumulation and de-repression of transcript targets (Han et al., 2004b; Kurihara et al., 2006). I then assessed the accumulation of four well characterized miRNAs, and target gene expression, in wild-type, *drb1* and *drb1* transformant lines. miRNA accumulation and target gene expression showed strong correlation with the phenotypes expressed by the *drb1* transformant lines (Figure 8-2 and Figure 8-3). In transformant lines displaying complemented wild-type-like phenotypes, including plant lines *drb1*/DRB-C1, *drb1*/DRB-C2, *drb1*/DRB-C4 and *drb1*/DRB-C9, the accumulation of miR164, miR165/166, miR398 and miR408 and the expression of their respective target genes *CUP SHAPED COTLEDONS2* (*CUC2*; miR164), *ARABIDOPSIS THALIANA HOMEBOX PROTEIN14* (*ATHB-14*; miR165/166), *REVOLUTA* (*REV*; miR165/166), *COPPER/ZINC SUPEROXIDE DISMUTASE2* (*CSD2*; miR398) and *PLANTACYANIN* (*ARPN*; miR408) returned to approximate wild-type levels. Furthermore, the degree of *drb1* phenotype complementation was supported by these molecular analyses. *drb1*/DRB-C1 transformants, which displayed the highest degree of complementation (Figure 8-2), had wild-type miRNA accumulation and target gene expression. However, *drb1*/DRB-C9 transformant lines, which showed partial complementation, had slightly reduced miRNA accumulation and a corresponding mild elevation in target gene expression. *drb1* transformed with DRB-C3, DRB-5, DRB-C6, DRB-C7 or DRB-C8 chimeric genes displayed *drb1*-like phenotypes, which also correlated with miRNA accumulation and target gene expression observed in *drb1* mutants. Taken together, the phenotypic and molecular analysis show that the primary role of the first dsRNA binding domains of DRB1 and DRB2 are similar to one another in function, which is likely to be restricted to dsRNA binding activity, and suggest that the second dsRNA binding domain defines their function in the miRNA pathway.

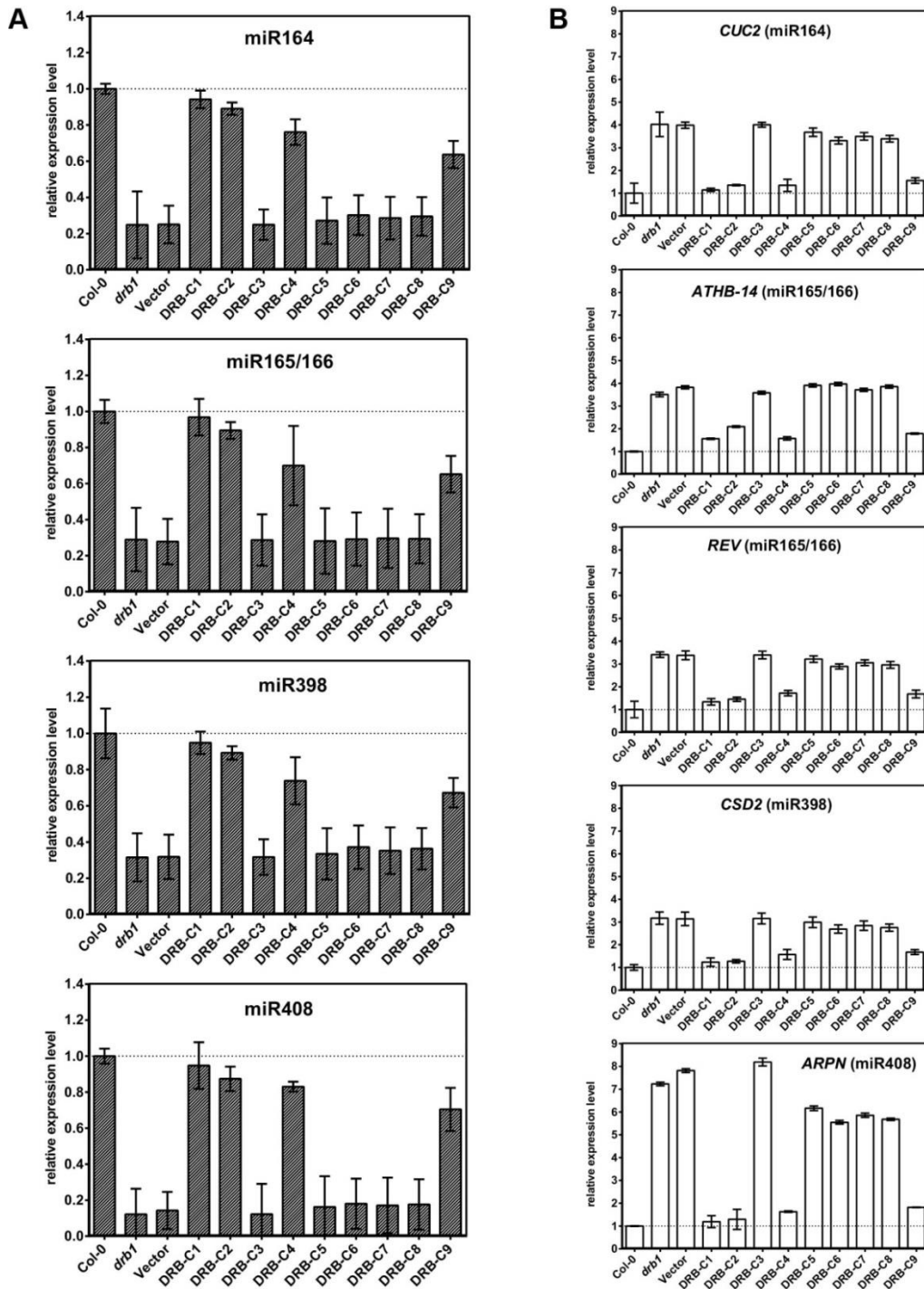


Figure 8-3. miRNA accumulation and their target levels in wild-type, *drb1* and transgenic plants.

(A) Stem-loop RT-PCR quantification of miRNA accumulation relative to Col-0 wild-type levels (dashed line) (n = 3). miRNA levels normalized to SnoR101 accumulation.

(B) RT-PCR quantification of miRNA target gene expression relative to Col-0 wild-type levels (dashed line) (n = 3). Gene expression levels normalized to *ACTIN2* (AT3G18780) expression.

8.4 Abscisic acid treatment of the *drb1* transformant lines

It has been previously shown that germination of *drb1* mutant seeds can be completely inhibited by exogenous addition of abscisic acid (ABA) (Lu and Fedoroff, 2000). To further characterize the transformant lines resulting from *drb1* transformation, seed was collected from these plant lines and their respective germination efficiencies assessed via their germination under an inhibiting concentration of ABA (Figure 8-4). In contrast to seed germinated on water-soaked filter paper, all assessed plant lines showed reduced to completely abolished germination in the presence of ABA. The germination of seed collected from the four transformant lines expressing the RDB2 of DRB1, and that displayed wild-type-like phenotypes (*see* Figure 8-2, plant lines *drb1*/DRB-C1, *drb1*/DRB-C2, *drb1*/DRB-C4 and *drb1*/DRB-C9), all showed limited sensitivity to ABA (Figure 8-4). Seed collected from the *drb1*/DRB-C3, *drb1*/DRB-C5, *drb1*/DRB-C6, *drb1*/DRB-C7 and *drb1*/DRB-C8 transformant lines was, however, highly sensitive to ABA treatment. The observed ABA hypersensitive of *drb1* transformant lines expressing the DRB-C3, DRB-C5, DRB-C6, DRB-C7 and DRB-C8 chimeric vectors was not surprising considering that the expression of these chimeric genes in the *drb1* mutant background failed to complement the *drb1* phenotype (Figure 8-2). ABA treatment reveals a clear correlation between *drb1* phenotype complementation and ABA sensitivity; that is, *drb1* transformant lines that complemented the *drb1* phenotype were not hypersensitive to ABA treatment, while those lines that failed to complement *drb1* were hypersensitive.

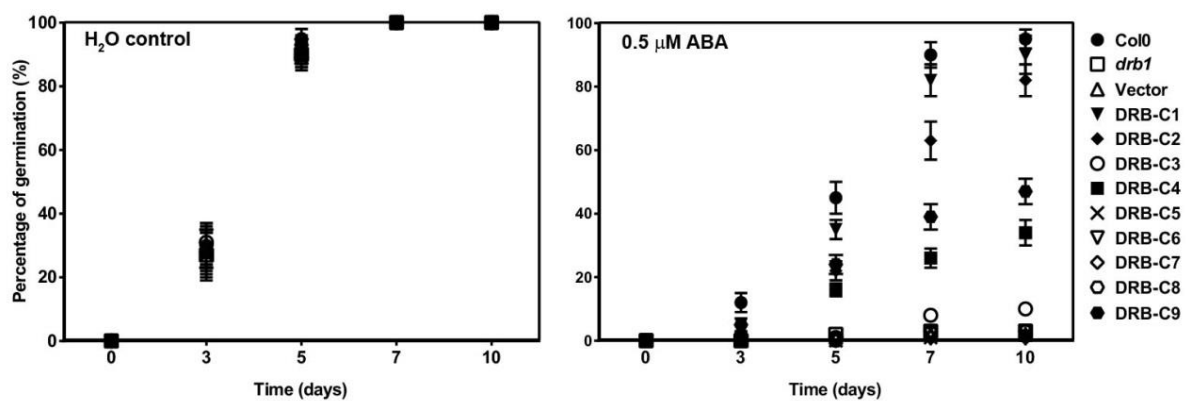
















Figure 8-4. Effects of exogenous ABA on wild-type, *drb1* and transgenic plants.

Seed of wild-type, *drb1* mutant and *drb1* transformant lines were germinated on filter paper saturated with either water (left) or 0.5 mM ABA (right) ($n = 3$). Seeds were incubated at 4°C for 48 h and then transferred to room temperature for assessment of their germination efficiency over a period of ten days.

8.5 Chapter highlights

-  All dsRNA binding domains of DRB2, DRB3, DRB4 and DRB5 were predicted to fold to give canonical structures, contrasting with the non-canonical RBD2 of DRB1.
-  The critical loop linking $\beta 1$ and $\beta 2$ (region 2) of the dsRNA binding domains, required for dsRNA minor groove recognition, was only re-oriented in RBD2 of DRB1.
-  An arginine residue has been selected in evolution, over histidine, in the critical loop (region 2) for DRB1 activity.
-  Amino acid alignment suggests that region 2 is an important structural determinant for DRB1 in the miRNA pathway.
-  The structural determinants of DRB1 function, and possibly DRB2, are complex and involve elements other than histidine in region 2.
-  The N-terminal dsRNA binding domains fulfill the function of the whole DRB1 when expression is driven by a constitutive promoter or *DRB1* endogenous promoter.
-  Transformation of a *drb1* mutant with chimeric genes lacking the non-canonical dsRNA binding domain of DRB1 failed to complement its phenotype.
-  RDB2 of DRB2 probably mediates specific protein-protein interactions that are different of those of DRB1.
-  miRNA accumulation and target gene expression showed strong correlation with the phenotypes expressed by the *drb1* transformant lines.
-  Germination of seed collected from transformant lines expressing RDB2 of DRB1, and that displayed wild-type-like phenotypes, showed limited sensitivity to ABA.
-  ABA treatment reveals a clear correlation between *drb1* phenotype complementation and ABA sensitivity.
-  The C-terminal of DRB2 can impair DRB1 function in the absence of DRB2 RBD1.
-  The first dsRNA binding domains of DRB1 and DRB2 are functionally similar, which are likely to be restricted to dsRNA binding activity.
-  The second dsRNA binding domain appears to define the function of DRB1 and DRB2 in the miRNA pathway.

PART IV – GENERAL DISCUSSION AND CONCLUSION

**Chapter 9 – General discussion,
conclusion and future directions**

miRNA activity has been almost exclusively studied at the transcript level of the target genes, while translation inhibition has been thought to be an alternative pathway in plants (Rogers and Chen, 2013). However, recent evidence suggests that miRNA-guided translational inhibition is a main component of miRNA activity. For instance, in floral tissue miRNA targets undergo preferentially translational inhibition, as opposed to cleavage of target transcript (Chen, 2004b; Grant-Downton et al., 2013; Reis et al., 2015). Furthermore, Li and colleagues (Li et al., 2013a) recently demonstrated that expression of artificial miRNAs (amiRNAs) predominantly mediate highly specific translational repression with limited mRNA decay or cleavage. The well-characterized miR398 plays an important role in environmental adaptation, and regulates its targets through both translation inhibition and cleavage (Sunkar et al., 2012; Zhu et al., 2011). More recently, we showed that DRB2 selects the miRNA regulatory mechanism by determining translational inhibition and repressing transcript cleavage (this thesis; Reis et al., 2015). We also showed that DRB2 has been much more conserved in evolution than DRB1, which is required for transcript cleavage, suggesting that translation inhibition is the ancient miRNA regulatory mechanism.

In this chapter I discuss the results presented in this thesis and how they have advanced our current knowledge.

9.1 Role of translation inhibition in plants

The role played by miRNAs in translation inhibition is still unclear but recent reports, as outlined above, suggest that it is distinct from the role in transcript cleavage. The current model is that miRNAs and siRNA-guided translational inhibition is a reversible process, allowing for rapid response under specific conditions, particularly stress (Voinnet, 2009). Although the reversibility of translation repression can be intuitively understood, it has not yet been experimentally validated in plants. The results presented in this thesis demonstrate that cleavage and translation inhibition are processes that can be studied independently using *drb1* and *drb2* mutants, respectively. By studying the changes in protein accumulation in these mutants, it was possible to identify salt stress as a candidate condition to test the role of translation inhibition in a stress response. This analysis showed that DRB1 and DRB2 play different roles in salt stress, and the release of translational inhibition in *drb2* resulted in plants that are more resistant to salt stress.

Plant miRNAs are master regulators, and the metabolic labeling approach presented here has identified and quantified ten of their targets, as well as several hundred non-miRNA targets.

PART IV – DISCUSSION AND CONCLUSION

It was found that proteins with altered abundance in *drb1* tend more towards increased than reduced levels. Reduced proteins had GO enrichment mostly related to the chloroplast. It has been reported that *drb1* has fewer stomata per leaf than wild-type plants (Jover-Gil et al., 2012), indicating that photosynthesis and respiration are compromised in this mutant, corroborating our findings of reduced chloroplast-related protein accumulation. Conversely, proteins with increased accumulation were GO-enriched for both environment response and metabolic process. Proteins with altered accumulation were mapped to metabolic pathways, and this showed a large number of proteins with altered accumulation involved in metabolism of secondary metabolites, amino acids and carbon in *drb1*. These are key processes in plant development, suggesting that the severe phenotypes observed are probably caused by a loss in cellular homeostasis. Moreover, fatty acid metabolism had enzymes with increased accumulation specifically in the beta-oxidation pathway, possibly disfavouring fatty acid synthesis and storage. DRB1 partnering proteins, DCL1 and SERRATE (SE), have also been previously implicated in fatty acid metabolism (Voisin et al., 2009; Willmann et al., 2011). In embryos of *dcl1*, GO enrichment revealed over-representation of genes involved in storage lipid, and these genes were up-regulated (Willmann et al., 2011). This appears to contrast my findings that beta-oxidation was favoured over storage in *drb1*, suggesting that DRB1/DCL1 interaction in seed and shoot apex results in different regulation of fatty acid metabolism. SE has been implicated in leaf cuticle formation, and only down-regulated genes in the *se* mutant were GO-enriched for this process (Voisin et al., 2009). This also contrasts with the results for *drb1* in the shoot apex, further suggesting that fatty acid metabolism is highly regulated by proteins required for miRNA biogenesis in a tissue-specific manner.

Although this thesis presented putative novel roles for DRB1, particularly in metabolic processes, DRB1 has been previously extensively studied together with DCL1 and SE in the miRNA pathway. In contrast, DRB2 has only recently been shown to be required in this pathway (Eamens et al., 2012a) and to participate in the selection of regulatory mechanism for plant miRNAs (this thesis, Reis et al., 2015). Here I found that protein accumulation in *drb2* correlates with environmental response and, to a much lesser extent, with certain metabolic processes. The most affected metabolic processes were similar to those in *drb1* (metabolism of secondary metabolites, amino acids and carbon), suggesting a common function. Moreover, proteins with increase accumulation in *drb2* were exclusively GO-enriched for biotic and abiotic response. This is in great contrast with the various GO terms enriched for proteins accumulated in *drb1*, suggesting that DRB2 plays a role in environmental adaptation, whereas DRB1 has a ubiquitous role.

9.2 Auto-regulation of the miRNA pathway

An important aspect of the miRNA pathway is its auto-regulation via a number of miRNA-mediated negative feedback loops, including the miR162/*DCL1*, miR168/*AGO1* and miR863/*SE* pathway checkpoints (Li et al., 2012; Vaucheret, 2006; Xie et al., 2003). The miR168/*AGO1* and miR162/*DCL1* interactions are well characterized (Vaucheret, 2006; Xie et al., 2003). In contrast, the miR863/*SE* relationship is poorly documented, although miR863 is known to regulate *SE* via a mRNA cleavage mechanism of silencing (Li et al., 2012; Xie et al., 2003). My results show that both cleavage and translation inhibition are required for miRNA pathway auto-regulation in the shoot apex and floral tissues. Translation inhibition was particularly pronounced in the regulation of *SE* and *AGO1*, core proteins in the miRNA biogenesis and activity, respectively. Furthermore, I also show that the non-miRNA targeted *DRB1* is transcriptionally regulated in the presence of *DRB2*, uncoupling cleavage and translation inhibition at the cellular level.

9.3 DRBs as scaffold proteins

In addition to *DCL1*, *DRB1* and *SE*, several other functionally diverse proteins have recently been implicated in the production of miRNAs. These include *TOUGH* (*TGH*), *DRB2*, *C-TERMINAL DOMAIN PHOSPHATASE-LIKE1* (*CPL1*), *DAWDLE* (*DDL*), *MODIFIER OF SNC1,2* (*MOS2*), *NEGATIVE ON TATA LESS2A* (*NOT2*), *RECEPTOR FOR ACTIVATED C KINASE1* (*RACK1*), *SICKLE* (*SIC*) and *STABILIZED1* (*STA1*) (Ben Chaabane et al., 2013; Manavella et al., 2012; Ren et al., 2012; Speth et al., 2013; Wang et al., 2013; Wu et al., 2013; Yu et al., 2008a; Zhan et al., 2012). Their number suggests that miRNA production is a complex and highly regulated process. Eukaryotic DRB proteins play central roles in many cellular processes by forming bridges between RNAs and their associated proteins to form a diverse array of ribonucleoprotein (RNP) complexes (e.g. human homologous *TRBP*, as recently reviewed (Daniels and Gagnol, 2012)). My finding that *DRB1* and *DRB2* determine the functional fate of a miRNA during its biogenesis raises the possibility that these proteins determine the arrangement, composition or activation of different protein complexes that govern the differential sorting of miRNAs into mechanistically distinct silencing pathways. Such a model is shown in Figure 9-1.

9.4 Structural determinants for DRB1 and DRB2 *in vivo* activity

Eukaryotic DRB proteins often contain more than one dsRNA-binding domain (RBD) (Curtin et al., 2008; Lee et al., 2013; Sohn et al., 2007). In humans, siRNA and miRNA biogenesis appear to require the Dicer partnering proteins PACT and TRBP, respectively (Lee et al., 2013). These proteins have three RBD, with the two N-terminal RBD of each protein conferring dsRNA substrate recognition and processing specificity of Dicer-dsRNA-binding protein complexes (Lee et al., 2013). *Caenorhabditis elegans* RDE-4 facilitates cleavage of long dsRNA to small interfering RNA (siRNA). A study using RDE-4/TRBP chimeric genes showed that RDE-4 promotes activity using its RBD2 to bind dsRNA, its linker region to interact with Dicer, and its C-terminus for Dicer activation (Parker et al., 2008). In *Drosophila*, the Dicer-binding partner protein, Loquacious, changes the choice of cleavage site by Dicer, producing miRNAs with target specificities different from those made by Dicer alone or Dicer bound to alternative protein partners (Fukunaga et al., 2012). The results presented in this thesis provide the structural determinants for Arabidopsis Dicer-binding partner proteins, DRB1 and DRB2. Arabidopsis DRB proteins contain two N-terminal dsRNA binding domains (Curtin et al., 2008), and I show that the first dsRNA binding domain of DRB1 is functionally similar to its counterpart in DRB2, while the second RBD appears to define their different function *in vivo*.

9.5 Conclusion

Although our knowledge of the biogenesis of plant miRNAs has dramatically improved in recent years, several of the latest findings indicate that some important mechanisms remain poorly understood. The biogenesis of miRNA/miRNA* from miRNA-containing intermediates occurs in dicing bodies (D-bodies), and a growing number of genes, in addition to well characterized core components (e.g., DCL1, SE and DRB1), have been shown to be required in this process (reviewed by Rogers and Chen, 2013). Thus, it is likely that the D-bodies are dynamic and may vary in protein composition accordingly to developmental stage, environmental conditions and even precursor transcript structure. Although DRB1 is a well characterized DCL1 partnering protein, the results presented in this thesis revealed that DRB2 has been much more conserved during plant evolution, that it represses the expression of *DRB1* and that it is required for miRNAs that guide translation inhibition. In addition, DRB1 and DRB2 have similar but functionally different domains, such as their dsRBD2 and C-terminus. The results presented here suggest that D-bodies are dynamic and different

components can be assembled, such as DRB1 or DRB2, leading to different outcomes (i.e. transcript cleavage or translational inhibition). Moreover, it is suggested that cleavage and translation inhibition are independent mechanisms and the later play a major role in environmental adaptation, insights that have not been experimentally shown before.

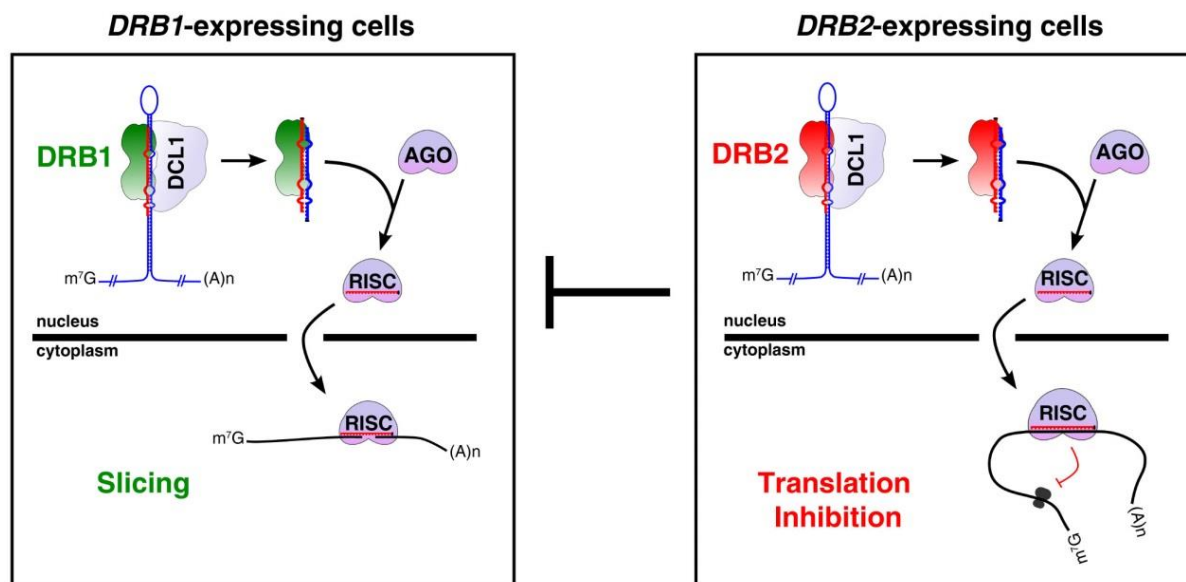


Figure 9-1. Proposed model for the role of DRB1 and DRB2 in the miRNA pathway.

Pri-miRNAs are processed in the nucleus by DCL1 bound to a DRB partner. miRNA/miRNA* bound to DRB is loaded onto an AGO protein to form the RNA-induced silencing complex (RISC) – a process that might define the destiny of RISC. In DRB1-expressing cells, RISC is guided to the cleavage (slicing) pathway. Conversely, in DRB2-expressing cells, DRB1 expression is repressed and DRB2 guides RISC to the translation inhibition pathway.

9.6 Future directions

The results presented in this thesis demonstrated that the selection of regulatory mechanisms for plant miRNAs is determined by the dicer partnering protein DRB2. However, AGO1, the main catalytic component of RISC, is clearly capable of cleaving its targets, and the mechanism by which DRB2 suppresses this activity is still unknown. I speculate that DRB2 may aid a posttranslational modification (e.g., phosphorylation) of AGO proteins, thereby hindering their cleavage activity, as reported for human Ago2 after phosphorylation by Akt kinase (Horman et al., 2013). This could occur, for instance, through the bridging activity of DRB2 linking AGO proteins to a kinase, a process that would not occur with DRB1. However, such kinase or other AGO modifier that hinders the cleavage activity of AGO has

PART IV – DISCUSSION AND CONCLUSION

not yet been identified; thus, how DRB2 activity leads to cleavage-impaired AGO proteins is still unknown.

This thesis presents evidences that DRB2 is conserved and plays a major role in response to salt stress. It is suggested that DRB2 is also involved in other environmental adaptive processes, but this needs to be further verified experimentally. It would be important to investigate the role of DRB2 in stress responses in crop plants. This has a major potential as miRNAs are known key players in environmental adaptation, and DRB2 has been shown in this thesis to be required for their biogenesis in the translation inhibition pathway.

PART V – SUPPLEMENTARY DATA

Sequence of synthesized DNA

Sequence of synthesized DNA used to construct vectors to transform *drb1* mutants. Each sequence is identified as “gBlock” (Integrated DNA Technologies, IDT) of DRB gene (DRBgBlock), and are followed by numbers that identify its components, such as, DRBgBlock-1 1.2-1.L-1.1 (5’ – RDB1 of DRB2; inter-domain loop of DRB1; RDB1 of DRB1 – 3’).

DRBgBlock-1 1.2-1.L-1.1

atCAATTGctatTTATGCAAGAACCTACTTCAAGAATACGCTCAAAAGATGAATTACGCGAT
TCCATTGTATCAGTGCCAGAAGGTCGAAACTCTTGGGAGAGTTACACAATTCACATGTAC
TGTAGAGATTGGAGGCATAAAGTACACAGGAGCTGCAACAAGA ACTAAAAAGATGCT
GAGATTAGCGCTGGGAGA ACTGCTCTTTTAGCGATCCAGTCATCCAGTGAGCTAAGCCAA
TGTGTTTCACAACCTGTTACGAAACGGGAGTTTTCAAAAGTCCGTTGCAGGAGTATGCT
CAGAAGTACAAGCTCCCAACGCCTGTTTATGAGATCGTTAAAGAAGGCCCTTCACACAA
ATCTTTATTTCAATCGACTGTGATACTGGATGGTGTGAGATATAATTCTTTGCCTGGATTC
TTCAATCGTAAGGCTGCAGAGCAATCAGCTGCCGAGGTTGCTCTCCGGAATTAGCAAA
AACTAGTtaatgaGGATCCat

DRBgBlock-4 2.1-1.L-1.2

atCAATTGctatATGTATAAGAACCAGCTACAAGAGTTGGCTCAGAGGAGCTGCTTTAATCTT
CCTTCGTATACTTGTATTAGGGAAGGTCCTGACCACGCGCCGCGATTCAAGGCTACTGTT
AACTTTAACGGCGAGATCTTTGAGAGTCTCAGTATTGTTCTACTCTTCGTC AAGCTGAA
CACTCTGCTGCTGAAGTTGCTCTCAATGCTCTCTCTAATTCAGTGAGCTAAGCCAATGTG
TTTCAACAACCTGTTACGAAACGGGATTATGCAAGAACCTACTTCAAGAATACGCTCAAA
AGATGAATTACGCGATTCCATTGTATCAGTGCCAGAAGGTCGAAACTCTTGGGAGAGTTA
CACAATTCACATGTACTGTAGAGATTGGAGGCATAAAGTACACAGGAGCTGCAACAAGA
ACTAAAAAGATGCTGAGATTAGCGCTGGGAGAACTGCTCTTTTAGCGATCCAGTCAACT
AGTtaatgaGGATCCat

DRBgBlock-5 1.1-1.L-2.2

atatCAATTGctatGTTTTCAAAAGTCGGTTGCAGGAGTATGCTCAGAAGTACAAGCTCCCAA
CGCCTGTTTATGAGATCGTTAAAGAAGGCCCTTCACACAAATCTTTATTTCAATCGACTG
TGATACTGGATGGTGTGAGATATAATTCTTTGCCTGGATTCTTCAATCGTAAGGCTGCAG
AGCAATCAGCTGCCGAGGTTGCTCTCCGGAATTAGCAAAATCCAGTGAGCTAAGCCAA
TGTGTTTCACAACCTGTTACGAAACGGGAGTGTATAAGAATCTTTTGCAAGAGATAGCT
CAAAGAGTGGGAGCTCCTTTACCGCATATACTACTTTTCAGGTCAGGTCCTTGGTCACCAA
CCTGTGTTTACTGGTACTGTAGAATTGGCTGGAATTACGTTCACTGGAGATCCAGCTAAG
AACAGAAGCAAGCAGAGAAGAATGCTGCAATGGCTGCTTGGTCTTCCCTAAAACAAAC
TAGTtaatgaGGATCCata

DRBgBlock-6 2.2-1.L-1.2

PART V – SUPPLEMENTARY DATA

atatCAATTGctatGTGTATAAGAATCTTTTGCAAGAGATAGCTCAAAGAGTGGGAGCTCCTTT
ACCGCGATATACTACTTTTCAGGTCAGGTCCTGGTCACCAACCTGTGTTTACTGGTACTGTA
GAATTGGCTGGAATTACGTTCACTGGAGATCCAGCTAAGAACAAGAAGCAAGCAGAGAA
GAATGCTGCAATGGCTGCTTGGTCTTCCCTAAAACAATCCAGTGAGCTAAGCCAATGTGT
TTCACAACCTGTTACGAAACGGGATTATGCAAGAACCTACTTCAAGAATACGCTCAAA
AGATGAATTACGCGATTCCATTGTATCAGTGCCAGAAGGTCGAAACTCTTGGGAGAGTTA
CACAATTCACATGTACTGTAGAGATTGGAGGCATAAAGTACACAGGAGCTGCAACAAGA
ACTAAAAAAGATGCTGAGATTAGCGCTGGGAGAAGTCTCTTTTAGCGATCCAGTCAACT
AGTtaatgaGGATCCata

DRBgBlock-7 4.1-1.L-1.2

atCAATTGctatGTATACAAAGGTCAACTGCAAGCGTATGCCCTGCAACATAATCTGGAGCT
ACCAGTGTATGCGAATGAGAGAGAAGGGCCTCCTCATGCTCCTAGATTTAGATGTAATGT
TACATTCTGTGGACAGACTTTCCAGAGCTCTGAATTCTTTCCGACACTAAAATCGGCTGA
ACATGCCGCTGCAAAAATTGCAGTTGCTTCTTTGACGCCATCCAGTGAGCTAAGCCAATG
TGTTTCACAACCTGTTACGAAACGGGATTATGCAAGAACCTACTTCAAGAATACGCTCA
AAAGATGAATTACGCGATTCCATTGTATCAGTGCCAGAAGGTCGAAACTCTTGGGAGAG
TTACACAATTCACATGTACTGTAGAGATTGGAGGCATAAAGTACACAGGAGCTGCAACA
AGAACTAAAAAAGATGCTGAGATTAGCGCTGGGAGAAGTCTCTTTTAGCGATCCAGTC
AACTAGTtaatgaGGATCCat

DRBgBlock-8 1.1-1.L-4.2

atatCAATTGctatGTTTTCAAAGTTCGGTTGCAGGAGTATGCTCAGAAGTACAAGCTCCCAA
CGCCTGTTTATGAGATCGTTAAAGAAGGCCCTTCACACAAATCTTTATTTCAATCGACTG
TGATACTGGATGGTGTGAGATATAATTCTTTGCCTGGATTCTTCAATCGTAAGGCTGCAG
AGCAATCAGCTGCCGAGGTTGCTCTCCGGGAATTAGCAAAATCCAGTGAGCTAAGCCAA
TGTGTTTCACAACCTGTTACGAAACGGGAGCCTACAAGAACCTGTTACAAGAAATTGCA
CAGAAAGAGAGTTCTCTGTTACCATTTTATGCAACTGCTACATCTGGTCCATCGCATGCG
CCTACTTTTACTTCAACTGTTGAGTTTGCTGGTAAAGTTTTTCAGTGGAGAAGAGGCGAAA
ACCAAAAAGTTGGCTGAAATGAGCGCTGCTAAAGTTGCATTCATGAGTATCAAAAATAC
TAGTtaatgaGGATCCata

DRBgBlock-9 4.2-1.L-1.2

atatCAATTGctatGCCTACAAGAACCTGTTACAAGAAATTGCACAGAAAGAGAGTTCTCTGT
TACCATTTTATGCAACTGCTACATCTGGTCCATCGCATGCGCCTACTTTTACTTCAACTGT
TGAGTTTGCTGGTAAAGTTTTTCAGTGGAGAAGAGGCGAAAACCAAAAAGTTGGCTGAAA
TGAGCGCTGCTAAAGTTGCATTCATGAGTATCAAAAATTCAGTGAGCTAAGCCAATGTG
TTTACAACCTGTTACGAAACGGGATTATGCAAGAACCTACTTCAAGAATACGCTCAAA
AGATGAATTACGCGATTCCATTGTATCAGTGCCAGAAGGTCGAAACTCTTGGGAGAGTTA
CACAATTCACATGTACTGTAGAGATTGGAGGCATAAAGTACACAGGAGCTGCAACAAGA
ACTAAAAAAGATGCTGAGATTAGCGCTGGGAGAAGTCTCTTTTAGCGATCCAGTCAACT
AGTtaatgaGGATCCata

DRBgBlock-10 1.1-2.L-1.2

atCAATTGctatGTTTTCAAAGTTCGGTTGCAGGAGTATGCTCAGAAGTACAAGCTCCCAAC
GCCTGTTTATGAGATCGTTAAAGAAGGCCCTTCACACAAATCTTTATTTCAATCGACTGT
GATACTGGATGGTGTGAGATATAATTCTTTGCCTGGATTCTTCAATCGTAAGGCTGCAGA
GCAATCAGCTGCCGAGGTTGCTCTCCGGGAATTAGCAAAACGTGGTCTTCTCACTCTCT
TGCCGCCAGGATCTTGATGAGACGGGTTTATGCAAGAACCTACTTCAAGAATACGCTCA

PART V – SUPPLEMENTARY DATA

AAAGATGAATTACGCGATTCCATTGTATCAGTGCCAGAAGGTCGAAACTCTTGGGAGAG
TTACACAATTCACATGTAAGTACTGTAGAGATTGGAGGCATAAAGTACACAGGAGCTGCAACA
AGAACTAAAAAAGATGCTGAGATTAGCGCTGGGAGAAGTCTCTTTTAGCGATCCAGTC
AACTAGTtaatgaGGATCCat

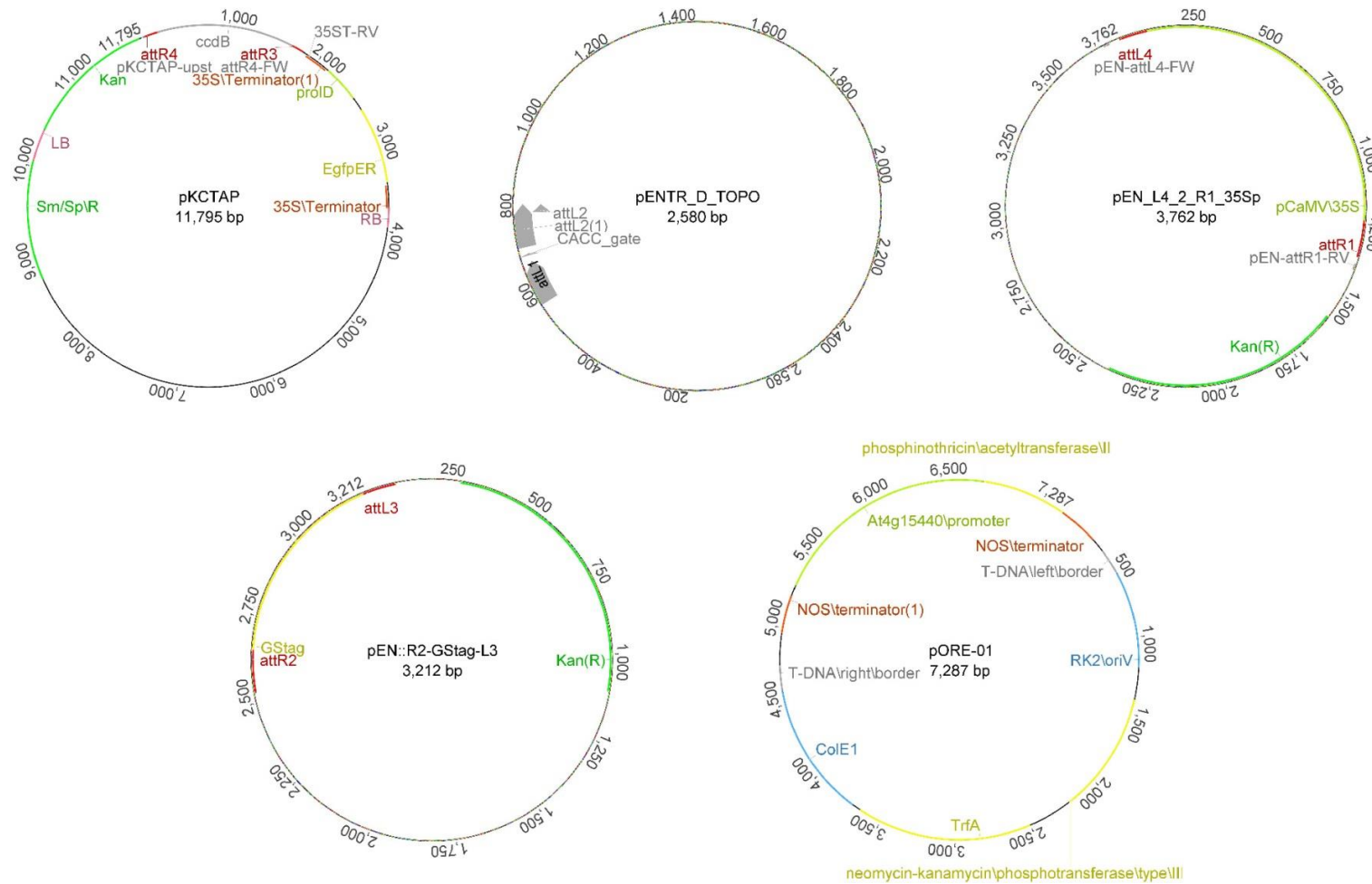
DRBgBlock-11 1.1-4.L-1.2

atataaCAATTGctatGTTTTCAAAGTCGGTTGCAGGAGTATGCTCAGAAGTACAAGCTCCCA
ACGCTGTTTATGAGATCGTTAAAGAAGGCCCTTCACACAAATCTTTATTTCAATCGACT
GTGATACTGGATGGTGTGATATAAATTCTTTGCCTGGATTCTTCAATCGTAAGGCTGCA
GAGCAATCAGCTGCCGAGGTTGCTCTCCGGGAATTAGCAAAACAAAGTCCAGAGGGAAT
TGATGTTTTATGCAAGAACCTACTTCAAGAATACGCTCAAAGATGAATTACGCGATTCC
ATTGTATCAGTGCCAGAAGGTCGAAACTCTTGGGAGAGTTACACAATTCACATGTAAGT
AGAGATTGGAGGCATAAAGTACACAGGAGCTGCAACAAGAACTAAAAAAGATGCTGAG
ATTAGCGCTGGGAGAAGTCTCTTTTAGCGATCCAGTCAACTAGTtaatgaGGATCCatataa

DRBgBlock-12 4.1-1.L-4.2

atatCAATTGctatGTATACAAAGGTCAACTGCAAGCGTATGCCCTGCAACATAATCTGGAGC
TACCAGTGTATGCGAATGAGAGAGAAGGGCCTCCTCATGCTCCTAGATTTAGATGTAATG
TTACATTCTGTGGACAGACTTTCCAGAGCTCTGAATTCTTTCCGACACTAAAATCGGCTG
AACATGCCGCTGCAAAAATTGCAGTTGCTTCTTTGACGCCATCCAGTGAGCTAAGCCAAT
GTGTTTCACAACCTGTTTACGAAACGGGAGCCTACAAGAACCTGTTACAAGAAATTGCA
CAGAAAGAGAGTTCTCTGTTACCATTTTATGCAACTGCTACATCTGGTCCATCGCATGCG
CCTACTTTTACTTCAACTGTTGAGTTTGGTAAAGTTTTTCAGTGGAGAAGAGGGCGAAA
ACCAAAAAGTTGGCTGAAATGAGCGCTGCTAAAGTTGCATTCATGAGTATCAAAAATAC
TAGTtaatgaGGATCCata

Map of cloning vectors



Vector maps were created using Geneious v5.6.4.

Microarray data

Table 9-1. Transcript expression level of miRNA targets in shoot apex in *drb2* and wild-type.

Targeted locus (validated or predicted)	Fold Change (drb2vsCol0)	ANOVA p-value (drb2vsCol0)	FDR p-value (drb2vsCol0)	miRNA*	Ref.†
AT2G33810(V)	-1.43	0.005721	0.038831	miR156	1,2
AT5G43270(V)	-1.19	0.00136	0.016984	miR156	3
AT1G53160(V)	-2.5	0.000005	0.001927	miR156	4
AT3G15270(V)	-1.69	0.000064	0.003802	miR156	1
AT2G42200(P)	-1.17	0.006637	0.042356	miR156	5
AT1G27360(P)	-1.11	0.13333	0.295838	miR156	5
AT3G19553(P)	-1	0.88282	0.939073	miR157	2
AT2G34960(P)	1.18	0.275935	0.470338	miR157	6
AT2G03220(P)	-1.02	0.956075	0.979238	miR158	4
AT3G03580(P)	1.17	0.065439	0.186466	miR158	4
AT5G55930(V)	-1.56	0.003583	0.029088	miR159	7
AT2G26960(P)	-1.36	0.036457	0.125779	miR159	5
AT5G55020(P)	-1.14	0.257033	0.450104	miR159	5,8
AT2G26950(P)	-1.07	0.151662	0.321009	miR159	5,8
AT4G26930(P)	1.02	0.388141	0.581447	miR159	5
AT2G32460(V)	1.14	0.170883	0.346767	miR159	9
AT4G37770(P)	1.3	0.063793	0.183342	miR159	7
AT5G06100(V)	-1.11	0.00841	0.049121	miR159/miR319	10,11
AT3G11440(V)	-1.04	0.026448	0.101927	miR159/miR319	10-12
AT2G28350(V)	-1.14	0.402587	0.594851	miR160	3,13
AT4G30080(V)	-1.1	0.174174	0.351422	miR160	4,13
AT1G77850(V)	1.01	0.600188	0.754344	miR160	3,12,13
AT5G52060(P)	1.27	0.00012	0.005025	miR160	6
AT1G62670(P)	-1.2	0.376576	0.571274	miR161/miR400	14
AT1G62670(P)	-1.2	0.376576	0.571274	miR161/miR400	14
AT1G01040(V)	1.27	0.0032	0.027204	miR162	15
AT4G24160(P)	-1.49	0.0006	0.011018	miR163	6
AT3G44870(P)	1.06	0.431649	0.619971	miR163	16
AT1G66690(V)	1.18	0.518024	0.691178	miR163	16
AT1G66720(V)	1.27	0.730318	0.844593	miR163	16
AT1G66700(V)	1.33	0.011782	0.060685	miR163	16
AT3G44860(V)	3.8	0.000168	0.00584	miR163	16
AT1G15125(P)	5.53	0.00000366	0.001339	miR163	17
AT5G53950(V)	-1.16	0.701059	0.824585	miR164	3,18,19
AT5G07680(V)	-1.07	0.047311	0.149559	miR164	19
AT5G39610(P)	-1.07	0.378839	0.572904	miR164	20
AT5G61430(V)	-1.03	0.682675	0.812626	miR164	1,19
AT3G15170(V)	-1	0.897197	0.947654	miR164	3,18,19
AT3G12977(P)	1.01	0.950523	0.97575	miR164	21
AT1G56010(V)	1.1	0.016243	0.07443	miR164	4,22
AT1G52150(V)	1.34	0.000042	0.003355	miR165/miR166	4,13
AT1G30490(V)	1.39	0.000043	0.003355	miR165/miR166	19,23
AT2G34710(V)	1.47	0.000059	0.003683	miR165/miR166	19
AT2G34710(V)	1.47	0.000059	0.003683	miR165/miR166	19
AT5G60690(V)	1.51	0.000603	0.011033	miR165/miR166	19,24
AT4G32880(V)	1.55	0.000031	0.00302	miR165/miR166	19
AT1G30330(V)	1.1	0.000609	0.011068	miR167	4

PART V – SUPPLEMENTARY DATA

AT5G37020(V)	1.13	0.000275	0.007432	miR167	3,12
AT1G48410(V)	1.19	0.000333	0.008143	miR168	12,25
AT5G12840(P)	-1.21	0.001387	0.017171	miR169	20
AT5G06510(V)	1.11	0.080673	0.21275	miR169	20
AT3G05690(V)	1.25	0.008422	0.049129	miR169	4,20
AT1G17590(V)	1.43	0.001702	0.01923	miR169	4
AT1G72830(V)	1.87	0.000018	0.002643	miR169	4
AT4G00150(V)	-1.44	0.006008	0.039826	miR170/miR171	3,26
AT3G60630(V)	1.22	0.0015	0.017961	miR170/miR171	3,12,26
AT2G45160(P)	1.24	0.005583	0.038235	miR170/miR171	5,26
AT5G60120(V)	1.06	0.042235	0.138491	miR172	3,7,27
AT2G28550(V)	1.1	0.071356	0.196519	miR172	3,7,27
AT5G67180(V)	1.23	0.000079	0.004137	miR172	3
AT4G36920(V)	1.34	0.00148	0.017847	miR172	3,7,28
AT3G27150(V)	1.12	0.14997	0.318842	miR2111	29
AT2G31070(V)	-1.57	0.000411	0.009058	miR319	11
AT1G53230(V)	-1.31	0.000327	0.008071	miR319	11
AT3G15030(V)	-1.22	0.010879	0.057707	miR319	11
AT1G30210(V)	-1.18	0.002977	0.026145	miR319	11
AT4G18390(V)	-1.12	0.003606	0.029175	miR319	11
AT1G12820(V)	-1.12	0.001996	0.02115	miR393	20
AT3G62980(V)	1.02	0.414096	0.60572	miR393	20
AT3G26810(V)	1.09	0.008468	0.049253	miR393	20,30
AT4G03190(V)	1.54	0.000035	0.003129	miR393	20
AT1G27340(V)	1.17	0.00024	0.006978	miR394	20
AT3G22890(V)	-1.1	0.027538	0.104674	miR395	4
AT2G28780(V)	-1.09	0.026279	0.101451	miR395	31
AT5G10180(V)	1.06	0.000807	0.012904	miR395	4
AT5G43780(V)	1.22	0.083265	0.217584	miR395	20
AT4G14680(V)	1.29	0.000088	0.004331	miR395	31
AT4G24150(V)	-1.83	0.010382	0.056038	miR396	20
AT4G37740(V)	-1.18	0.000199	0.006359	miR396	20
AT3G52910(P)	-1.11	0.009176	0.051684	miR396	20
AT2G45480(V)	-1.08	0.045191	0.145064	miR396	20
AT2G36400(V)	-1.04	0.103185	0.249705	miR396	20
AT2G22840(V)	-1.01	0.628058	0.774666	miR396	20
AT5G53660(V)	1.09	0.317442	0.511531	miR396	20
AT2G29130(V)	-3.08	0.000007	0.002123	miR397	20
AT5G60020(V)	-1.3	0.000103	0.004637	miR397	20
AT2G38080(V)	-1.25	0.004164	0.031834	miR397	20
AT3G60250(P)	-1.04	0.631288	0.776097	miR397	14
AT2G28190(V)	-1.2	0.001031	0.014832	miR398	20,32
AT3G15640(V)	1.03	0.119292	0.274638	miR398	20
AT1G08830(V)	1.27	0.011301	0.059102	miR398	20,32
AT3G06370(P)	1.74	0.000087	0.004331	miR398	33
AT2G33770(V)	-1.39	0.000148	0.005521	miR399	4
AT1G06580(P)	-1.06	0.473348	0.655242	miR400	14
AT2G31400(P)	-1.03	0.427364	0.617086	miR400	14
AT3G16010(P)	-1	0.961741	0.982713	miR400	34
AT1G22960(P)	1.05	0.938414	0.969875	miR400	34
AT1G62720(P)	1.1	0.56053	0.724501	miR400	14
AT1G62590(P)	1.13	0.377398	0.572024	miR400	34
AT4G19440(P)	1.16	0.023947	0.095599	miR400	14
AT1G63130(P)	1.02	0.784676	0.878193	miR400	6
AT1G62930(P)	1.29	0.078852	0.209675	miR400	6
AT1G31280(V)	1.45	0.000353	0.008358	miR403	4
AT2G30210(V)	-2.64	0.000346	0.008281	miR408	7
AT2G47020(P)	-1.21	0.01573	0.072956	miR408	14

PART V – SUPPLEMENTARY DATA

AT5G07130(P)	-1.06	0.162031	0.335449	miR408	7
AT2G02850(P)	1.06	0.055124	0.165901	miR408	14
AT5G05390(P)	1.08	0.12691	0.285886	miR408	7
AT5G60760(V)	-1.15	0.034638	0.121542	miR447	4
AT5G39370(V)	-1.12	0.237198	0.427532	miR447	35
AT3G45090(P)	1.13	0.000312	0.00785	miR447	4
AT5G43740(V)	-1.19	0.09837	0.242151	miR472	36
AT1G51480(V)	1.04	0.753305	0.860781	miR472	36,37
AT1G53290(V)	1.11	0.181851	0.361052	miR775	37
AT5G53890(P)	1.1	0.09158	0.231621	miR779	6
AT4G15310(P)	1.17	0.973549	0.98751	miR779	6
AT5G23480(P)	-1.1	0.126041	0.284629	miR781	37
AT1G44900(P)	1.3	0.000032	0.003045	miR781	37
AT1G52820(P)	1.29	0.038989	0.131475	miR781	6
AT5G02350(P)	-1.3	0.033482	0.11871	miR822	38
AT2G13900(P)	-1.02	0.455777	0.639751	miR822	38
AT2G02620(P)	1.1	0.390517	0.583274	miR822	38
AT5G02330(P)	1.18	0.713522	0.833332	miR822	38
AT1G69770(P)	-1.02	0.214958	0.401836	miR823	37,38
AT3G57230(V)	1.1	0.31312	0.507192	miR824	37
AT1G02860(V)	1.07	0.042343	0.138746	miR827	37
AT5G18560(P)	1.01	0.465211	0.648019	miR829	38
AT2G02740(P)	-1.01	0.424324	0.614974	miR840	38
AT4G13570(P)	1.11	0.740447	0.851852	miR841	38
AT2G38810(P)	1.16	0.012236	0.062211	miR841	38
AT1G70470(P)	1.33	0.008093	0.047995	miR841	38
AT1G52070(P)	-1.14	0.713139	0.833217	miR846	38
AT5G28520(V)	1.02	0.929631	0.965034	miR846	38
AT1G57570(P)	1.04	0.320419	0.514643	miR846	38
AT1G52040(P)	1.16	0.024001	0.095763	miR846	38
AT1G52030(P)	1.31	0.024001	0.010663	miR846	38
AT1G52050(P)	1.2	0.184486	0.364635	miR846	38
AT5G49870(P)	1.3	0.389464	0.58252	miR846	37,38
AT1G52060(P)	1.33	0.133964	0.296952	miR846	38
AT2G25980(P)	1.33	0.050994	0.15748	miR846	37,38
AT5G38550(V)	1.48	0.000093	0.004445	miR846	37
AT3G09220(V)	-1.16	0.136551	0.300622	miR857	37
AT5G49330(P)	-1.72	0.005914	0.039518	miR858	37
AT1G66230(P)	-1.61	0.006346	0.041141	miR858	37
AT3G08500(V)	-1.35	0.006653	0.04242	miR858	37
AT4G12350(P)	-1.18	0.206135	0.391283	miR858	37
AT3G24310(P)	-1.13	0.23691	0.427234	miR858	37
AT2G47460(V)	-1.11	0.34947	0.544463	miR858	37
AT5G35550(P)	-1.07	0.712756	0.833029	miR858	37
AT3G62610(P)	1.03	0.671206	0.804886	miR858	37
AT1G06180(P)	1.12	0.023727	0.095009	miR858	37
AT1G19100(P)	1.24	0.001052	0.014993	miR869	6

* Only miRNAs identified in this work were considered.

† Reference refers to the identification of miRNA (*) that target a transcript locus.

SUPPLEMENTARY REFERENCES

- 1 Wu, G. & Poethig, R. S. Temporal regulation of shoot development in *Arabidopsis thaliana* by miR156 and its target SPL3. *Development* **133**, 3539-3547, doi:10.1242/dev.02521 (2006).

- 2 Gandikota, M. *et al.* The miRNA156/157 recognition element in the 3' UTR of the Arabidopsis SBP box gene SPL3 prevents early flowering by translational inhibition in seedlings. *The Plant Journal* **49**, 683-693, doi:10.1111/j.1365-313X.2006.02983.x (2007).
- 3 Kasschau, K. D. *et al.* P1/HC-Pro, a Viral Suppressor of RNA Silencing, Interferes with Arabidopsis Development and miRNA Function. *Developmental Cell* **4**, 205-217, doi:http://dx.doi.org/10.1016/S1534-5807(03)00025-X (2003).
- 4 Allen, E., Xie, Z., Gustafson, A. M. & Carrington, J. C. microRNA-Directed Phasing during Trans-Acting siRNA Biogenesis in Plants. *Cell* **121**, 207-221, doi:http://dx.doi.org/10.1016/j.cell.2005.04.004 (2005).
- 5 Rhoades, M. W. *et al.* Prediction of Plant MicroRNA Targets. *Cell* **110**, 513-520, doi:http://dx.doi.org/10.1016/S0092-8674(02)00863-2 (2002).
- 6 Alves-Junior, L., Niemeier, S., Hauenschild, A., Rehmsmeier, M. & Merkle, T. Comprehensive prediction of novel microRNA targets in Arabidopsis thaliana. *Nucleic Acids Research* **37**, 4010-4021, doi:10.1093/nar/gkp272 (2009).
- 7 Schwab, R. *et al.* Specific Effects of MicroRNAs on the Plant Transcriptome. *Developmental Cell* **8**, 517-527, doi:http://dx.doi.org/10.1016/j.devcel.2005.01.018 (2005).
- 8 Park, W., Li, J., Song, R., Messing, J. & Chen, X. CARPEL FACTORY, a Dicer Homolog, and HEN1, a Novel Protein, Act in microRNA Metabolism in Arabidopsis thaliana. *Current Biology* **12**, 1484-1495, doi:http://dx.doi.org/10.1016/S0960-9822(02)01017-5 (2002).
- 9 Reyes, J. L. & Chua, N.-H. ABA induction of miR159 controls transcript levels of two MYB factors during Arabidopsis seed germination. *The Plant Journal* **49**, 592-606, doi:10.1111/j.1365-313X.2006.02980.x (2007).
- 10 Millar, A. A. & Gubler, F. The Arabidopsis GAMYB-Like Genes, MYB33 and MYB65, Are MicroRNA-Regulated Genes That Redundantly Facilitate Anther Development. *The Plant Cell Online* **17**, 705-721, doi:10.1105/tpc.104.027920 (2005).
- 11 Palatnik, J. F. *et al.* Control of leaf morphogenesis by microRNAs. *Nature* **425**, 257-263 (2003).
- 12 Vazquez, F., Gascioli, V., Cr  t  , P. & Vaucheret, H. The Nuclear dsRNA Binding Protein HYL1 Is Required for MicroRNA Accumulation and Plant Development, but Not Posttranscriptional Transgene Silencing. *Current Biology* **14**, 346-351, doi:http://dx.doi.org/10.1016/j.cub.2004.01.035 (2004).
- 13 Mallory, A. C., Bartel, D. P. & Bartel, B. MicroRNA-Directed Regulation of Arabidopsis AUXIN RESPONSE FACTOR17 Is Essential for Proper Development and Modulates Expression of Early Auxin Response Genes. *The Plant Cell Online* **17**, 1360-1375, doi:10.1105/tpc.105.031716 (2005).
- 14 Sunkar, R. & Zhu, J.-K. Novel and Stress-Regulated MicroRNAs and Other Small RNAs from Arabidopsis. *The Plant Cell Online* **16**, 2001-2019, doi:10.1105/tpc.104.022830 (2004).
- 15 Xie, Z., Kasschau, K. D. & Carrington, J. C. Negative Feedback Regulation of Dicer-Like1 in Arabidopsis by microRNA-Guided mRNA Degradation. *Current Biology* **13**, 784-789, doi:http://dx.doi.org/10.1016/S0960-9822(03)00281-1 (2003).
- 16 Allen, E. *et al.* Evolution of microRNA genes by inverted duplication of target gene sequences in Arabidopsis thaliana. *Nature genetics* **36**, 1282-1290 (2004).
- 17 Bhargava, A. *et al.* Identification of Cytokinin-Responsive Genes Using Microarray Meta-Analysis and RNA-Seq in Arabidopsis. *Plant Physiology* **162**, 272-294, doi:10.1104/pp.113.217026 (2013).
- 18 Baker, C. C., Sieber, P., Wellmer, F. & Meyerowitz, E. M. The early extra petals1 Mutant Uncovers a Role for MicroRNA miR164c in Regulating Petal Number in Arabidopsis. *Current Biology* **15**, 303-315, doi:http://dx.doi.org/10.1016/j.cub.2005.02.017 (2005).
- 19 Mallory, A. C., Dugas, D. V., Bartel, D. P. & Bartel, B. MicroRNA Regulation of NAC-Domain Targets Is Required for Proper Formation and Separation of Adjacent Embryonic,

- Vegetative, and Floral Organs. *Current Biology* **14**, 1035-1046, doi:http://dx.doi.org/10.1016/j.cub.2004.06.022 (2004).
- 20 Jones-Rhoades, M. W. & Bartel, D. P. Computational Identification of Plant MicroRNAs and Their Targets, Including a Stress-Induced miRNA. *Molecular Cell* **14**, 787-799, doi:http://dx.doi.org/10.1016/j.molcel.2004.05.027 (2004).
- 21 Gustafson, A. M. *et al.* ASRP: the Arabidopsis Small RNA Project Database. *Nucleic Acids Research* **33**, D637-D640, doi:10.1093/nar/gki127 (2005).
- 22 Guo, H.-S., Xie, Q., Fei, J.-F. & Chua, N.-H. MicroRNA Directs mRNA Cleavage of the Transcription Factor NAC1 to Downregulate Auxin Signals for Arabidopsis Lateral Root Development. *The Plant Cell Online* **17**, 1376-1386, doi:10.1105/tpc.105.030841 (2005).
- 23 Tang, G., Reinhart, B. J., Bartel, D. P. & Zamore, P. D. A biochemical framework for RNA silencing in plants. *Genes & Development* **17**, 49-63, doi:10.1101/gad.1048103 (2003).
- 24 Emery, J. F. *et al.* Radial Patterning of Arabidopsis Shoots by Class III HD-ZIP and KANADI Genes. *Current Biology* **13**, 1768-1774, doi:http://dx.doi.org/10.1016/j.cub.2003.09.035 (2003).
- 25 Vaucheret, H., Vazquez, F., Cr  t  , P. & Bartel, D. P. The action of ARGONAUTE1 in the miRNA pathway and its regulation by the miRNA pathway are crucial for plant development. *Genes & Development* **18**, 1187-1197, doi:10.1101/gad.1201404 (2004).
- 26 Llave, C., Xie, Z., Kasschau, K. D. & Carrington, J. C. Cleavage of Scarecrow-like mRNA Targets Directed by a Class of Arabidopsis miRNA. *Science* **297**, 2053-2056, doi:10.1126/science.1076311 (2002).
- 27 Aukerman, M. J. & Sakai, H. Regulation of Flowering Time and Floral Organ Identity by a MicroRNA and Its APETALA2-Like Target Genes. *The Plant Cell Online* **15**, 2730-2741, doi:10.1105/tpc.016238 (2003).
- 28 Chen, X. A MicroRNA as a Translational Repressor of APETALA2 in Arabidopsis Flower Development. *Science* **303**, 2022-2025, doi:10.1126/science.1088060 (2004).
- 29 Hsieh, L.-C. *et al.* Uncovering Small RNA-Mediated Responses to Phosphate Deficiency in Arabidopsis by Deep Sequencing. *Plant Physiology* **151**, 2120-2132, doi:10.1104/pp.109.147280 (2009).
- 30 Wang, X.-J., Reyes, J., Chua, N.-H. & Gaasterland, T. Prediction and identification of Arabidopsis thaliana microRNAs and their mRNA targets. *Genome Biology* **5**, R65 (2004).
- 31 Kawashima, C. G. *et al.* Sulphur starvation induces the expression of microRNA-395 and one of its target genes but in different cell types. *The Plant Journal* **57**, 313-321, doi:10.1111/j.1365-313X.2008.03690.x (2009).
- 32 Sunkar, R., Kapoor, A. & Zhu, J.-K. Posttranscriptional Induction of Two Cu/Zn Superoxide Dismutase Genes in Arabidopsis Is Mediated by Downregulation of miR398 and Important for Oxidative Stress Tolerance. *The Plant Cell Online* **18**, 2051-2065, doi:10.1105/tpc.106.041673 (2006).
- 33 Adai, A. *et al.* Computational prediction of miRNAs in Arabidopsis thaliana. *Genome Research* **15**, 78-91, doi:10.1101/gr.2908205 (2005).
- 34 Howell, M. D. *et al.* Genome-Wide Analysis of the RNA-DEPENDENT RNA POLYMERASE6/DICER-LIKE4 Pathway in Arabidopsis Reveals Dependency on miRNA- and tasiRNA-Directed Targeting. *The Plant Cell Online* **19**, 926-942, doi:10.1105/tpc.107.050062 (2007).
- 35 Chen, H.-M., Li, Y.-H. & Wu, S.-H. Bioinformatic prediction and experimental validation of a microRNA-directed tandem trans-acting siRNA cascade in Arabidopsis. *Proceedings of the National Academy of Sciences* **104**, 3318-3323, doi:10.1073/pnas.0611119104 (2007).
- 36 Lu, C. *et al.* Elucidation of the Small RNA Component of the Transcriptome. *Science* **309**, 1567-1569, doi:10.1126/science.1114112 (2005).

- 37 Fahlgren, N. *et al.* High-Throughput Sequencing of *Arabidopsis* microRNAs: Evidence for Frequent Birth and Death of *MIRNA* Genes. *PLoS ONE* **2**, e219, doi:10.1371/journal.pone.0000219 (2007).
- 38 Rajagopalan, R., Vaucheret, H., Trejo, J. & Bartel, D. P. A diverse and evolutionarily fluid set of microRNAs in *Arabidopsis thaliana*. *Genes & Development* **20**, 3407-3425, doi:10.1101/gad.1476406 (2006).

Gene ontology enrichment and protein accumulation

Table 9-2. Accumulation of proteins enriched in GO terms (p-value<0.05).

GO cluster ¹	UniProt	Protein accumulation			
		<i>drb1</i> (log2FC)	<i>p</i> -Value (<i>drb1</i>)	<i>drb2</i> (log2FC)	<i>p</i> -Value (<i>drb2</i>)
cellular response to stress; response to endogenous stimulus; response to hydrogen peroxide (Cluster #1)					
AT1G19570	Q9FWR4	1.68	0.00	0.77	0.00
AT1G20620	Q42547	0.48	0.03	0.47	0.02
AT1G20620	Q42547	0.48	0.03	0.47	0.02
AT1G24100	O48676	0.41	0.02	-0.15	0.10
AT1G35720	Q9SYT0	0.43	0.02	0.44	0.02
AT1G48410	O04379	-0.46	0.01	0.87	0.00
AT1G54100	Q9SYG7	0.89	0.06	0.31	0.02
AT1G55020	Q06327	-0.10	0.27	0.32	0.05
AT1G59870	Q9XIE2	0.65	0.00	0.14	0.59
AT2G18960	P20649	0.34	0.80	0.36	0.03
AT2G28900	Q9ZV24	0.36	0.01	0.45	0.01
AT2G39800	P54887	-0.23	0.12	0.97	0.04
AT3G15730	Q38882	0.40	0.10	0.23	0.05
AT3G16420	O04314	-0.13	0.09	0.56	0.02
AT3G16470	O04309	1.79	0.00	0.80	0.01
AT3G45140	P38418	-0.40	0.24	3.07	0.00
AT3G49110	P24101	0.25	0.03	0.06	0.80
AT3G49120	Q9SMU8	1.03	0.00	0.66	0.01
AT3G52880	Q9LFA3	0.41	0.02	0.14	0.28
AT4G31500	O65782	1.07	0.00	-0.64	0.82
AT4G33030	O48917	0.67	0.00	-0.13	0.12
AT5G24770	O82122	2.20	0.00	1.86	0.00
AT5G24780	O49195	2.85	0.00	1.55	0.01
AT1G76180	P42763	ND	ND	0.33	0.03
AT2G38750	Q9ZVJ6	ND	ND	0.26	0.05
AT2G39770	O22287	ND	ND	0.33	0.03
AT3G09940	Q9SR59	ND	ND	0.61	0.01
AT3G12500	P19171	2.66	0.03	ND	ND
AT3G54640	Q42529	0.91	0.01	ND	ND
AT3G54960	Q8VX13	0.51	0.02	ND	ND
AT4G21960	Q9SB81	ND	ND	0.65	0.01
AT4G23600	Q9SUR6	ND	ND	0.93	0.01
AT5G01600	Q39101	ND	ND	1.37	0.00
response to abiotic stimulus (Cluster #2)	UniProt	<i>drb1</i> (log2FC)	<i>p</i>-Value (<i>drb1</i>)	<i>drb2</i> (log2FC)	<i>p</i>-Value (<i>drb2</i>)
AT1G02930	P42760	1.09	0.00	1.03	0.00
AT1G09210	Q38858	-0.11	0.39	-0.47	0.01
AT1G10760	Q9SAC6	0.62	0.00	0.24	0.04
AT1G20620	Q42547	0.48	0.03	0.47	0.02
AT1G24180	Q8H1Y0	-0.20	0.08	0.20	0.05

PART V – SUPPLEMENTARY DATA

AT1G35680	P51412	-0.67	0.02	-0.40	0.04
AT1G35720	Q9SYT0	0.43	0.02	0.44	0.02
AT1G37130	P11035	0.12	0.88	0.33	0.05
AT1G48410	O04379	-0.46	0.01	0.87	0.00
AT1G52340	Q9C826	-0.06	0.75	-1.35	0.01
AT1G54100	Q9SYG7	0.89	0.06	0.31	0.02
AT1G55490	P21240	-0.34	0.05	-0.43	0.01
AT1G67280	Q8W593	0.08	0.23	0.34	0.02
AT1G77120	P06525	1.16	0.00	1.14	0.00
AT1G77510	Q9SRG3	-1.05	0.00	0.03	0.97
AT1G78380	Q9ZRW8	0.01	0.64	0.23	0.05
AT2G06850	Q39099	-1.29	0.00	-0.11	0.51
AT2G18960	P20649	0.34	0.80	0.36	0.03
AT2G21660	Q03250	-0.46	0.01	0.22	0.09
AT2G26250	Q570B4	-0.51	0.04	-0.43	0.01
AT2G28900	Q9ZV24	0.36	0.01	0.45	0.01
AT2G30490	P92994	0.37	0.02	0.22	0.28
AT2G30870	P42761	0.29	0.03	0.12	0.21
AT2G31610	Q9SIP7	-0.13	0.08	-0.26	0.03
AT2G37220	Q9ZUU4	-0.73	0.00	-0.47	0.01
AT2G39730	P10896	-0.40	0.06	-0.28	0.03
AT2G39800	P54887	-0.23	0.12	0.97	0.04
AT2G40100	Q9S7W1	1.46	0.00	0.32	0.15
AT2G45790	O80840	0.42	0.03	0.19	0.07
AT2G45960	Q06611	-0.60	0.02	0.14	0.10
AT2G47730	Q96266	0.44	0.07	0.32	0.02
AT3G02230	Q9SRT9	-0.29	0.04	0.17	0.06
AT3G02360	Q9FWA3	0.29	0.03	0.27	0.27
AT3G04720	P43082	1.53	0.00	0.44	0.07
AT3G09260	Q9SR37	-0.49	0.02	0.43	0.01
AT3G12490	Q8H0X6	0.48	0.01	0.28	0.33
AT3G12780	Q9LD57	0.31	0.03	-0.09	0.27
AT3G14210	Q9LJG3	0.44	0.01	0.33	0.29
AT3G16470	O04309	1.79	0.00	0.80	0.01
AT3G17390	Q9LUT2	0.58	0.03	0.60	0.02
AT3G18780	Q96292	-0.43	0.01	0.03	0.63
AT3G19820	Q39085	-0.39	0.04	0.01	0.30
AT3G29320	Q9LIB2	0.51	0.01	0.26	0.03
AT3G45140	P38418	-0.40	0.24	3.07	0.00
AT3G46970	Q9SD76	0.58	0.00	0.21	0.12
AT3G49110	P24101	0.25	0.03	0.06	0.80
AT3G49120	Q9SMU8	1.03	0.00	0.66	0.01
AT3G53420	P43286	-0.68	0.00	-0.06	0.42
AT3G56240	O82089	-0.58	0.81	-0.56	0.01
AT4G02520	P46422	1.53	0.00	-0.19	0.06
AT4G11600	O48646	0.45	0.01	0.17	0.06
AT4G13770	P48421	0.21	0.25	-1.72	0.00
AT4G24280	Q9STW6	-0.21	0.15	-0.31	0.03
AT4G31500	O65782	1.07	0.00	-0.64	0.82
AT4G35830	Q42560	0.19	0.11	0.21	0.04
AT5G03630	Q93WJ8	0.42	0.01	0.40	0.02
AT5G04530	Q9LZ72	-0.43	0.03	0.05	0.72
AT5G07440	Q38946	0.63	0.02	-0.08	0.86

PART V – SUPPLEMENTARY DATA

AT5G09590	Q9LDZ0	0.41	0.03	0.07	0.34
AT5G14200	Q9FMT1	-0.03	0.20	-0.92	0.01
AT5G20630	P94072	0.87	0.00	0.17	0.25
AT5G24770	O82122	2.20	0.00	1.86	0.00
AT5G27600	Q8LKS5	0.93	0.02	0.38	0.01
AT5G38420	P10796	-0.07	0.59	-0.30	0.03
AT5G49720	Q38890	0.38	0.01	0.34	0.03
AT5G49910	Q9LTX9	-0.09	0.70	-0.26	0.05
AT5G54770	Q38814	-0.69	0.00	-0.49	0.01
AT5G54810	P14671	1.00	0.02	-0.03	0.36
AT5G63570	P42799	-0.18	0.50	-0.37	0.03
AT5G63860	Q9FN03	0.34	0.04	0.14	0.40
AT1G31812	ND	ND	ND	-0.26	0.03
AT1G53580	Q9C8L4	0.38	0.01	ND	ND
AT1G76180	ND	ND	ND	0.33	0.03
AT2G33380	O22788	2.17	0.00	ND	ND
AT2G38750	ND	ND	ND	0.26	0.05
AT2G39770	ND	ND	ND	0.33	0.03
AT2G39810	ND	ND	ND	-0.28	0.04
AT3G01500	P27140	0.48	0.02	ND	ND
AT3G02870	ND	ND	ND	0.22	0.05
AT3G09940	ND	ND	ND	0.61	0.01
AT3G51240	ND	ND	ND	0.65	0.01
AT3G55120	P41088	0.37	0.03	ND	ND
AT4G04020	O81439	0.65	0.04	ND	ND
AT4G23600	ND	ND	ND	0.93	0.01
AT4G32410	ND	ND	ND	0.28	0.04
AT5G01600	ND	ND	ND	1.37	0.00
AT5G15970	P31169	0.89	0.01	ND	ND
AT5G17990	Q02166	0.60	0.00	ND	ND
AT5G20830	P49040	1.42	0.00	ND	ND
AT5G38430	P10796	-0.07	0.59	ND	ND
AT5G65940	Q9LKJ1	0.47	0.03		
response to metal ion; response to cadmium ion (Cluster #2a)	UniProt	<i>drb1</i> (log2FC)	<i>p</i>-Value (<i>drb1</i>)	<i>drb2</i> (log2FC)	<i>p</i>-Value (<i>drb2</i>)
AT1G02930	P42760	1.09	0.00	1.03	0.00
AT1G17290	F4I7I0	0.54	0.03	0.13	0.10
AT1G20620	Q42547	0.48	0.03	0.47	0.02
AT1G27130	Q9FUS6	-0.12	0.21	0.41	0.01
AT1G35720	Q9SYT0	0.43	0.02	0.44	0.02
AT1G45145	Q39241	1.89	0.00	0.62	0.03
AT1G49760	Q9FXA2	-0.31	0.04	-0.13	0.14
AT1G49760	Q9FXA2	-0.31	0.04	-0.13	0.14
AT1G50480	Q9SPK5	0.44	0.03	0.26	0.08
AT1G60420	O80763	0.44	0.02	0.17	0.12
AT1G60710	Q93ZN2	0.07	0.95	0.27	0.04
AT1G64550	Q8H0V6	-0.39	0.02	-0.35	0.26
AT1G75280	P52577	1.85	0.00	2.81	0.00
AT1G76680	Q8LAH7	1.29	0.01	1.92	0.00
AT1G77120	P06525	1.16	0.00	1.14	0.00
AT1G77510	Q9SRG3	-1.05	0.00	0.03	0.97

PART V – SUPPLEMENTARY DATA

AT1G78380	Q9ZRW8	0.01	0.64	0.23	0.05
AT2G21660	Q03250	-0.46	0.01	0.22	0.09
AT2G23350	O22173	-0.29	0.03	-0.04	0.25
AT2G30870	P42761	0.29	0.03	0.12	0.21
AT2G35840	Q9SJ66	0.44	0.01	-0.17	0.75
AT2G37760	O80944	1.20	0.00	0.99	0.01
AT2G41530	Q8LAS8	0.32	0.04	0.07	0.17
AT2G43750	P47999	0.49	0.03	0.51	0.01
AT2G44350	P20115	0.16	0.22	0.25	0.03
AT2G45290	F4IW47	0.50	0.01	0.33	0.15
AT3G06050	Q9M7T0	0.42	0.03	0.26	0.04
AT3G12780	Q9LD57	0.31	0.03	-0.09	0.27
AT3G14990	Q9FPF0	0.80	0.04	1.29	0.00
AT3G15730	Q38882	0.40	0.10	0.23	0.05
AT3G17820	Q9LVI8	0.63	0.00	0.24	0.04
AT3G19170	Q9LJL3	-0.14	0.68	-0.21	0.05
AT3G22890	Q9LIK9	0.22	0.17	-0.58	0.01
AT3G27300	Q9LK23	0.19	0.05	0.48	0.02
AT3G46970	Q9SD76	0.58	0.00	0.21	0.12
AT3G48000	Q9SU63	0.65	0.00	-0.09	0.30
AT3G52880	Q9LFA3	0.41	0.02	0.14	0.28
AT3G56240	O82089	-0.58	0.81	-0.56	0.01
AT4G02520	P46422	1.53	0.00	-0.19	0.06
AT4G11600	O48646	0.45	0.01	0.17	0.06
AT4G13430	Q94AR8	-0.27	0.03	-0.47	0.01
AT4G14030	O23264	0.32	0.02	0.83	0.00
AT4G16760	O65202	0.68	0.01	0.21	0.86
AT4G24280	Q9STW6	-0.21	0.15	-0.31	0.03
AT4G24280	Q9STW6	-0.21	0.15	-0.31	0.03
AT4G37870	Q9T074	0.88	0.00	0.41	0.03
AT5G03630	Q93WJ8	0.42	0.01	0.40	0.02
AT5G07440	Q38946	0.63	0.02	-0.08	0.86
AT5G09590	Q9LDZ0	0.41	0.03	0.07	0.34
AT5G11170	Q56XG6	-0.29	0.07	-0.38	0.01
AT5G11670	Q9LYG3	0.41	0.03	0.35	0.05
AT5G14780	Q9S7E4	0.94	0.02	0.25	0.12
AT5G24770	O82122	2.20	0.00	1.86	0.00
AT5G49910	Q9LTX9	-0.09	0.70	-0.26	0.05
AT5G52920	Q9FLW9	-0.40	0.01	-0.37	0.02
AT5G53460	Q9LV03	-0.42	0.01	-0.70	0.00
AT3G12500	P19171	2.66	0.03	ND	ND
AT3G13110	Q39218	0.59	0.00	ND	ND
AT3G56090	ND	ND	ND	-1.18	0.00
AT5G01600	ND	ND	ND	1.37	0.00
AT5G02790	Q9LZ06	0.75	0.01	ND	ND
AT5G17990	Q02166	0.60	0.00	ND	ND
AT5G20830	P49040	1.42	0.00	ND	ND
response to salt stress; response to osmotic stress (Cluster #2b)	UniProt	<i>drb1</i> (log2FC)	<i>p</i>-Value (<i>drb1</i>)	<i>drb2</i> (log2FC)	<i>p</i>-Value (<i>drb2</i>)
AT2G21660	Q03250	-0.46	0.01	0.22	0.09
AT1G02930	P42760	1.09	0.00	1.03	0.00

PART V – SUPPLEMENTARY DATA

AT1G24180	Q8H1Y0	-0.20	0.08	0.20	0.05
AT1G35720	Q9SYT0	0.43	0.02	0.44	0.02
AT1G54100	Q9SYG7	0.89	0.06	0.31	0.02
AT1G77120	P06525	1.16	0.00	1.14	0.00
AT2G39800	P54887	-0.23	0.12	0.97	0.04
AT2G45790	O80840	0.42	0.03	0.19	0.07
AT2G47730	Q96266	0.44	0.07	0.32	0.02
AT3G02360	Q9FWA3	0.29	0.03	0.27	0.27
AT3G04720	P43082	1.53	0.00	0.44	0.07
AT3G04720	P43082	1.53	0.00	0.44	0.07
AT3G09260	Q9SR37	-0.49	0.02	0.43	0.01
AT3G16470	O04309	1.79	0.00	0.80	0.01
AT4G02520	P46422	1.53	0.00	-0.19	0.06
AT4G11600	O48646	0.45	0.01	0.17	0.06
AT4G35830	Q42560	0.19	0.11	0.21	0.04
AT5G03630	Q93WJ8	0.42	0.01	0.40	0.02
AT5G07440	Q38946	0.63	0.02	-0.08	0.86
AT5G09590	Q9LDZ0	0.41	0.03	0.07	0.34
AT5G24770	O82122	2.20	0.00	1.86	0.00
AT5G27600	Q8LKS5	0.93	0.02	0.38	0.01
AT5G49720	Q38890	0.38	0.01	0.34	0.03
AT5G54810	P14671	1.00	0.02	-0.03	0.36
AT1G53580	Q9C8L4	0.38	0.01	ND	ND
AT2G33380	O22788	2.17	0.00	ND	ND
AT2G38750	Q9ZVJ6	ND	ND	0.26	0.05
AT2G39770	O22287	ND	ND	0.33	0.03
AT3G09940	Q9SR59	ND	ND	0.61	0.01
AT4G23600	Q9SUR6	ND	ND	0.93	0.01
AT4G32410	O48946	ND	ND	0.28	0.04
AT5G15970	P31169	0.89	0.01	ND	ND
AT5G17990	Q02166	0.60	0.00	ND	ND
AT5G20830	P49040	1.42	0.00	ND	ND
response to cold; response to temperature stimulus (Cluster #2c)	UniProt	<i>drb1</i> (log2FC)	<i>p</i>-Value (<i>drb1</i>)	<i>drb2</i> (log2FC)	<i>p</i>-Value (<i>drb2</i>)
AT1G35680	P51412	-0.67	0.02	-0.40	0.04
AT1G52340	Q9C826	-0.06	0.75	-1.35	0.01
AT1G55490	P21240	-0.34	0.05	-0.43	0.01
AT2G21660	Q03250	-0.46	0.01	0.22	0.09
AT2G26250	Q570B4	-0.51	0.04	-0.43	0.01
AT2G37220	Q9ZUU4	-0.73	0.00	-0.47	0.01
AT2G39730	P10896	-0.40	0.06	-0.28	0.03
AT4G24280	Q9STW6	-0.21	0.15	-0.31	0.03
AT5G04530	Q9LZ72	-0.43	0.03	0.05	0.72
AT5G49910	Q9LTX9	-0.09	0.70	-0.26	0.05
AT5G54770	Q38814	-0.69	0.00	-0.49	0.01
AT1G31812	P57752	ND	ND	-0.26	0.03
AT2G39810	Q84JU6	ND	ND	-0.28	0.04
defense response; glycosinolate metabolic process; cell wall	UniProt	<i>drb1</i> (log2FC)	<i>p</i>-Value (<i>drb1</i>)	<i>drb2</i> (log2FC)	<i>p</i>-Value (<i>drb2</i>)

PART V – SUPPLEMENTARY DATA

thickening during defense response (Cluster #3)					
AT1G02930	P42760	1.09	0.00	1.03	0.00
AT1G18590	Q9FZ80	0.09	0.71	-0.73	0.00
AT1G24100	O48676	0.41	0.02	-0.15	0.10
AT1G59870	Q9XIE2	0.65	0.00	0.14	0.59
AT1G62560	Q9SXE1	-0.04	0.21	-0.96	0.00
AT1G74090	Q9C9C9	0.08	0.49	-0.67	0.01
AT1G74100	Q9C9D0	0.42	0.01	-0.07	0.23
AT2G25450	Q9SKK4	-0.15	0.07	-1.29	0.00
AT3G04720	P43082	1.53	0.00	0.44	0.07
AT3G14210	Q9LJG3	0.44	0.01	0.33	0.29
AT3G19710	Q9LE06	-0.07	0.14	-3.09	0.00
AT3G49110	P24101	0.25	0.03	0.06	0.80
AT3G49120	Q9SMU8	1.03	0.00	0.66	0.01
AT3G54640	P46422	1.53	0.00	-0.19	0.06
AT4G13770	P48421	0.21	0.25	-1.72	0.00
AT4G31500	O65782	1.07	0.00	-0.64	0.82
AT5G14740	P42737	0.42	0.03	-0.94	0.01
AT5G25980	Q9C5C2	0.24	0.29	-1.34	0.00
AT5G26000	P37702	0.04	0.97	-1.21	0.01
AT5G48180	Q93XW5	0.72	0.00	2.54	0.00
AT5G64440	Q7XJJ7	0.33	0.03	ND	ND
AT3G01500	P27140	0.48	0.02	ND	ND
AT4G02520	P46422	1.53	0.00	ND	ND
response to jasmonic acid stimulus; jasmonic acid biosynthetic process; oxylipin metabolic process; oxylipin biosynthetic process (Cluster #4)	UniProt	<i>drb1</i> (log2FC)	<i>p</i>-Value (<i>drb1</i>)	<i>drb2</i> (log2FC)	<i>p</i>-Value (<i>drb2</i>)
AT1G13280	Q93ZC5	0.68	0.01	0.62	0.01
AT1G19570	Q9FWR4	1.68	0.00	0.77	0.00
AT1G55020	Q06327	-0.10	0.27	0.32	0.05
AT1G74100	Q9C9D0	0.42	0.01	-0.07	0.23
AT1G76680	Q8LAH7	1.29	0.01	1.92	0.00
AT2G06050	Q9FUP0	0.96	0.00	0.47	0.01
AT2G28900	Q9ZV24	0.36	0.01	0.45	0.01
AT3G16470	O04309	1.79	0.00	0.80	0.01
AT3G45140	P38418	-0.40	0.24	3.07	0.00
AT4G16760	O65202	0.68	0.01	0.21	0.86
AT5G24770	O82122	2.20	0.00	1.86	0.00
AT5G24780	O49195	2.85	0.00	1.55	0.01
AT5G42650	Q96242	2.82	0.00	ND	ND
AT5G48880	Q570C8	1.31	0.00	ND	ND
AT2G33380	O22788	2.17	0.00	ND	ND
AT2G39770	O22287	ND	ND	0.33	0.03
AT3G09940	Q9SR59	ND	ND	0.61	0.01
AT4G05160	Q9M0X9	0.47	0.01	ND	ND
AT4G23600	Q9SUR6	ND	ND	0.93	0.01

PART V – SUPPLEMENTARY DATA

AT5G17990	Q02166	0.60	0.00	ND	ND
response to bacterium; response to fungus; response to symbiotic fungus (Cluster #5)	UniProt	<i>drb1</i> (log2FC)	<i>p</i>-Value (<i>drb1</i>)	<i>drb2</i> (log2FC)	<i>p</i>-Value (<i>drb2</i>)
AT4G16760	O65202	0.68	0.01	0.21	0.86
AT2G33380	O22788	2.17	0.00	ND	ND
AT1G02930	P42760	1.09	0.00	1.03	0.00
AT1G24100	O48676	0.41	0.02	-0.15	0.10
AT1G59870	Q9XIE2	0.65	0.00	0.14	0.59
AT3G04720	P43082	1.53	0.00	0.44	0.07
AT3G14210	Q9LJG3	0.44	0.01	0.33	0.29
AT3G49110	P24101	0.25	0.03	0.06	0.80
AT3G49120	Q9SMU8	1.03	0.00	0.66	0.01
AT4G02520	P46422	1.53	0.00	-0.19	0.06
AT4G31500	O65782	1.07	0.00	-0.64	0.82
AT4G39980	P29976	0.54	0.00	0.05	0.19
AT5G05730	P32068	0.96	0.00	0.03	0.54
AT5G14740	P42737	0.42	0.03	-0.94	0.01
AT5G64440	Q7XJJ7	0.33	0.03	ND	ND
AT3G01500	P27140	0.48	0.02	ND	ND
AT3G54640	Q42529	0.91	0.01	ND	ND
AT1G10760	Q9SAC6	0.62	0.00	0.24	0.04
AT1G11580	Q1JPL7	1.39	0.00	1.21	0.01
AT1G19570	Q9FWR4	1.68	0.00	0.77	0.00
AT1G37130	P11035	0.12	0.88	0.33	0.05
AT1G45145	Q39241	1.89	0.00	0.62	0.03
AT1G52400	Q9SE50	1.90	0.00	0.77	0.00
AT2G06050	Q9FUP0	0.96	0.00	0.47	0.01
AT3G09260	Q9SR37	-0.49	0.02	0.43	0.01
AT3G45140	P38418	-0.40	0.24	3.07	0.00
AT3G49120	Q9SMU8	1.03	0.00	0.66	0.01
AT3G09940	Q9SR59	ND	ND	0.61	0.01
response to bacterium (Cluster #5a)	UniProt	<i>drb1</i> (log2FC)	<i>p</i>-Value (<i>drb1</i>)	<i>drb2</i> (log2FC)	<i>p</i>-Value (<i>drb2</i>)
AT1G02930	P42760	1.09	0.00	1.03	0.00
AT1G24100	O48676	0.41	0.02	-0.15	0.10
AT1G59870	Q9XIE2	0.65	0.00	0.14	0.59
AT3G04720	P43082	1.53	0.00	0.44	0.07
AT3G14210	Q9LJG3	0.44	0.01	0.33	0.29
AT3G49110	P24101	0.25	0.03	0.06	0.80
AT3G49120	Q9SMU8	1.03	0.00	0.66	0.01
AT4G02520	P46422	1.53	0.00	-0.19	0.06
AT4G31500	O65782	1.07	0.00	-0.64	0.82
AT4G39980	P29976	0.54	0.00	0.05	0.19
AT5G05730	P32068	0.96	0.00	0.03	0.54
AT5G14740	P42737	0.42	0.03	-0.94	0.01
AT5G64440	Q7XJJ7	0.33	0.03	ND	ND
AT3G01500	P27140	0.48	0.02	ND	ND
AT3G54640	Q42529	0.91	0.01	ND	ND
response to fungus;	UniProt	<i>drb1</i>	<i>p</i>-Value	<i>drb2</i>	<i>p</i>-Value

PART V – SUPPLEMENTARY DATA

response to symbiotic fungus (Cluster #5b)		(log2FC)	(<i>drb1</i>)	(log2FC)	(<i>drb2</i>)
AT1G10760	Q9SAC6	0.62	0.00	0.24	0.04
AT1G11580	Q1JPL7	1.39	0.00	1.21	0.01
AT1G19570	Q9FWR4	1.68	0.00	0.77	0.00
AT1G37130	P11035	0.12	0.88	0.33	0.05
AT1G45145	Q39241	1.89	0.00	0.62	0.03
AT1G52400	Q9SE50	1.90	0.00	0.77	0.00
AT2G06050	Q9FUP0	0.96	0.00	0.47	0.01
AT3G09260	Q9SR37	-0.49	0.02	0.43	0.01
AT3G45140	P38418	-0.40	0.24	3.07	0.00
AT3G49120	Q9SMU8	1.03	0.00	0.66	0.01
AT3G09940	Q9SR59	ND	ND	0.61	0.01
toxin catabolic process (Cluster #6)	UniProt	<i>drb1</i> (log2FC)	<i>p</i>-Value (<i>drb1</i>)	<i>drb2</i> (log2FC)	<i>p</i>-Value (<i>drb2</i>)
AT1G02930	P42760	1.09	0.00	1.03	0.00
AT1G27130	Q9FUS6	-0.12	0.21	0.41	0.01
AT1G78380	Q9ZRW8	0.01	0.64	0.23	0.05
AT2G29450	P46421	0.81	0.00	0.36	0.04
AT2G47730	Q96266	0.44	0.07	0.32	0.02
AT5G17220	Q9FE46	-0.14	0.84	1.21	0.00
response to wounding (Cluster #7)	UniProt	<i>drb1</i> (log2FC)	<i>p</i>-Value (<i>drb1</i>)	<i>drb2</i> (log2FC)	<i>p</i>-Value (<i>drb2</i>)
AT1G52030	Q9SAV1	3.11	0.00	0.81	0.00
AT1G55020	Q06327	-0.10	0.27	0.32	0.05
AT1G76680	Q8LAH7	1.29	0.01	1.92	0.00
AT2G06050	Q9FUP0	0.96	0.00	0.47	0.01
AT2G28900	Q9ZV24	0.36	0.01	0.45	0.01
AT3G16470	O04309	1.79	0.00	0.80	0.01
AT3G45140	P38418	-0.40	0.24	3.07	0.00
AT5G24770	O82122	2.20	0.00	1.86	0.00
AT4G23600	Q9SUR6	0.93	0.01	ND	ND
senescence (Cluster #8)	UniProt	<i>drb1</i> (log2FC)	<i>p</i>-Value (<i>drb1</i>)	<i>drb2</i> (log2FC)	<i>p</i>-Value (<i>drb2</i>)
AT1G76680	Q8LAH7	1.29	0.01	1.92	0.00
AT5G11520	P46644	0.41	0.03	0.28	0.19
AT5G24770	O82122	2.20	0.00	1.86	0.00
AT1G17020	Q39224	1.41	0.00	ND	ND
negative regulation of organelle organization; regulation of cellular component size; plastid organization; peroxisome fission (Cluster #9)	UniProt	<i>drb1</i> (log2FC)	<i>p</i>-Value (<i>drb1</i>)	<i>drb2</i> (log2FC)	<i>p</i>-Value (<i>drb2</i>)
AT1G14410	Q9M9S3	-0.75	0.00	-0.09	0.26
AT1G62750	Q9SI75	-0.50	0.08	-0.41	0.01
AT2G06850	Q39099	-1.29	0.00	-0.11	0.51
AT2G19520	O22607	-0.59	0.03	-0.01	0.26

PART V – SUPPLEMENTARY DATA

AT2G28000	P21238	-0.20	0.17	-0.34	0.02
AT2G41740	O81644	-0.29	0.04	0.14	0.54
AT2G45740	O80845	0.40	0.02	0.04	0.80
AT3G18780	Q96292	-0.43	0.01	0.03	0.63
AT3G19820	Q39085	-0.39	0.04	0.01	0.30
AT3G46740	Q9STE8	-0.43	0.05	-0.24	0.03
AT3G48870	Q9SXJ7	-0.80	0.01	-0.41	0.01
AT3G57410	O81645	-0.25	0.03	0.00	0.54
AT4G28250	Q9M0I2	-1.90	0.02	ND	ND
AT1G01820	Q9LQ73	0.34	0.02	ND	ND
AT1G47750	Q9FZF1	0.47	0.02	ND	ND
AT2G28800	Q8LBP4	ND	ND	-0.43	0.01
AT3G03220	Q9M9P0	-0.36	0.02	ND	ND
chlorophyll biosynthetic process; protein targeting to chloroplast; chlorophyll biosynthetic process (Cluster #10)	UniProt	<i>drb1</i> (log2FC)	<i>p</i>-Value (<i>drb1</i>)	<i>drb2</i> (log2FC)	<i>p</i>-Value (<i>drb2</i>)
AT1G08520	Q9SJE1	-0.47	0.05	-0.32	0.03
AT3G03710	Q8GZQ3	-1.76	0.09	-0.53	0.03
AT3G46740	Q9STE8	-0.43	0.05	-0.24	0.03
AT3G48730	Q42522	-0.45	0.02	-0.36	0.02
AT3G48870	Q9SXJ7	-0.80	0.01	-0.41	0.01
AT3G56940	Q9M591	-0.33	0.05	-0.18	0.54
AT4G02510	O81283	-0.40	0.18	-0.37	0.02
AT4G18480	P16127	-0.66	0.01	-0.27	0.03
AT4G27440	P21218	-0.45	0.01	0.06	0.91
AT5G08280	Q43316	-0.35	0.03	-0.30	0.05
AT5G13630	Q9FNB0	-0.45	0.01	-0.35	0.03
AT5G16440	Q38929	-0.17	0.72	-0.29	0.03
AT5G63570	P42799	-0.18	0.50	-0.37	0.03
AT2G28800	Q8LBP4	ND	ND	-0.43	0.01
mRNA metabolic process (Cluster #11)	UniProt	<i>drb1</i> (log2FC)	<i>p</i>-Value (<i>drb1</i>)	<i>drb2</i> (log2FC)	<i>p</i>-Value (<i>drb2</i>)
AT2G37220	Q9ZUU4	-0.73	0.00	-0.47	0.01
AT3G03710	Q8GZQ3	-1.76	0.09	-0.53	0.03
AT3G53460	Q43349	-0.97	0.00	-0.46	0.01
AT5G11170	Q56XG6	-0.29	0.07	-0.38	0.01
AT5G47010	Q9FJR0	-0.12	0.48	-0.26	0.04
nitrogen compound biosynthetic process (Cluster #12)	UniProt	<i>drb1</i> (log2FC)	<i>p</i>-Value (<i>drb1</i>)	<i>drb2</i> (log2FC)	<i>p</i>-Value (<i>drb2</i>)
AT1G08520	Q9SJE1	-0.47	0.05	-0.32	0.03
AT1G17745	O04130	0.75	0.02	0.91	0.05
AT1G31230	Q9SA18	-0.04	0.20	-0.38	0.03
AT1G37130	P11035	0.12	0.88	0.33	0.05
AT1G52340	Q9C826	-0.06	0.75	-1.35	0.01
AT1G58080	Q9S762	-0.30	0.04	-0.18	0.07
AT1G70310	O48661	0.29	0.09	0.27	0.04

PART V – SUPPLEMENTARY DATA

AT1G75330	O50039	0.24	0.04	-0.04	0.37
AT2G04400	P49572	0.72	0.00	0.21	0.26
AT2G14750	Q43295	0.22	0.06	-0.37	0.02
AT2G18960	P20649	0.34	0.80	0.36	0.03
AT2G31810	Q93YZ7	-0.12	0.52	-0.69	0.01
AT2G39800	P54887	-0.23	0.12	0.97	0.04
AT2G41220	Q9T0P4	0.30	0.02	0.15	0.09
AT2G43750	P47999	0.49	0.03	0.51	0.01
AT3G01120	P55217	-0.42	0.01	-0.53	0.01
AT3G03710	Q8GZQ3	-1.76	0.09	-0.53	0.03
AT3G14990	Q9FPF0	0.80	0.04	1.29	0.00
AT3G16400	Q9SDM9	0.19	0.10	0.38	0.05
AT3G17390	Q9LUT2	0.58	0.03	0.60	0.02
AT3G17820	Q9LVI8	0.63	0.00	0.24	0.04
AT3G44310	P32961	1.84	0.00	1.17	0.00
AT3G48730	Q42522	-0.45	0.02	-0.36	0.02
AT3G49680	Q9M401	-0.03	0.18	-0.71	0.00
AT3G56940	Q9M591	-0.33	0.05	-0.18	0.54
AT3G59760	Q43725	0.39	0.02	0.20	0.14
AT4G11010	O49203	0.38	0.02	0.25	0.09
AT4G13430	Q94AR8	-0.27	0.03	-0.47	0.01
AT4G18480	P16127	-0.66	0.01	-0.27	0.03
AT4G27440	P21218	-0.45	0.01	0.06	0.91
AT4G31500	O65782	1.07	0.00	-0.64	0.82
AT4G35630	Q96255	0.63	0.01	0.38	0.02
AT4G39080	Q8W4S4	-0.16	0.22	0.29	0.03
AT4G39980	P29976	0.54	0.00	0.05	0.19
AT5G05730	P32068	0.96	0.00	0.03	0.54
AT5G08280	Q43316	-0.35	0.03	-0.30	0.05
AT5G13630	Q9FNB0	-0.45	0.01	-0.35	0.03
AT5G14200	Q9FMT1	-0.03	0.20	-0.92	0.01
AT5G16440	Q38929	-0.17	0.72	-0.29	0.03
AT5G48180	Q93XW5	0.72	0.00	2.54	0.00
AT5G53460	Q9LV03	-0.42	0.01	-0.70	0.00
AT5G54770	Q38814	-0.69	0.00	-0.49	0.01
AT5G54810	P14671	1.00	0.02	-0.03	0.36
AT5G56760	P42799	-0.18	0.50	-0.37	0.03
AT5G63570	Q9LV77	-0.53	0.02	-0.14	0.12
AT1G15710	Q9LMR3	0.32	0.02	ND	ND
AT1G48850	P57720	0.25	0.04	ND	ND
AT1G50110	Q9LPM9	0.28	0.03	ND	ND
AT3G02020	Q9S702	-1.03	0.03	ND	ND
AT3G13110	Q39218	0.59	0.00	ND	ND
AT3G53900	Q9M336	-0.34	0.02	ND	ND
AT3G54640	Q42529	0.91	0.01	ND	ND
AT4G04610	P92979	0.97	0.02	ND	ND
AT5G04950	Q9FF79	-0.78	0.00	ND	ND
AT5G16290	Q9FFF4	0.25	0.03	ND	ND
AT5G17990	Q02166	0.60	0.00	ND	ND
AT5G62670	ND	ND	ND	-0.42	0.01
sulfur metabolic process; sulfur	UniProt	<i>drb1</i> (log2FC)	<i>p</i>-Value (<i>drb1</i>)	<i>drb2</i> (log2FC)	<i>p</i>-Value (<i>drb2</i>)

PART V – SUPPLEMENTARY DATA

compound biosynthetic process; serine family amino acid metabolic process (Cluster #13)					
AT1G18590	Q9FZ80	0.09	0.71	-0.73	0.00
AT1G19920	Q43870	0.14	0.96	-0.41	0.01
AT1G23310	Q9LR30	0.06	0.32	-0.37	0.04
AT1G24100	O48676	0.41	0.02	-0.15	0.10
AT1G31230	Q9SA18	-0.04	0.20	-0.38	0.03
AT1G62560	Q9SXE1	-0.04	0.21	-0.96	0.00
AT1G74090	Q9C9C9	0.08	0.49	-0.67	0.01
AT1G74100	Q9C9D0	0.42	0.01	-0.07	0.23
AT2G14750	Q43295	0.22	0.06	-0.37	0.02
AT2G25450	Q9SKK4	-0.15	0.07	-1.29	0.00
AT2G43750	P47999	0.49	0.03	0.51	0.01
AT3G01120	P55217	-0.42	0.01	-0.53	0.01
AT3G14990	Q9FPF0	0.80	0.04	1.29	0.00
AT3G17390	Q9LUT2	0.58	0.03	0.60	0.02
AT3G19710	Q9LE06	-0.07	0.14	-3.09	0.00
AT3G22890	Q9LIK9	0.22	0.17	-0.58	0.01
AT3G59760	Q43725	0.39	0.02	0.20	0.14
AT4G13770	P48421	0.21	0.25	-1.72	0.00
AT4G31500	O65782	1.07	0.00	-0.64	0.82
AT4G33030	O48917	0.67	0.00	-0.13	0.12
AT5G25980	Q9C5C2	0.24	0.29	-1.34	0.00
AT5G26000	P37702	0.04	0.97	-1.21	0.01
AT5G54770	Q38814	-0.69	0.00	-0.49	0.01
AT5G56760	Q42538	0.95	0.04	ND	ND
AT4G04610	P92979	0.97	0.02	ND	ND
AT3G13110	Q39218	0.59	0.00	ND	ND
cellular glucan metabolic process; polysaccharide localization (Cluster #14)	UniProt	<i>drb1</i> (log2FC)	<i>p</i>-Value (<i>drb1</i>)	<i>drb2</i> (log2FC)	<i>p</i>-Value (<i>drb2</i>)
AT1G10760	Q9SAC6	0.62	0.00	0.24	0.04
AT1G24100	O48676	0.41	0.02	-0.15	0.10
AT1G59870	Q9XIE2	0.65	0.00	0.14	0.59
AT3G52180	Q9FEB5	0.74	0.00	0.25	0.11
AT4G09020	Q9M0S5	0.58	0.01	0.77	0.01
AT4G31500	O65782	1.07	0.00	-0.64	0.82
AT5G26570	Q6ZY51	0.60	0.00	0.16	0.09
AT5G49720	Q38890	0.38	0.01	0.34	0.03
AT5G65020	Q9XEE2	0.74	0.01	0.22	0.07
AT1G11720	F4IAG2	0.34	0.03	ND	ND
AT2G39770	O22287	ND	ND	0.33	0.03
AT3G54640	Q42529	0.91	0.01	ND	ND
AT4G32410	O48946	ND	ND	0.28	0.04
glycoside metabolic process (Cluster #15)	UniProt	<i>drb1</i> (log2FC)	<i>p</i>-Value (<i>drb1</i>)	<i>drb2</i> (log2FC)	<i>p</i>-Value (<i>drb2</i>)
AT1G18590	Q9FZ80	0.09	0.71	-0.73	0.00

PART V – SUPPLEMENTARY DATA

AT1G24100	O48676	0.41	0.02	-0.15	0.10
AT1G59870	Q9XIE2	0.65	0.00	0.14	0.59
AT1G62560	Q9SXE1	-0.04	0.21	-0.96	0.00
AT1G74090	Q9C9C9	0.08	0.49	-0.67	0.01
AT1G74100	Q9C9D0	0.42	0.01	-0.07	0.23
AT2G25450	Q9SKK4	-0.15	0.07	-1.29	0.00
AT2G35840	Q9SJ66	0.44	0.01	-0.17	0.75
AT3G14210	Q9LJG3	0.44	0.01	0.33	0.29
AT3G19710	Q9LE06	-0.07	0.14	-3.09	0.00
AT4G13770	P48421	0.21	0.25	-1.72	0.00
AT4G31500	O65782	1.07	0.00	-0.64	0.82
AT5G25980	Q9C5C2	0.24	0.29	-1.34	0.00
AT5G26000	P37702	0.04	0.97	-1.21	0.01
AT5G48180	Q93XW5	0.72	0.00	2.54	0.00
AT1G73370	Q9FX32	0.23	0.04	ND	ND
AT5G20830	P49040	1.42	0.00	ND	ND
cellular respiration; acetyl-CoA catabolic process; cofactor catabolic process; coenzyme metabolic process; cell redox homeostasis (Cluster #16)	UniProt	<i>drb1</i> (log2FC)	<i>p</i>-Value (<i>drb1</i>)	<i>drb2</i> (log2FC)	<i>p</i>-Value (<i>drb2</i>)
AT1G19670	O22527	2.70	0.00	0.15	0.17
AT1G45145	Q39241	1.89	0.00	0.62	0.03
AT1G50480	Q9SPK5	0.44	0.03	0.26	0.08
AT1G53310	Q9MAH0	0.67	0.01	0.22	0.04
AT1G60420	O80763	0.44	0.02	0.17	0.12
AT1G77120	P06525	1.16	0.00	1.14	0.00
AT2G22780	O82399	0.52	0.01	0.37	0.02
AT2G44350	P20115	0.16	0.22	0.25	0.03
AT3G02360	Q9FWA3	0.29	0.03	0.27	0.27
AT3G06050	Q9M7T0	0.42	0.03	0.26	0.04
AT3G06850	Q9M7Z1	0.21	0.05	-0.17	0.15
AT3G27300	Q9LK23	0.19	0.05	0.48	0.02
AT4G35830	Q42560	0.19	0.11	0.21	0.04
AT4G37000	Q8LDU4	0.31	0.29	0.45	0.01
AT5G11670	Q9LYG3	0.41	0.03	0.35	0.05
AT5G40760	Q9FJI5	0.86	0.01	0.71	0.31
AT5G43330	P57106	0.42	0.03	0.19	0.96
AT5G55070	Q9FLQ4	0.24	0.17	0.33	0.04
AT3G26060	Q9LU86	0.26	0.04	ND	ND
AT3G54960	Q8VX13	0.51	0.02	ND	ND
AT4G04610	P92979	0.97	0.02	ND	ND
				ND	ND
dicarboxylic acid metabolic process; aromatic compound biosynthetic process; organic acid biosynthetic process;	UniProt	<i>drb1</i> (log2FC)	<i>p</i>-Value (<i>drb1</i>)	<i>drb2</i> (log2FC)	<i>p</i>-Value (<i>drb2</i>)

PART V – SUPPLEMENTARY DATA

carboxylic acid biosynthetic process (Cluster #17)					
AT1G13280	Q93ZC5	0.68	0.01	0.62	0.01
AT1G17745	O04130	0.75	0.02	0.91	0.05
AT1G31230	Q9SA18	-0.04	0.20	-0.38	0.03
AT1G52340	Q9C826	-0.06	0.75	-1.35	0.01
AT1G55020	Q06327	-0.10	0.27	0.32	0.05
AT1G58080	Q9S762	-0.30	0.04	-0.18	0.07
AT1G75330	O50039	0.24	0.04	-0.04	0.37
AT1G76680	Q8LAH7	1.29	0.01	1.92	0.00
AT2G04400	P49572	0.72	0.00	0.21	0.26
AT2G06050	Q9FUP0	0.96	0.00	0.47	0.01
AT2G14750	Q43295	0.22	0.06	-0.37	0.02
AT2G22780	O82399	0.52	0.01	0.37	0.02
AT2G26250	Q570B4	-0.51	0.04	-0.43	0.01
AT2G30490	P92994	0.37	0.02	0.22	0.28
AT2G31810	Q93YZ7	-0.12	0.52	-0.69	0.01
AT2G39800	P54887	-0.23	0.12	0.97	0.04
AT2G41220	Q9T0P4	0.30	0.02	0.15	0.09
AT2G43750	P47999	0.49	0.03	0.51	0.01
AT2G45790	O80840	0.42	0.03	0.19	0.07
AT2G47240	O22898	0.03	0.74	-0.41	0.02
AT3G01120	P55217	-0.42	0.01	-0.53	0.01
AT3G14990	Q9FPF0	0.80	0.04	1.29	0.00
AT3G17390	Q9LUT2	0.58	0.03	0.60	0.02
AT3G17820	Q9LVI8	0.63	0.00	0.24	0.04
AT3G44310	P32961	1.84	0.00	1.17	0.00
AT3G45140	P38418	-0.40	0.24	3.07	0.00
AT3G49680	Q9M401	-0.03	0.18	-0.71	0.00
AT3G59760	Q43725	0.39	0.02	0.20	0.14
AT4G13430	Q94AR8	-0.27	0.03	-0.47	0.01
AT4G16760	O65202	0.68	0.01	0.21	0.86
AT4G31500	O65782	1.07	0.00	-0.64	0.82
AT4G35630	Q96255	0.63	0.01	0.38	0.02
AT4G39980	P29976	0.54	0.00	0.05	0.19
AT5G04530	Q9LZ72	-0.43	0.03	0.05	0.72
AT5G05730	P32068	0.96	0.00	0.03	0.54
AT5G11670	Q9LYG3	0.41	0.03	0.35	0.05
AT5G14200	Q9FMT1	-0.03	0.20	-0.92	0.01
AT5G28840	Q93VR3	-0.28	0.10	-0.34	0.02
AT5G35360	O04983	-0.35	0.02	-0.19	0.12
AT5G43330	P57106	0.42	0.03	0.19	0.96
AT5G52920	Q9FLW9	-0.40	0.01	-0.37	0.02
AT5G53460	Q9LV03	-0.42	0.01	-0.70	0.00
AT5G54810	P14671	1.00	0.02	-0.03	0.36
AT5G65010	Q9LV77	-0.53	0.02	-0.14	0.12
AT1G15710	Q9LMR3	0.32	0.02	ND	ND
AT1G17020	Q39224	1.41	0.00	ND	ND
AT1G30530	Q9S9P6	0.86	0.00	ND	ND
AT1G48850	P57720	0.25	0.04	ND	ND
AT1G50110	Q9LPM9	0.28	0.03	ND	ND
AT2G39770	O22287	ND	ND	0.33	0.03

PART V – SUPPLEMENTARY DATA

AT3G02020	Q9S702	-1.03	0.03	ND	ND
AT3G02870	Q9M8S8	ND	ND	0.22	0.05
AT3G13110	Q39218	0.59	0.00	ND	ND
AT3G54640	Q42529	0.91	0.01	ND	ND
AT3G55120	P41088	0.37	0.03	ND	ND
AT4G04610	P92979	0.97	0.02	ND	ND
AT4G05160	Q9M0X9	0.47	0.01	ND	ND
AT5G05270	Q8VZW3	0.29	0.03	ND	ND
AT5G16290	Q9FFF4	0.25	0.03	ND	ND
AT5G17990	Q02166	0.60	0.00	ND	ND
AT5G42650	Q96242	2.82	0.00	ND	ND
AT5G48880	Q570C8	1.31	0.00	ND	ND
AT5G56760	Q42538	0.95	0.04	ND	ND
fatty acid metabolic process (Cluster #18)	UniProt	<i>drb1</i> (log2FC)	<i>p</i>-Value (<i>drb1</i>)	<i>drb2</i> (log2FC)	<i>p</i>-Value (<i>drb2</i>)
AT1G06550	Q9SHJ8	0.61	0.00	0.25	0.84
AT1G13280	Q93ZC5	0.68	0.01	0.62	0.01
AT1G55020	Q06327	-0.10	0.27	0.32	0.05
AT1G76680	Q8LAH7	1.29	0.01	1.92	0.00
AT2G06050	Q9FUP0	0.96	0.00	0.47	0.01
AT3G06860	Q9ZPI5	0.48	0.01	0.26	0.42
AT3G15730	Q38882	0.40	0.10	0.23	0.05
AT3G45140	P38418	-0.40	0.24	3.07	0.00
AT4G16760	O65202	0.68	0.01	0.21	0.86
AT4G29010	Q9ZPI6	0.43	0.01	0.19	0.06
AT5G27600	Q8LKS5	0.93	0.02	0.38	0.01
AT2G33380	O22788	2.17	0.00	ND	ND
AT4G05160	Q9M0X9	0.47	0.01	ND	ND
AT5G42650	Q96242	2.82	0.00	ND	ND
AT5G48880	Q570C8	1.31	0.00	ND	ND
AT5G65940	Q9LKJ1	0.47	0.03	ND	ND
glucose catabolic process; carbohydrate catabolic process (Cluster #19)	UniProt	<i>drb1</i> (log2FC)	<i>p</i>-Value (<i>drb1</i>)	<i>drb2</i> (log2FC)	<i>p</i>-Value (<i>drb2</i>)
AT1G01090	O24457	-0.37	0.03	-0.10	0.14
AT1G10760	Q9SAC6	0.62	0.00	0.24	0.04
AT1G24180	Q8H1Y0	-0.20	0.08	0.20	0.05
AT1G59870	Q9XIE2	0.65	0.00	0.14	0.59
AT2G22780	O82399	0.52	0.01	0.37	0.02
AT3G02360	Q9FWA3	0.29	0.03	0.27	0.27
AT3G04720	P43082	1.53	0.00	0.44	0.07
AT3G12780	Q9LD57	0.31	0.03	-0.09	0.27
AT3G14210	Q9LJG3	0.44	0.01	0.33	0.29
AT3G16400	Q9SDM9	0.19	0.10	0.38	0.05
AT3G27300	Q9LK23	0.19	0.05	0.48	0.02
AT4G09020	Q9M0S5	0.58	0.01	0.77	0.01
AT5G11670	Q9LYG3	0.41	0.03	0.35	0.05
AT5G26570	Q6ZY51	0.60	0.00	0.16	0.09
AT5G40760	Q9FJI5	0.86	0.01	0.71	0.31
AT5G43330	P57106	0.42	0.03	0.19	0.96
AT5G48180	Q93XW5	0.72	0.00	2.54	0.00

PART V – SUPPLEMENTARY DATA

AT5G49720	Q38890	0.38	0.01	0.34	0.03
AT5G52920	Q9FLW9	-0.40	0.01	-0.37	0.02
AT5G64570	Q9FLG1	1.45	0.00	0.18	0.07
AT2G29560	Q9ZW34	-0.38	0.03	ND	ND
AT3G12500	P19171	2.66	0.03	ND	ND
AT5G13110	Q9FY99	-0.47	0.02	ND	ND
response to hormone stimulus; response to abscisic acid stimulus (Cluster #20)	UniProt	<i>drb1</i> (log2FC)	<i>p</i>-Value (<i>drb1</i>)	<i>drb2</i> (log2FC)	<i>p</i>-Value (<i>drb2</i>)
AT1G35720	Q9SYT0	0.43	0.02	0.44	0.02
AT2G38750	Q9ZVJ6	ND	ND	0.26	0.05
AT2G39800	P54887	-0.23	0.12	0.97	0.04
AT2G33380	O22788	2.17	0.00	ND	ND
AT2G37220	Q9ZUU4	-0.73	0.00	-0.47	0.01
AT4G23600	Q9SUR6	ND	ND	0.93	0.01
AT5G17990	Q02166	0.60	0.00	ND	ND
AT4G02520	P46422	1.53	0.00	-0.19	0.06

¹Gene ontology clustered as follow:

Cluster #1 - cellular response to stress (GO:0033554); response to endogenous stimulus (GO:0009719); response to hydrogen peroxide (GO:0042542)

Cluster #2 - response to abiotic stimulus (GO:0009628)

Cluster #2a - response to metal ion (GO:0010038); response to cadmium ion (GO:0046686)

Cluster #2b - response to salt stress (GO:0009651); response to osmotic stress (GO:0006970)

Cluster #2c - response to cold (GO:0009409); response to temperature stimulus (GO:0009266)

Cluster #3 - defense response (GO:0006952); glycosinolate metabolic process (GO:0019757); cell wall thickening during defense response (GO:0052482)

Cluster #4 - response to jasmonic acid stimulus (GO:0009753); jasmonic acid biosynthetic process (GO:0009695); oxylipin metabolic process (GO:0031407); oxylipin biosynthetic process (GO:0031408)

Cluster #5a - response to bacterium (GO:0042742)

Cluster #5b - response to fungus (GO:0009620); response to symbiotic fungus (GO:0009610)

Cluster #6 - toxin catabolic process (GO:0009407)

Cluster #7 - response to wounding (GO:0009611)

Cluster #8 - senescence (GO:0010149)

Cluster #9 - negative regulation of organelle organization (GO:0010639); regulation of cellular component size (GO:0032535); plastid organization (GO:0009657); peroxisome fission (GO:0016559)

Cluster #10 - chlorophyll biosynthetic process (GO:0015995); protein targeting to chloroplast (GO:0045036); chlorophyll biosynthetic process (GO:0015995)

Cluster #11 - mRNA metabolic process (GO:0016071)

Cluster #12 - nitrogen compound biosynthetic process (GO:0044271)

Cluster #13 - sulfur metabolic process (GO:0006790); sulfur compound biosynthetic process (GO:0044272); serine family amino acid metabolic process (GO:0009069)

Cluster #14 - cellular glucan metabolic process (GO:0006073); polysaccharide localization (GO:0033037)

Cluster #15 - glycoside metabolic process (GO:0016137)

Cluster #16 - cellular respiration (GO:0045333); acetyl-CoA catabolic process (GO:0046356); cofactor catabolic process (GO:0051187); coenzyme metabolic process (GO:0006732); cell redox homeostasis (GO:0045454)

Cluster #17 - dicarboxylic acid metabolic process (GO:0043648); aromatic compound biosynthetic process (GO:0019438); organic acid biosynthetic process (GO:0016053)

Cluster #18 - fatty acid metabolic process (GO:0006631)

Cluster #19 - glucose catabolic process (GO:0006007); carbohydrate catabolic process (GO:0016052)

PART VI - BIBLIOGRAPHY

Bibliography

- Adams, D.R., Ron, D., and Kiely, P.A. (2011). RACK1, A multifaceted scaffolding protein: Structure and function. *Cell Commun. Signal.* *9*, 22.
- Ameres, S.L., and Zamore, P.D. (2013). Diversifying microRNA sequence and function. *Nat. Rev. Mol. Cell Biol.* *14*, 475–488.
- Angell, S.M., and Baulcombe, D.C. (1997). Consistent gene silencing in transgenic plants expressing a replicating potato virus X RNA. *EMBO J.* *16*, 3675–3684.
- Arabidopsis Interactome Mapping Consortium (2011). Evidence for network evolution in an Arabidopsis interactome map. *Science* *333*, 601–607.
- Arsova, B., Zauber, H., and Schulze, W.X. (2012a). Precision, Proteome Coverage, and Dynamic Range of Arabidopsis Proteome Profiling Using ¹⁵N Metabolic Labeling and Label-free Approaches. *Mol. Cell. Proteomics* *11*, 619–628.
- Arsova, B., Kierszniowska, S., and Schulze, W.X. (2012b). The use of heavy nitrogen in quantitative proteomics experiments in plants. *Trends Plant Sci.* *17*, 102–112.
- Baek, D., Villén, J., Shin, C., Camargo, F.D., Gygi, S.P., and Bartel, D.P. (2008). The impact of microRNAs on protein output. *Nature* *455*, 64–71.
- Baerenfaller, K., Grossmann, J., Grobei, M. a, Hull, R., Hirsch-Hoffmann, M., Yalovsky, S., Zimmermann, P., Grossniklaus, U., Gruissem, W., and Baginsky, S. (2008). Genome-scale proteomics reveals Arabidopsis thaliana gene models and proteome dynamics. *Science* *320*, 938–941.
- Baker, C.C., Sieber, P., Wellmer, F., and Meyerowitz, E.M. (2005). The early extra petals1 Mutant Uncovers a Role for MicroRNA miR164c in Regulating Petal Number in Arabidopsis. *Curr. Biol.* *15*, 303–315.
- Bartel, D. (2004). MicroRNAs: genomics, biogenesis, mechanism, and function. *Cell* *116*, 281–297.
- Baulcombe, D. (2004). RNA silencing in plants. *Nature* *431*, 356–363.
- Baulcombe, D.C. (1996). Mechanisms of Pathogen-Derived Resistance to Viruses in Transgenic Plants. *Plant Cell* *8*, 1833–1844.
- Baulcombe, D.C., and English, J.J. (1996). Ectopic pairing of homologous DNA and post-transcriptional gene silencing in transgenic plants. *Curr. Opin. Biotechnol.* *7*, 173–180.
- Baumberger, N., and Baulcombe, D.C. (2005). Arabidopsis ARGONAUTE1 is an RNA Slicer that selectively recruits microRNAs and short interfering RNAs. *Proc. Natl. Acad. Sci. U. S. A.* *102*, 11928–11933.
- Bernstein, E., Caudy, A.A., Hammond, S.M., and Hannon, G.J. (2001). Role for a bidentate ribonuclease in the initiation step of RNA interference. *Nature* *409*, 363–366.
- Bindschedler, L. V, Palmblad, M., and Cramer, R. (2008). Hydroponic isotope labelling of entire plants (HILEP) for quantitative plant proteomics; an oxidative stress case study. *Phytochemistry* *69*, 1962–1972.

- Bohmert, K., Camus, I., Bellini, C., Bouchez, D., Caboche, M., and Benning, C. (1998). AGO1 defines a novel locus of Arabidopsis controlling leaf development. *EMBO J.* *17*, 170–180.
- Bologna, N.G., and Voinnet, O. (2014). The Diversity, Biogenesis, and Activities of Endogenous Silencing Small RNAs in Arabidopsis. *Annu. Rev. Plant Biol.* *65*, 1–31.
- Boualem, A., Laporte, P., Jovanovic, M., Laffont, C., Plet, J., Combier, J.-P., Niebel, A., Crespi, M., and Frugier, F. (2008). MicroRNA166 controls root and nodule development in *Medicago truncatula*. *Plant J.* *54*, 876–887.
- Braun, P., Aubourg, S., Van Leene, J., De Jaeger, G., and Lurin, C. (2013). Plant protein interactomes. *Annu. Rev. Plant Biol.* *64*, 161–187.
- Brodersen, P., Sakvarelidze-Achard, L., Bruun-Rasmussen, M., Dunoyer, P., Yamamoto, Y.Y., Sieburth, L., and Voinnet, O. (2008). Widespread translational inhibition by plant miRNAs and siRNAs. *Science* *320*, 1185–1190.
- Burk, D.H., Zhong, R., and Ye, Z.-H. (2007). The Katanin Microtubule Severing Protein in Plants. *J. Integr. Plant Biol.* *49*, 1174–1182.
- Cabello, J. V., Lodeyro, A.F., and Zurbriggen, M.D. (2014). Novel perspectives for the engineering of abiotic stress tolerance in plants. *Curr. Opin. Biotechnol.* *26C*, 62–70.
- Calderon-villalobos, L.I.A., Kuhnle, C., Dohmann, E.M.N., Li, H., Bevan, M., and Schwechheimer, C. (2005). The Evolutionarily Conserved TOUGH Protein Is Required for Proper Development of *Arabidopsis thaliana*. *J. Biol. Chem.* *280*, 2473–2485.
- Carbonell, A., Fahlgren, N., Garcia-Ruiz, H., Gilbert, K.B., Montgomery, T. a, Nguyen, T., Cuperus, J.T., and Carrington, J.C. (2012). Functional analysis of three Arabidopsis ARGONAUTES using slicer-defective mutants. *Plant Cell* *24*, 3613–3629.
- Carmell, M. a, Xuan, Z., Zhang, M.Q., and Hannon, G.J. (2002). The Argonaute family: tentacles that reach into RNAi, developmental control, stem cell maintenance, and tumorigenesis. *Genes Dev.* *16*, 2733–2742.
- Carr, J.P., and Zaitlin, M. (1991). Resistance in Transgenic Tobacco Plants Expressing a Nonstructural Gene Sequence. *Mol. Plant-Microbe Interact.* *4*, 579–585.
- De Carvalho, F., Gheysen, G., Kushnir, S., Van Montagu, M., Inzé, D., and Castresana, C. (1992). Suppression of beta-1,3-glucanase transgene expression in homozygous plants. *EMBO J.* *11*, 2595–2602.
- Causier, B., Ashworth, M., Guo, W., and Davies, B. (2012). The TOPLESS interactome: a framework for gene repression in Arabidopsis. *Plant Physiol.* *158*, 423–438.
- Ceci, M., Gaviraghi, C., Gorrini, C., Sala, L.A., Offenhäuser, N., Marchisio, P.C., and Biffo, S. (2003). Release of eIF6 (p27BBP) from the 60S subunit allows 80S ribosome assembly. *Nature* *426*, 579–584.
- Ben Chaabane, S., Liu, R., Chinnusamy, V., Kwon, Y., Park, J., Kim, S.Y., Zhu, J.-K., Yang, S.W., and Lee, B. (2013). STA1, an Arabidopsis pre-mRNA processing factor 6 homolog, is a new player involved in miRNA biogenesis. *Nucleic Acids Res.* *41*, 1984–1997.

- Chang, K.-Y., and Ramos, A. (2005). The double-stranded RNA-binding motif, a versatile macromolecular docking platform. *FEBS J.* 272, 2109–2117.
- Chang, S.-S., Zhang, Z., and Liu, Y. (2012). RNA Interference Pathways in Fungi: Mechanisms and Functions. *Annu. Rev. Microbiol.* 66, 305–323.
- Chatr-Aryamontri, A., Breitkreutz, B.-J., Heinicke, S., Boucher, L., Winter, A., Stark, C., Nixon, J., Ramage, L., Kolas, N., O'Donnell, L., et al. (2013). The BioGRID interaction database: 2013 update. *Nucleic Acids Res.* 41, D816–D823.
- Chen, X. (2004a). A microRNA as a translational repressor of *APETALA2* in Arabidopsis flower development. *Science* 303, 2022–2025.
- Chen, X. (2004b). A MicroRNA as a Translational Repressor of *APETALA2* in Arabidopsis Flower Development. *Science* 303, 2022–2025.
- Chen, C., Ridzon, D. a, Broomer, A.J., Zhou, Z., Lee, D.H., Nguyen, J.T., Barbisin, M., Xu, N.L., Mahuvakar, V.R., Andersen, M.R., et al. (2005). Real-time quantification of microRNAs by stem-loop RT-PCR. *Nucleic Acids Res.* 33, e179.
- Christie, M., and Carroll, B.J. (2011). *SERRATE* is required for intron suppression of RNA silencing in Arabidopsis. *Plant Signal. Behav.* 6, 2035–2037.
- Chuang, C.F., and Meyerowitz, E.M. (2000). Specific and heritable genetic interference by double-stranded RNA in *Arabidopsis thaliana*. *Proc. Natl. Acad. Sci. U. S. A.* 97, 4985–4990.
- Clough, S.J., and Bent, a F. (1998). Floral dip: a simplified method for *Agrobacterium*-mediated transformation of *Arabidopsis thaliana*. *Plant J.* 16, 735–743.
- Cogoni, C., and Macino, G. (1997). Isolation of quelling-defective (*qde*) mutants impaired in posttranscriptional transgene-induced gene silencing in *Neurospora crassa*. *Proc. Natl. Acad. Sci. U. S. A.* 94, 10233–10238.
- Cogoni, C., and Macino, G. (1999). Gene silencing in *Neurospora crassa* requires a protein homologous to RNA-dependent RNA polymerase. *Nature* 399, 166–169.
- Cogoni, C., and Macino, G. (2000). Post-transcriptional gene silencing across kingdoms. *Curr. Opin. Genet. Dev.* 10, 638–643.
- Combiér, J.-P., Frugier, F., de Billy, F., Boualem, A., El-Yahyaoui, F., Moreau, S., Vernié, T., Ott, T., Gamas, P., Crespi, M., et al. (2006). *MtHAP2-1* is a key transcriptional regulator of symbiotic nodule development regulated by microRNA169 in *Medicago truncatula*. *Genes Dev.* 20, 3084–3088.
- Coutu, C., Brandle, J., Brown, D., and Brown, K. (2007). pORE: a modular binary vector series suited for both monocot and dicot plant transformation. *Transgenic Res.* 771–781.
- Cui, J., Li, P., Li, G., Xu, F., Zhao, C., Li, Y., Yang, Z., Wang, G., Yu, Q., Li, Y., et al. (2008). AtPID: Arabidopsis thaliana protein interactome database--an integrative platform for plant systems biology. *Nucleic Acids Res.* 36, D999–D1008.
- Curtin, S.J., Watson, J.M., Smith, N.A., Eamens, A.L., Blanchard, C.L., and Waterhouse, P.M. (2008). The roles of plant dsRNA-binding proteins in RNAi-like pathways. *FEBS Lett.* 582, 2753–2760.

- Czech, B., and Hannon, G.J. (2010). Small RNA sorting: matchmaking for Argonautes. *Nat. Rev. Genet.* *12*, 19–31.
- Dalmay, T., Hamilton, a, Rudd, S., Angell, S., and Baulcombe, D.C. (2000). An RNA-dependent RNA polymerase gene in *Arabidopsis* is required for posttranscriptional gene silencing mediated by a transgene but not by a virus. *Cell* *101*, 543–553.
- Daniels, S.M., and Gatignol, A. (2012). The Multiple Functions of TRBP, at the Hub of Cell Responses to Viruses, Stress, and Cancer. *Microbiol. Mol. Biol. Rev.* *76*, 652–666.
- Davis, B.N., Hilyard, A.C., Lagna, G., and Hata, A. (2008). SMAD proteins control DROSHA-mediated microRNA maturation. *Nature* *454*, 56–61.
- Ding, Y., Tao, Y., and Zhu, C. (2013). Emerging roles of microRNAs in the mediation of drought stress response in plants. *J. Exp. Bot.* *64*, 3077–3086.
- Doench, J.G., Petersen, C.P., and Sharp, P. a (2003). siRNAs can function as miRNAs. *Genes Dev.* *17*, 438–442.
- Dong, Z., Han, M.-H., and Fedoroff, N. (2008). The RNA-binding proteins HYL1 and SE promote accurate in vitro processing of pri-miRNA by DCL1. *Proc. Natl. Acad. Sci. U. S. A.* *105*, 9970–9975.
- Dugas, D., and Bartel, B. (2008). Sucrose induction of *Arabidopsis* miR398 represses two Cu/Zn superoxide dismutases. *Plant Mol. Biol.* *67*, 403–417.
- Eamens, A.L., Smith, N.A., Curtin, S.J., Wang, M.-B., and Waterhouse, P.M. (2009). The *Arabidopsis thaliana* double-stranded RNA binding protein DRB1 directs guide strand selection from microRNA duplexes. *RNA* *15*, 2219–2235.
- Eamens, A.L., Kim, K.W., Curtin, S.J., and Waterhouse, P.M. (2012a). DRB2 Is Required for MicroRNA Biogenesis in *Arabidopsis thaliana*. *PLoS One* *7*, e35933.
- Eamens, A.L., Wook Kim, K., Waterhouse, P.M., and Kim, K.W. (2012b). DRB2, DRB3 and DRB5 function in a non-canonical microRNA pathway in *Arabidopsis thaliana*. *Plant Signal. Behav.* *7*, 1224–1229.
- Elbashir, S.M., Lendeckel, W., and Tuschl, T. (2001a). RNA interference is mediated by 21- and 22-nucleotide RNAs. *Genes Dev.* *15*, 188–200.
- Elbashir, S.M., Martinez, J., Patkaniowska, A., Lendeckel, W., and Tuschl, T. (2001b). Functional anatomy of siRNAs for mediating efficient RNAi in *Drosophila melanogaster* embryo lysate. *EMBO J.* *20*, 6877–6888.
- Engelsberger, W.R., and Schulze, W.X. (2012). Nitrate and ammonium lead to distinct global dynamic phosphorylation patterns when resupplied to nitrogen-starved *Arabidopsis* seedlings. *Plant J.* *69*, 978–995.
- Errampalli, D., Patton, D., Castle, L., Mickelson, L., Hansen, K., Schnall, J., Feldmann, K., and Meinke, D. (1991). Embryonic Lethals and T-DNA Insertional Mutagenesis in *Arabidopsis*. *Plant Cell* *3*, 149–157.
- Fagard, M., Boutet, S., Morel, J.-B., Bellini, C., and Vaucheret, H. (2000). AGO1, QDE-2, and RDE-1 are related proteins required for post-transcriptional gene silencing in plants, quelling in fungi, and RNA interference in animals. *Proc. Natl. Acad. Sci. U. S. A.* *97*, 11650–11654.

- Faino, L., and Thomma, B.P.H.J. (2014). Get your high-quality low-cost genome sequence. *Trends Plant Sci.* *19*, 288–291.
- Fei, Q., Xia, R., and Meyers, B.C. (2013). Phased, secondary, small interfering RNAs in posttranscriptional regulatory networks. *Plant Cell* *25*, 2400–2415.
- Filipowicz, W., Jaskiewicz, L., Kolb, F. a, and Pillai, R.S. (2005). Post-transcriptional gene silencing by siRNAs and miRNAs. *Curr. Opin. Struct. Biol.* *15*, 331–341.
- Finnegan, E.J., Margis, R., and Waterhouse, P.M. (2003). Posttranscriptional gene silencing is not compromised in the Arabidopsis *CARPEL FACTORY(DICER-LIKE1)* mutant, a homolog of Dicer-1 from *Drosophila*. *Curr. Biol.* *13*, 236–240.
- Fire, A., Xu, S., Montgomery, M.K., Kostas, S.A., Driver, S.E., and Mello, C.C. (1998). Potent and specific genetic interference by double-stranded RNA in *Caenorhabditis elegans*. *Nature* *391*, 806–811.
- Floyd, S.K., and Bowman, J.L. (2004). Gene regulation: ancient microRNA target sequences in plants. *Nature* *428*, 485–486.
- Franco-Zorrilla, J.M., Valli, A., Todesco, M., Mateos, I., Puga, M.I., Rubio-Somoza, I., Leyva, A., Weigel, D., García, J.A., and Paz-Ares, J. (2007). Target mimicry provides a new mechanism for regulation of microRNA activity. *Nat. Genet.* *39*, 1033–1037.
- Friedman, R.C., Farh, K.K.-H., Burge, C.B., and Bartel, D.P. (2009). Most mammalian mRNAs are conserved targets of microRNAs. *Genome Res.* *19*, 92–105.
- Fukunaga, R., Han, B.W., Hung, J.-H., Xu, J., Weng, Z., and Zamore, P.D. (2012). Dicer Partner Proteins Tune the Length of Mature miRNAs in Flies and Mammals. *Cell* *151*, 533–546.
- Fung, D.C.Y., Li, S.S., Goel, A., Hong, S.-H., and Wilkins, M.R. (2012). Visualization of the interactome: what are we looking at? *Proteomics* *12*, 1669–1686.
- Gandikota, M., Birkenbihl, R.P., Höhmann, S., Cardon, G.H., Saedler, H., and Huijser, P. (2007). The miRNA156/157 recognition element in the 3' UTR of the Arabidopsis SBP box gene *SPL3* prevents early flowering by translational inhibition in seedlings. *Plant J.* *49*, 683–693.
- Geisler-Lee, J., O'Toole, N., Ammar, R., Provart, N.J., Millar, A.H., and Geisler, M. (2007). A predicted interactome for Arabidopsis. *Plant Physiol.* *145*, 317–329.
- German, M.A., Pillay, M., Jeong, D.-H., Hetawal, A., Luo, S., Janardhanan, P., Kannan, V., Rymarquis, L.A., Nobuta, K., and German, R. (2008). Global identification of microRNA–target RNA pairs by parallel analysis of RNA ends. *Nat. Biotechnol.* *26*, 941–946.
- Goel, A., and Wilkins, M.R. (2012). Dynamic hubs show competitive and static hubs non-competitive regulation of their interaction partners. *PLoS One* *7*, e48209.
- Golden, T.T.A.T., Schauer, S.E.S., Lang, J.J.D., Mushegian, A.R., Grossniklaus, U., Meinke, D.W., and Ray, A. (2002). *SHORT INTEGUMENTS1/SUSPENSOR1/CARPEL FACTORY*, a Dicer homolog, is a maternal effect gene required for embryo development in Arabidopsis. *Plant Physiol.* *130*, 808–822.

- Grant-Downton, R., Kourmpetli, S., Hafidh, S., Khatab, H., Le Trionnaire, G., Dickinson, H., Twell, D., and Le, G. (2013). Artificial microRNAs reveal cell-specific differences in small RNA activity in pollen. *Curr. Biol.* *23*, R599–R601.
- Gregory, R.I., Yan, K., Amuthan, G., Chendrimada, T., Doratotaj, B., Cooch, N., and Shiekhattar, R. (2004). The Microprocessor complex mediates the genesis of microRNAs. *Nature* *432*, 235–240.
- Griffin, N.M., Yu, J., Long, F., Oh, P., Shore, S., Li, Y., Koziol, J.A., and Schnitzer, J.E. (2010). Label-free, normalized quantification of complex mass spectrometry data for proteomic analysis. *Nat. Biotechnol.* *28*, 83–89.
- Grimson, A., Farh, K.K.-H., Johnston, W.K., Garrett-Engle, P., Lim, L.P., and Bartel, D.P. (2007). MicroRNA Targeting Specificity in Mammals: Determinants beyond Seed Pairing. *Mol. Cell* *27*, 91–105.
- Gu, H., Zhu, P., Jiao, Y., Meng, Y., and Chen, M. (2011). PRIN: a predicted rice interactome network. *BMC Bioinformatics* *12*, 161.
- Guo, S., and Kemphues, K.J. (1995). *par-1*, a gene required for establishing polarity in *C. elegans* embryos, encodes a putative Ser/Thr kinase that is asymmetrically distributed. *Cell* *81*, 611–620.
- Guo, H., Ingolia, N.T., Weissman, J.S., and Bartel, D.P. (2010). Mammalian microRNAs predominantly act to decrease target mRNA levels. *Nature* *466*, 835–840.
- Guo, J., Wang, S., Valerius, O., Hall, H., Zeng, Q., Li, J.-F., Weston, D.J., Ellis, B.E., and Chen, J.-G. (2011). Involvement of Arabidopsis RACK1 in protein translation and its regulation by abscisic acid. *Plant Physiol.* *155*, 370–383.
- Guruharsha, K.G., Rual, J.-F., Zhai, B., Mintseris, J., Vaidya, P., Vaidya, N., Beekman, C., Wong, C., Rhee, D.Y., Cenaj, O., et al. (2011). A protein complex network of *Drosophila melanogaster*. *Cell* *147*, 690–703.
- Hamilton, A.J., and Baulcombe, D.C. (1999). A Species of Small Antisense RNA in Posttranscriptional Gene Silencing in Plants. *Science* *286*, 950–952.
- Hamilton, A.J., Lycett, G.W., and Grierson, D. (1990). Antisense gene that inhibits synthesis of the hormone ethylene in transgenic plants. *Nature* *346*, 284–287.
- Hammond, S.M., Bernstein, E., Beach, D., and Hannon, G.J. (2000). An RNA-directed nuclease mediates post-transcriptional gene silencing in *Drosophila* cells. *Nature* *404*, 293–296.
- Hammond, S.M., Boettcher, S., Caudy, a a, Kobayashi, R., and Hannon, G.J. (2001). Argonaute2, a link between genetic and biochemical analyses of RNAi. *Science* *293*, 1146–1150.
- Han, J., Lee, Y., Yeom, K.-H., Kim, Y.-K., Jin, H., and Kim, V.N. (2004a). The Drosha-DGCR8 complex in primary microRNA processing. *Genes Dev.* *18*, 3016–3027.
- Han, M.-H., Goud, S., Song, L., and Fedoroff, N. (2004b). The Arabidopsis double-stranded RNA-binding protein HYL1 plays a role in microRNA-mediated gene regulation. *Proc. Natl. Acad. Sci. U. S. A.* *101*, 1093–1098.
- Hart-Smith, G., and Raftery, M. (2012). Detection and Characterization of Low Abundance Glycopeptides Via Higher-Energy C-Trap Dissociation and Orbitrap Mass Analysis. *J. Am. Soc. Mass Spectrom.* *23*, 124–140.

- He, F., Zhou, Y., and Zhang, Z. (2010). Deciphering the Arabidopsis floral transition process by integrating a protein-protein interaction network and gene expression data. *Plant Physiol.* 153, 1492–1505.
- Horman, S.R., Janas, M.M., Litterst, C., Wang, B., MacRae, I.J., Sever, M.J., Morrissey, D. V, Graves, P., Luo, B., Umesalma, S., et al. (2013). Akt-Mediated Phosphorylation of Argonaute 2 Downregulates Cleavage and Upregulates Translational Repression of MicroRNA Targets. *Mol. Cell* 50, 356–367.
- Huang, D.W., Sherman, B.T., and Lempicki, R. a (2009). Bioinformatics enrichment tools: paths toward the comprehensive functional analysis of large gene lists. *Nucleic Acids Res.* 37, 1–13.
- Hutvagner, G., McLachlan, J., Pasquinelli, A.E., Bálint, E., Tuschl, T., Zamore, P.D., and Bálint, É. (2001). A Cellular Function for the RNA-Interference Enzyme Dicer in the Maturation of the let-7 Small Temporal RNA. *Science* 293, 834–838.
- Ideker, T., Galitski, T., and Hood, L. (2001). A new approach to decoding life: systems biology. *Annu. Rev. Genomics Hum. Genet.* 2, 343–372.
- Iki, T., Yoshikawa, M., Nishikiori, M., Jaudal, M.C., Matsumoto-Yokoyama, E., Mitsuhashi, I., Meshi, T., and Ishikawa, M. (2010). In vitro assembly of plant RNA-induced silencing complexes facilitated by molecular chaperone HSP90. *Mol. Cell* 39, 282–291.
- Iki, T., Yoshikawa, M., Meshi, T., and Ishikawa, M. (2012). Cyclophilin 40 facilitates HSP90-mediated RISC assembly in plants. *EMBO J.* 31, 267–278.
- Jacobsen, S.E., Running, M.P., and Meyerowitz, E.M. (1999). Disruption of an RNA helicase/RNase III gene in Arabidopsis causes unregulated cell division in floral meristems. *Development* 126, 5231–5243.
- Jannot, G., Bajan, S., Giguère, N.J., Bouasker, S., Banville, I.H., Piquet, S., Hutvagner, G., and Simard, M.J. (2011). The ribosomal protein RACK1 is required for microRNA function in both *C. elegans* and humans. *EMBO Rep.* 12, 581–586.
- Jefferson, R.A., Kavanagh, T.A., and Bevan, M.W. (1987). GUS fusions: beta-glucuronidase as a sensitive and versatile gene fusion marker in higher plants. *EMBO J.* 6, 3901.
- Jorgensen, R.A. (1995). Cosuppression, flower color patterns, and metastable gene expression States. *Science* 268, 686–691.
- Jover-Gil, S., Candela, H., Robles, P., Aguilera, V., Barrero, J.M., Micol, J.L., and Ponce, M.R. (2012). The microRNA pathway genes AGO1, HEN1 and HYL1 participate in leaf proximal-distal venation and stomatal patterning in Arabidopsis. *Plant Cell Physiol.* 53, 1322–1333.
- Karginov, F. V, Cheloufi, S., Chong, M.M.W., Stark, A., Smith, A.D., and Hannon, G.J. (2010). Diverse Endonucleolytic Cleavage Sites in the Mammalian Transcriptome Depend upon MicroRNAs, Drosha, and Additional Nucleases. *Mol. Cell* 38, 781–788.
- Kawashima, C.G., Yoshimoto, N., Maruyama-Nakashita, A., Tsuchiya, Y.N., Saito, K., Takahashi, H., and Dalmay, T. (2009). Sulphur starvation induces the expression of microRNA-395 and one of its target genes but in different cell types. *Plant J.* 57, 313–321.
- Kemmeren, P., Sameith, K., van de Pasch, L. a L., Benschop, J.J., Lenstra, T.L., Margaritis, T., O’Duibhir, E., Apweiler, E., van Wageningen, S., Ko, C.W., et al. (2014). Large-scale genetic

- perturbations reveal regulatory networks and an abundance of gene-specific repressors. *Cell* 157, 740–752.
- Kennerdell, J.R., and Carthew, R.W. (1998). Use of dsRNA-mediated genetic interference to demonstrate that *frizzled* and *frizzled 2* act in the wingless pathway. *Cell* 95, 1017–1026.
- Khraiwesh, B., and Zhu, J.J.-K. (2012). Role of miRNAs and siRNAs in biotic and abiotic stress responses of plants. *Biochim. Biophys. Acta* 1819, 137–148.
- Kim, Y.J., Zheng, B., Yu, Y., Won, S.Y., Mo, B., and Chen, X. (2011). The role of Mediator in small and long noncoding RNA production in *Arabidopsis thaliana*. *EMBO J.* 30, 814–822.
- Van der Krol, A.R. (1990). Flavonoid Genes in *Petunia*: Addition of a Limited Number of Gene Copies May Lead to a Suppression of Gene Expression. *Plant Cell* 2, 291–299.
- Kurihara, Y., and Watanabe, Y. (2004). *Arabidopsis* micro-RNA biogenesis through Dicer-like 1 protein functions. *Proc. Natl. Acad. Sci. U. S. A.* 101, 12753–12758.
- Kurihara, Y., Takashi, Y., and Watanabe, Y. (2006). The interaction between DCL1 and HYL1 is important for efficient and precise processing of pri-miRNA in plant microRNA biogenesis. *RNA* 12, 206–212.
- Lage, K., Karlberg, E.O., Størling, Z.M., Olason, P.I., Pedersen, A.G., Rigina, O., Hinsby, A.M., Tümer, Z., Pociot, F., Tommerup, N., et al. (2007). A human phenome-interactome network of protein complexes implicated in genetic disorders. *Nat. Biotechnol.* 25, 309–316.
- Lagos-Quintana, M., Rauhut, R., Lendeckel, W., and Tuschl, T. (2001). Identification of novel genes coding for small expressed RNAs. *Science* 294, 853–858.
- Landthaler, M., Yalcin, A., and Tuschl, T. (2004). The Human DiGeorge Syndrome Critical Region Gene 8 and Its *D. melanogaster* Homolog Are Required for miRNA Biogenesis. *Curr. Biol.* 14, 2162–2167.
- Lanet, E., Delannoy, E., Sormani, R., Floris, M., Brodersen, P., Créte, P., Voinnet, O., and Robaglia, C. (2009). Biochemical Evidence for Translational Repression by *Arabidopsis* MicroRNAs. *Plant Cell* 21, 1762–1768.
- Lanquar, V., Kuhn, L., Lelièvre, F., Khafif, M., Espagne, C., Bruley, C., Barbier-Brygoo, H., Garin, J., and Thomine, S. (2007). ¹⁵N-metabolic labeling for comparative plasma membrane proteomics in *Arabidopsis* cells. *Proteomics* 7, 750–754.
- Lau, N.C., Lim, L.P., Weinstein, E.G., and Bartel, D.P. (2001). An abundant class of tiny RNAs with probable regulatory roles in *Caenorhabditis elegans*. *Science* 294, 858–862.
- Laubinger, S., Sachsenberg, T., Zeller, G., Busch, W., Lohmann, J.U., Ratsch, G., and Weigel, D. (2008). Dual roles of the nuclear cap-binding complex and SERRATE in pre-mRNA splicing and microRNA processing in *Arabidopsis thaliana*. *Proc. Natl. Acad. Sci. U. S. A.* 105, 8795–8800.
- Leal Valentim, F., Neven, F., Boyen, P., and van Dijk, A.D.J. (2012). Interactome-wide prediction of protein-protein binding sites reveals effects of protein sequence variation in *Arabidopsis thaliana*. *PLoS One* 7, e47022.
- Lee, R.C., and Ambros, V. (2001). An extensive class of small RNAs in *Caenorhabditis elegans*. *Science* 294, 862–864.

- Lee, H.Y., Zhou, K., Smith, A.M., Noland, C.L., and Doudna, J. a (2013). Differential roles of human Dicer-binding proteins TRBP and PACT in small RNA processing. *Nucleic Acids Res.* *41*, 6568–6576.
- Lee, K., Thorneycroft, D., Achuthan, P., Hermjakob, H., and Ideker, T. (2010). Mapping plant interactomes using literature curated and predicted protein-protein interaction data sets. *Plant Cell* *22*, 997–1005.
- Lee, R.C., Feinbaum, R.L., and Ambros, V. (1993). The *C. elegans* heterochronic gene *lin-4* encodes small RNAs with antisense complementarity to *lin-14*. *Cell* *75*, 843–854.
- Lee, Y.S., Nakahara, K., Pham, J.W., Kim, K., He, Z., Sontheimer, E.J., and Carthew, R.W. (2004). Distinct Roles for *Drosophila* Dicer-1 and Dicer-2 in the siRNA/miRNA Silencing Pathways. *Cell* *117*, 69–81.
- Van Leene, J., Stals, H., Eeckhout, D., Persiau, G., Van De Slijke, E., Van Isterdael, G., De Clercq, A., Bonnet, E., Laukens, K., Remmerie, N., et al. (2007). A tandem affinity purification-based technology platform to study the cell cycle interactome in *Arabidopsis thaliana*. *Mol. Cell. Proteomics* *6*, 1226–1238.
- Lei, Z., Elmer, A.M., Watson, B.S., Dixon, R.A., Mendes, P.J., and Sumner, L.W. (2005). A two-dimensional electrophoresis proteomic reference map and systematic identification of 1367 proteins from a cell suspension culture of the model legume *Medicago truncatula*. *Mol. Cell. Proteomics* *4*, 1812–1825.
- Li, J.-F., Chung, H.S., Niu, Y., Bush, J., McCormack, M., and Sheen, J. (2013a). Comprehensive protein-based artificial microRNA screens for effective gene silencing in plants. *Plant Cell* *25*, 1507–1522.
- Li, S., Liu, L., Zhuang, X., Yu, Y., Liu, X., Cui, X., Ji, L., Pan, Z., Cao, X., Mo, B., et al. (2013b). MicroRNAs Inhibit the Translation of Target mRNAs on the Endoplasmic Reticulum in *Arabidopsis*. *Cell* *153*, 562–574.
- Li, W., Cui, X., Meng, Z., Huang, X., Xie, Q., Wu, H., Jin, H., Zhang, D., and Liang, W. (2012). Transcriptional regulation of *Arabidopsis* MIR168a and argonaute1 homeostasis in abscisic acid and abiotic stress responses. *Plant Physiol.* *158*, 1279–1292.
- Lian, H., Li, X., Liu, Z., and He, Y. (2013). HYL1 is required for establishment of stamen architecture with four microsporangia in *Arabidopsis*. *J. Exp. Bot.* *64*, 3397–3410.
- Lin, M., Shen, X., and Chen, X. (2011). PAIR: the predicted *Arabidopsis* interactome resource. *Nucleic Acids Res.* *39*, D1134–D1140.
- Lindbo, J.A., Silva-Rosales, L., Proebsting, W.M., and Dougherty, W.G. (1993). Induction of a Highly Specific Antiviral State in Transgenic Plants: Implications for Regulation of Gene Expression and Virus Resistance. *Plant Cell* *5*, 1749–1759.
- Liu, J., Carmell, M. a, Rivas, F. V, Marsden, C.G., Thomson, J.M., Song, J.-J., Hammond, S.M., Joshua-Tor, L., and Hannon, G.J. (2004). Argonaute2 is the catalytic engine of mammalian RNAi. *Science* *305*, 1437–1441.
- Llave, C., Xie, Z., Kasschau, K.D., and Carrington, J.C. (2002). Cleavage of Scarecrow-like mRNA targets directed by a class of *Arabidopsis* miRNA. *Science* *297*, 2053–2056.

- Lobbes, D., Rallapalli, G., Schmidt, D.D., Martin, C., and Clarke, J. (2006). SERRATE: a new player on the plant microRNA scene. *EMBO Rep.* 7, 1052–1058.
- Lu, C., and Fedoroff, N. (2000). A Mutation in the Arabidopsis HYL1 Gene Encoding a dsRNA Binding Protein Affects Responses to Abscisic Acid, Auxin, and Cytokinin. *Plant Cell* 12, 2351–2365.
- Machida, S., and Yuan, Y.A. (2013). Crystal structure of *Arabidopsis thaliana* Dax1 forkhead-associated domain reveals a conserved phospho-threonine recognition cleft for dicer-like 1 binding. *Mol. Plant* 6, 1290–1300.
- Macino, G., Cogoni, C., Catalanotto, C., and Azzalin, G. (2000). Transcription: Gene silencing in worms and fungi. *Nature* 404, 245.
- Mallick, P., and Kuster, B. (2010). Proteomics: a pragmatic perspective. *Nat. Biotechnol.* 28, 695–709.
- Mallory, A., and Vaucheret, H. (2010). Form, function, and regulation of ARGONAUTE proteins. *Plant Cell* 22, 3879–3889.
- Mallory, A.C., Bartel, D.P., and Bartel, B. (2005). MicroRNA-Directed Regulation of Arabidopsis AUXIN RESPONSE FACTOR17 Is Essential for Proper Development and Modulates Expression of Early Auxin Response Genes. *Plant Cell* 17, 1360–1375.
- Manavella, P.A., Hagmann, J., Ott, F., Laubinger, S., Franz, M., Macek, B., and Weigel, D. (2012). Fast-Forward Genetics Identifies Plant CPL Phosphatases as Regulators of miRNA Processing Factor HYL1. *Cell* 151, 859–870.
- Matzke, M.A., Primig, M., Trnovsky, J., and Matzke, A.J. (1989). Reversible methylation and inactivation of marker genes in sequentially transformed tobacco plants. *EMBO J.* 8, 643–649.
- Meijer, H.A., Kong, Y.W., Lu, W.T., Wilczynska, A., Spriggs, R. V, Robinson, S.W., Godfrey, J.D., Willis, A.E., and Bushell, M. (2013). Translational Repression and eIF4A2 Activity Are Critical for MicroRNA-Mediated Gene Regulation. *Science* 340, 82–85.
- Metzlaff, M., O’Dell, M., Cluster, P., and Flavell, R.. (1997). RNA-Mediated RNA Degradation and Chalcone Synthase A Silencing in Petunia. *Cell* 88, 845–854.
- Mourrain, P., Béclin, C., Elmayan, T., Feuerbach, F., Godon, C., Morel, J.B., Jouette, D., Lacombe, M., Nikic, S., Picault, N., et al. (2000). Arabidopsis SGS2 and SGS3 genes are required for posttranscriptional gene silencing and natural virus resistance. *Cell* 101, 533–542.
- Mueller, E., Gilbert, J., Davenport, G., Brigneti, G., and Baulcombe, D.C. (1995). Homology-dependent resistance: transgenic virus resistance in plants related to homology-dependent gene silencing. *Plant J.* 7, 1001–1013.
- Mukhtar, M.S., Carvunis, A.-R., Dreze, M., Epple, P., Steinbrenner, J., Moore, J., Tasan, M., Galli, M., Hao, T., Nishimura, M.T., et al. (2011). Independently evolved virulence effectors converge onto hubs in a plant immune system network. *Science* 333, 596–601.
- Napoli, C., Lemieux, C., and Jorgensen, R. (1990). Introduction of a Chimeric Chalcone Synthase Gene into Petunia Results in Reversible Co-Suppression of Homologous Genes in trans. *Plant Cell* 2, 279–289.

- Nellen, W., and Lichtenstein, C. (1993). What makes an mRNA anti-sense-itive? *Trends Biochem. Sci.* *18*, 419–423.
- Ngô, H., Tschudi, C., Gull, K., and Ullu, E. (1998). Double-stranded RNA induces mRNA degradation in *Trypanosoma brucei*. *Proc. Natl. Acad. Sci. U. S. A.* *95*, 14687–14692.
- Parker, G.S., Maity, T.S., and Bass, B.L. (2008). dsRNA binding properties of RDE-4 and TRBP reflect their distinct roles in RNAi. *J. Mol. Biol.* *384*, 967–979.
- Parrish, S., Fleenor, J., Xu, S., Mello, C., and Fire, a (2000). Functional anatomy of a dsRNA trigger: differential requirement for the two trigger strands in RNA interference. *Mol. Cell* *6*, 1077–1087.
- Pélissier, T., Clavel, M., Chaparro, C., Pouch-Pélissier, M.-N., Vaucheret, H., and Deragon, J.-M. (2011). Double-stranded RNA binding proteins DRB2 and DRB4 have an antagonistic impact on polymerase IV-dependent siRNA levels in *Arabidopsis*. *RNA* *17*, 1502–1510.
- Picotti, P., Bodenmiller, B., Mueller, L.N., Domon, B., and Aebersold, R. (2009). Full dynamic range proteome analysis of *S. cerevisiae* by targeted proteomics. *Cell* *138*, 795–806.
- Praefcke, G.J.K., Hofmann, K., and Dohmen, R.J. (2012). SUMO playing tag with ubiquitin. *Trends Biochem. Sci.* *37*, 23–31.
- Raczynska, K.D., Simpson, C.G., Ciesiolka, A., Szewc, L., Lewandowska, D., McNicol, J., Szweykowska-Kulinska, Z., Brown, J.W.S., and Jarmolowski, A. (2010). Involvement of the nuclear cap-binding protein complex in alternative splicing in *Arabidopsis thaliana*. *Nucleic Acids Res.* *38*, 265–278.
- Rajagopalan, R., Vaucheret, H., Trejo, J., and Bartel, D.P. (2006). A diverse and evolutionarily fluid set of microRNAs in *Arabidopsis thaliana*. *Genes Dev.* *20*, 3407–3425.
- Ratcliff, F. (1997). A Similarity Between Viral Defense and Gene Silencing in Plants. *Science* *276*, 1558–1560.
- Reece-Hoyes, J.S., Pons, C., Diallo, A., Mori, A., Shrestha, S., Kadreppa, S., Nelson, J., Diprima, S., Dricot, A., Lajoie, B.R., et al. (2013). Extensive rewiring and complex evolutionary dynamics in a *C. elegans* multiparameter transcription factor network. *Mol. Cell* *51*, 116–127.
- Reinhart, B.J., Slack, F.J., Basson, M., Pasquinelli, a E., Bettinger, J.C., Rougvie, a E., Horvitz, H.R., and Ruvkun, G. (2000). The 21-nucleotide let-7 RNA regulates developmental timing in *Caenorhabditis elegans*. *Nature* *403*, 901–906.
- Reis, R.S., Hart-Smith, G., Eamens, A.L., Wilkins, M.R., and Waterhouse, P.M. (2015). Gene regulation by translational inhibition is determined by Dicer partnering proteins. *Nat. Plants* *1*, 14027.
- Ren, G., Xie, M., Dou, Y., Zhang, S., Zhang, C., and Yu, B. (2012). Regulation of miRNA abundance by RNA binding protein TOUGH in *Arabidopsis*. *Proc. Natl. Acad. Sci. U. S. A.* *109*, 12817–12821.
- Reynoso, M.A., Blanco, F.A., Bailey-Serres, J., Crespi, M., and Zanetti, M.E. (2013). Selective recruitment of mRNAs and miRNAs to polyribosomes in response to rhizobia infection in *Medicago truncatula*. *Plant J.* *73*, 289–301.
- Robinson-Beers, K., Pruitt, R.E., and Gasser, C.S. (1992). Ovule Development in Wild-Type *Arabidopsis* and Two Female-Sterile Mutants. *Plant Cell* *4*, 1237–1249.

- Rogers, K., and Chen, X. (2013). Biogenesis, Turnover, and Mode of Action of Plant MicroRNAs. *Plant Cell* 25, 2383–2399.
- Rubio-Somoza, I., and Weigel, D. (2011). MicroRNA networks and developmental plasticity in plants. *Trends Plant Sci.* 16, 258–264.
- Ruiz, M.T. (1998). Initiation and Maintenance of Virus-Induced Gene Silencing. *Plant Cell* 10, 937–946.
- Saito, R., Smoot, M., Ono, K., and Ruschinski, J. (2012). A travel guide to Cytoscape plugins. *Nat. Methods* 9, 1069–1076.
- Salvucci, M.E. (2008). Association of Rubisco activase with chaperonin-60beta: a possible mechanism for protecting photosynthesis during heat stress. *J. Exp. Bot.* 59, 1923–1933.
- Schauer, S.E., Jacobsen, S.E., Meinke, D.W., and Ray, A. (2002). DICER-LIKE1: blind men and elephants in Arabidopsis development. *Trends Plant Sci.* 7, 487–491.
- Schiebel, W., Haas, B., Marinkovic, S., Klanner, A., and Sangers, H.L. (1993). RNA-directed RNA polymerase from tomato leaves. II. Catalytic in vitro properties. *J. Biol. Chem.* 268, 11858–11867.
- Schwab, R., Ossowski, S., Riester, M., Warthmann, N., and Weigel, D. (2006). Highly specific gene silencing by artificial microRNAs in Arabidopsis. *Plant Cell* 18, 1121–1133.
- Seo, Y.-S., Chern, M., Bartley, L.E., Han, M., Jung, K.-H., Lee, I., Walia, H., Richter, T., Xu, X., Cao, P., et al. (2011). Towards establishment of a rice stress response interactome. *PLoS Genet.* 7, e1002020.
- Sharma, A., Gulbahce, N., Pevzner, S.J., Menche, J., Ladenvall, C., Folkersen, L., Eriksson, P., Orho-Melander, M., and Barabási, A.-L. (2013). Network-based analysis of genome wide association data provides novel candidate genes for lipid and lipoprotein traits. *Mol. Cell. Proteomics* 12, 3398–3408.
- Shevchenko, A., Wilm, M., Vorm, O., and Mann, M. (1996). Mass Spectrometric Sequencing of Proteins from Silver-Stained Polyacrylamide Gels. *Anal. Chem.* 68, 850–858.
- Skirycz, A., Memmi, S., De Bodt, S., Maleux, K., Obata, T., Fernie, A.R., Devreese, B., Inzé, D., and Inzé, D. (2011). A reciprocal 15N-labeling proteomic analysis of expanding Arabidopsis leaves subjected to osmotic stress indicates importance of mitochondria in preserving plastid functions. *J. Proteome Res.* 10, 1018–1029.
- Slack, F.J., Basson, M., Liu, Z., Ambros, V., Horvitz, H.R., and Ruvkun, G. (2000). The *lin-41* RBCC gene acts in the *C. elegans* heterochronic pathway between the *let-7* regulatory RNA and the LIN-29 transcription factor. *Mol. Cell* 5, 659–669.
- Smardon, a, Spoerke, J.M., Stacey, S.C., Klein, M.E., Mackin, N., and Maine, E.M. (2000). EGO-1 is related to RNA-directed RNA polymerase and functions in germ-line development and RNA interference in *C. elegans*. *Curr. Biol.* 10, 169–178.
- Smith, S.E., and Smith, F.A. (2011). Roles of arbuscular mycorrhizas in plant nutrition and growth: new paradigms from cellular to ecosystem scales. *Annu. Rev. Plant Biol.* 62, 227–250.
- Smith, C.J.S., Watson, C.F., Bird, C.R., Ray, J., Schuch, W., and Grierson, D. (1990). Expression of a truncated tomato polygalacturonase gene inhibits expression of the endogenous gene in transgenic plants. *Mol. Gen. Genet.* 224.

- Sohn, S.Y., Bae, W.J., Kim, J.J., Yeom, K.-H., Kim, V.N., and Cho, Y. (2007). Crystal structure of human DGCR8 core. *Nat. Struct. Mol. Biol.* *14*, 847–853.
- Song, J.-J., Smith, S.K., Hannon, G.J., and Joshua-Tor, L. (2004). Crystal structure of Argonaute and its implications for RISC slicer activity. *Science* *305*, 1434–1437.
- Speth, C., Willing, E.-M., Rausch, S., Schneeberger, K., and Laubinger, S. (2013). RACK1 scaffold proteins influence miRNA abundance in Arabidopsis. *Plant J.* *76*, 433–445.
- Stark, C., Breitkreutz, B.-J., Reguly, T., Boucher, L., Breitkreutz, A., and Tyers, M. (2006). BioGRID: a general repository for interaction datasets. *Nucleic Acids Res.* *34*, D535–D539.
- Stocks, M.B., Moxon, S., Mapleson, D., Woolfenden, H.C., Mohorianu, I., Folkes, L., Schwach, F., Dalmay, T., and Moulton, V. (2012). The UEA sRNA workbench: a suite of tools for analysing and visualizing next generation sequencing microRNA and small RNA datasets. *Bioinformatics* *28*, 2059–2061.
- Sunkar, R., Li, Y.-F., and Jagadeeswaran, G. (2012). Functions of microRNAs in plant stress responses. *Trends Plant Sci.* *17*, 196–203.
- Tabara, H., Sarkissian, M., Kelly, W.G., Fleenor, J., Grishok, A., Timmons, L., Fire, A., and Mello, C.C. (1999). The *rde-1* gene, RNA interference, and transposon silencing in *C. elegans*. *Cell* *99*, 123–132.
- Tang, G., Reinhart, B.J., Bartel, D.P., and Zamore, P.D. (2003). A biochemical framework for RNA silencing in plants. *Genes Dev.* *17*, 49–63.
- Ting, L., Cowley, M.J., Hoon, S.L., Guilhaus, M., Raftery, M.J., and Cavicchioli, R. (2009). Normalization and statistical analysis of quantitative proteomics data generated by metabolic labeling. *Mol. Cell. Proteomics* *8*, 2227–2242.
- Tobias, P. a, and Guest, D.I. (2014). Tree immunity: growing old without antibodies. *Trends Plant Sci.* 1–4.
- Vaistij, F., Jones, L., and Baulcombe, D. (2002). Spreading of RNA targeting and DNA methylation in RNA silencing requires transcription of the target gene and a putative RNA-dependent RNA polymerase. *Plant Cell* *14*, 857–867.
- Vanhée-Brossollet, C., and Vaquero, C. (1998). Do natural antisense transcripts make sense in eukaryotes? *Gene* *211*, 1–9.
- Vaucheret, H. (2006). Post-transcriptional small RNA pathways in plants: mechanisms and regulations. *Genes Dev.* *20*, 759–771.
- Vaucheret, H., Palauqui, J.-C., Elmayan, T., and Moffatt, B. (1995). Molecular and genetic analysis of nitrite reductase co-suppression in transgenic tobacco plants. *Mol. Gen. Genet.* *248*, 311–317.
- Vazquez, F., Gascioli, V., Crété, P., and Vaucheret, H. (2004). The Nuclear dsRNA Binding Protein HYL1 Is Required for MicroRNA Accumulation and Plant Development, but Not Posttranscriptional Transgene Silencing. *Curr. Biol.* *14*, 346–351.
- Vidal, M., Cusick, M.E., and Barabási, A.-L. (2011). Interactome networks and human disease. *Cell* *144*, 986–998.

- Vogel, C., and Marcotte, E.M. (2012). Insights into the regulation of protein abundance from proteomic and transcriptomic analyses. *Nat. Rev. Genet.* *13*, 227–232.
- Voïnnet, O. (2009). Origin, Biogenesis, and Activity of Plant MicroRNAs. *Cell* *136*, 669–687.
- Voisin, D., Nawrath, C., Kurdyukov, S., Franke, R.B., Reina-Pinto, J.J., Efremova, N., Will, I., Schreiber, L., and Yephremov, A. (2009). Dissection of the complex phenotype in cuticular mutants of *Arabidopsis* reveals a role of *SERRATE* as a mediator. *PLoS Genet.* *5*.
- Wagner, E., and Simons, R. (1994). Antisense RNA control in bacteria, phages, and plasmids. *Annu. Rev. Microbiol.* *48*, 713–742.
- Wang, L., Song, X., Gu, L., Li, X., Cao, S., Chu, C., Cui, X., Chen, X., and Cao, X. (2013). NOT2 Proteins Promote Polymerase II–Dependent Transcription and Interact with Multiple MicroRNA Biogenesis Factors in *Arabidopsis*. *Plant Cell* *25*, 715–727.
- Wang, W., Ye, R., Xin, Y., Fang, X., Li, C., Shi, H., Zhou, X., and Qi, Y. (2011). An importin β protein negatively regulates MicroRNA activity in *Arabidopsis*. *Plant Cell* *23*, 3565–3576.
- Wang, Y., Juranek, S., Li, H., Sheng, G., Wardle, G.S., Tuschl, T., and Patel, D.J. (2009). Nucleation, propagation and cleavage of target RNAs in Ago silencing complexes. *Nature* *461*, 754–761.
- Waterhouse, P.M., Graham, M.W., and Wang, M.B. (1998). Virus resistance and gene silencing in plants can be induced by simultaneous expression of sense and antisense RNA. *Proc. Natl. Acad. Sci. U. S. A.* *95*, 13959–13964.
- Da Wei Huang, B.T.S., Lempicki, R. a, Huang, D.W., and Sherman, B.T. (2008). Systematic and integrative analysis of large gene lists using DAVID bioinformatics resources. *Nat. Protoc.* *4*, 44–57.
- Wesley, S. V, Helliwell, C. a, Smith, N. a, Wang, M.B., Rouse, D.T., Liu, Q., Gooding, P.S., Singh, S.P., Abbott, D., Stoutjesdijk, P. a, et al. (2001). Construct design for efficient, effective and high-throughput gene silencing in plants. *Plant J.* *27*, 581–590.
- Wianny, F., and Zernicka-Goetz, M. (2000). Specific interference with gene function by double-stranded RNA in early mouse development. *Nat. Cell Biol.* *2*, 70–75.
- Willmann, M.R., Mehalick, A.J., Packer, R.L., and Jenik, P.D. (2011). MicroRNAs regulate the timing of embryo maturation in *Arabidopsis*. *Plant Physiol.* *155*, 1871–1884.
- Wingard, S.A. (1928). Hosts and symptoms of ring spot, a virus disease of plants. *J. Agric. Res.* *37*, 127–153.
- Wodak, S., Vlasblom, J., Turinsky, A., and Pu, S. (2013). Protein–protein interaction networks: the puzzling riches. *Curr. Opin. Struct. Biol.* *23*, 941–953.
- Wu, F., Yu, L., Cao, W., Mao, Y., Liu, Z., and He, Y. (2007). The N-terminal double-stranded RNA binding domains of *Arabidopsis* *HYPONASTIC LEAVES1* are sufficient for pre-microRNA processing. *Plant Cell* *19*, 914–925.
- Wu, X., Shi, Y., Li, J., Xu, L., Fang, Y., Li, X., and Qi, Y. (2013). A role for the RNA-binding protein *MOS2* in microRNA maturation in *Arabidopsis*. *Cell Res.* *23*, 645–657.
- Xie, Z., Kasschau, K.D., and Carrington, J.C. (2003). Negative Feedback Regulation of Dicer-Like 1 in *Arabidopsis* by microRNA-Guided mRNA Degradation. *Curr. Biol.* *13*, 784–789.

- Yan, J., Gu, Y., Jia, X., Kang, W., Pan, S., Tang, X., Chen, X., and Tang, G. (2012a). Effective small RNA destruction by the expression of a short tandem target mimic in *Arabidopsis*. *Plant Cell* *24*, 415–427.
- Yan, K., Liu, P., Wu, C.-A., Yang, G.-D., Xu, R., Guo, Q.-H., Huang, J.-G., and Zheng, C.-C. (2012b). Stress-induced alternative splicing provides a mechanism for the regulation of microRNA processing in *Arabidopsis thaliana*. *Mol. Cell* *48*, 521–531.
- Yang, L., Wu, G., and Poethig, R.S. (2012). Mutations in the GW-repeat protein SUO reveal a developmental function for microRNA-mediated translational repression in *Arabidopsis*. *Proc. Natl. Acad. Sci. U. S. A.* *109*, 315–320.
- Yang, S.W., Chen, H.-Y., Yang, J., Machida, S., Chua, N.-H., and Yuan, Y.A. (2010). Structure of *Arabidopsis* HYPOPLASTIC LEAVES1 and Its Molecular Implications for miRNA Processing. *Structure* *18*, 594–605.
- Yu, B., Yang, Z., Li, J., Minakhina, S., Yang, M., Padgett, R.W., Steward, R., and Chen, X. (2005). Methylation as a crucial step in plant microRNA biogenesis. *Science* *307*, 932–935.
- Yu, B., Bi, L., Zheng, B., Ji, L., Chevalier, D., Agarwal, M., Ramachandran, V., Li, W., Lagrange, T., Walker, J.C., et al. (2008a). The FHA domain proteins DAWDLE in *Arabidopsis* and SNIP1 in humans act in small RNA biogenesis. *Proc. Natl. Acad. Sci. U. S. A.* *105*, 10073–10078.
- Yu, H., Braun, P., Yildirim, M. a, Lemmens, I., Venkatesan, K., Sahalie, J., Hirozane-Kishikawa, T., Gebreab, F., Li, N., Simonis, N., et al. (2008b). High-quality binary protein interaction map of the yeast interactome network. *Science* *322*, 104–110.
- Zamore, P.D., Tuschl, T., Sharp, P. a, and Bartel, D.P. (2000). RNAi: double-stranded RNA directs the ATP-dependent cleavage of mRNA at 21 to 23 nucleotide intervals. *Cell* *101*, 25–33.
- Zeng, Y., Yi, R., and Cullen, B.R. (2003). MicroRNAs and small interfering RNAs can inhibit mRNA expression by similar mechanisms. *Proc. Natl. Acad. Sci. U. S. A.* *100*, 9779–9784.
- Zhai, J., Jeong, D.-H., De Paoli, E., Park, S., Rosen, B.D., Li, Y., Gonzalez, A.J., Yan, Z., Kitto, S.L., Grusak, M.A., et al. (2011). MicroRNAs as master regulators of the plant NB-LRR defense gene family via the production of phased, trans-acting siRNAs. *Genes Dev.* *25*, 2540–2553.
- Zhan, X., Wang, B., Li, H., Liu, R., Kalia, R.K., Zhu, J.-K., and Chinnusamy, V. (2012). *Arabidopsis* proline-rich protein important for development and abiotic stress tolerance is involved in microRNA biogenesis. *Proc. Natl. Acad. Sci. U. S. A.* *109*, 18198–18203.
- Zhang, S., Xie, M., Ren, G., and Yu, B. (2013). CDC5, a DNA binding protein, positively regulates posttranscriptional processing and/or transcription of primary microRNA transcripts. *Proc. Natl. Acad. Sci. U. S. A.* *110*, 17588–17593.
- Zhu, C., Ding, Y., and Liu, H. (2011). MiR398 and plant stress responses. *Physiol. Plant.* *143*, 1–9.